
SOILWATER CONSULTANTS

TERRAIN ANALYSIS AND MATERIALS CHARACTERISATION FOR THE MULGA ROCK URANIUM PROJECT

Prepared for: **VIMY RESOURCES**

Date of Issue: 21 October 2015

Project No.: VMY-001/002

Document Ref: Terrain Analysis and Materials
Characterisation for the MRUP RevC2



Distribution:

Electronic Copy – Vimy Resources

Soilwater Group (Perth Office)

A Member of the SOILWATER GROUP

SOILWATER CONSULTANTS | SOILWATER ANALYSIS | SOILWATER TECHNOLOGIES

www.soilwatergroup.com

45 Gladstone Street, East Perth, WA 6004 | Tel: +61 8 9228 3060 | Email: swc@soilwatergroup.com

DOCUMENT STATUS RECORD

Project Title:	TERRAIN ANALYSIS AND MATERIALS CHARACTERISATION FOR THE MULGA ROCK URANIUM PROJECT
Project No.:	VMY-001/002
Client:	VIMY RESOURCES

Revision History

Revision Code ¹	Date Revised	Revision Comments	Signatures		
			Originator	Reviewer	Approved
A	01/05/2015	Draft report issued for internal review	ASP	SC	ASP
B	04/05/2015	Draft report issued for Vimy review	ASP	GB	ASP
C	08/06/2015	Final report issued to Vimy	ASP	GB	ASP
C2	21/10/15	Updated report issued to Vimy	JP	ASP	JP

Revision Code¹

- A - Report issued for internal review
- B - Draft report issued for client review
- C - Final report issued to client

LIMITATIONS

The sole purpose of this report and the associated services performed by Soil Water Consultants (SWC) was to undertake a Terrain Analysis and Material Characterisation for the proposed Mulga Rock Uranium Project (MRUP). This work was conducted in accordance with the Scope of Work presented to Vimy Resources ('the Client'). SWC performed the services in a manner consistent with the normal level of care and expertise exercised by members of the earth sciences profession. Subject to the Scope of Work, the Terrain Analysis and Material Characterisation was primarily confined to the proposed MRUP Development Extent, defined in the Environmental Scoping Document (ESD). No extrapolation of the results and recommendations reported in this study should be made to areas external to this project area. In preparing this study, SWC has relied on relevant published reports and guidelines, and information provided by the Client. All information is presumed accurate and SWC has not attempted to verify the accuracy or completeness of such information. While normal assessments of data reliability have been made, SWC assumes no responsibility or liability for errors in this information. All conclusions and recommendations are the professional opinions of SWC personnel. SWC is not engaged in reporting for the purpose of advertising, sales, promoting or endorsement of any client interests. No warranties, expressed or implied, are made with respect to the data reported or to the findings, observations and conclusions expressed in this report. All data, findings, observations and conclusions are based solely upon site conditions at the time of the investigation and information provided by the Client. This report has been prepared on behalf of and for the exclusive use of the Client, its representatives and advisors. SWC accepts no liability or responsibility for the use of this report by any third party.

© Soilwater Consultants, 2015. No part of this document may be reproduced or transmitted in any form or by any means, electronic, mechanical, photocopying, recording, or otherwise, without prior written permission of Soilwater Consultants.

CONTENTS

CONTENTS

1	INTRODUCTION.....	1-1
1.1	Objectives of work	1-1
1.2	Scope of Work	1-1
2	EXISTING ENVIRONMENT	2-1
2.1	Climate	2-1
2.1.1	REGIONAL CLIMATE	2-1
2.1.2	LOCAL CLIMATE.....	2-1
2.2	Geology	2-8
2.2.1	REGIONAL.....	2-8
2.2.2	LOCAL	2-8
2.3	Hydrogeology	2-9
2.3.1	REGIONAL.....	2-9
2.3.2	LOCAL	2-9
2.4	Geomorphology – Terrain Analysis.....	2-19
2.5	Terrain Dating	2-36
2.6	Hydrology	2-39
2.6.1	REGIONAL.....	2-39
2.6.2	LOCAL	2-39
2.7	Regional Soils.....	2-42
2.8	Flora and Vegetation	2-45
2.9	Fire	2-50
3	STUDY METHODOLOGY	3-1
3.1	Soil Sampling.....	3-1
3.1.1	TRENCH EXCAVATION	3-1
3.1.2	COLLECTION OF SOIL SAMPLES.....	3-1
3.1.3	SOIL PROFILE DESCRIPTION	3-2
3.1.4	SEMI-QUANTITATIVE ASSESSMENT OF ROOT ABUNDANCE	3-2
3.2	Laboratory Analysis	3-6
3.2.1	PHYSICAL, CHEMICAL AND HYDRAULIC PROPERTIES	3-6
3.2.2	GEOCHEMICAL TESTING	3-7
3.2.3	EROSION TESTING	3-8
4	STUDY RESULTS.....	4-1
4.1	Soil Distribution.....	4-1
4.2	SMU 1: Deep Dunal Sands.....	4-7
4.2.1	PHYSICAL AND HYDRAULIC PROPERTIES	4-12

CONTENTS

4.2.2	CHEMICAL PROPERTIES	4-14
4.3	SMU 2: Sandy Duplex Soils.....	4-16
4.3.1	PHYSICAL PROPERTIES	4-16
4.3.2	CHEMICAL PROPERTIES.....	4-17
4.4	SMU 3: Calcareous Loamy Soils	4-21
4.4.1	PHYSICAL AND HYDRAULIC PROPERTIES.....	4-22
4.4.2	CHEMICAL PROPERTIES.....	4-25
4.5	Soil Material Management Units (SMMU).....	4-27
4.5.1	TOPSOIL	4-27
4.5.2	YELLOW DUNAL SAND.....	4-28
4.5.3	RED DUNAL SAND	4-28
4.5.4	RED BROWN LOAM	4-29
4.5.5	CALCRETE	4-29
4.6	Erosional Stability	4-30
4.6.1	WEPP EROSION MODELLING	4-30
4.6.2	SIBERIA EROSION MODELLING.....	4-31
4.7	Overburden Materials	4-36
4.7.1	MIOCENE SEDIMENTS.....	4-36
4.7.2	OXIDISED EOCENE SEDIMENTS	4-39
4.7.3	REHABILITATION POTENTIAL OF OVERBURDEN MATERIALS.....	4-41
5	STUDY CONCLUSIONS AND RECOMMENDATIONS.....	5-1
5.1	Management of Soil and Waste Materials	5-1
5.2	Vegetation Management.....	5-1
5.2.1	VEGETATION STRIPPING.....	5-1
5.2.2	VEGETATION DEBRIS STOCKPILING.....	5-1
5.2.3	VEGETATION DEBRIS UTILISATION	5-2
5.3	Mulching	5-2
5.3.1	EFFECTS OF FIRE ON VEGETATION SOURCES	5-4
6	REFERENCES.....	6-1

LIST OF FIGURES

Figure 2.1: Long-term monthly average A) Rainfall and B) Pan Evaporation.....	2-2
Figure 2.2: Map showing the location of the on-site weather stations	2-3
Figure 2.3: Local monthly average A) rainfall and B) pan evaporation.....	2-5
Figure 2.4: Local monthly average A) maximum temperature and B) wind speed	2-6
Figure 2.5: Wind rose data for the MRUP	2-7
Figure 2.6: Regional geology of A) south-eastern portion of the Yilgarn Craton, and B) Narnoo Basin showing location of MRUP	2-10
Figure 2.7: A) Thickness and B) Stratigraphy of the Gunbarrel and Narnoo Basins	2-11

Figure 2.8: Geological cross-sections through the MRUP (See Figure 2.6B for cross-section locations)	2–12
Figure 2.9: A) Eocene paleodrainage channel incised into the Narnoo Basin and B) Conceptual Hydrogeological Model for the MRUP	2–13
Figure 2.10: Basement depth of the paleodrainage channel within the MRUP	2–14
Figure 2.11: Location of the MRUP in relation to the paleovalleys draining the southeastern portion of the Yilgarn Craton	2–15
Figure 2.12: Groundwater levels (blue lines) within the Narnoo Paleodrainage System	2–16
Figure 2.13: Groundwater quality observation locations	2–18
Figure 2.14: Regional landforms within the MRUP.....	2–22
Figure 2.15: Primary dune formations identified near the Mulga Rocks Project: (A) Linear Dunes, (B) Barchan Dunes, (C) Parabolic Dunes, and (C) Complex/Irregular Dunes. Adapted from Short (2010).....	2–23
Figure 2.16: Location of landsurface cross-sections	2–24
Figure 2.17: Characteristic linear dunes within the MRUP	2–25
Figure 2.18: Characteristic barchan dunes within the MRUP	2–26
Figure 2.19: Characteristic parabolic dunes within the MRUP	2–27
Figure 2.20: Characteristic complex or irregular dunes within the MRUP	2–29
Figure 2.21: Landsurface within the Emperor Deposit	2–31
Figure 2.22: Landsurface within the Shogun Deposit.....	2–32
Figure 2.23: Landsurface within the Ambassador West Deposit.....	2–33
Figure 2.24: Landsurface within the Ambassador East Deposit.....	2–34
Figure 2.25: Landsurface within the Princess Deposit	2–35
Figure 2.26: Recorded ages for Quaternary Dunes within the GVD and broader arid zone of Australia.....	2–38
Figure 2.27: Regional surface hydrology.....	2–40
Figure 2.28: Local-scale hydrological processes, showing convergence of surface flows into topographic depressions..	2–41
Figure 2.29: Regional soil-landscape units.....	2–44
Figure 2.30: Vegetation distribution throughout the MRUP (MCPL, 2015a) – See Table 2.6).....	2–49
Figure 2.31: Complexity of fire scars within the MRUP region	2–53
Figure 2.32: Bushfires from 1995 to 2014 (Data collated from the Landgate’s Firewatch).....	2–54
Figure 3.1: Map showing the soil and geochemical sampling locations within the Shogun Deposit.....	3–3
Figure 3.2: Map showing the soil and geochemical sampling locations within the Ambassador West and East Deposits	3–4
Figure 3.3: A) 24-hour and B) mean monthly rainfall data.....	3–12
Figure 3.4: Annual rainfall data	3–13
Figure 4.1: Mapping of broad soil landform associations across the MRUP	4–3
Figure 4.2: SMU Map across the MRUP	4–4
Figure 4.3: SMU map across the Mulga Rock West Deposits.....	4–5
Figure 4.4: SMU map across the Mulga Rock East Deposits.....	4–6
Figure 4.5: Typical profile of SMU 1 – Deep dunal sands	4–11
Figure 4.6: Moisture profiles with water retention information for SMU 1	4–13
Figure 4.7: pH and EC depth profiles for SMU 1	4–15
Figure 4.8: Characteristic soil profile of SMU 2	4–18
Figure 4.9: Moisture profiles with water retention information for SMU 2.....	4–19

CONTENTS

Figure 4.10: pH and EC depth profiles for SMU 2	4-20
Figure 4.11: Characteristic soil profile for SMU 3	4-23
Figure 4.12: Moisture profiles for SMU 3.....	4-24
Figure 4.13: pH and EC depth profiles for SMU 3	4-26
Figure 4.14: Modelled slope erosion rates	4-33
Figure 4.15: Regional SIBERIA model results.....	4-34
Figure 4.16: Layered SIBERIA landform model results.....	4-35
Figure 4.17: Screen test results for the overburden materials within the Shogun Deposit	4-42
Figure 4.18: Screen test results for the overburden materials within the Ambassador East Deposit	4-44
Figure 4.19: Screen test results for the overburden materials within the Ambassador West Deposit	4-45
Figure 4.20: Screen test results for the overburden materials within the Princess Deposit.....	4-47
Figure 4.21: Trial mining slot within the Shogun Deposit	4-49

LIST OF TABLES

Table 2.1: IFD data for the MRUP (BOM, 2015a)	2-1
Table 2.2: Location of on-site weather stations	2-4
Table 2.3: Summary of groundwater quality from the Narnoo paleodrainage channel.....	2-17
Table 2.4: Soil-landscape units within the MRUP region.....	2-42
Table 2.5: Priority species recorded within the MRUP area	2-45
Table 2.6: Description of VCTs recorded within the MRUP (MCPL, 2015a).....	2-45
Table 3.1: Details of the deep trenches examined in this investigation	3-2
Table 3.2: Semi-quantitative assessment of root abundance (McDonald <i>et al.</i> , 2009).....	3-6
Table 3.3: Physical and chemical properties examined in the laboratory.....	3-6
Table 3.4: Drillholes screen tested in this investigation.....	3-7
Table 3.5: Key soil parameters used in the WEPP model.....	3-14
Table 3.6: Key input parameters used in the SIBERIA model.....	3-14
Table 4.1: Relationship of identified SMU to Australian soil classification schemes.....	4-1
Table 4.2: SMU coverage within the Development Area and Disturbance Area	4-2
Table 4.3: Average physical and hydraulic properties for SMU 1	4-12
Table 4.4: Average chemical properties for SMU 1	4-14
Table 4.5: Average physical and hydraulic properties of SMU 2	4-16
Table 4.6: Average chemical properties of SMU 2	4-17
Table 4.7: Average physical and hydraulic properties of SMU 3	4-22
Table 4.8 Average chemical properties of SMU 3	4-25
Table 4.9: Summary physical and hydraulic properties of the identified SMMU	4-29
Table 4.10: Summary chemical properties of the identified SMMU	4-30
Table 4.11: Summary of WEPP erosion modelling results.....	4-31
Table 4.12: Characteristic chemical properties of the Miocene sediments.....	4-37
Table 4.13: Multi-element composition of Miocene sediments (Values in bold exceed the corresponding EIL).....	4-38
Table 4.14: Characteristic chemical properties of the Oxidised Eocene sediments	4-40
Table 4.15: Multi-element composition of Oxidised Eocene sediments (Values in bold exceed the corresponding EIL) ..	4-40
Table 5.1: Key properties of the soil and overburden materials, and their management requirements.....	5-5

LIST OF PLATES

Plate 2.1: Weather station at the Emperor Deposit	2-4
Plate 2.2: Dunal surface with repeating sand dunes and localised interdunal topographic depressions.....	2-21
Plate 2.3: Broad alluvial plain	2-21
Plate 2.4: OSL sampling locations from the MRUP rubbish trench	2-37
Plate 2.5: OSL dating of surficial dunal sands near the Kakarook Borefield by the GSWA.....	2-37
Plate 2.6: Localised flooding with a topographic depression within the MRUP in response to Cyclone Carlos.....	2-39
Plate 2.7: Extent of the November 2014 bushfire within the MRUP	2-50
Plate 2.8: Intensity of the November 2014 bushfire within the MRUP	2-51
Plate 2.9: Complexity of the fire front leaving some area unburnt.....	2-52
Plate 2.10: Fire refuge areas.....	2-52
Plate 3.1: Deep trench excavation directly adjacent to existing vegetation for this study	3-1
Plate 3.2: Exposed soil profile achieved through deep trench excavation in this investigation	3-5
Plate 3.3: Collection of soil samples from the exposed soil profile surface	3-5
Plate 3.4: Laboratory rainfall simulator. (A) sample C1, (B) sample E3	3-9
Plate 3.5: Laboratory-scale, rill erosion flume (sample E5).....	3-10
Plate 4.1: Layer of cryptogam below thin surface layer of active sand.....	4-8
Plate 4.2: Tap roots extending below bottom of trench within dunal sands (SMU 1).....	4-8
Plate 4.3: Typical density of plant species	4-9
Plate 4.4: Abundance of tap roots effectively anchoring the large sand dunes	4-9
Plate 4.5: Root growth through the soil matrix of the yellow sand material	4-10
Plate 4.6: Occurrence of SMU 3 directly overlying the Miocene sediments within the Shogun Deposit.....	4-21
Plate 4.7: Abrupt boundary between the surficial loam overlying the calcrete in SMU 3.....	4-22
Plate 4.8: Absence of organic matter accumulation following a fire within the MRUP.....	4-27
Plate 4.9: Overburden profile comprising the Miocene and Oxidised Eocene Sediments.....	4-36
Plate 4.10: Dispersive properties of the Miocene sediments, as influenced by salinity.....	4-37
Plate 4.11: Dispersive properties of the Oxidised Eocene sediments, as influenced by salinity.....	4-40
Plate 4.12: Reconstructed soil profile exposed at Trench 19	4-50
Plate 4.13: Reconstructed soil profile exposed at Trench 20	4-50
Plate 4.14: Characteristic rehabilitation of the mined slot within the Shogun Deposit	4-51
Plate 5.1: Satisfactory utilisation of vegetation debris providing a continuous cover across a slope surface	5-2
Plate 5.2: Unsatisfactory utilisation of vegetation debris providing insufficient surface cover.....	5-3
Plate 5.3: Pre- and post-fire vegetation sources	5-4

1 INTRODUCTION

Soil Water Consultants (SWC) were commissioned by Vimy Resources (Vimy) to undertake a pre-mine terrain analysis and materials characterisation for the proposed Mulga Rock Uranium Project (MRUP). The purpose of this assessment was to identify and characterise the existing landforms within the MRUP and to establish their likely formation and functioning to determine the potential risks associated with the mining of this deposit. This work provides the necessary information to manage the identified risks and to ensure adequate provisioning and implementation for future rehabilitation and closure plans.

The information presented in this terrain and materials characterisation provides baseline data that can be used to assist in the mining of these materials, and in the construction and rehabilitation of the post-mine landforms. Implementation of the management recommendations suggested in this report will ensure that all materials are used appropriately in the reconstruction of the various post-mine landforms and that these landforms are constructed in a safe, stable and sustainable manner to facilitate closure of this site in the future.

1.1 OBJECTIVES OF WORK

The objectives of the terrain analysis and materials characterisation were to:

- Characterise and spatially analysis the pre-existing landforms within the MRUP;
- Identify the distribution of distinctly different material types within the proposed mine disturbance area;
- Characterise the physical, chemical and hydraulic properties of the soil and overburden materials to be disturbed during mining;
- Identify materials that may develop adverse properties during mining and rehabilitation (e.g. hard-setting, dispersive or erosive soils);
- Identify materials which exhibit optimal or favourable characteristics for use in rehabilitation (e.g. topsoils or subsoils) so that these materials can be managed appropriately during the mining and rehabilitation process;
- Propose management strategies for the handling and utilisation of all materials during mining and rehabilitation; and
- Suggest management recommendations for the reconstruction of the various post-mine landforms.

1.2 SCOPE OF WORK

The Scope of Work completed by SWC included:

- Detailed review of regional and local-scale topographic data to characterise the pre-existing landforms within the MRUP;
- Field survey and collection of soil samples from the MRUP;
- Undertake field and laboratory analysis to characterise the physical, chemical and hydraulic properties of all materials to be disturbed during mining;
- Utilising data from the laboratory analysis conduct WEPP and SIBERIA landform evolution modelling to predict long-term evolution of the post-mine landforms;
- Establish management prescriptions for the handling and utilisation of all materials to be disturbed during mining of the MRUP; and
- Prepare preliminary rehabilitation and closure designs for the MRUP.

2 EXISTING ENVIRONMENT

2.1 CLIMATE

2.1.1 REGIONAL CLIMATE

The climate of the MRUP is classified as semi-arid to arid with hot summers and cool – mild winters. Rainfall throughout the year does not vary considerably with 20 – 40 mm/month falling in the summer months (November – March), often associated with cyclonic events, and 10 – 30 mm/month in winter (April – October), with a total annual average rainfall of approximately 280 mm. Pan evaporation (around 2,650 mm/yr) greatly exceeds rainfall throughout the year and thus the environment exists in a water deficit condition. Daily pan evaporation rates vary from 11 – 12 mm/day (330 – 360 mm/month) in summer to 2 – 3 mm/day (75 – 100 mm/month) in winter. Long term monthly total rainfall and pan evaporation for the three closest Bureau of Meteorology (BOM) weather stations (Balgair, Laverton and Kalgoorlie) is provided in Figure 2.1.

Intensity-Frequency-Duration (IFD) data for the MRUP (as determined at 568,000 mE and 6,688,000 mN; GDA94 Zone 51) is presented in

Table 2.1: IFD data for the MRUP (BOM, 2015a)

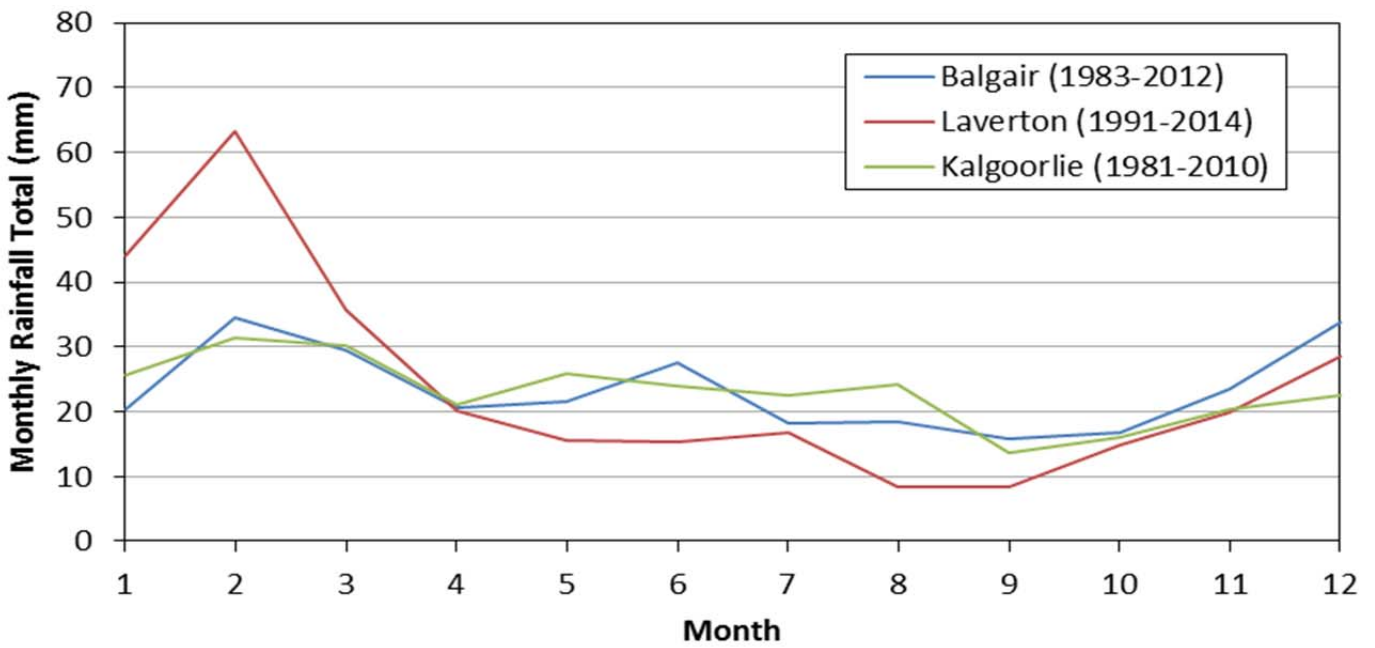
DURATION	1 Year	2 years	5 years	10 years	20 years	50 years	100 years
5Mins	36.8	50.0	73.5	89.7	111	140	165
6Mins	34.2	46.4	68.2	83.3	103	130	153
10Mins	27.4	37.2	54.5	66.4	81.7	104	122
20Mins	19.5	26.4	38.3	46.4	56.8	71.7	84.0
30Mins	15.5	20.9	30.3	36.6	44.8	56.5	66.0
1Hr	10.1	13.6	19.6	23.7	28.9	36.4	42.6
2Hrs	6.34	8.56	12.4	15.0	18.3	23.0	26.9
3Hrs	4.81	6.50	9.40	11.4	13.9	17.5	20.5
6Hrs	2.97	4.03	5.86	7.11	8.72	11.0	12.9
12Hrs	1.81	2.47	3.62	4.42	5.44	6.91	8.12
24Hrs	1.07	1.46	2.18	2.69	3.34	4.27	5.04
48Hrs	.597	.819	1.26	1.57	1.97	2.55	3.04
72Hrs	.410	.571	.891	1.11	1.41	1.84	2.20

2.1.2 LOCAL CLIMATE

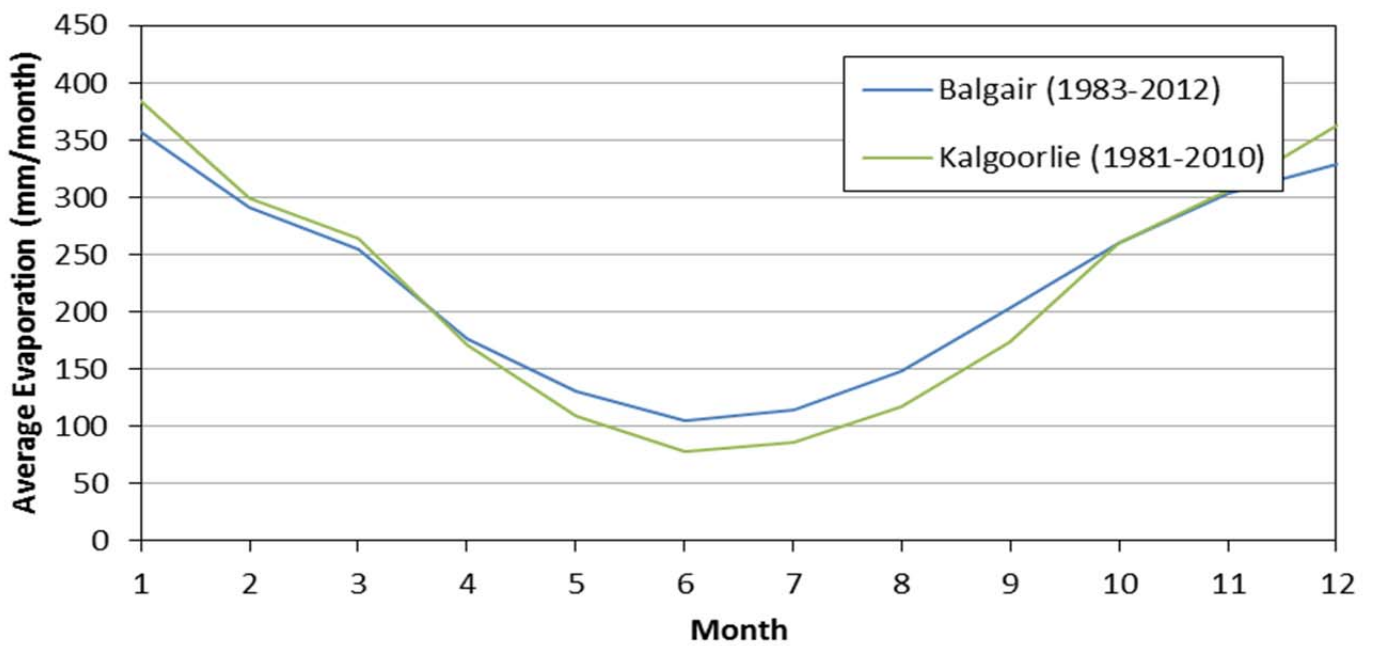
The local climate within the MRUP is captured at four locations to assess spatial variability across the site. The locations of the weather stations are provided in Table 2.2 and Figure 2.2. Data currently collected on an hourly basis includes: air temperature, barometric pressure, relative humidity, rainfall depth, wind speed, and wind direction. Data collection started in March 2009 and a summary of the data to September 2014 is provided in Figure 2.3 to Figure 2.4.

An example of the on-site weather station at the Emperor Deposit is shown in Plate 2.1.

A)



B)

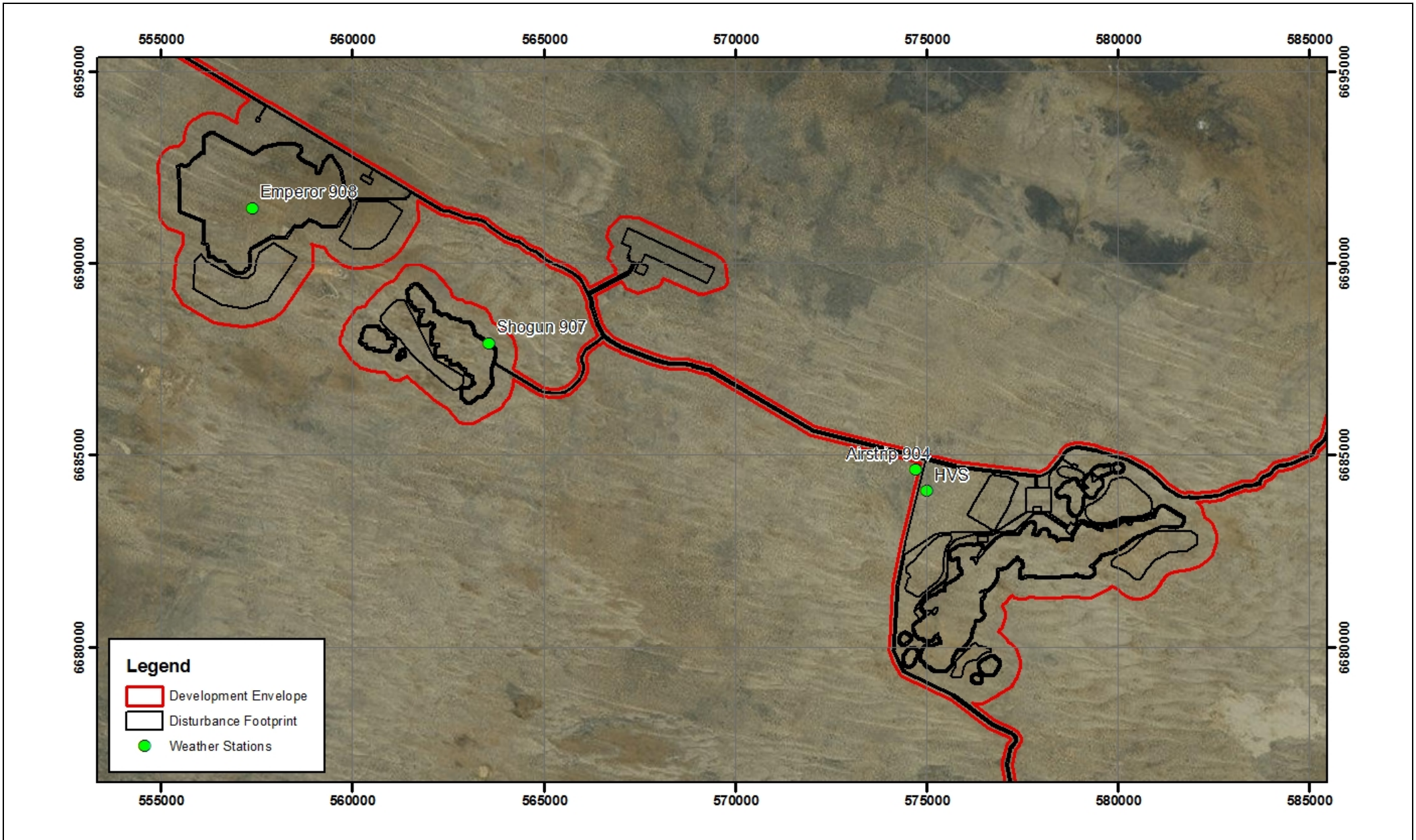


VIMY RESOURCES

TERRAIN ANALYSIS AND MATERIALS
CHARACTERISATION FOR THE MULGA
ROCK URANIUM PROJECT

Figure 2.1: Long-term monthly average A) Rainfall and B) Pan Evaporation





VIMY RESOURCES

TERRAIN ANALYSIS AND MATERIALS CHARACTERISATION
FOR THE MULGA ROCK URANIUM PROJECT

Figure 2.2: Map showing the location of the on-site weather stations



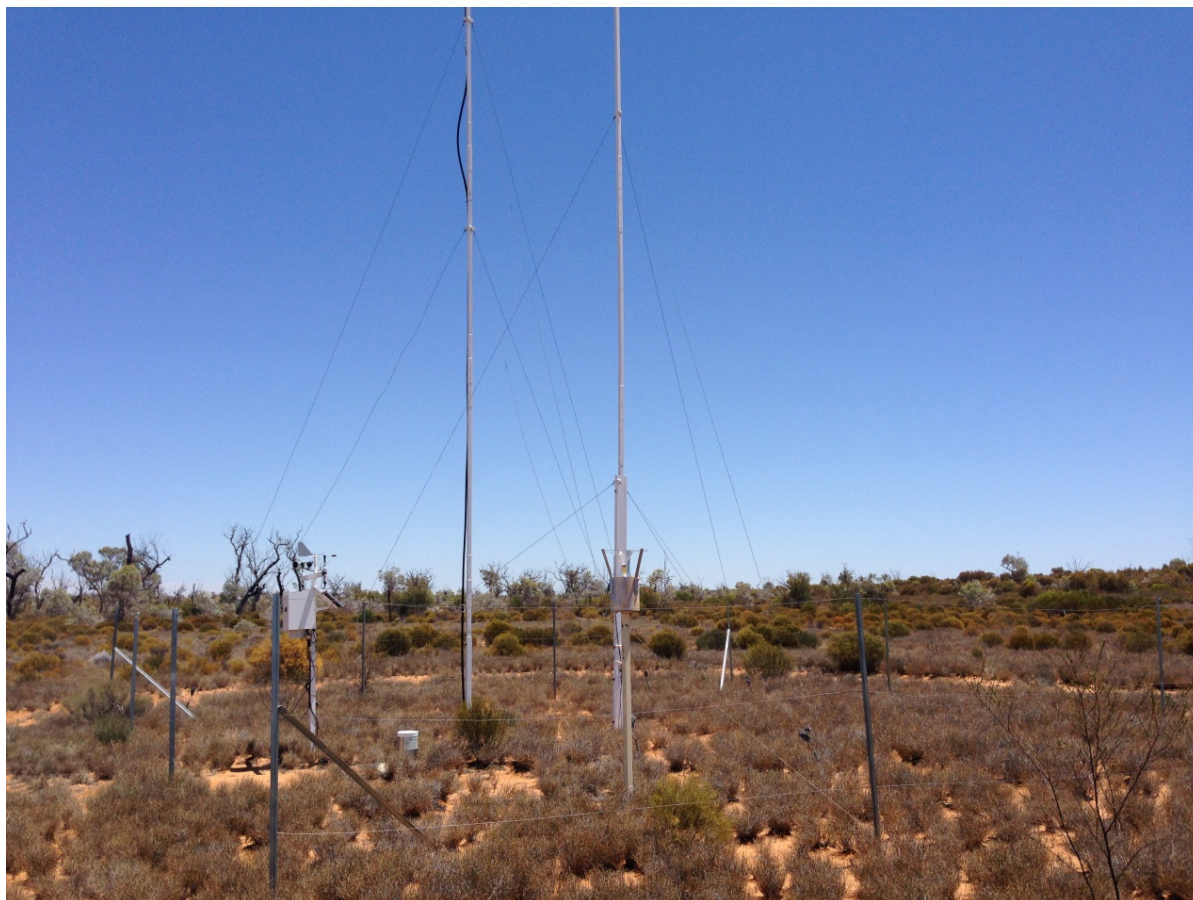
Table 2.2: Location of on-site weather stations

Station	Easting (GDA MGA zone 51)	Northing (GDA MGA zone 51)
Airstrip 904	574715	6684600
Emperor 908	557391	6691424
Shogun 907	563569	6687909
High Volume Sampler (HVS)	575003	6684055

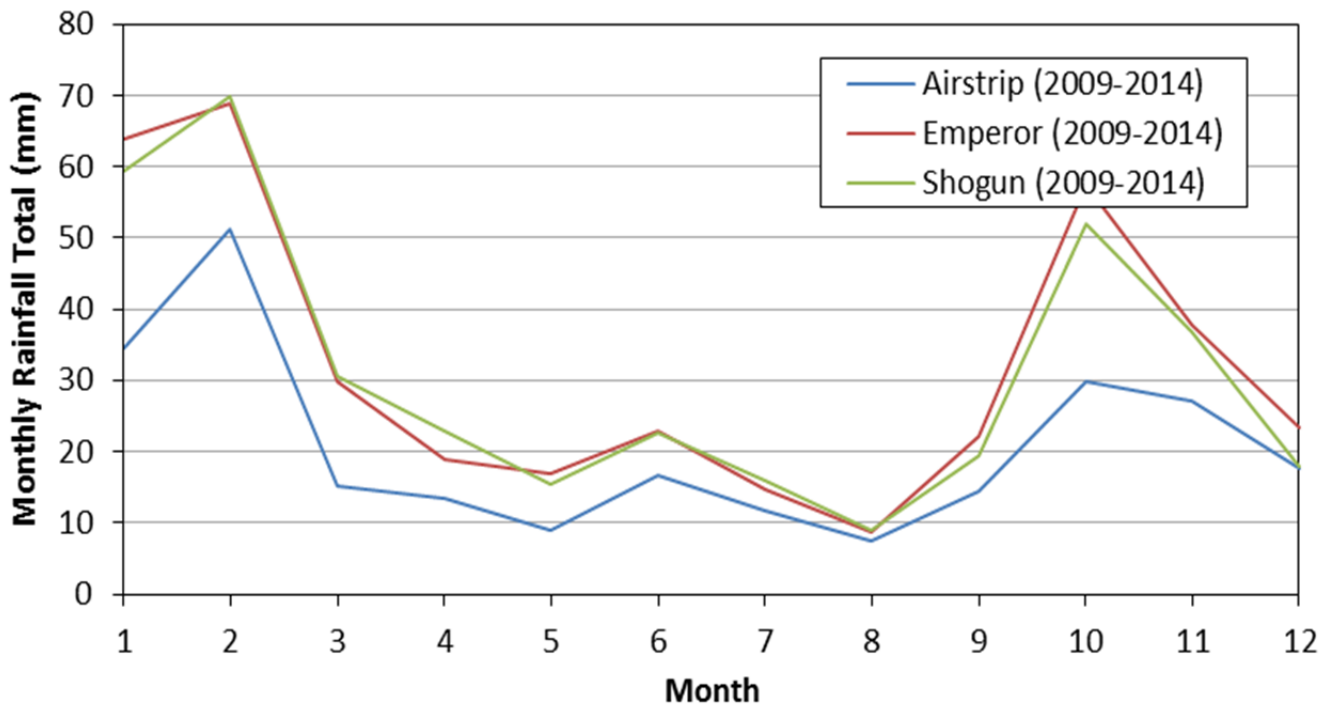
Local rainfall within the MRUP shows a defined seasonality with summer (November – March) rainfall varying from 20 – 70 mm/month, whilst rainfall varies from 10 – 20 mm/month during winter (April – October; Figure 2.3A). In contrast calculated pan evaporation data varies from 75 – 100 mm/month during winter to 280 – 290 mm/month during summer (Figure 2.3B). The western side of the MRUP (i.e. Shogun and Emperor Deposits) is noticeably wetter and experiences less evaporation than the eastern side (i.e. Ambassador and Princess Deposits).

Over the MRUP, 9 am wind speeds vary from around 5 km/hr during winter to around 11 km/hr in summer. During the summer months, wind direction is predominately (50 – 80%) from the south-east (i.e. blowing to the northwest), whilst in winter the prevailing wind direction is easterly (Figure 2.5).

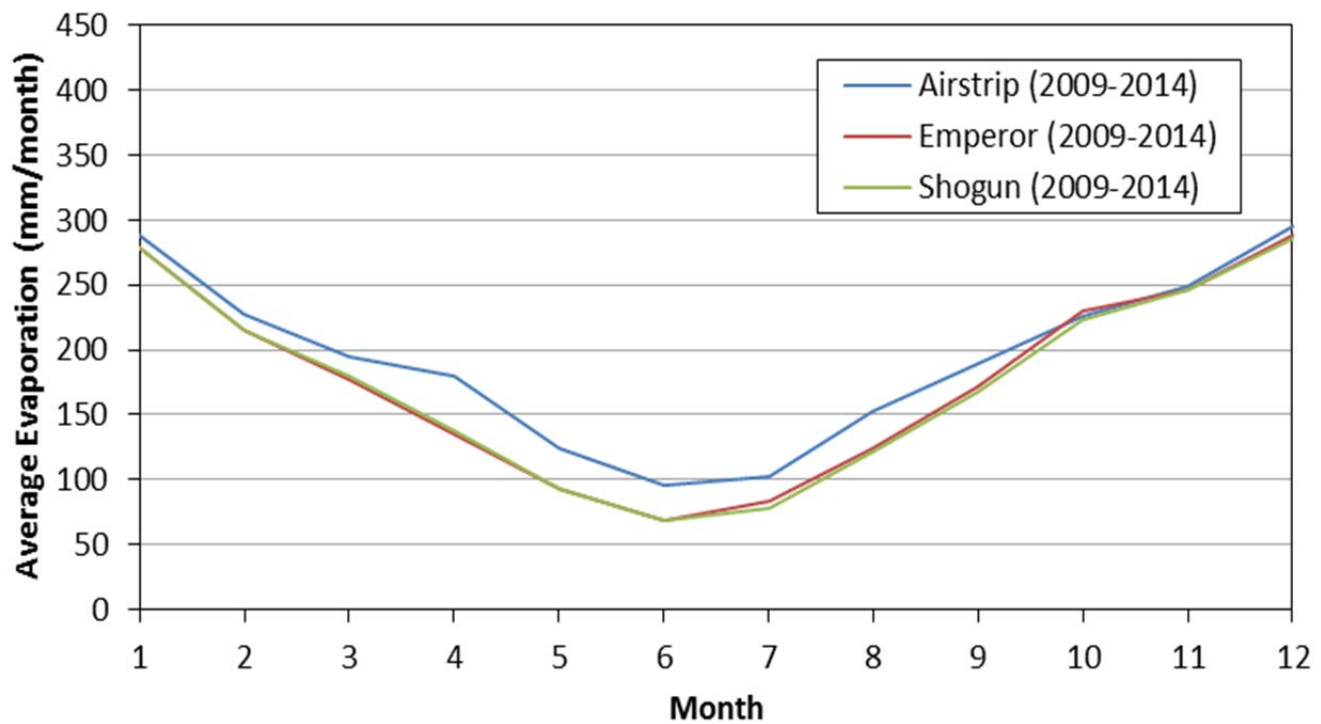
Plate 2.1: Weather station at the Emperor Deposit



A)



B)



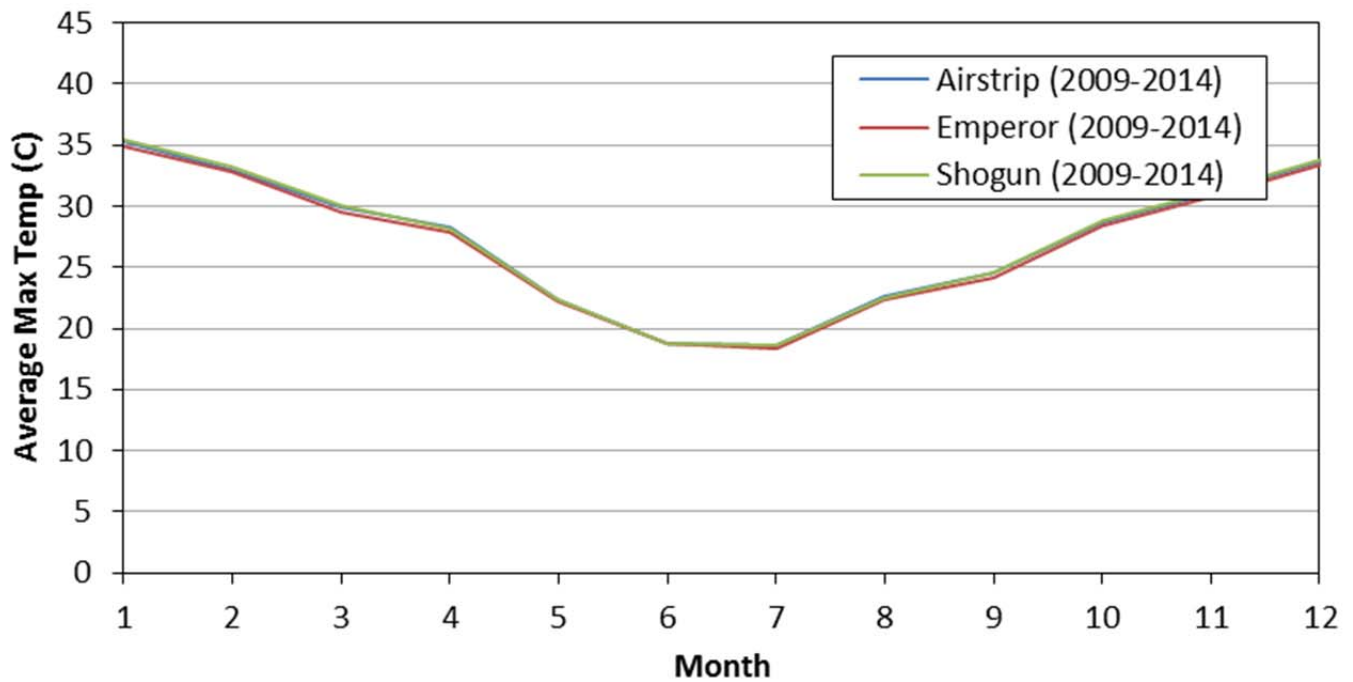
VIMY RESOURCES

TERRAIN ANALYSIS AND MATERIALS
CHARACTERISATION FOR THE MULGA
ROCK URANIUM PROJECT

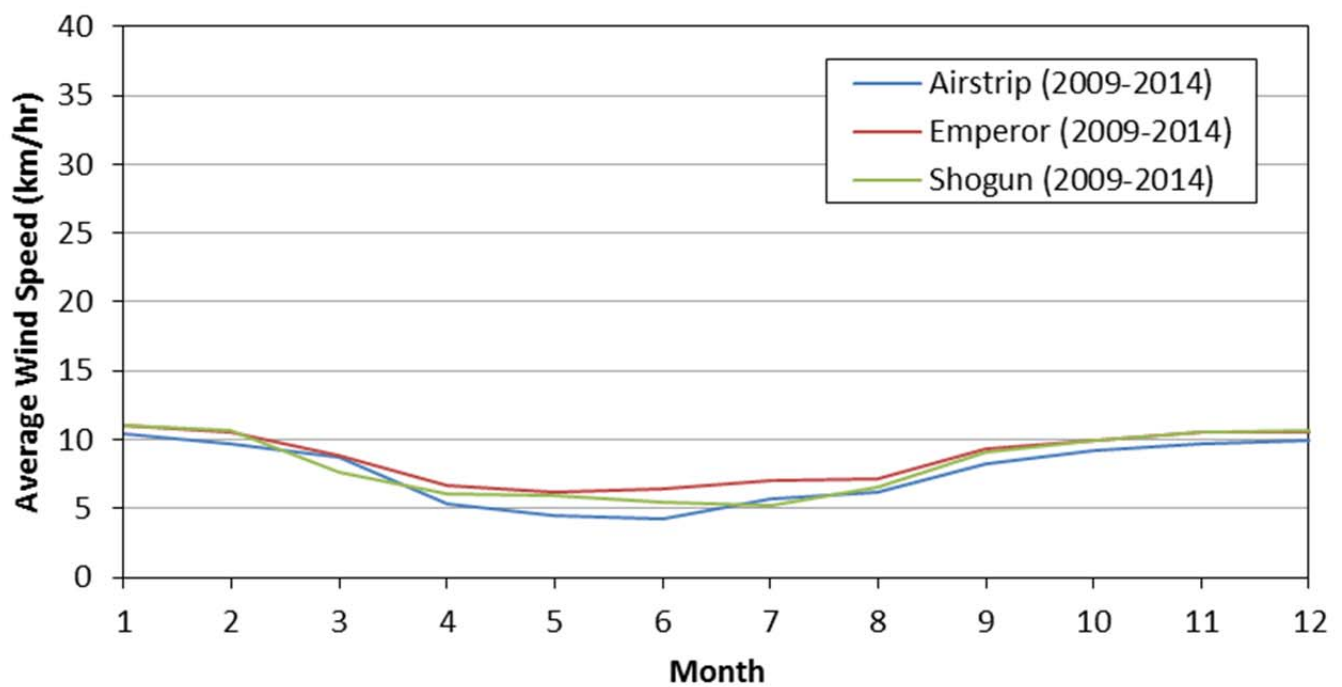
Figure 2.3: Local monthly average A) rainfall and B) pan evaporation



A)



B)

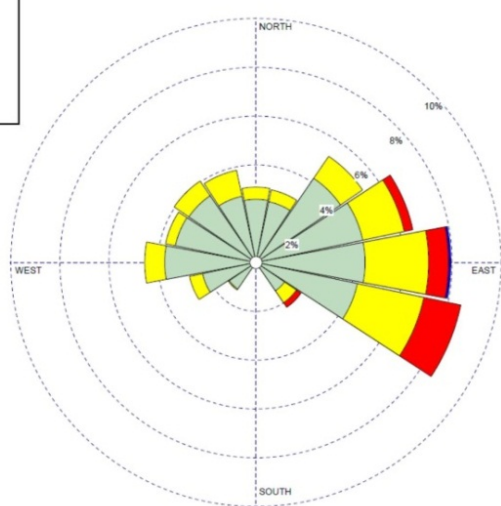
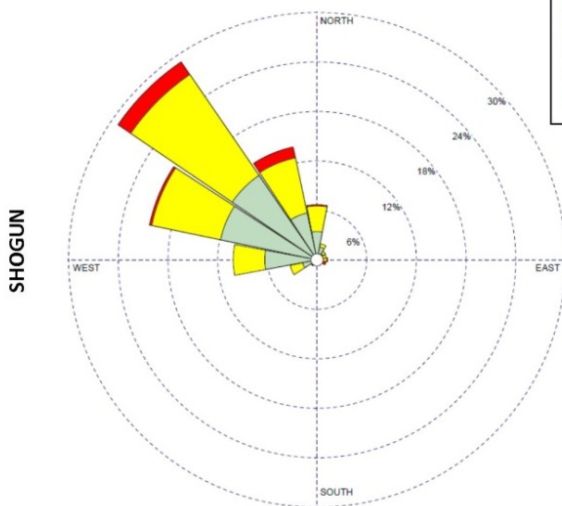
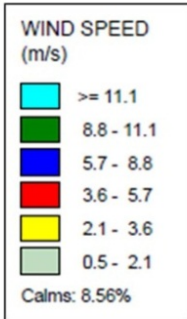
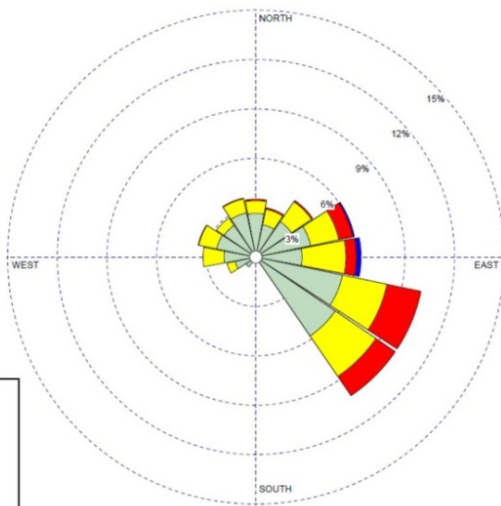
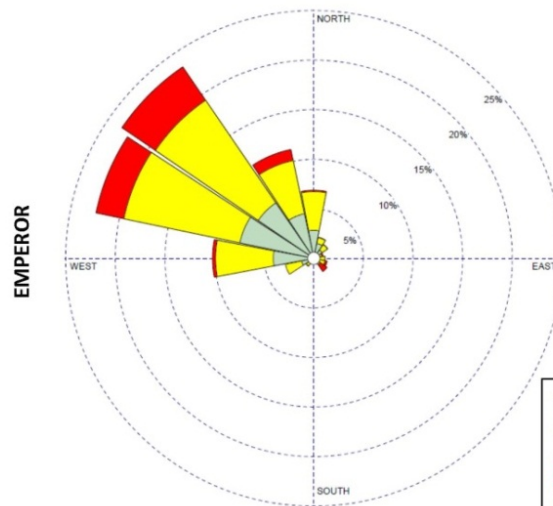
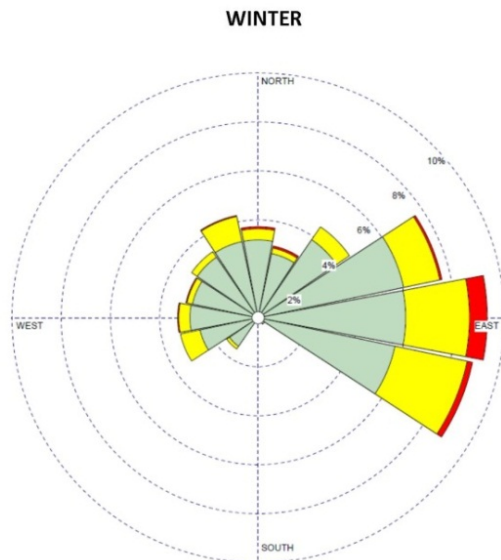
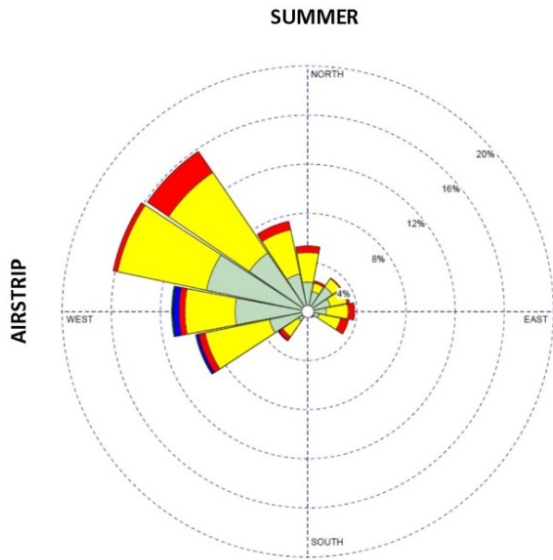


VIMY RESOURCES

TERRAIN ANALYSIS AND MATERIALS
CHARACTERISATION FOR THE MULGA
ROCK URANIUM PROJECT

Figure 2.4: Local monthly average A) maximum temperature and B) wind speed





VIMY RESOURCES

TERRAIN ANALYSIS AND MATERIALS
CHARACTERISATION FOR THE MULGA
ROCK URANIUM PROJECT

Figure 2.5: Wind rose data for the MRUP



2.2 GEOLOGY

2.2.1 REGIONAL

Regionally the MRUP is located within the Late Cretaceous to Early Cenozoic (Paleocene) Narnoo Basin, a small fault-bounded sedimentary basin within the larger Middle Cambrian to Cretaceous Gunbarrel Basin. Within the vicinity of the MRUP the underlying Gunbarrel basin directly overlies the Yilgarn Craton, corresponding to the Kingston Shelf (Figure 2.6A), whilst its eastern extension is terminated by the Neo-Proterozoic Albany-Fraser Province (Biranup Complex) along the Cundelee Fault (Figure 2.6B). Sediments within the Gunbarrel Basin, in the vicinity of the MRUP, achieve a thickness of around 600 m (Figure 2.7A), and correspond primarily to the Paterson Formation, being composed of inter- and cross-bedded shale, siltstone, claystone and sandstone deposited in subglacial, glaciolacustrine and fluvio-glacial environments, with some potential for marine influence (Figure 2.7B; Jackson and van de Graff, 1981).

The Narnoo Basin occurs within the Gunbarrel Basin as a series of complex Cretaceous to Paleocene grabens that were subsequently filled with Mid to Late Eocene, often carbonaceous, claystone, siltstone and sandstone deposited under a range of alluvial, fluvial, and lacustrine conditions (Figure 2.8). These sediments typically obtain thicknesses of up to 100 m, of which the surface 40 m is completely oxidised, whilst the remaining 60 m remains reduced.

2.2.2 LOCAL

At a local scale, the MRUP is associated with an oxbow-shaped mid-Eocene paleodrainage channel that was incised into the existing Cretaceous Narnoo Basin sediments. The geometry of the paleovalley is shown in Figure 2.9A, whilst the base of the paleodrainage channel is shown in Figure 2.10. Within this palaeochannel a range of materials were deposited under varying high and low-energy fluvial and lacustrine conditions, resulting (simplistically) in layers of claystone, siltstone and sandstone, which experienced varying levels of post-depositional weathering, prior to groundwater inundation. This paleodrainage system is likely to have exhibited geomorphological, and resulting fluvial, complexity, whereby zones of accumulation and more lacustrine conditions are likely to have existed; this effectively is where the mineralised U deposit to be mined by Vimy is captured (i.e. associated with defined zones of lignite).

A Conceptual Hydrogeological Site Model is shown in Figure 2.9B. The MRUP will primarily target the uranium-enriched carbonaceous Eocene sediments that have been deposited within a paleodrainage channel within the Narnoo Basin. The surface 30 – 40 m of these sediments have been extensively oxidised and weathered, and subsequently the current uranium orebody occurs and is enriched at the redox boundary, with it typically only extends 2 – 5 m below the groundwater level. The distribution of the enriched uranium, and other metals and metalloids, is strongly associated with the distribution of the organic-rich carbonaceous sediments, as the uranium is strongly bound to the organic matter through complex ion exchange and/or functional group assemblages (i.e. the positively charged uranyl ion binding with the negatively charged carboxylate anion: $\text{UO}_2^{2+} + \text{R-COO}^-$; Douglas *et al.*, 1996). This organic-rich layer effectively acts as a Passive or Permeable Reactive Barrier (PRB) stripping uranium and other solutes from the groundwater as it passes through this material.

Strong density stratification exists with the palaeochannel aquifer, with TDS varying from around 60 – 70 g/L within the basal highly transmissive (i.e. 10 – 140 m/day) sands to 40 – 50 g/L within the central lower permeable (i.e. 0.2 – 9 m/day) portion of the paleovalley. Within the orebody the salinity varies from 25 – 35 g/L, with these predominately finer textured, organic rich sediments having a much reduced permeability of only 0.02 – 0.7 m/day. The reactivity of the

sediment show a strong decreasing trend with depth, coinciding with the reduction in organic matter from 10 – 50% in the orebody to 0.5 – 2% within the basal sands.

Hydraulic gradients within the palaeodrainage channel are very small (i.e. <0.001; Rockwater, 2015) and subsequently groundwater movement within and into or out of the aquifer is sluggish and inconsequential (i.e. it represents a very slow meandering oxbow section of the larger Ponton Creek paleochannel located some 65 km to the south (Rockwater, 2015).

2.3 HYDROGEOLOGY

2.3.1 REGIONAL

At a regional scale groundwater is associated with structurally controlled palaeodrainage channels or isolated graben – horst structures. Formation of these groundwater systems, or their reactivation, is generally associated with extensional faulting of the accreted Australian continent, and subsequent subsidence during the Neoproterozoic, leading to the formation of the Centralian Superbasin (Walter *et al.*, 1995). This resulted in paleovalleys trending in an easterly or south-easterly direction towards the Eucla Basin. The occurrence of these drainage channels, representing topographic lows in the landscape, allowed incoming marine waters, during marine transgression events in the Eocene, to extend considerable distances into the Yilgarn Craton.

It has been hypothesised that the Eocene palaeodrainage channel hosting the MRUP represented a southern extension of the Carey Paleodrainage system, which effectively linked up with the Raeside Paleovalley to the south (Figure 2.11). Localised uplift along the south eastern margin of the Yilgarn Craton is considered to have terminated the south easterly trend of the Carey Paleovalley forcing it to its current position to the north and now coinciding with Lake Rason, approximately 150 km to the north of the MRUP. This uplift subsequently created the oxbow-shape of the now Narnoo Paleodrainage channel, which is connected to the Ponton Creek and the Raeside Paleodrainage system approximately 50 km south of the MRUP.

2.3.2 LOCAL

2.3.2.1 Palaeodrainage Channel

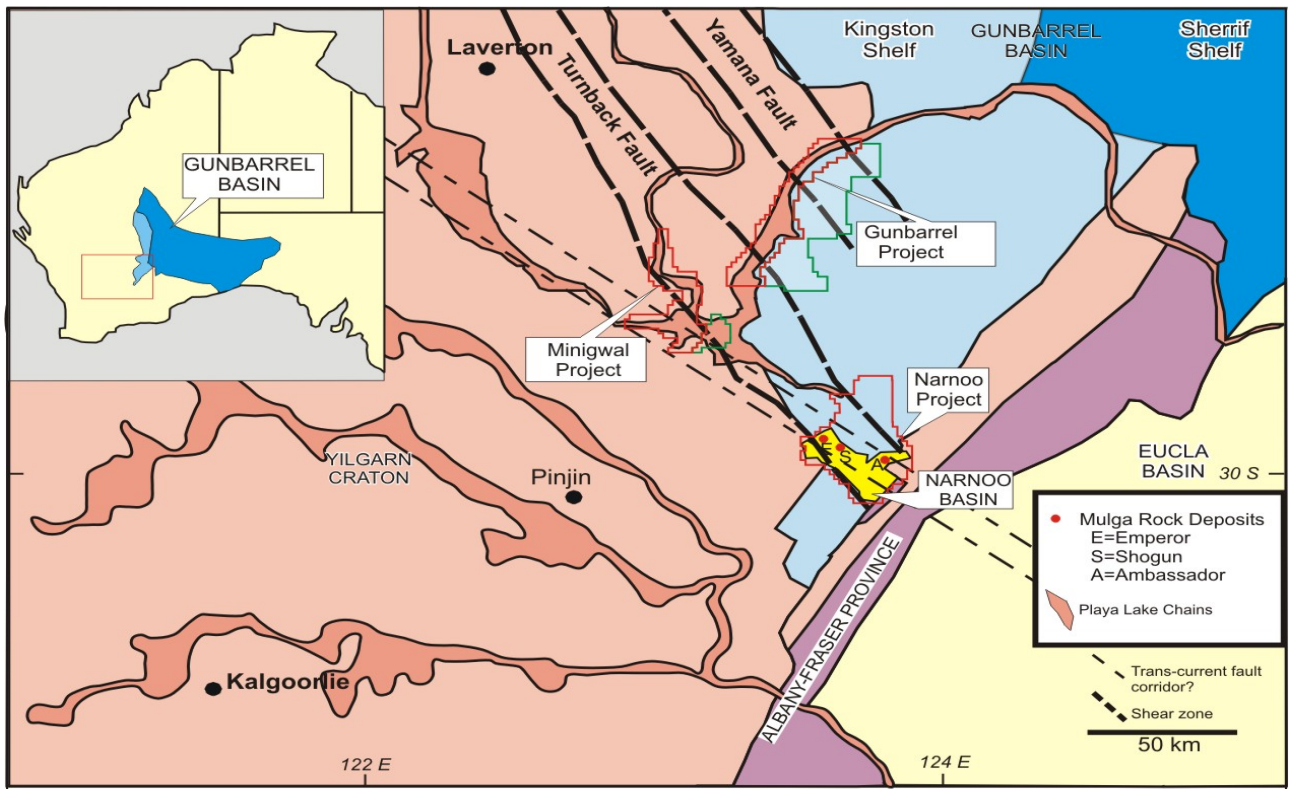
The hydrogeological condition within the palaeodrainage channel and that which will be intersected during mining and requiring dewatering, has been investigated by Rockwater (2015). It is important to note that the proposed mine pits will only extend 2 – 5 m below the phreatic surface (redox boundary), and thus the dewatering requirement is limited to this top portion of groundwater.

2.3.2.1.1 Groundwater Level

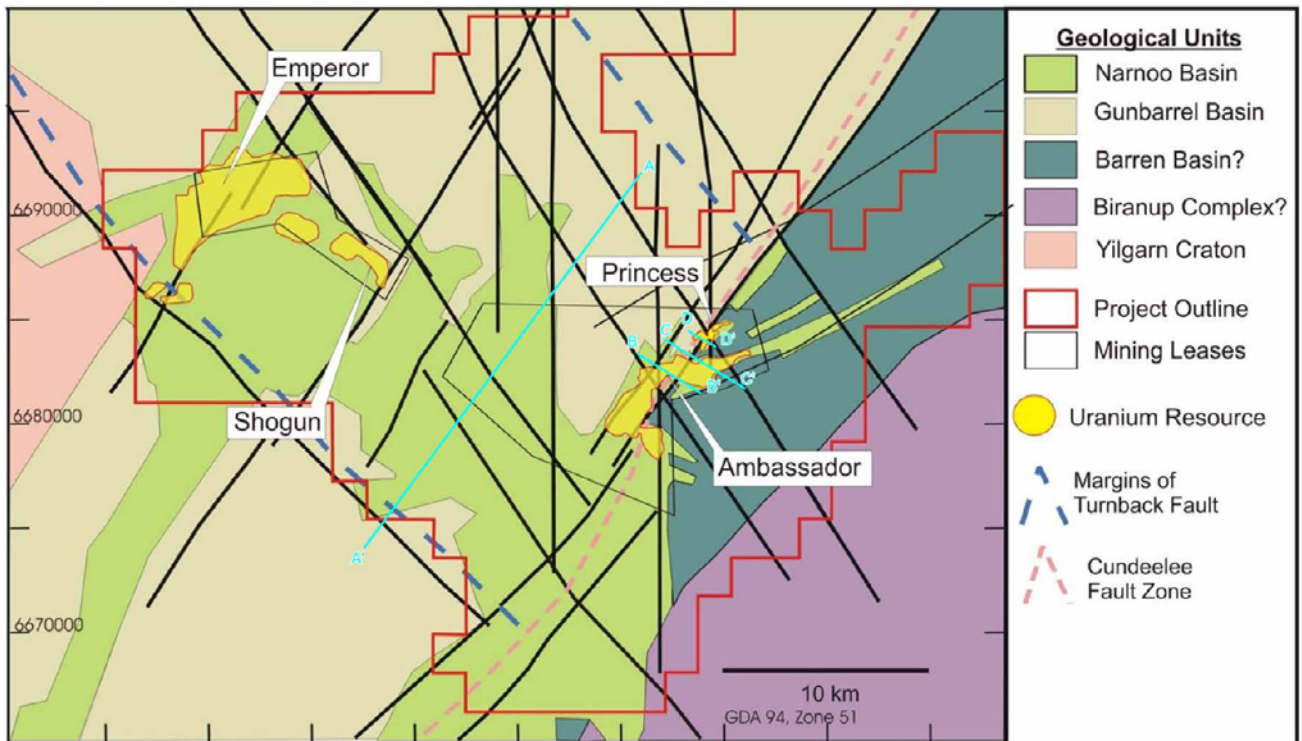
Groundwater levels within the palaeodrainage channel occur at between 38 – 40m below the surface at an elevation of approximately 290m AHD (Figure 2.12). Given the maximum depth of the palaeochannel is around 240m AHD (Figure 2.10), this results in a maximum groundwater thickness of around 50m. Groundwater (hydraulic) gradients within the palaeodrainage channel are very small (i.e. around 0.0022; Rockwater, 2015), and consequently groundwater movement through this system is very sluggish and to the south towards Ponton Creek.

Groundwater within the MRUP is generally restricted to the palaeodrainage channel and negligible flow or connection with the surrounding Cretaceous sediments occurs.

A)



B)



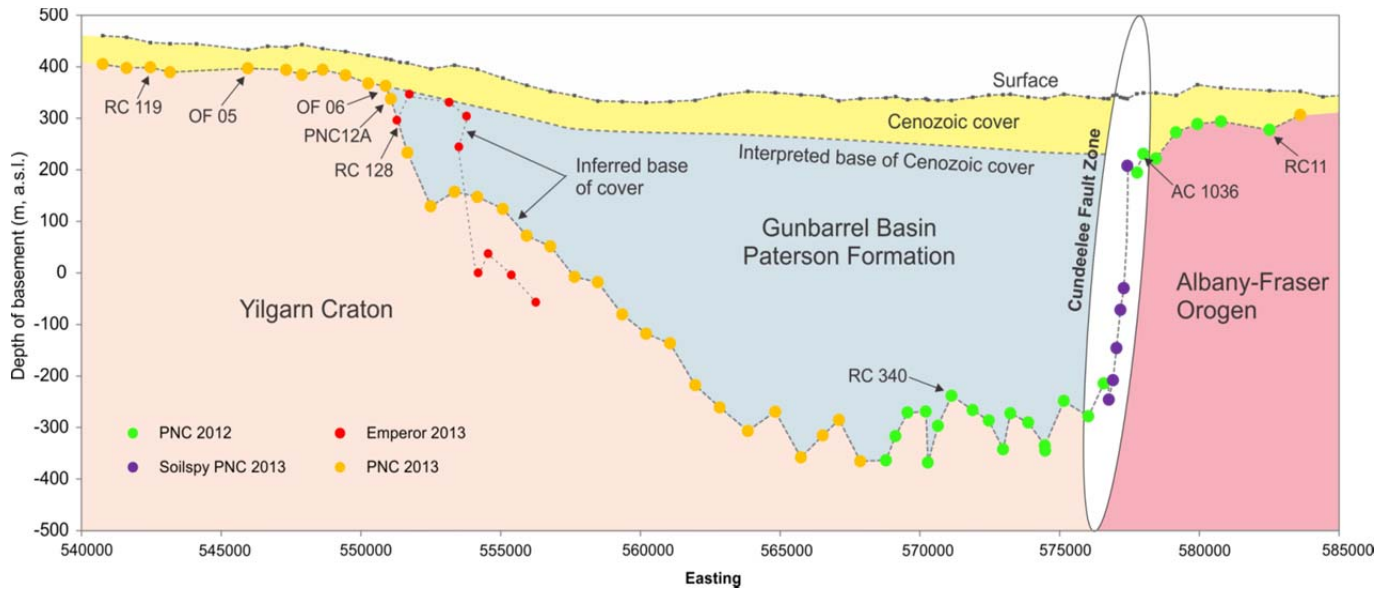
VIMY RESOURCES

TERRAIN ANALYSIS AND MATERIALS CHARACTERISATION FOR THE MULGA ROCK URANIUM PROJECT

Figure 2.6: Regional geology of A) south-eastern portion of the Yilgarn Craton, and B) Narnoo Basin showing location of MRUP



A)



B)

Seq.	AGE	Mulga Rock Graph log	Minon	EMA Unit	LITHOLOGY	
Upper Narnoo	L Pleistocene			Qa	Aeolian sand, orange-yellow. (<10 m, typically <3m)	
				Qb	Aeolian sand, red-brown. (<5 m) higher clay content	
	M Pleistocene			K	Sandstone, rare granulestone <5 m, limited distribution	
	Pliocene			J	Lithic diamicite, sandstone, calcrite and gypsum, <5m	
	Late Miocene			I	Lithic diamicite and conglomerate, rare claystone. Fe-rich. (<20m).	
Narnoo Basin	Early-Mid Miocene			H	Claystone, sandy clay, sandstone, local conglomerate at base. Red-brown with minor grey-green laminations. Very Fe-rich, some silcrete & calcrite. (<25 m).	
	Late Eocene			G2	Sandstone, VC-FG, well-sorted, fining-up (<5m). Glassy silcrete cap.	
				G1	Silt-sandstone, well-sorted. Many silcrete bands. Spicules in Kakarook area.	
	Mid-Late Eocene			F2c/Mc	Claystone, multi-coloured (green-red-brown; Emperor area only), or kaolinitic.	
				F2s	Sandstone, well-sorted or diamicite (Shogun area).	
	Mid-Late Eocene			F1c	Claystone, sandy, kaolinitic, overlying lenticular sandstone or diamicite	
				F1s	Claystone, carbonaceous, oxidised at top. (1-4 m)	
	Gunbarrel Basin	Mid-Late Eocene		U+BM	E3	Lignite, siltstone and carbonaceous claystone.
				BM-U	E2	Sandstone, very carbonaceous, fining-up (1-20m, typically <5m).
		Late-Mid Eocene		U-BM	Dcbc	Claystone; carbonaceous at base, oxidised at top. (1-4 m)
			-Au	Dcbs	Sandstone (carbonaceous), stacked packages fining-up to claystone, rare lignite and carb claystone (locally at base). (<30 m).	
				Dcblc	Claystone; carbonaceous-lignitic, limited distribution.	
				Dwsic	Claystone, grey, locally oxidised at top. (<15 m).	
				Dwsis	Sandstone, med-fine, fining up, well sorted. (<15 m)	
			U	Dwsc	Conglomerate. Ravinement deposit (<2 m).	
Late-Mid Eocene		U-Au	Dwsa	Conglomerate and sandstone, poorly sorted, fining and coarsening-up. Locally absent. (<20m).		
Gunbarrel Basin	Middle Cretaceous			C2c	Claystone. Bright white, locally micaceous (sericite?). (<10 m).	
				C2s	Sandstone/conglom, fining-up, very clayey, sericite clasts in Amb area. (<15 m)	
	Earliest Cretaceous			C1c	Siltstone grading to claystone. Black and carbonaceous where beneath water table, bright white when oxidised. (<20 m).	
				C1s	Sandstone, fining-up, very clayey. Carbonaceous where preserved beneath water-table. (<10m).	
	E Permian?			A5	SST, fine-grained (<100m?). Thickest mostly along eastern GB margin?	
Late Carboniferous			A4	Siltstone- very fine arkose, pyritic <500 m? Distributed in central and eastern NB Regions		
			A3	Carbonaceous shale, brown to blue-grey, <500m Thick? Grades into A4.		
Early-Prot?			A1-2	Diamicite and shale		
Archaean			Zn-Pb-Ag?	Barren Basin Meta-sediments		
				Basement	Yilgarn Craton Granite-Greenstone	

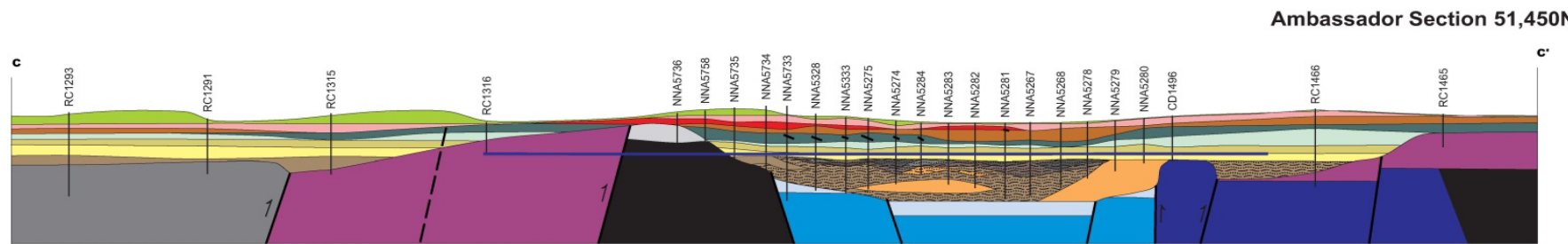
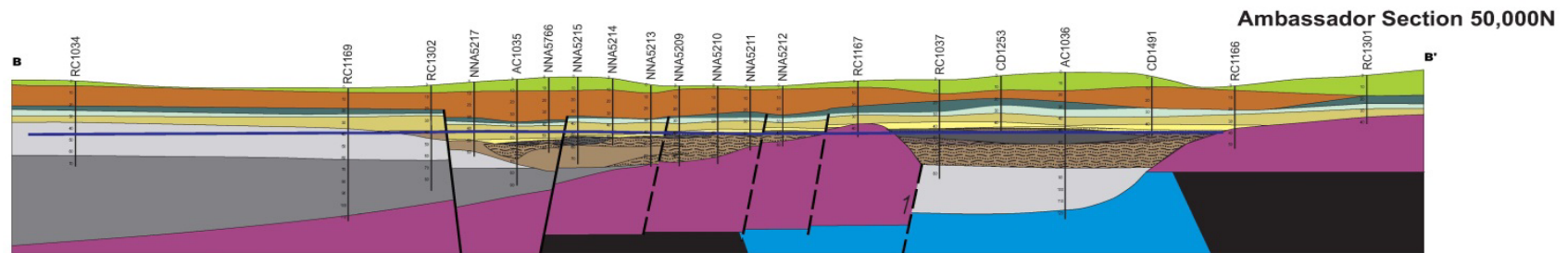
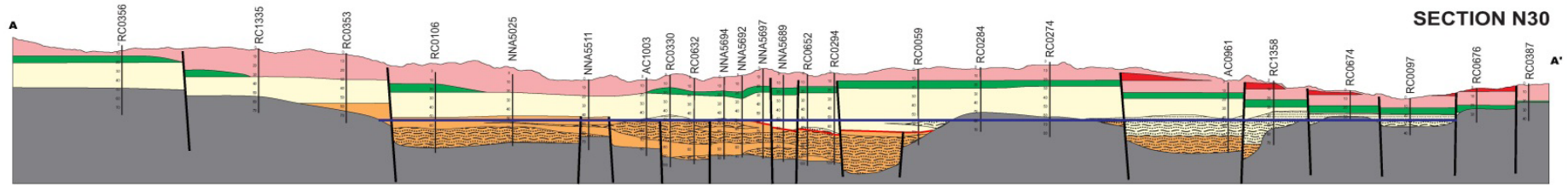
U = Uranium, BM = Ni, Co, Cu (and REE in Units E2-E3), Au = Gold

VIMY RESOURCES

TERRAIN ANALYSIS AND MATERIALS CHARACTERISATION FOR THE MULGA ROCK URANIUM PROJECT

Figure 2.7: A) Thickness and B) Stratigraphy of the Gunbarrel and Narnoo Basins





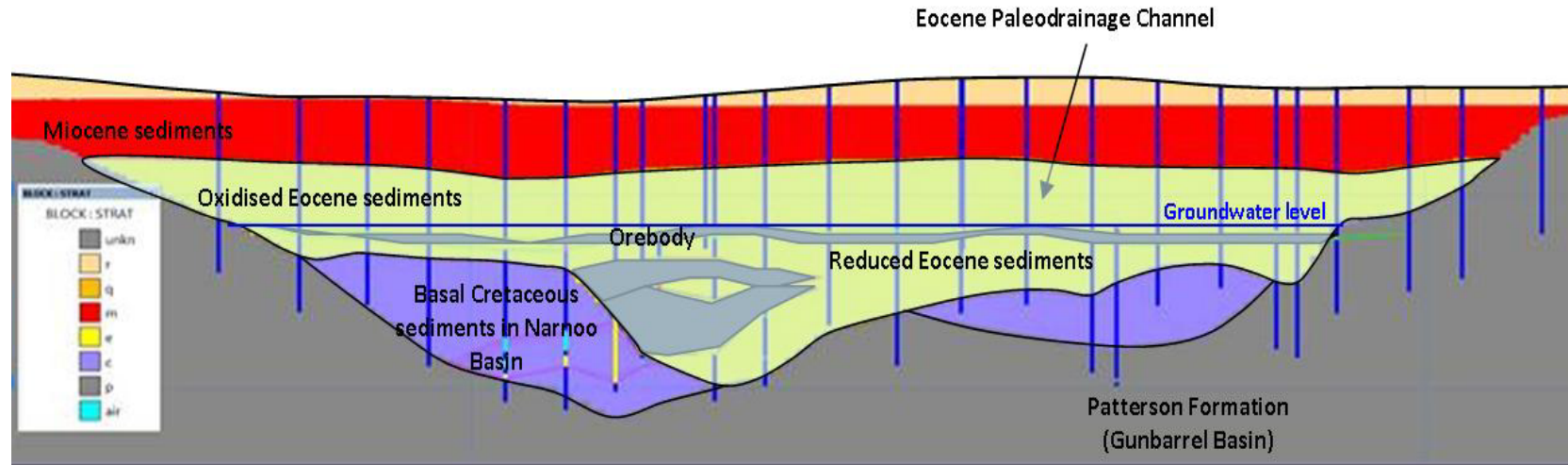
VIMY RESOURCES

TERRAIN ANALYSIS AND MATERIALS
CHARACTERISATION FOR THE MULGA ROCK URANIUM
PROJECT

Figure 2.8: Geological cross-sections through the MRUP (See Figure 2.6B for cross-section locations)



A)



B)

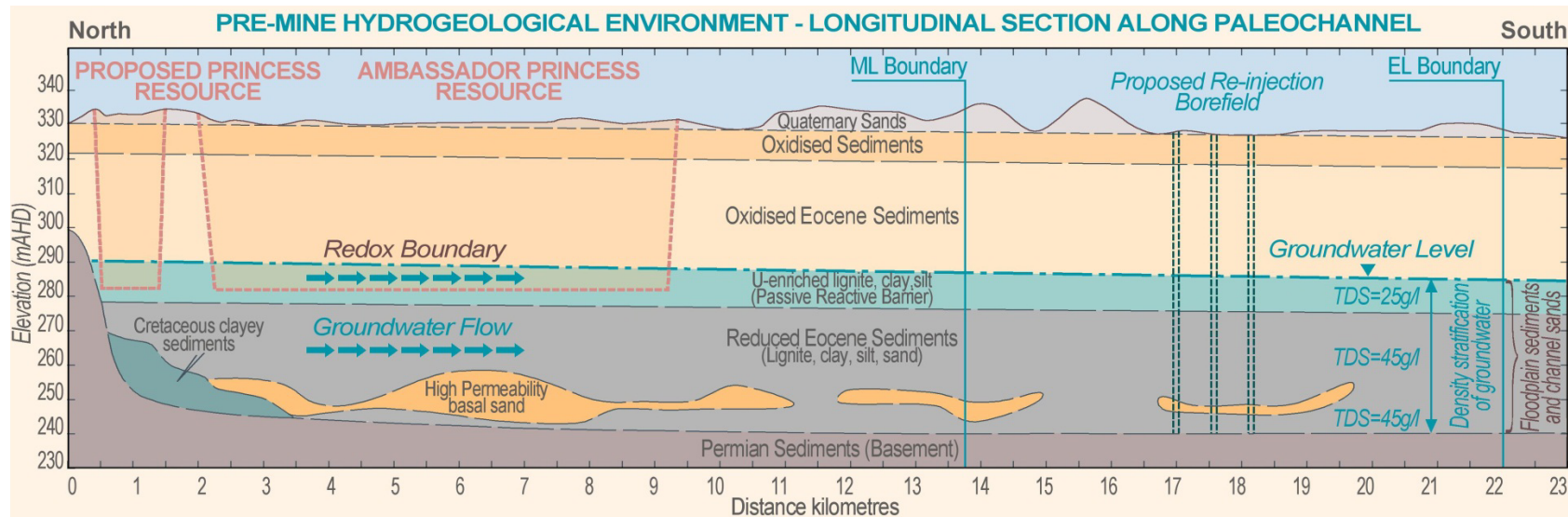
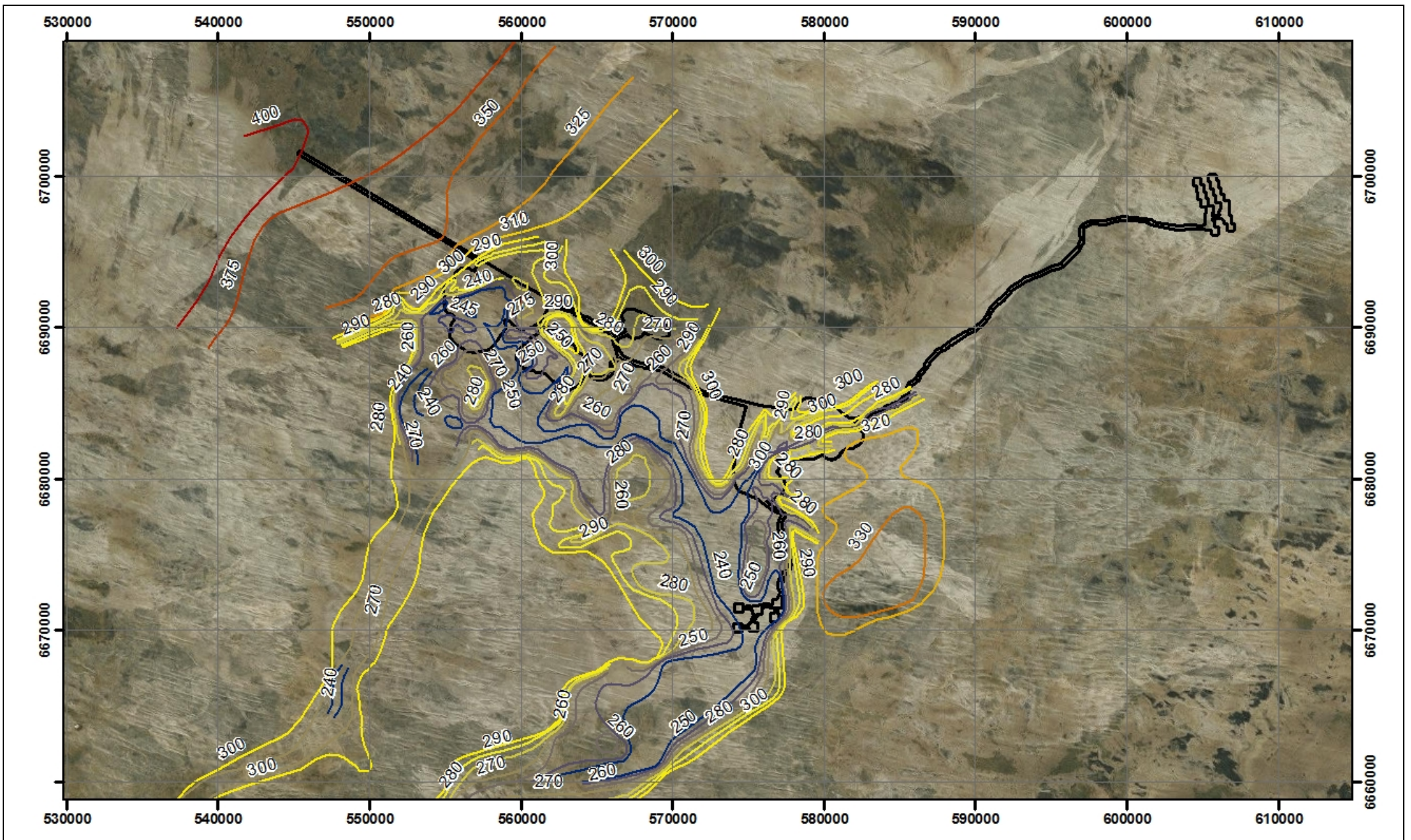


Figure 2.9: A) Eocene paleodrainage channel incised into the Narnoo Basin and B) Conceptual Hydrogeological Model for the MRUP

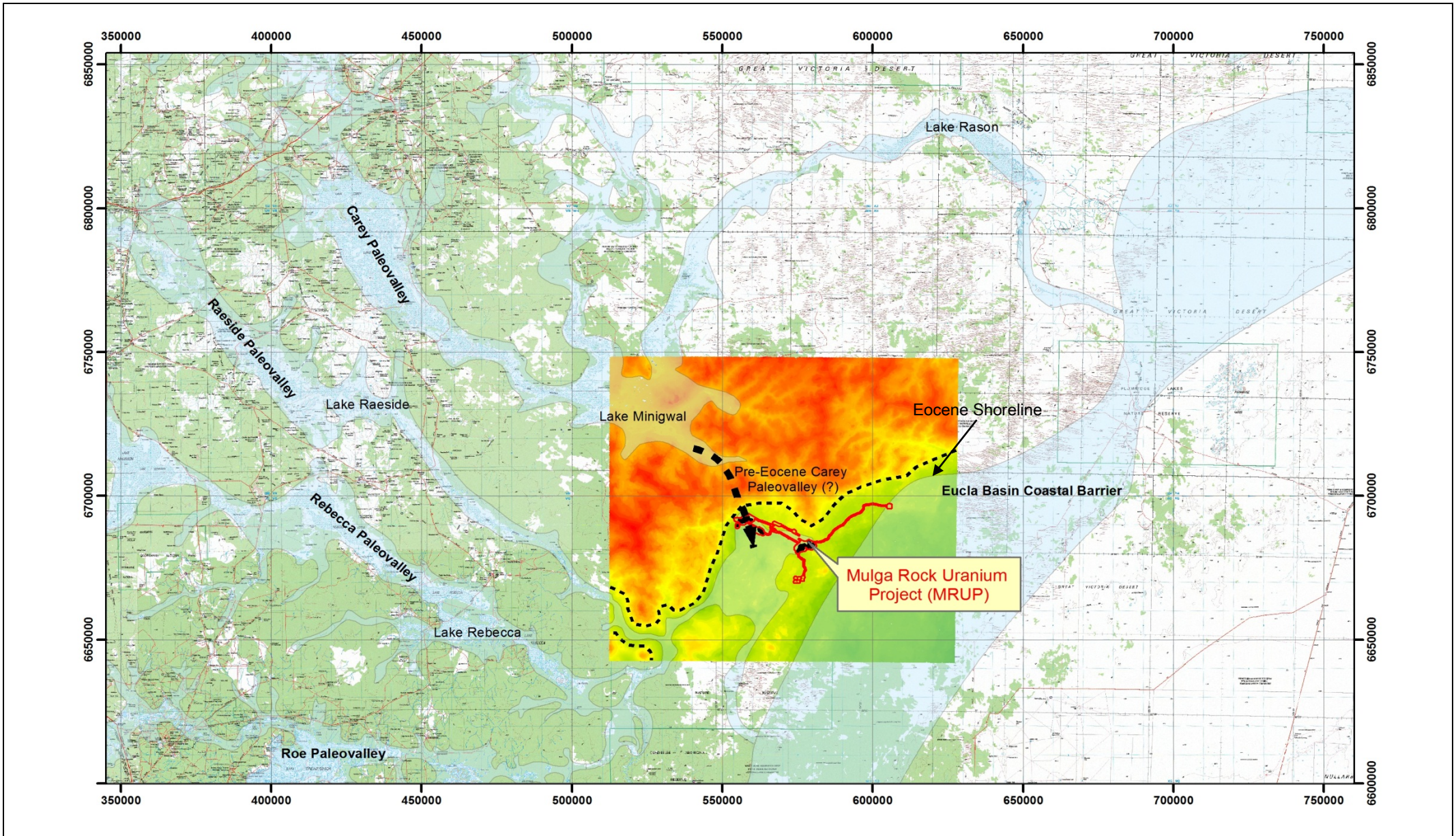


VIMY RESOURCES

TERRAIN ANALYSIS AND MATERIALS CHARACTERISATION
FOR THE MULGA ROCK URANIUM PROJECT

Figure 2.10: Basement depth of the paleodrainage channel within the MRUP



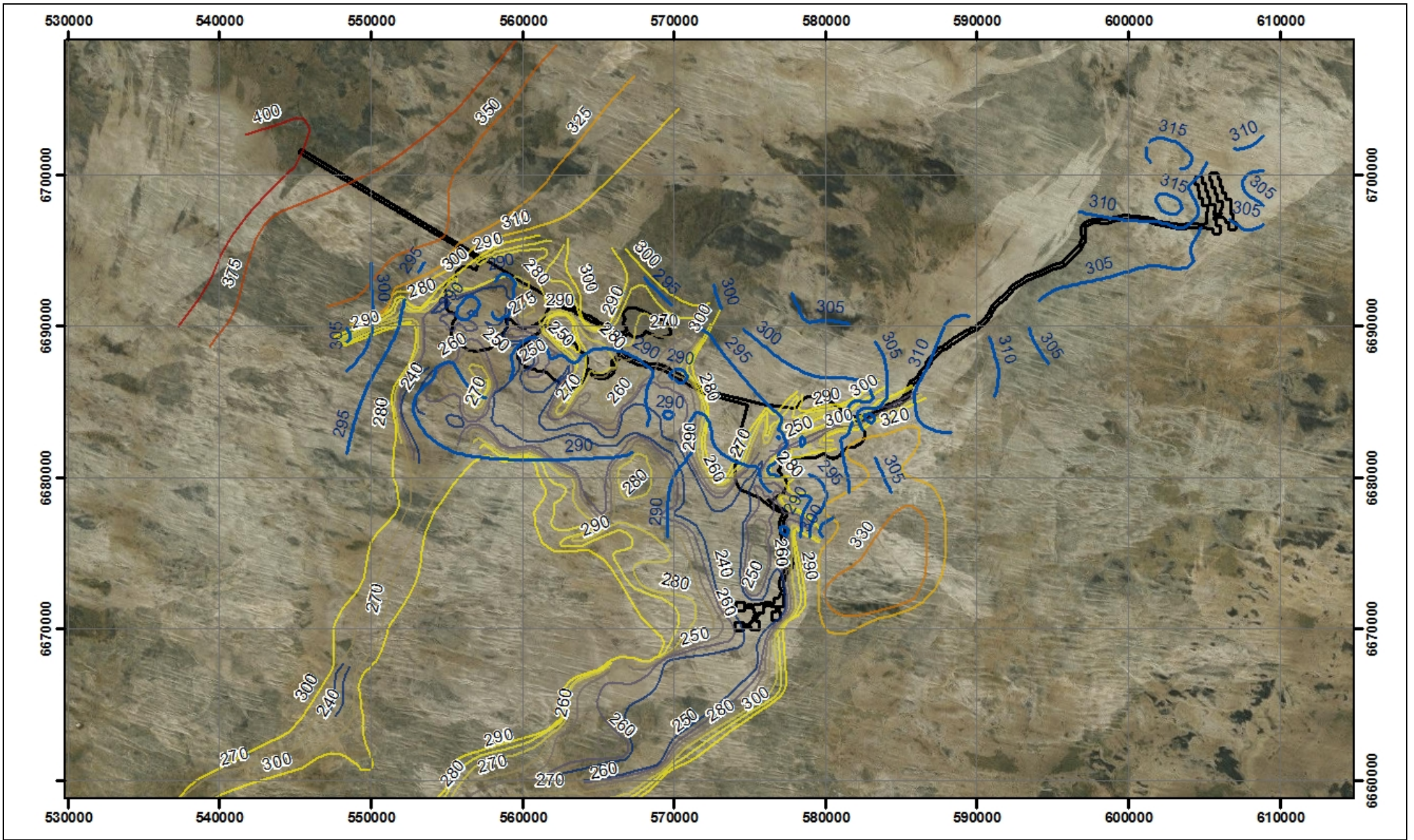


VIMY RESOURCES

TERRAIN ANALYSIS AND MATERIALS
CHARACTERISATION FOR THE MULGA ROCK URANIUM
PROJECT

Figure 2.11: Location of the MRUP in relation to the paleovalleys draining the southeastern portion of the Yilgarn Craton





VIMY RESOURCES

TERRAIN ANALYSIS AND MATERIALS CHARACTERISATION
FOR THE MULGA ROCK URANIUM PROJECT

Figure 2.12: Groundwater levels (blue lines) within the Narnoo Paleodrainage System

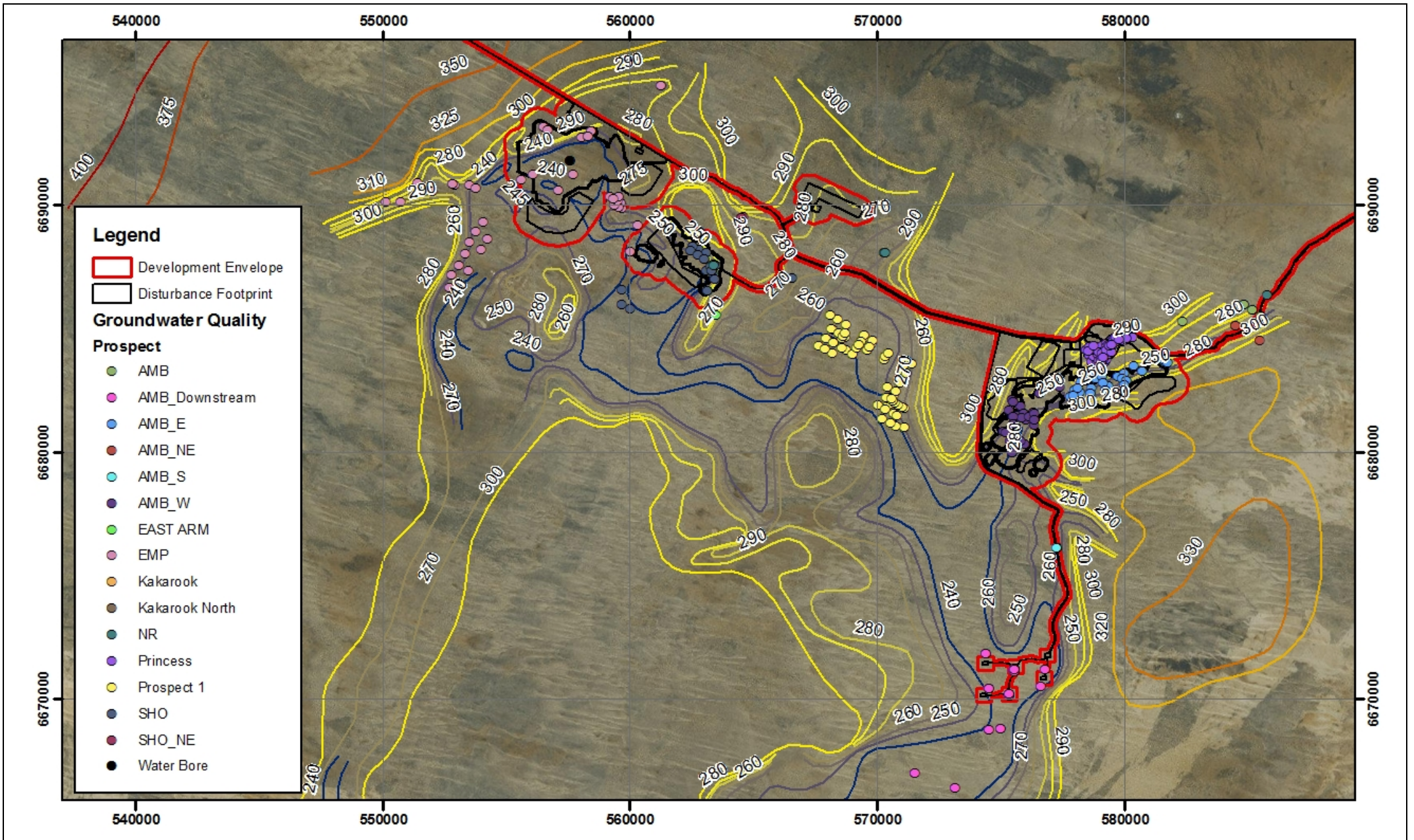


2.3.2.1.2 Groundwater Quality

At the MRUP groundwater quality and its spatial distribution has been measured from 495 geological drillholes (Figure 2.13). A summary of groundwater quality data from these drillholes is provided in Table 2.3. Groundwater within the Narnoo paleodrainage channel is classified as moderately to strongly acidic, with an average pH of 4.91; however pH values up to 8.05 (i.e. moderately alkaline) occur indicating the complexity of the groundwater system. The groundwater is moderately saline to hypersaline, with Total Dissolved Solids (TDS) averaging varying 41,846 mg/L, but salinities up to 146,900 have been recorded. The aquifer is a NaCl-type, with elevated levels of Cd, Co, Cu, Ni, Pb and Zn.

Table 2.3: Summary of groundwater quality from the Narnoo paleodrainage channel

Parameter	Maximum	Average	Parameter	Maximum	Average
pH	8.05	4.91	Mg (mg/L)	3995	1368
TDS (mg/L)	146900	41846	Mn (mg/L)	3.10	0.94
ORP_Field	335	100	Mo (mg/L)	0.035	0.018
Cl (mg/L)	75620	23945	Na (mg/L)	45000	14098
F (mg/L)	0.8	0.5	Ni (mg/L)	3.80	0.29
Al (mg/L)	2	0.9	Pb (mg/L)	3.10	0.15
As (mg/L)	0.03	0.03	Sb (mg/L)	0.015	0.010
Ba (mg/L)	0.155	0.045	Se (mg/L)	0.100	0.039
Be (mg/L)	0.02	0.013	Si (mg/L)	53	16
Ca (mg/L)	1185	483	Sr (mg/L)	11.80	6.62
Cd (mg/L)	0.319	0.034	Th (mg/L)	10.00	1.00
Co (mg/L)	4.00	0.47	Tl (mg/L)	0.0005	0.0005
Cr (mg/L)	0.077	0.015	U (mg/L)	0.068	0.02
Cu (mg/L)	2.800	0.372	V (mg/L)	0.009	0.005
Fe (mg/L)	190	17	Zn (mg/L)	13.00	0.96
K (mg/L)	935	362			



VIMY RESOURCES

TERRAIN ANALYSIS AND MATERIALS CHARACTERISATION FOR
THE MULGA ROCK URANIUM PROJECT

Figure 2.13: Groundwater quality observation locations



2.4 GEOMORPHOLOGY – TERRAIN ANALYSIS

The land surface within the vicinity of the MRUP is dominated by regions comprising irregularly-spaced sand dunes, with small inter-dunal topographic depressions (Plate 2.2), and broad alluvial plains (Plate 2.3). This sequence is clearly highlighted in the modified Total Dose Radiometric data shown in Figure 2.14. The dunes are not uniformly spread across the MRUP landsurface, and instead are concentrated within localised regions, interspersed by large relatively flat alluvial plains (Figure 2.14).

Given the importance of the aeolian sand dunes to the characteristic of the Great Victoria Desert and Yellow Sand Plain (YSP), of which the MRUP forms a part of, a more detailed investigation was undertaken to characterise the 'form' or the different 'types' of dunes present within the MRUP. For this purpose detailed aerial LiDAR elevation data was used to create a detailed digital elevation model (DEM) of the MRUP area and, subsequently, to identify the range of different dunal formations across the East and West project areas. The following primary dune types were identified within the MRUP:

- Linear (or Longitudinal) Dunes (Figure 2.15a): A dune with its crest running parallel to the direction of the prevailing wind (Clark, 1998). Linear dunes are the most abundant desert dune forms globally and, in Australia, linear dunes occupy approximately one-third of the continental land surface (Fitzsimmons, 2007);
- Barchan Dunes (Figure 2.15b): A crescent-shaped dune formed when the direction of the wind varies only very slightly or not at all. The windward side is convex, with a gentle slope, the steeper leeward side is concave, and the 'horns' point downwind. It occurs singly, or in groups. Height can range from quite low to over 30 m. (Clark, 1998);
- Parabolic Dunes (Figure 2.15c): A crescent-shaped dune. The windward side is concave and gently-sloping, with a steep face downwind. These dunes are found particularly on sandy shores and plateaus inland where sudden wind eddies and blowouts whisk away the central part of the dune and carry it downwind. (Clark, 1998); and
- Complex/Irregular dune shapes (Figure 2.15d): A number of closely-spaced dune formations were present that were not easily classified. The dunes have likely formed within more complex wind eddies, characteristic of their setting within the landscape or close proximity other dune formations.

In order to assess the specific geometry of the dunes, 30 elevation cross-sections were extracted from the DEM, resulting in a range of dune profiles of approximately 5 m horizontal resolution. The location of the cross-sections is shown on Figure 2.16, and the 30 cross-sectional elevation profiles are provided in Figure 2.17 to Figure 2.20, organised by dune type:

- Figure 2.17: Linear Dunes;
- Figure 2.18: Barchan Dunes;
- Figure 2.19: Parabolic Dunes; and
- Figure 2.20: Complex/Irregular Dunes

In general, the dune morphology indicates that the prevailing wind direction, during dune formation, was most likely from the West or West-North-West. This is further supported by particle size distribution data presented in Section 4.5.2. This is in contrast to the present-day prevailing wind direction, which is from an East or South-Easterly direction, and is evidenced by:

- A more gradual slope on the western edge of nearly all of the dunes, combined with a steeper slope on the eastern edge;

- The orientation of the Barchan and Parabolic dune types is in a predominately West or West-North-West direction; and
- The symmetrical cross-sectional shape of the Linear dunes indicates they were formed parallel to the wind direction, and they are generally orientated in a West or West-North-West direction

Dune heights were variable across the MRUP, ranging up to approximately 30 m above the adjacent inter-dunal areas. Linear dunes were found to be the most common dune type regionally, but these were typically lower-lying than other dune types, at approximately 10 m in height. Parabolic dunes were also found to be common across the region, and these were typically 15-20 m in height at the crest. Barchan Dunes were also found to be typically 15-20 m in height, but were far less common than the other dune types.

Dunes in this region are generally considered to be non-active (i.e. fixed), and abundant plant growth exists. The results of the soils works clearly show that dunal species have large singular taproots which effectively 'anchor' the dunes, whilst the surface of the dunes is stabilised by a defined cryptogam cover which occurs over most of the landforms within the MRUP. The shape of the dunes is therefore not expected to be majorly affected by the present day wind direction, which is generally from an East or South-Easterly direction.

Landsurface cross sections for each of the four deposits to be mined at the MRUP are provided in Figure 2.21 to Figure 2.25.

The dunes with the MRUP were deposited by aeolian processes directly onto either a truncated post-Miocene surface or a contemporaneous Miocene surface. Evidence for this deposit onto a pre-existing surface is clearly evident within the inter-dunal topographic depressions, whereby the soil profile in these areas is continuous underneath the dunes. Further discussed in Section 4.1, directly underlying the aeolian dunes is an approximately 1 m thick reddish brown loam. This loam was either deposited directly onto an existing calcrete surface, which is often outcropping in these topographic lows, or forms the upper pedogenic horizon of the calcrete layer. There is clear evidence from the morphology of the calcrete layer that it has experienced a complex, protracted history, with it varying from a relatively thin (i.e. < 1 m thick) poorly consolidated (and potentially forming today) to a thick (often up to 4 m in thickness) consolidated layer, comprising transported well-rounded calcrete pisoliths (gravels). The calcrete is uniform and consistent across the entire MRUP. The calcrete layer has formed on top of the Miocene sediments and therefore its basal surface represents the top of the Miocene surface.

Based on the above understanding, and from the landscape cross-sections provided in Figure 2.21 to Figure 2.25, the basal surface elevation for the dunes or the top of the loam/calcrete surface is set as follows:

- Emperor Deposit: 316 – 317 m AHD
- Shogun Deposit: 316 m AHD
- Ambassador West: 324 m AHD in the south to 330 m AHD in the north (i.e. the existing land and underlying Miocene surfaces gently slope to the south at an angle of approximately 0.1° or 0.2%)
- Ambassador East: 330 m AHD in the south to 335 m AHD in the north (i.e. the existing land and underlying Miocene surfaces gently slope to the south at an angle of approximately 0.1° or 0.2%)
- Princess: 338 m AHD

Based on the above elevations, the current landsurface and the previous Miocene (and potentially Eocene) landsurface gently slope down the two arms of the paleodrainage channel.

Plate 2.2: Dunal surface with repeating sand dunes and localised interdunal topographic depressions

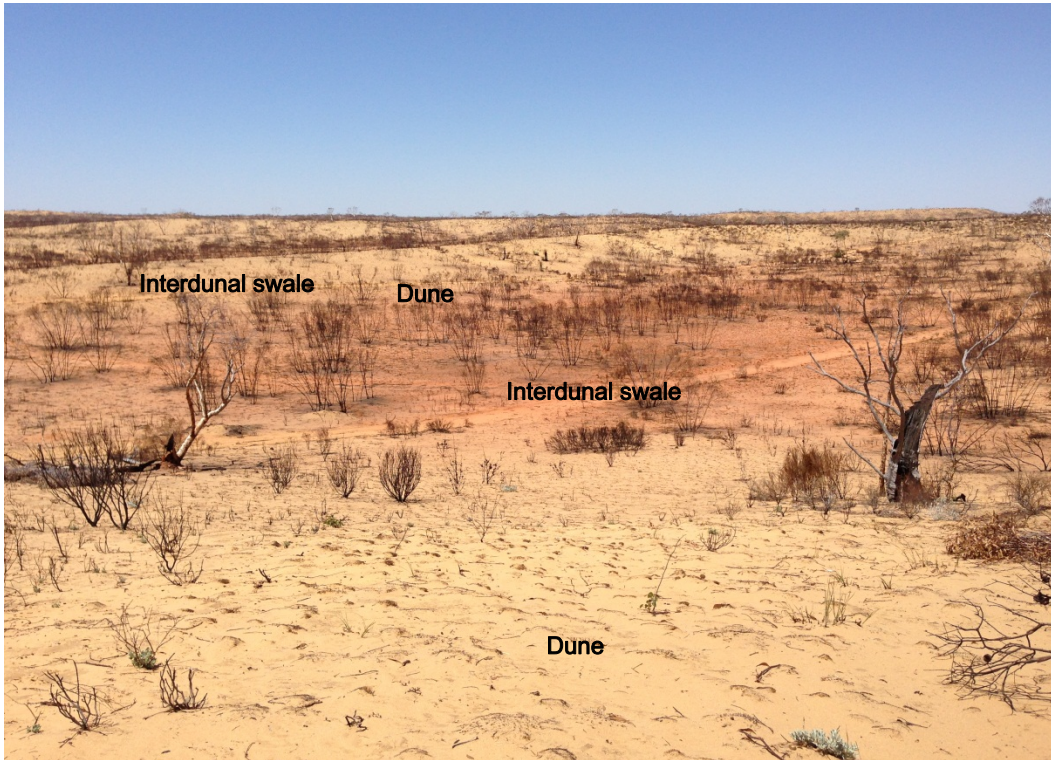
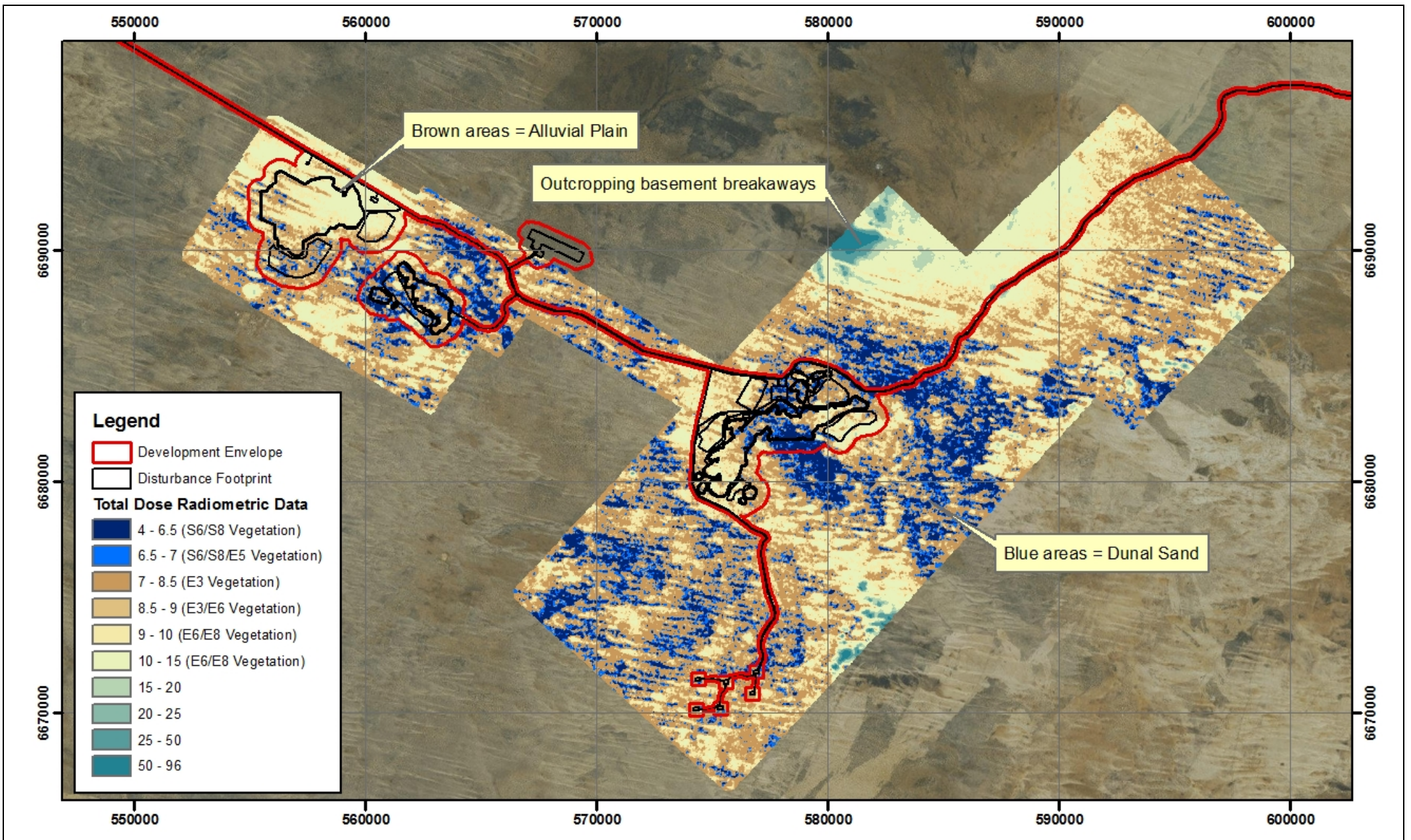


Plate 2.3: Broad alluvial plain



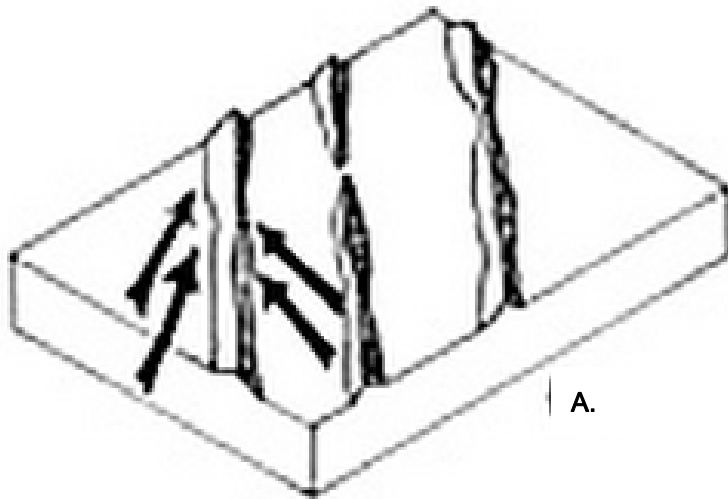


VIMY RESOURCES

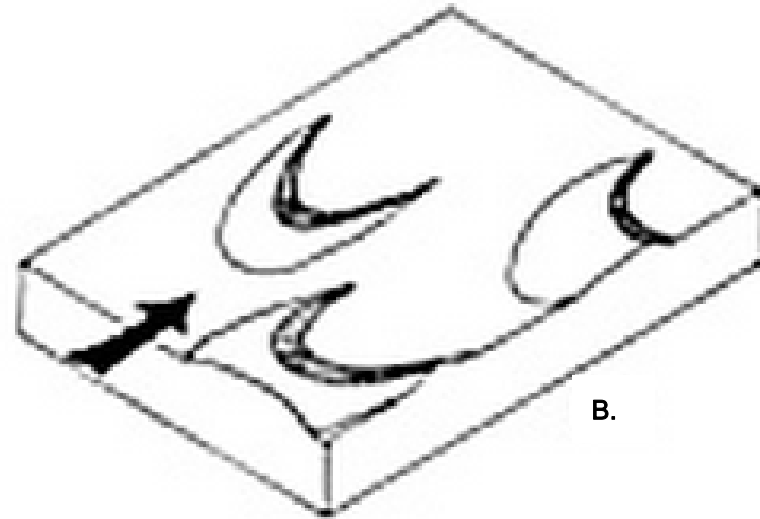
TERRAIN ANALYSIS AND MATERIALS CHARACTERISATION
FOR THE MULGA ROCK URANIUM PROJECT

Figure 2.14: Regional landforms within the MRUP

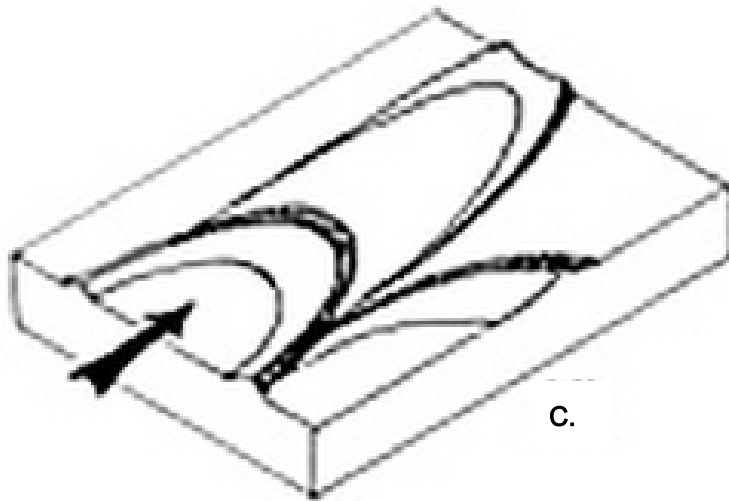




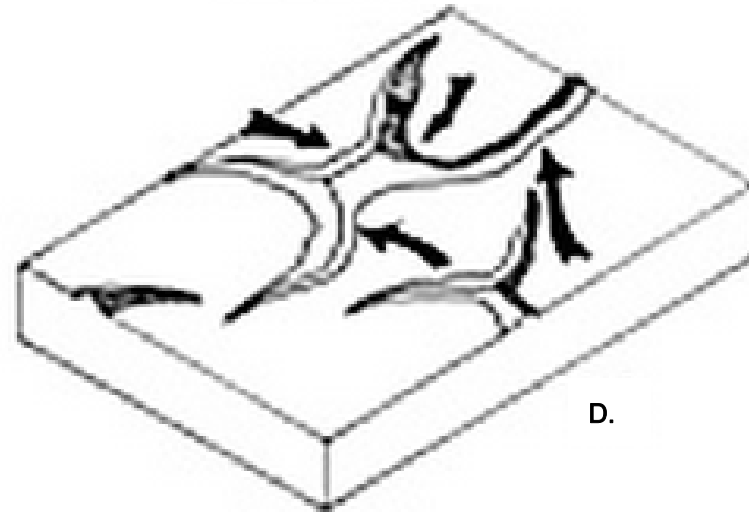
A.



B.



C.



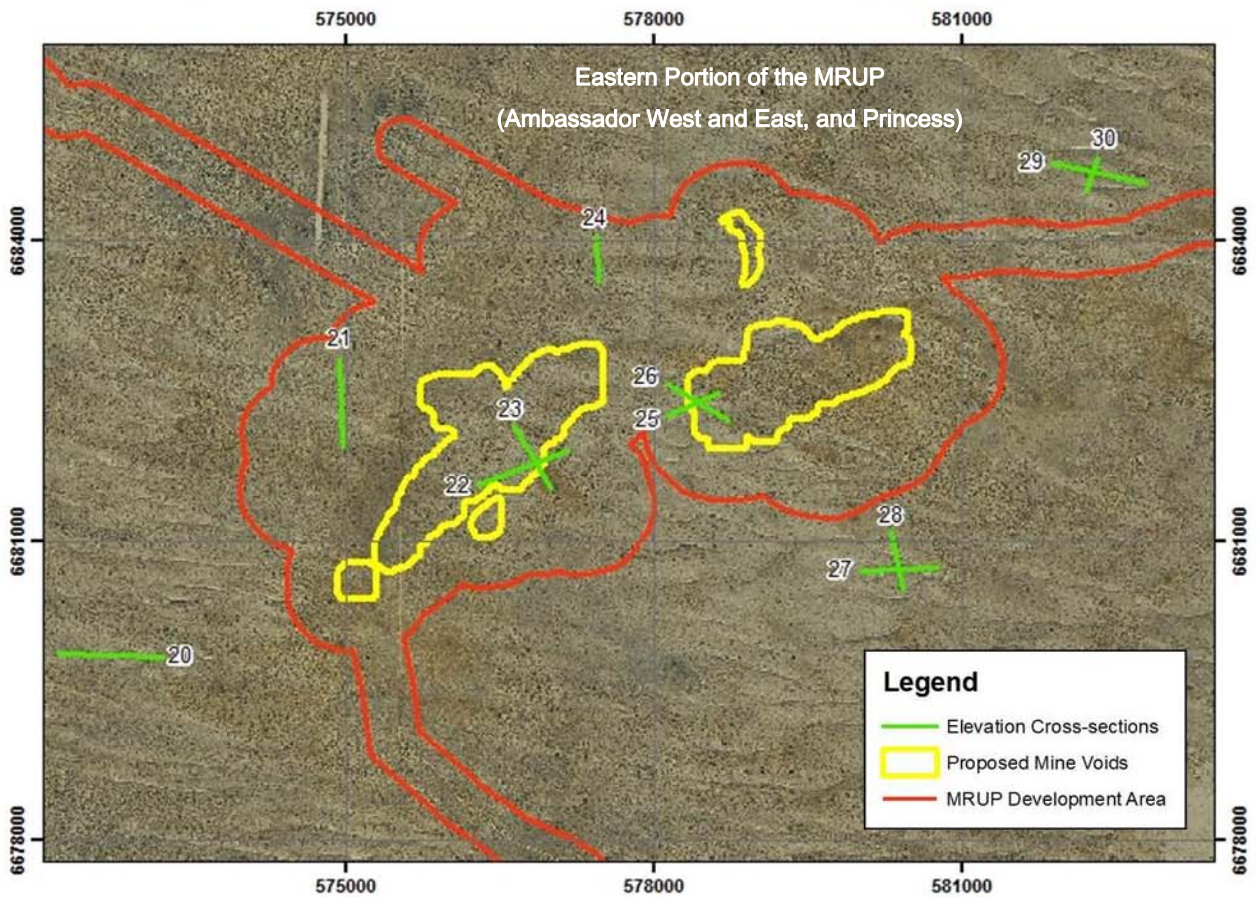
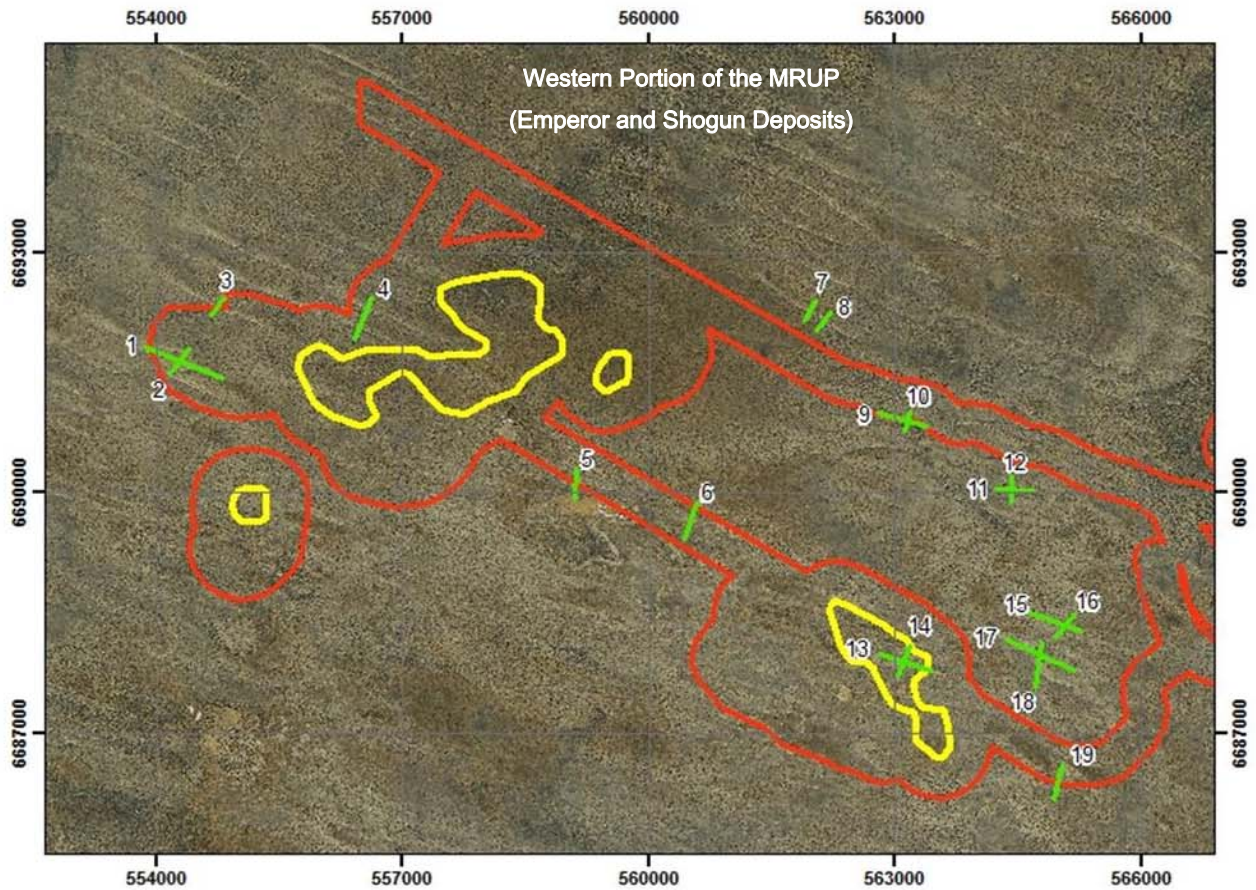
D.

VIMY RESOURCES

TERRAIN ANALYSIS AND MATERIALS
CHARACTERISATION FOR THE MULGA ROCK URANIUM
PROJECT

Figure 2.15: Primary dune formations identified near the Mulga Rocks Project: (A) Linear Dunes, (B) Barchan Dunes, (C) Parabolic Dunes, and (C) Complex/Irregular Dunes. Adapted from Short (2010).



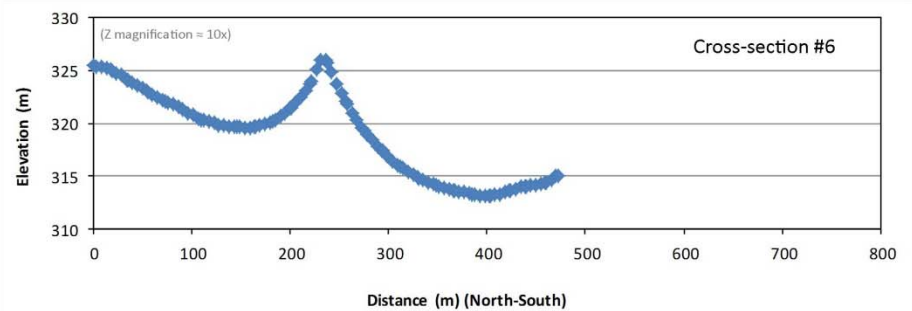
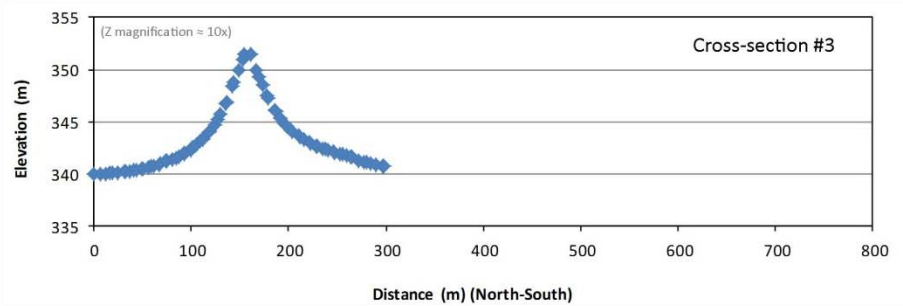
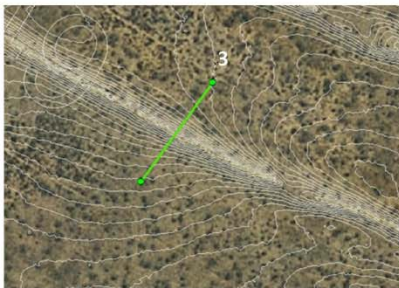
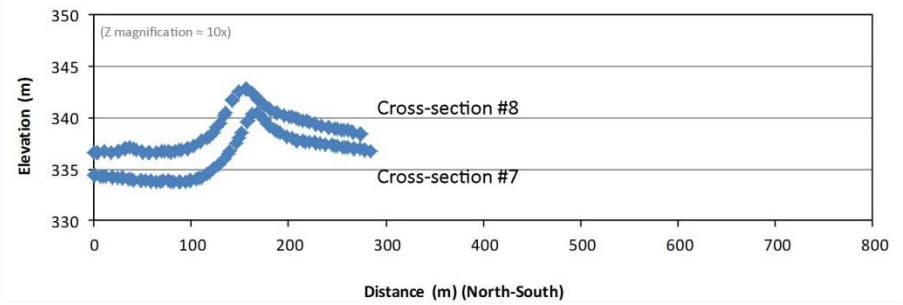
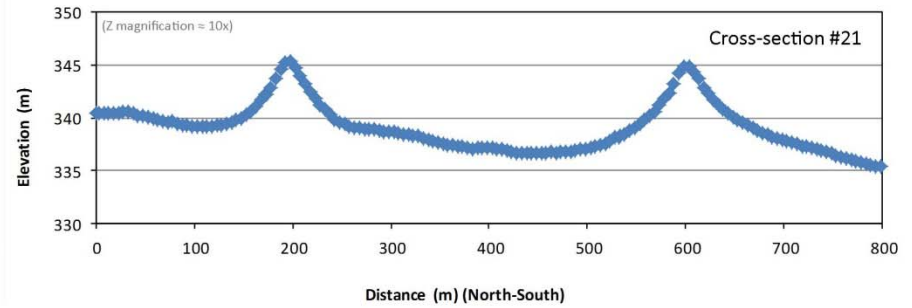
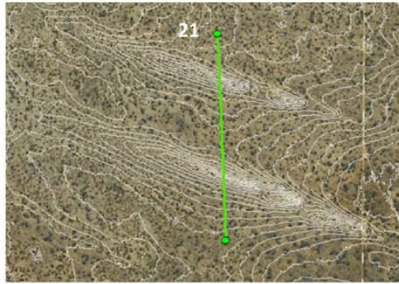
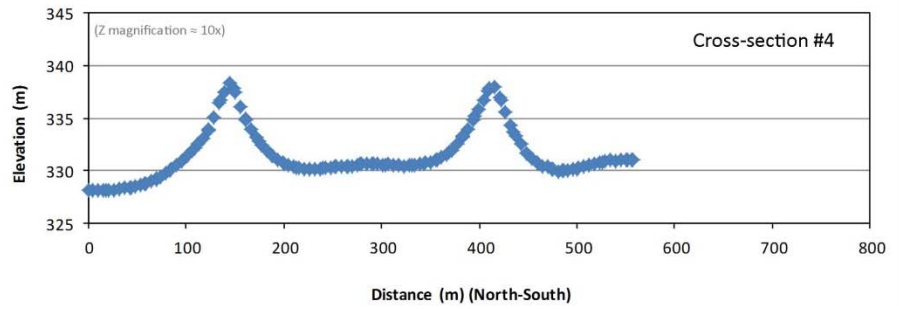
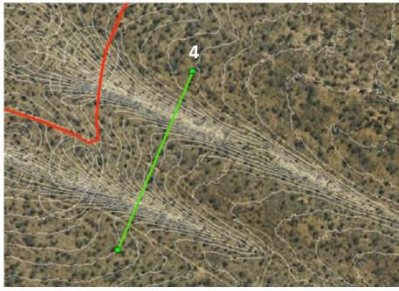


VIMY RESOURCES

TERRAIN ANALYSIS AND MATERIALS
CHARACTERISATION FOR THE MULGA ROCK
URANIUM PROJECT

Figure 2.16: Location of landsurface cross-sections



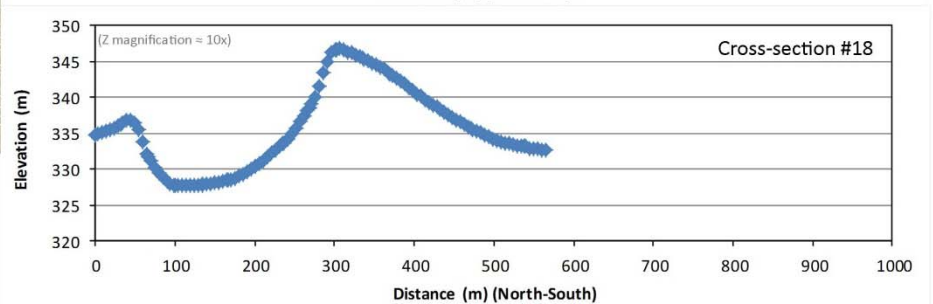
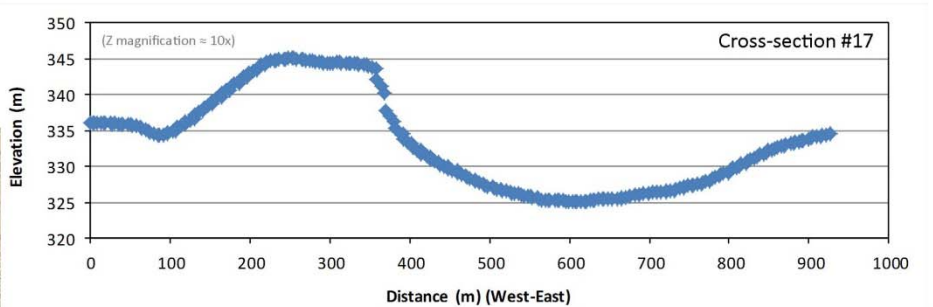
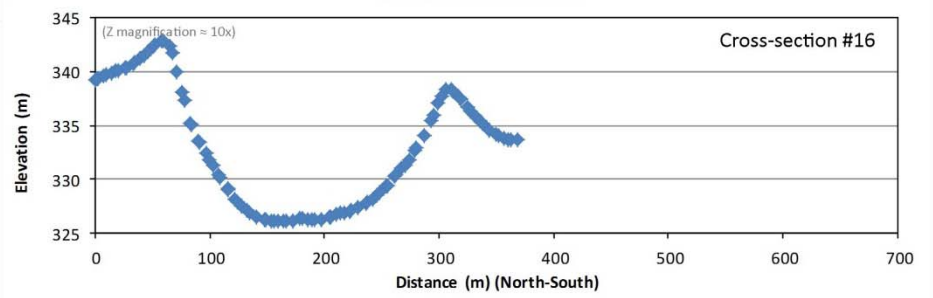
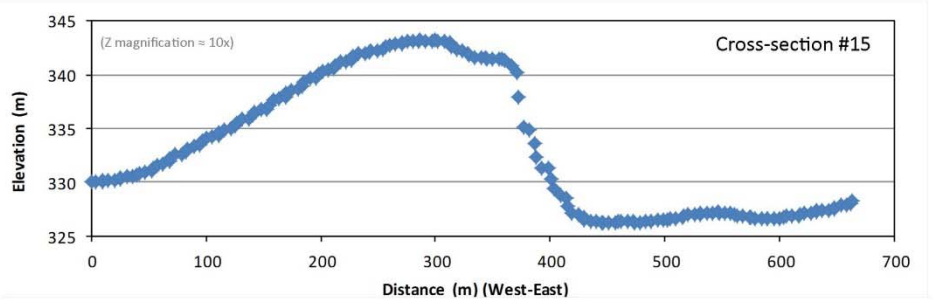
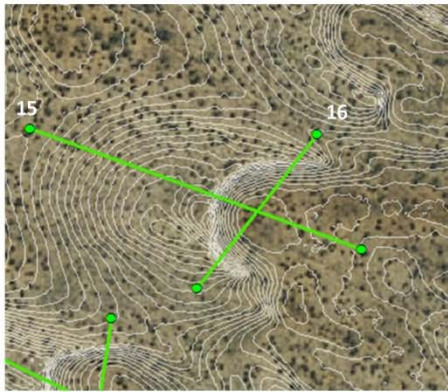


VIMY RESOURCES

TERRAIN ANALYSIS AND MATERIALS CHARACTERISATION FOR THE MULGA ROCK URANIUM PROJECT

Figure 2.17: Characteristic linear dunes within the MRUP



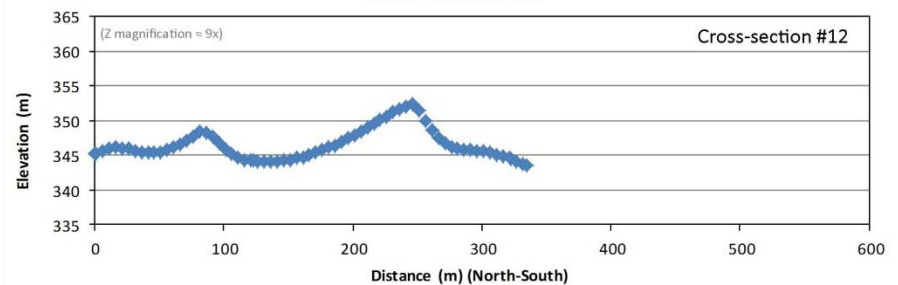
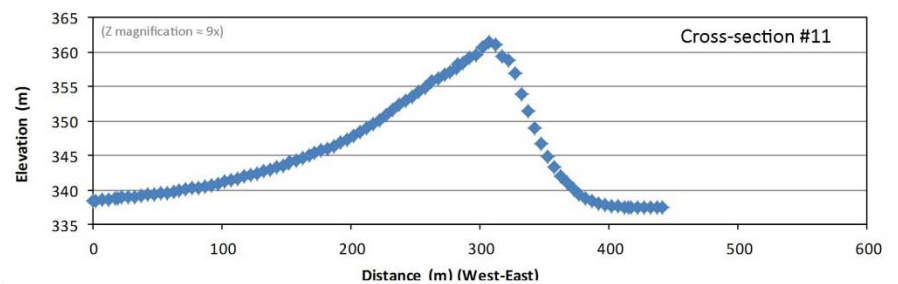
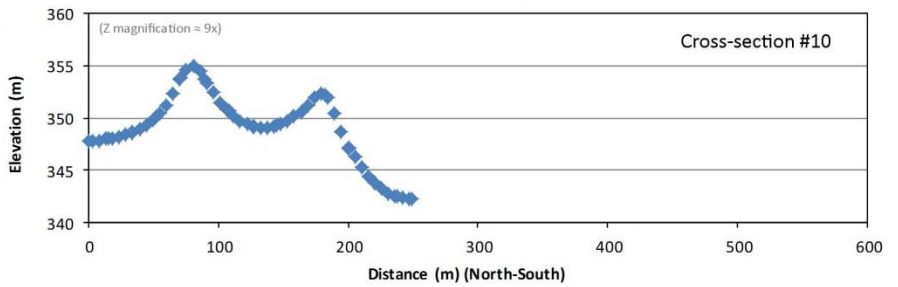
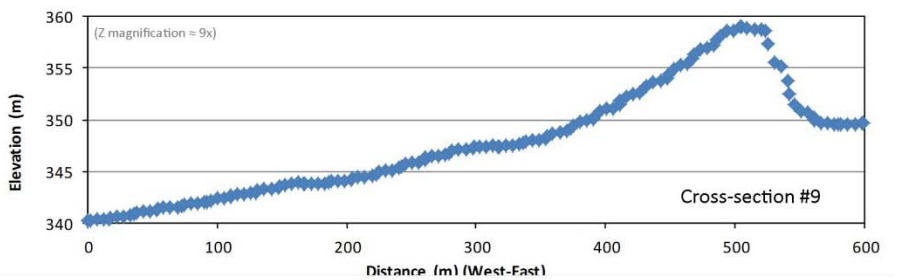
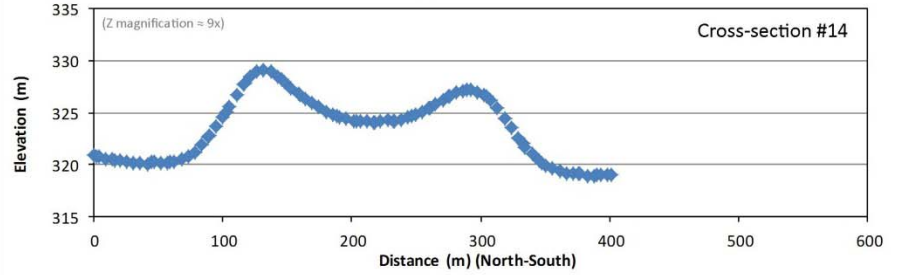
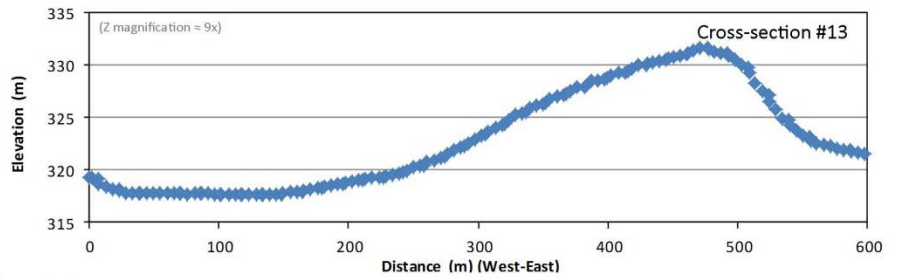


VIMY RESOURCES

TERRAIN ANALYSIS AND MATERIALS CHARACTERISATION FOR THE MULGA ROCK URANIUM PROJECT

Figure 2.18: Characteristic barchan dunes within the MRUP



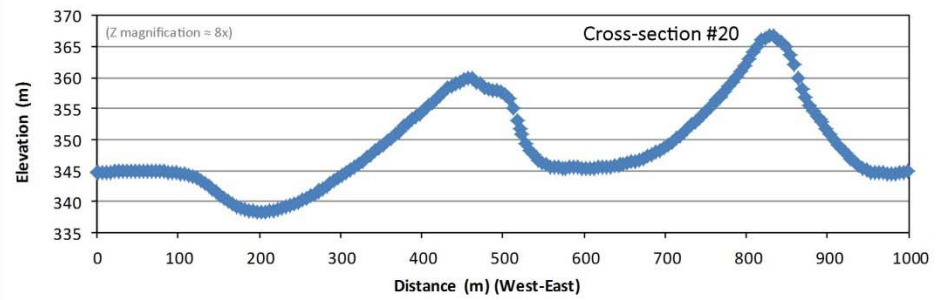
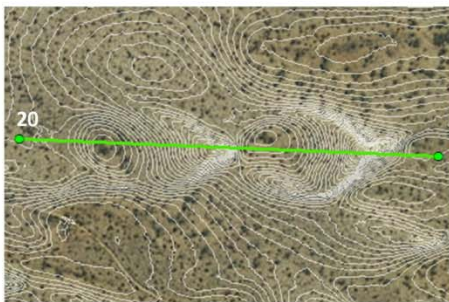
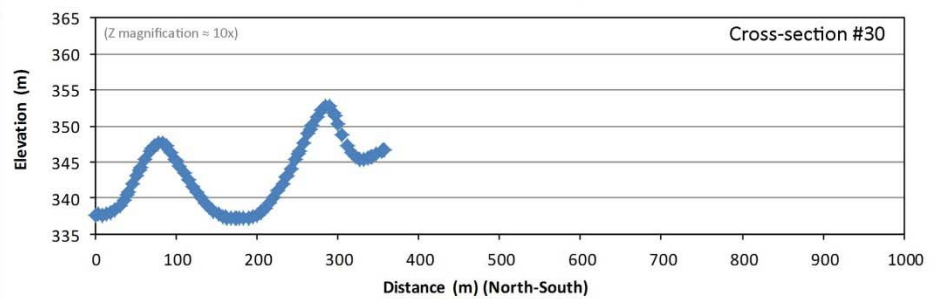
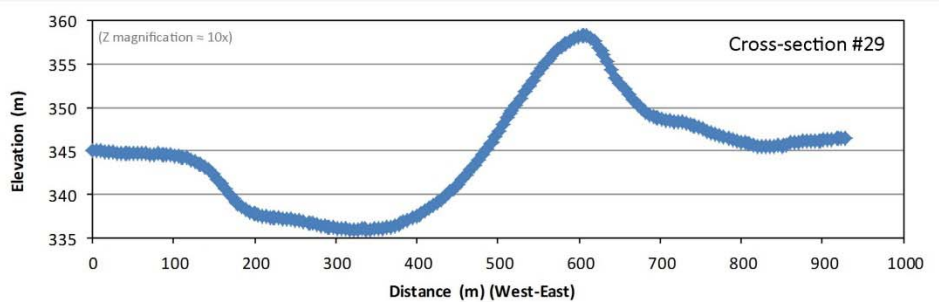
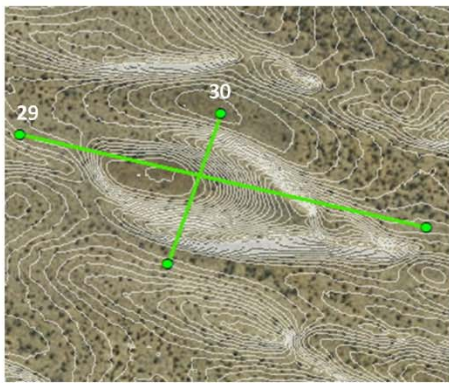
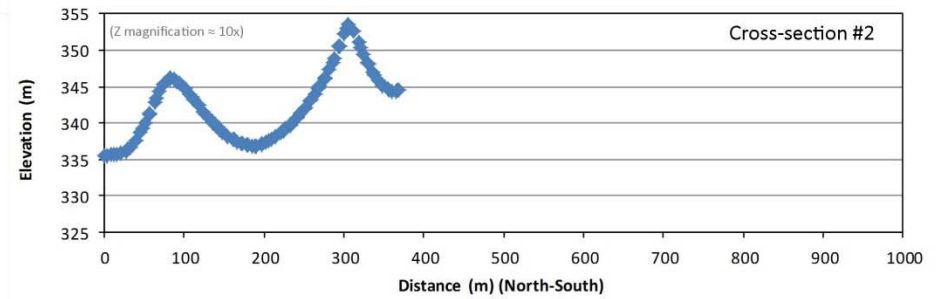
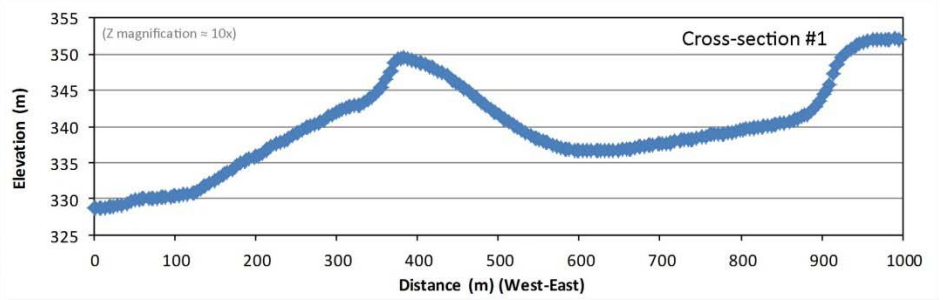
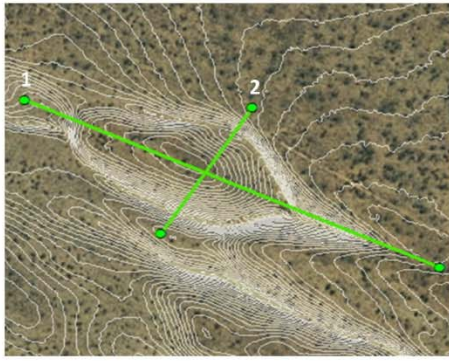


VIMY RESOURCES

TERRAIN ANALYSIS AND MATERIALS
CHARACTERISATION FOR THE MULGA
ROCK URANIUM PROJECT

Figure 2.19: Characteristic parabolic dunes within the MRUP



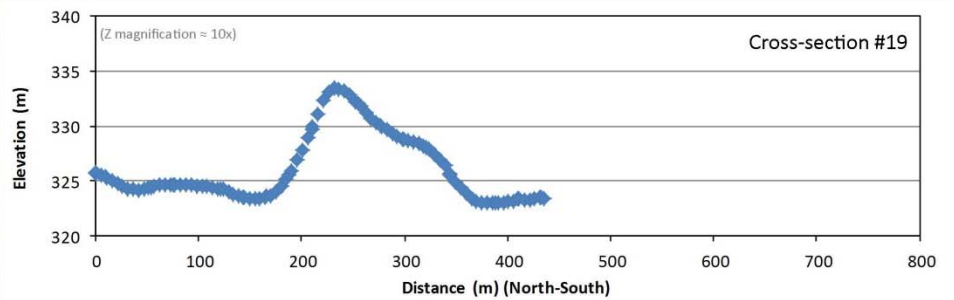
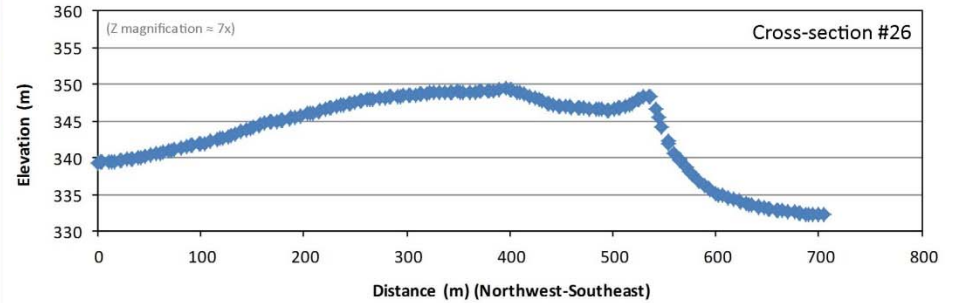
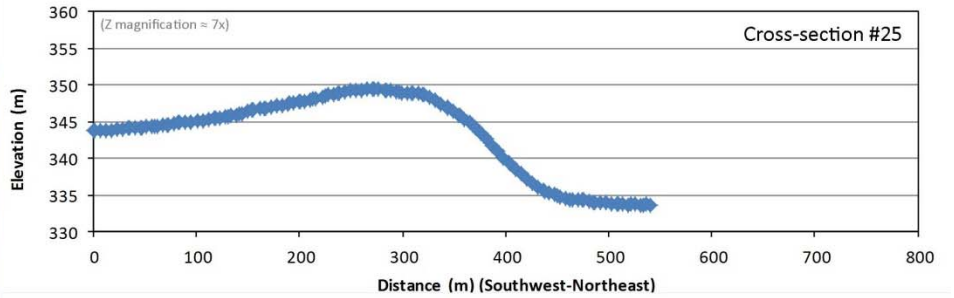
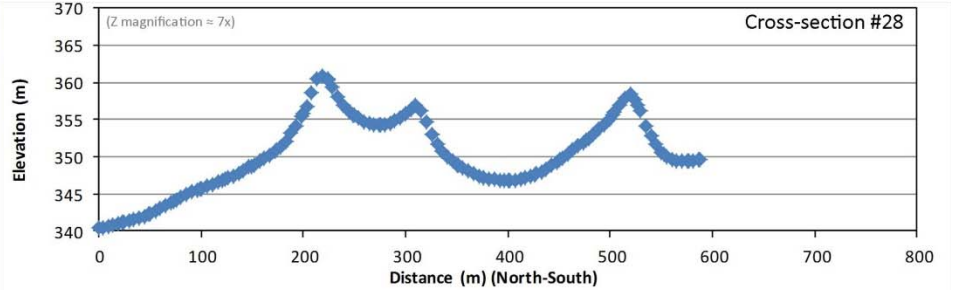
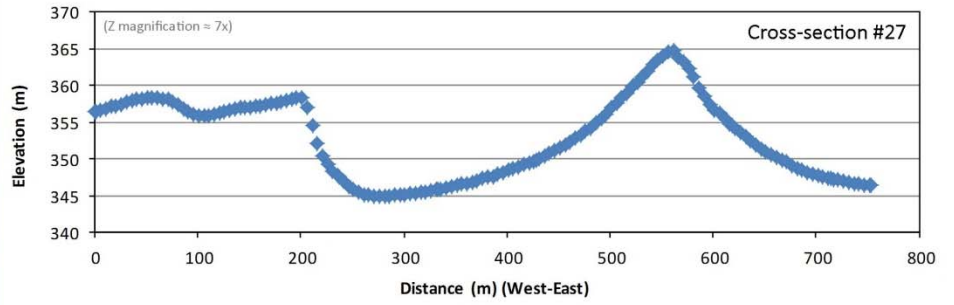
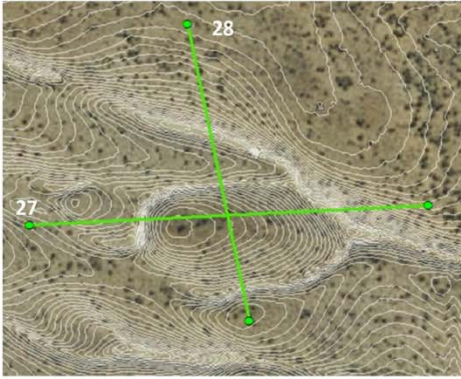


VIMY RESOURCES

TERRAIN ANALYSIS AND MATERIALS
CHARACTERISATION FOR THE MULGA
ROCK URANIUM PROJECT

Figure 2.14 continued...



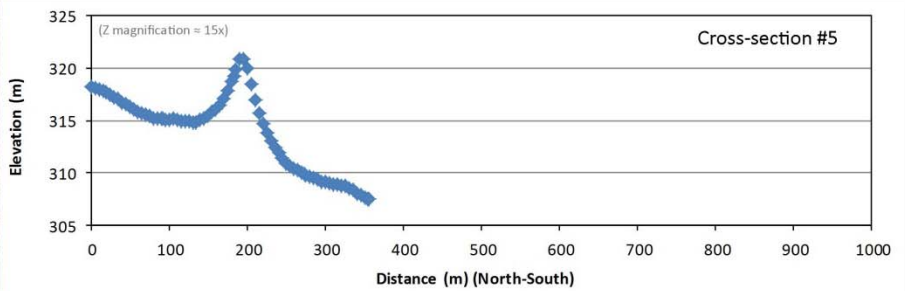
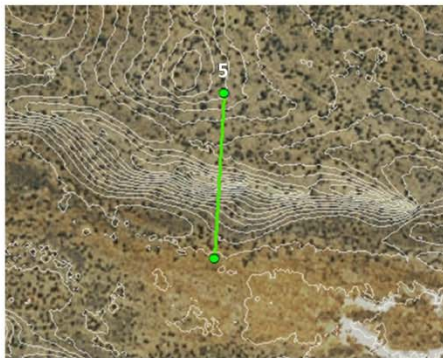
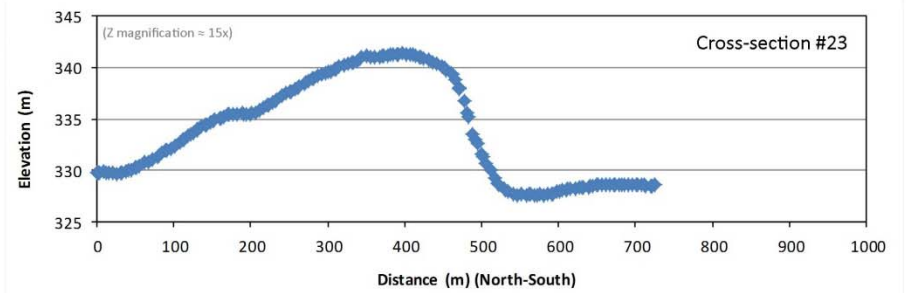
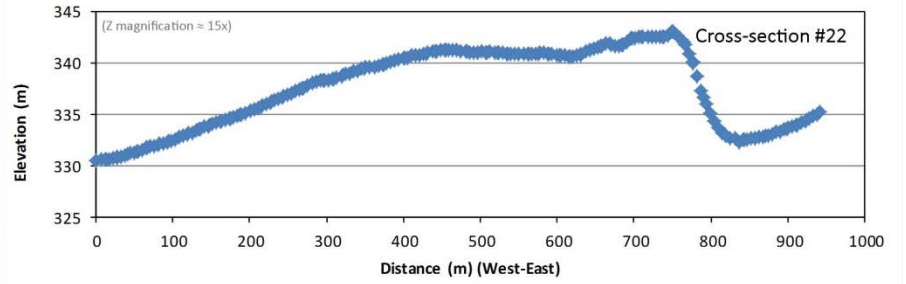
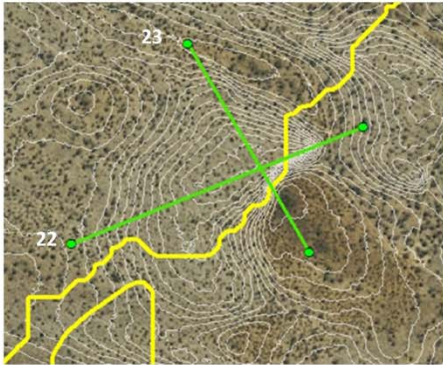


VIMY RESOURCES

TERRAIN ANALYSIS AND MATERIALS
CHARACTERISATION FOR THE MULGA
ROCK URANIUM PROJECT

Figure 2.20: Characteristic complex or irregular dunes within the MRUP



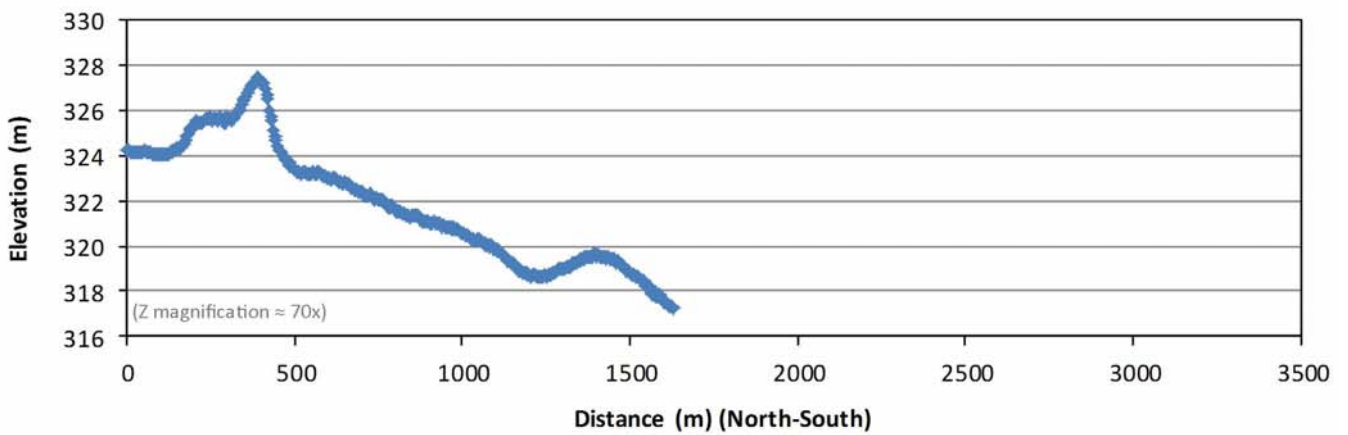
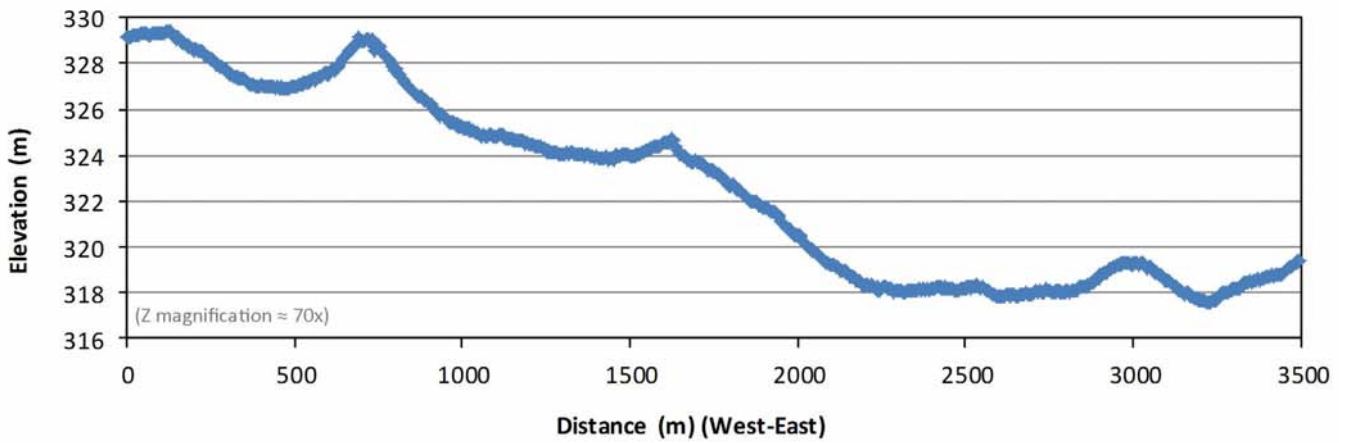
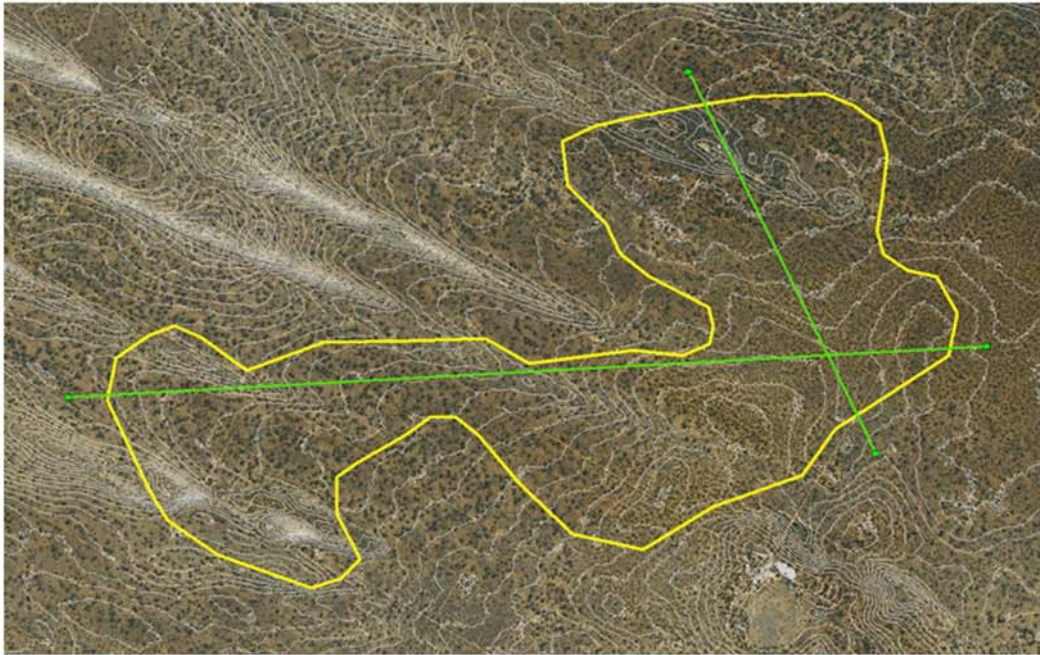


VIMY RESOURCES

TERRAIN ANALYSIS AND MATERIALS
CHARACTERISATION FOR THE MULGA
ROCK URANIUM PROJECT

Figure 2.15 continued...



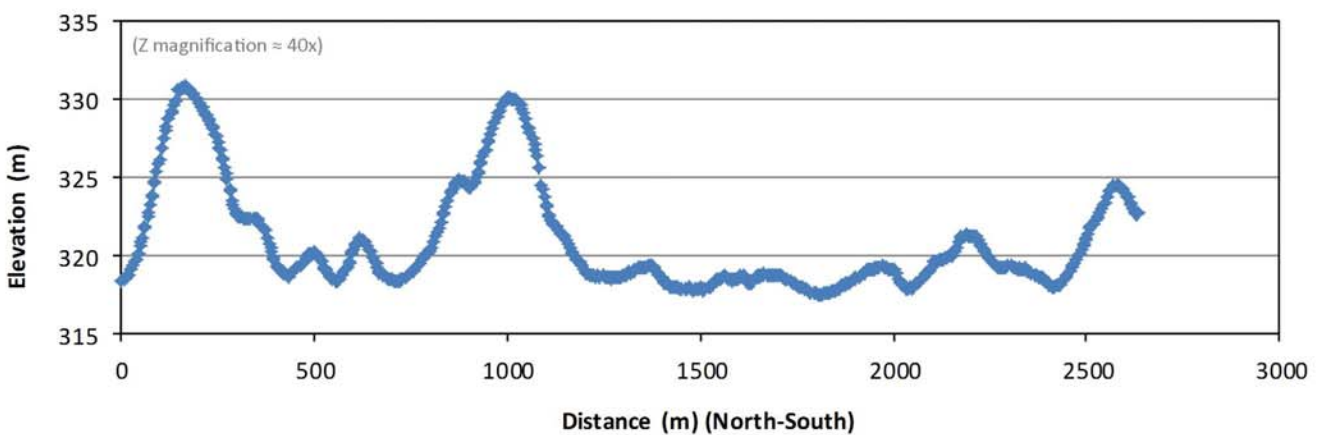
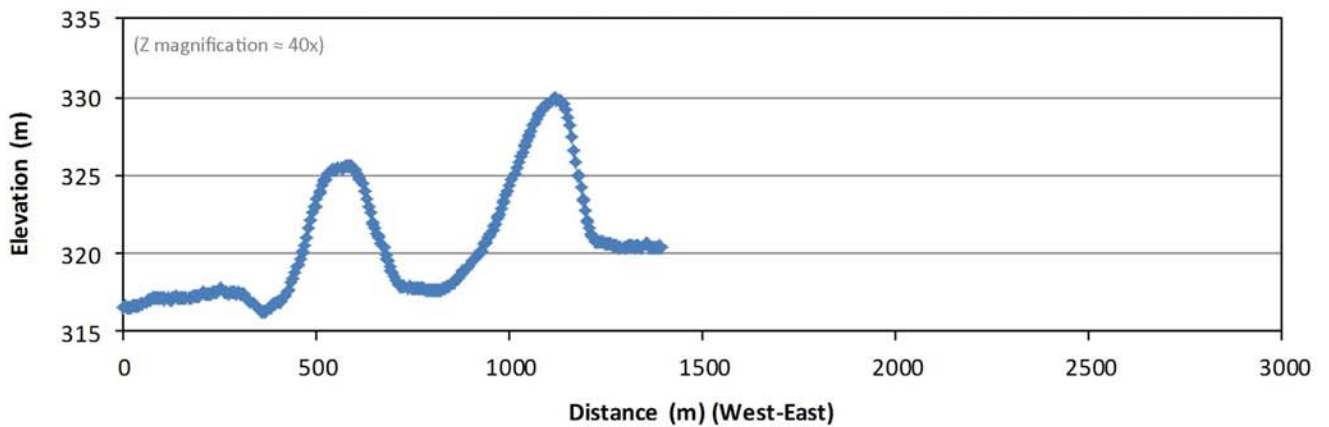
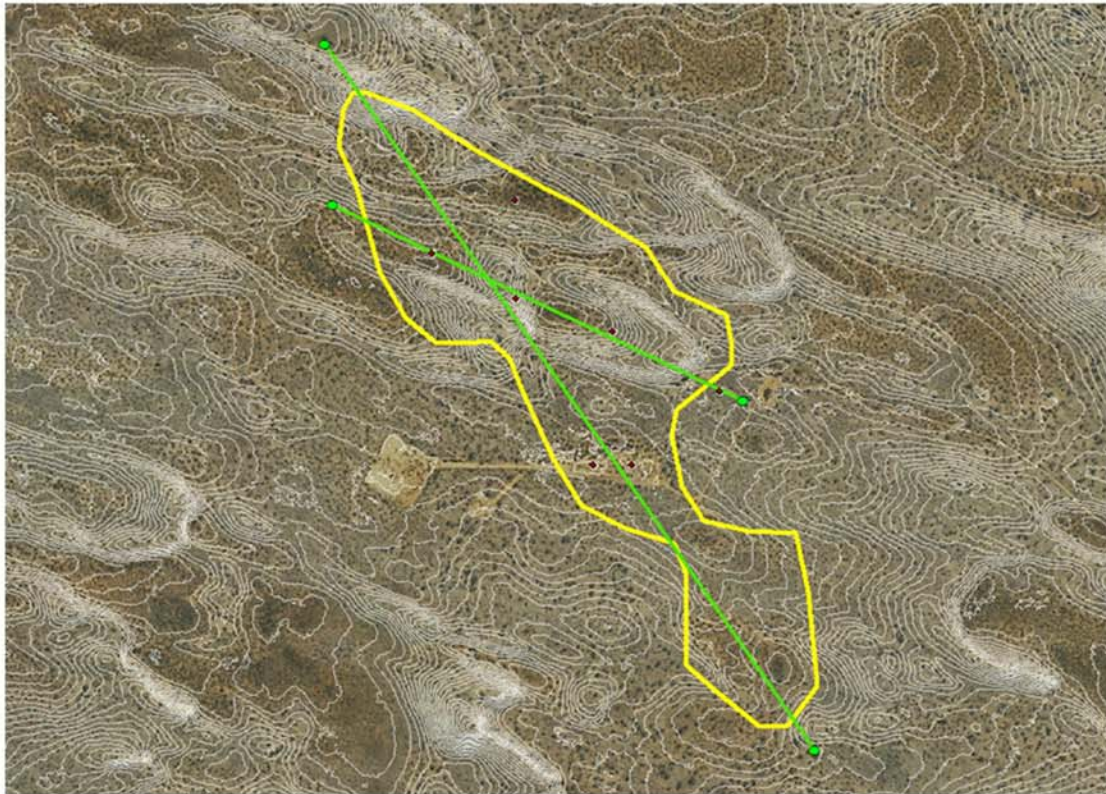


VIMY RESOURCES

TERRAIN ANALYSIS AND MATERIALS
CHARACTERISATION FOR THE MULGA
ROCK URANIUM PROJECT

Figure 2.21: Landsurface within the Emperor Deposit



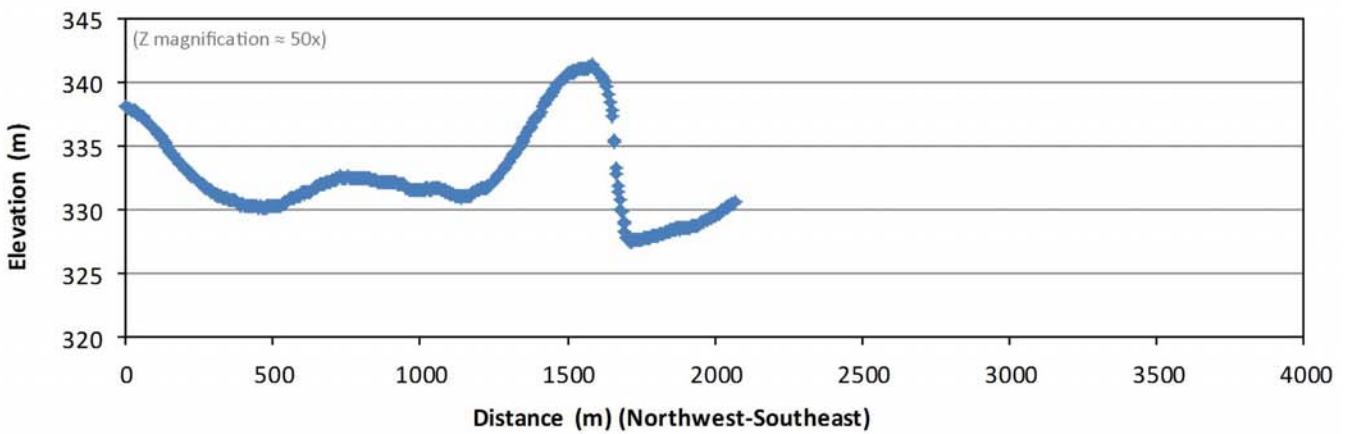
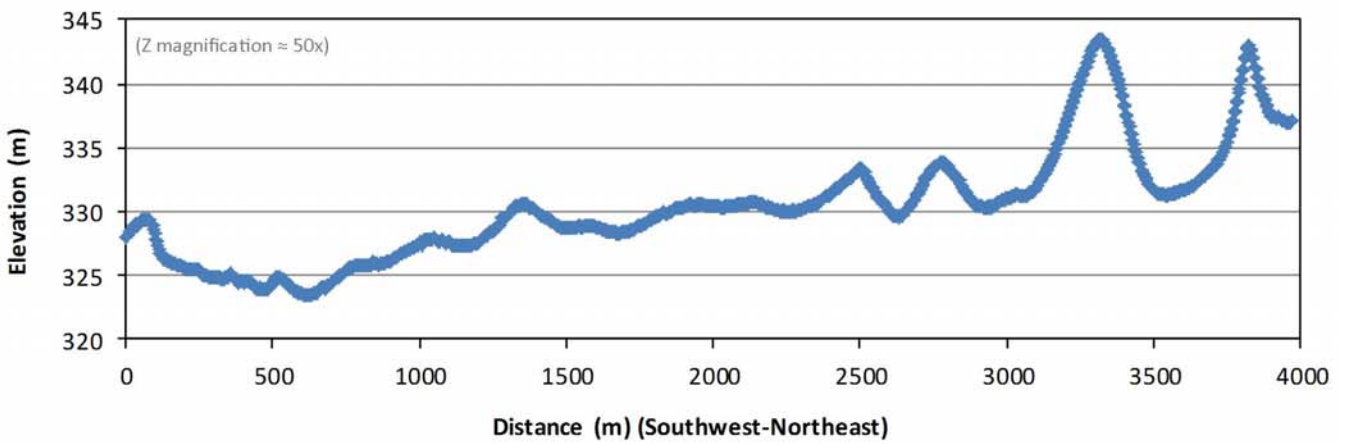
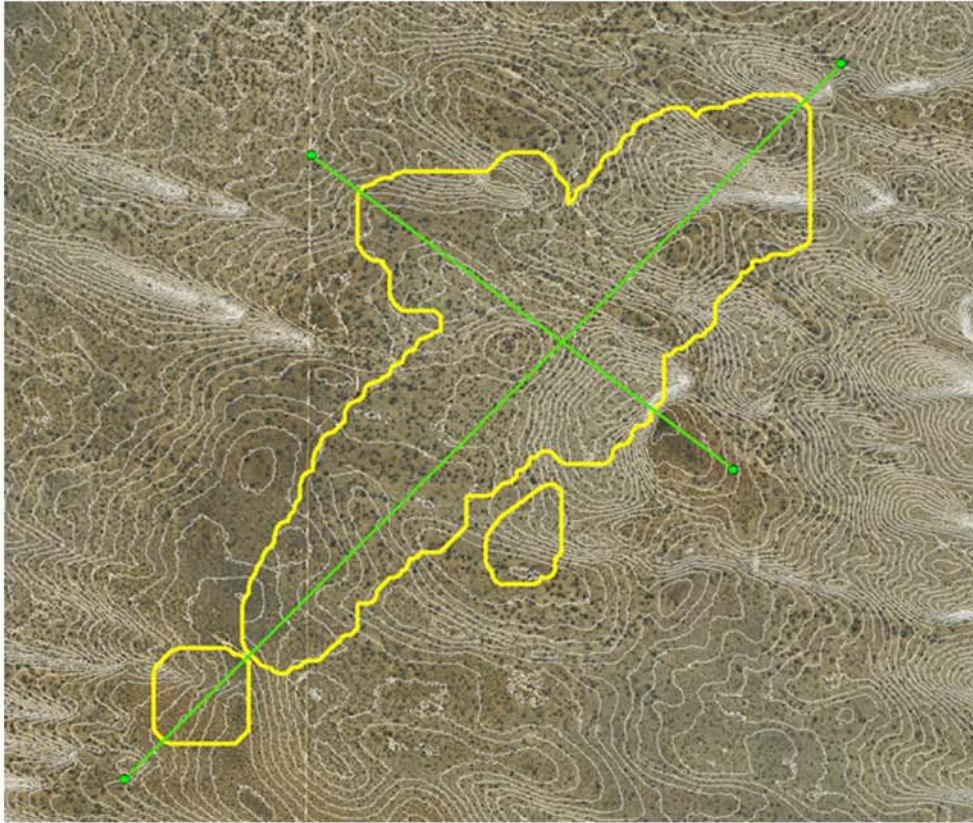


VIMY RESOURCES

TERRAIN ANALYSIS AND MATERIALS
CHARACTERISATION FOR THE MULGA
ROCK URANIUM PROJECT

Figure 2.22: Landsurface within the Shogun Deposit



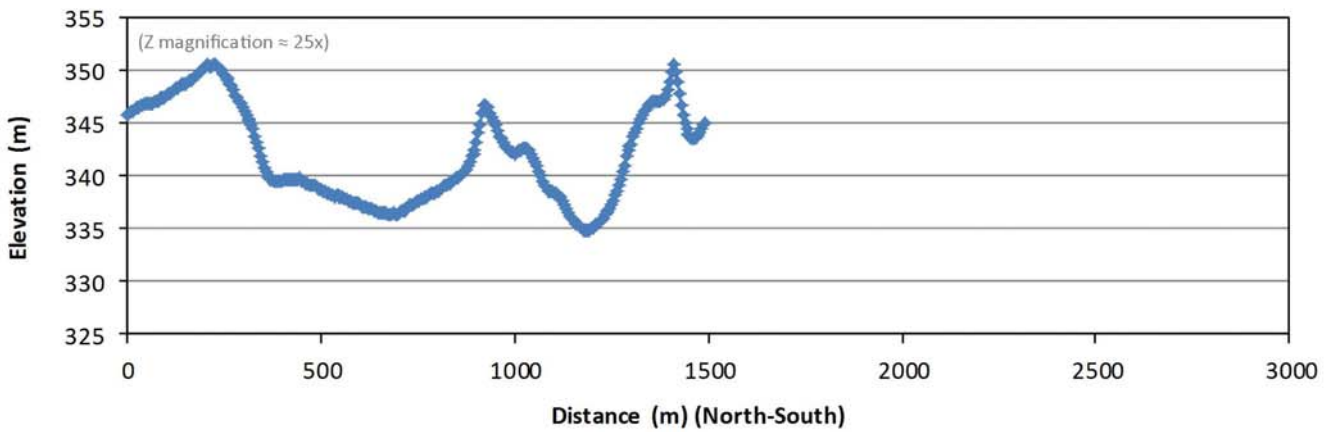
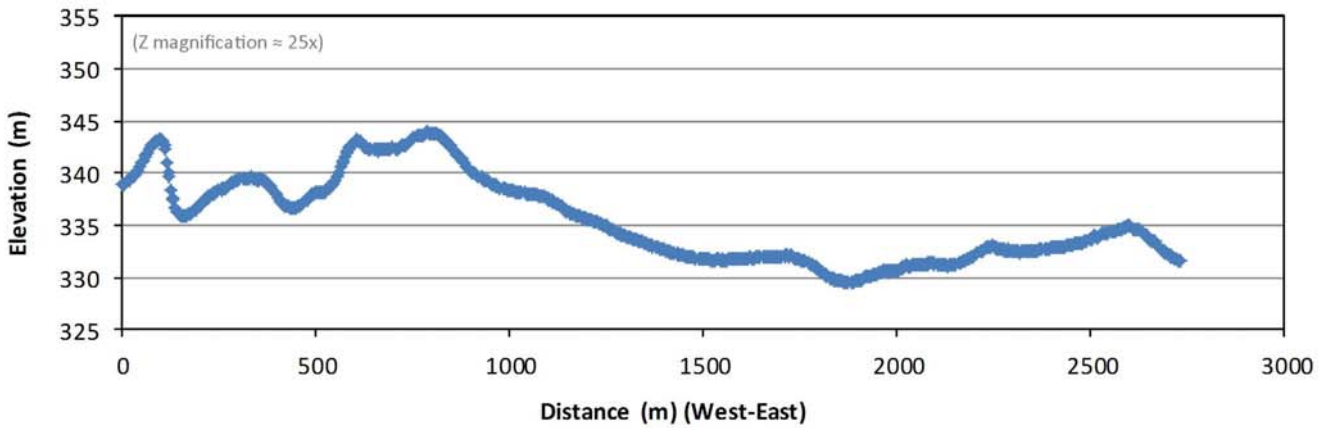
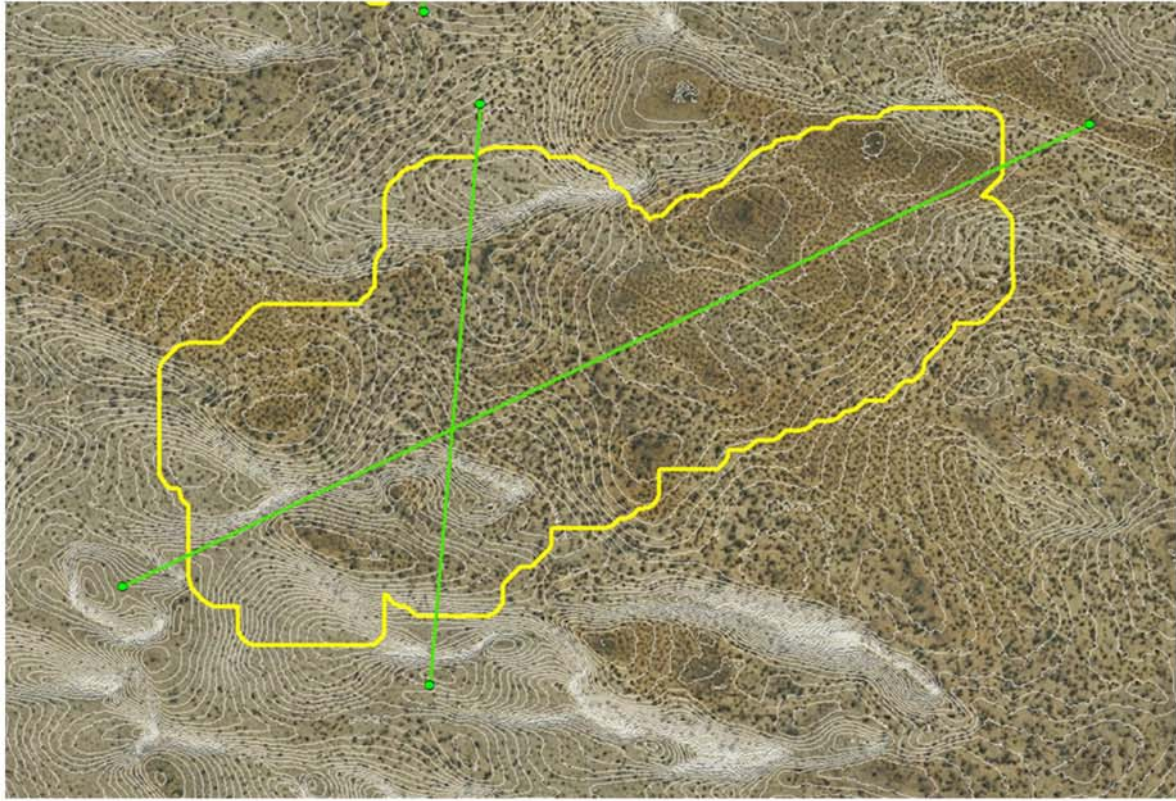


VIMY RESOURCES

TERRAIN ANALYSIS AND MATERIALS
CHARACTERISATION FOR THE MULGA
ROCK URANIUM PROJECT

Figure 2.23: Landsurface within the Ambassador West Deposit



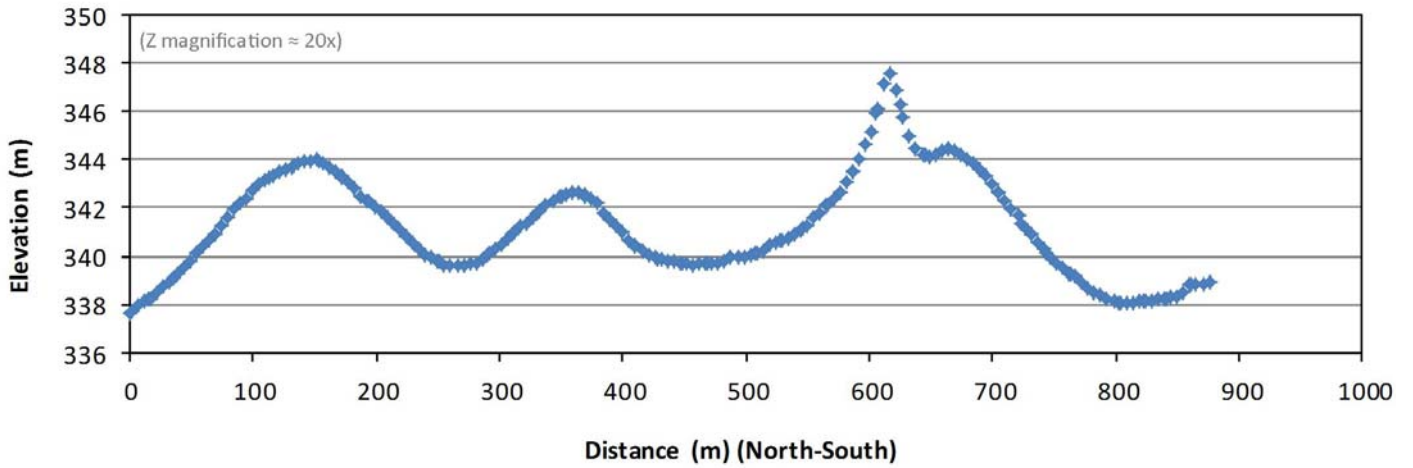
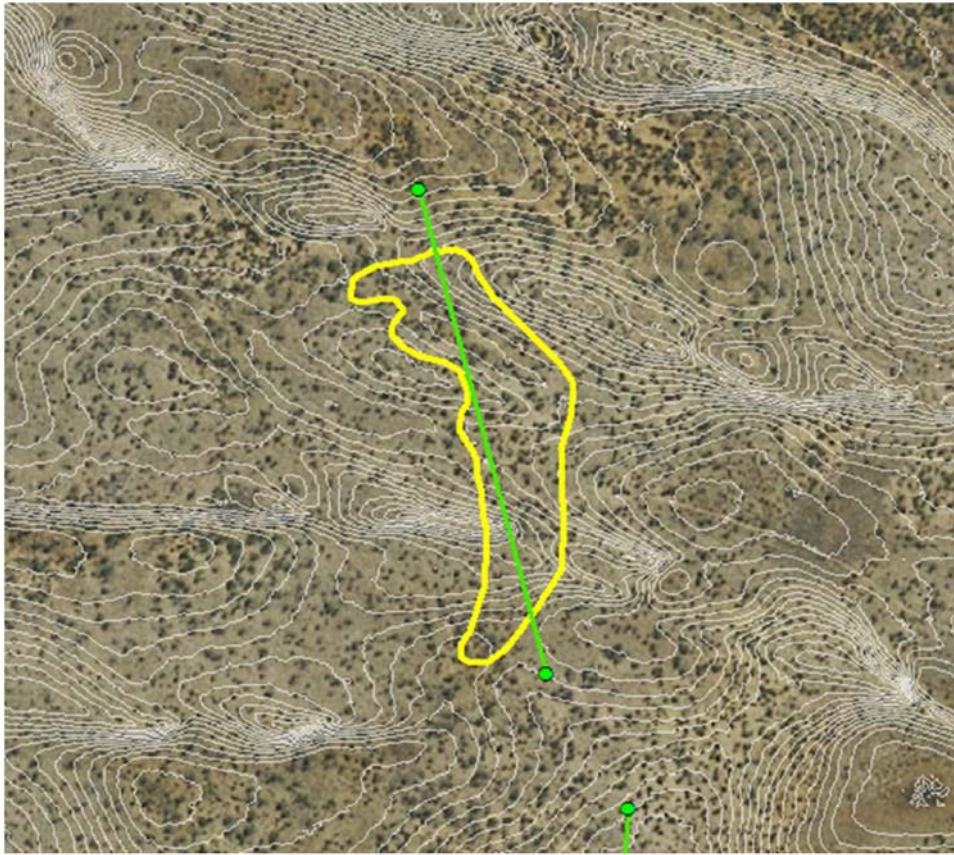


VIMY RESOURCES

TERRAIN ANALYSIS AND MATERIALS
CHARACTERISATION FOR THE MULGA
ROCK URANIUM PROJECT

Figure 2.24: Landsurface within the Ambassador East
Deposit





VIMY RESOURCES

TERRAIN ANALYSIS AND MATERIALS
CHARACTERISATION FOR THE MULGA
ROCK URANIUM PROJECT

Figure 2.25: Landsurface within the Princess Deposit



2.5 TERRAIN DATING

The landscape within the MRUP represents a complex arrangement of soils / sediments that span a significant time period, dating back to the Eocene (around 55 mya). During this time there have been a number of discrete soil formation or deposition episodes, likely driven by changing climatic conditions (i.e. glacial / interglacial periods), and at least two distinct paleo-landsurfaces are present within the MRUP; these are:

- Tertiary surface – located at the contact between the lower Eocene (55 – 34 mya) and the overlying Miocene (23 – 5 mya) sediments. This surface is widespread throughout Western Australia and distinguished by the presence of a lateritic or ferruginous hardpan that has cemented the original surficial parent material (often a conglomerate); and
- Miocene surface – located at the contact between the Miocene sediments and the overlying Quaternary Dunal Sands. This surface is typically distinguished by the occurrence of calcrete layer that has formed during a climatic period that is not too dissimilar from the current climate (i.e. semi-arid), but which likely experienced a higher rainfall than currently occurs to allow for the infiltration of soluble salts followed by a dry period to evaporate and precipitate them in the profile.

The complexity of the landscape is evident in the 'missing' sediments from the Oligocene (34 – 23 mya) and potentially the Pliocene (5 – 2.5 mya), which suggests widespread truncation of the profile prior to deposition of the younger sediments. It is important to reiterate that the MRUP occurs within once active paleodrainage channel that has been extensively faulted, and displaying a complex graben and horst structure; this is clearly shown in Figure 2.8.

To help constrain the depositional and formation ages of the surficial Quaternary aeolian sands, several studies have been recently (2012 – 2013) undertaken within the MRUP region by Geological Survey of Western Australia (GSWA; unpublished). One of the locations investigated was the old rubbish tip at the Vimy MRUP Exploration Camp (located at 51J 573,752 mE and 6,683,942 mN). Optically Stimulated Luminescence (OSL) dating was undertaken on the side wall of the tip trench at various depths down the surficial sandy profile (Plate 2.4). Sand deposition dates of between 9.1 (\pm 2.8) ka at 50 cm depth, 50.4 (\pm 14.2) ka at 110 cm depth and 92.3 (\pm 14.0) ka at 190 cm depth were reported (i.e. early Holocene to Late-Pleistocene), overlying an older, possibly reworked, basement of age 166.9 (\pm 46.6) ka. The dates of the surficial dunal sands correspond to those obtained from a similar OSL study undertaken by the GSWA at a location near the proposed Kakarook Borefield (). The dates for the dunal sands varied from 6.7 (\pm 2.8) ka at 60 cm depth, 38.9 (\pm 19.7) ka at 120 cm depth to 90.9 (\pm 19.0) ka at 180 cm depth.

The dates reported by the GSWA for the surficial sands within the MRUP coincide with the broad dune building dates established for the wider Great Victoria Desert (GVD) dunes and more regional arid zone within Australia (Figure 2.26). This figure shows that formation of the dunes has occurred over a protracted time period (up to 250 ka) and dune building has occurred multiple times, likely corresponding to glacial maxima where drier conditions prevail.

Plate 2.4: OSL sampling locations from the MRUP rubbish trench

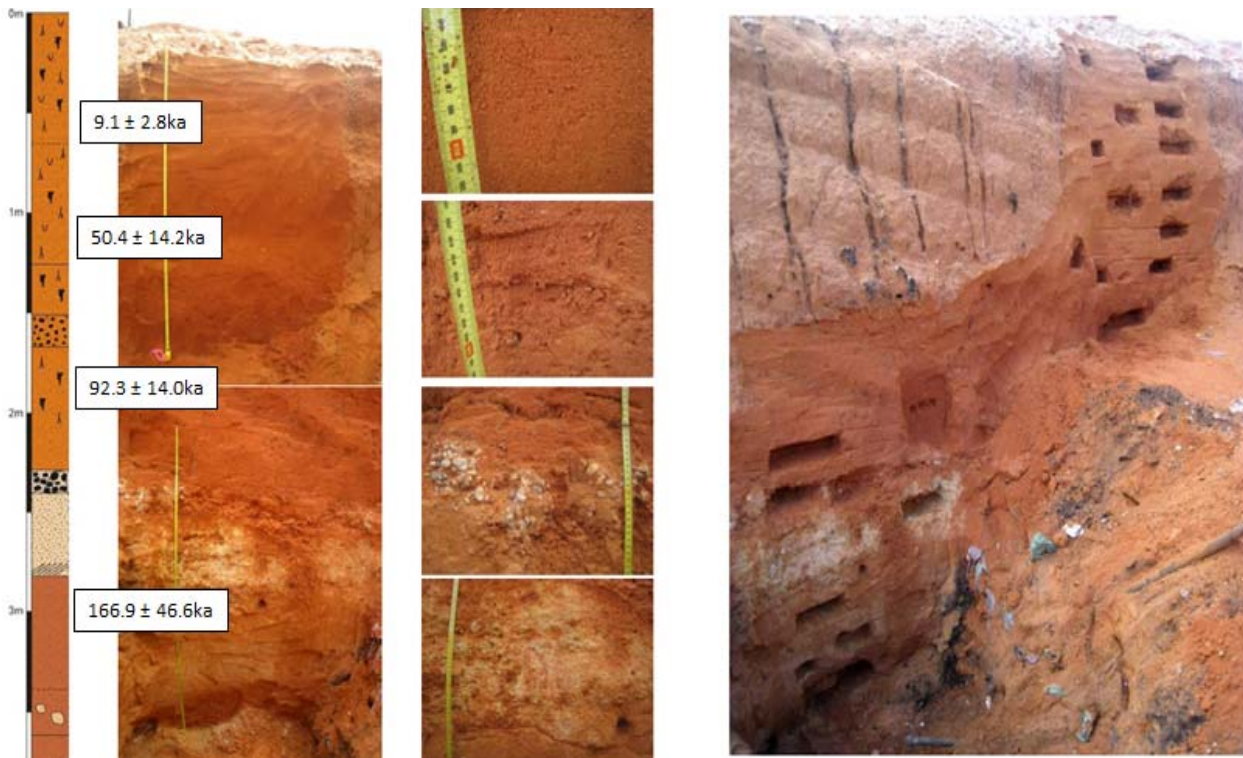


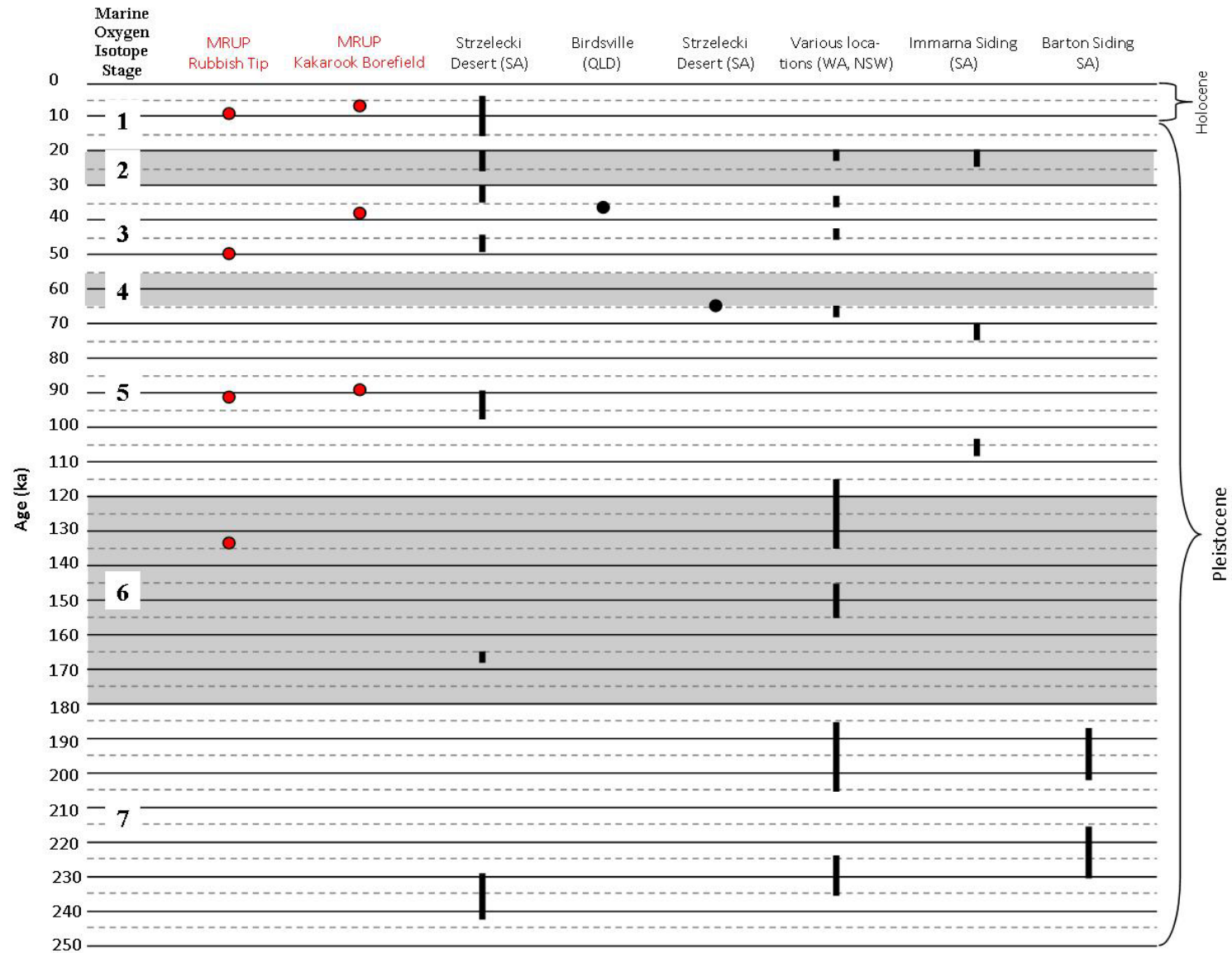
Plate 2.5: OSL dating of surficial dunal sands near the Kakarook Borefield by the GSWA



Sandpit excavation



OSL sampling



Highlighted ages represent glacial periods within the Pleistocene (Martinson *et al.*, 1987).

VIMY RESOURCES

TERRAIN ANALYSIS AND MATERIALS CHARACTERISATION FOR THE MULGA ROCK URANIUM PROJECT

Figure 2.26: Recorded ages for Quaternary Dunes within the GVD and broader arid zone of Australia



2.6 HYDROLOGY

2.6.1 REGIONAL

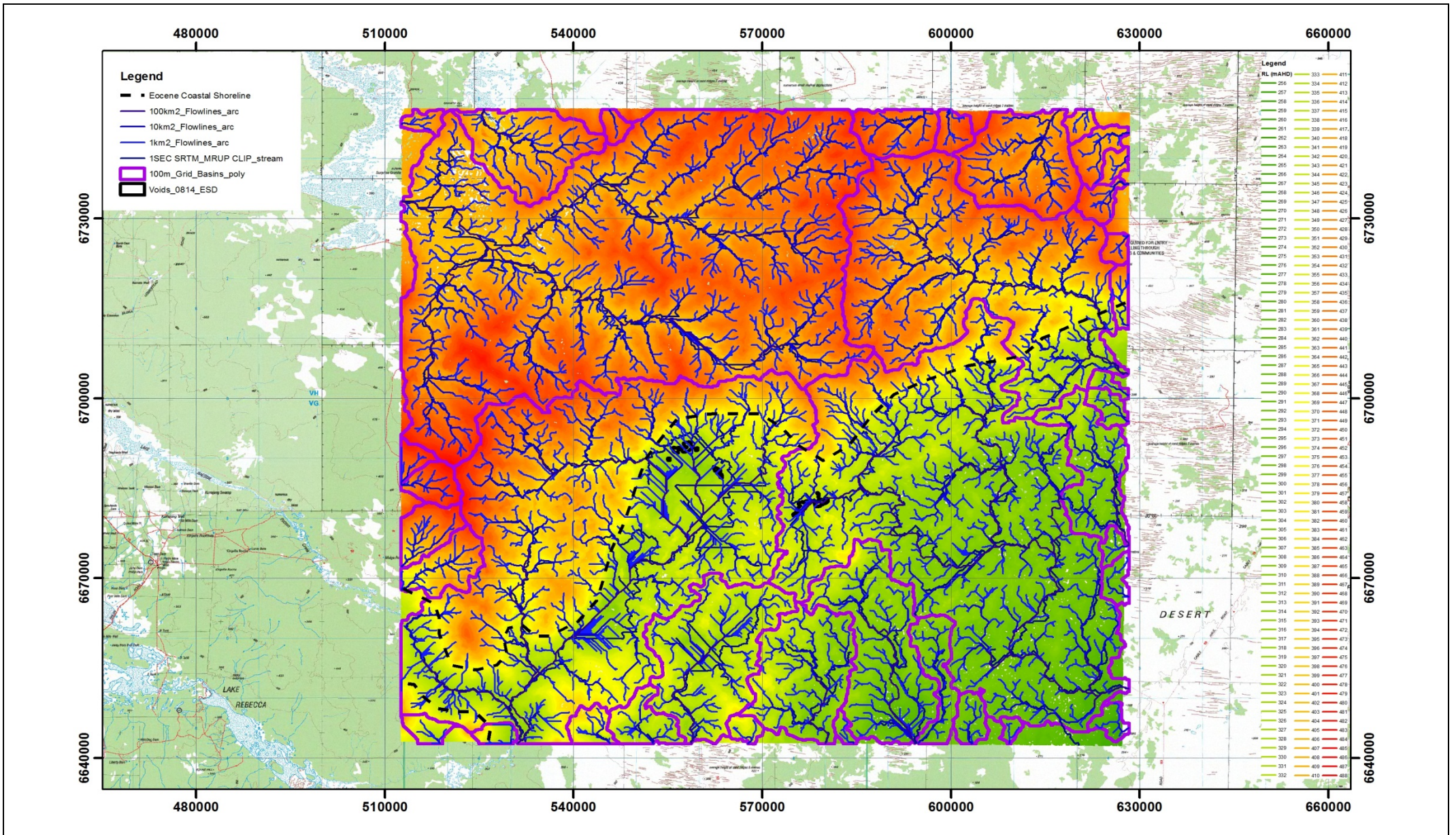
At a regional scale, the surface hydrology is effectively subdivided by the outcropping basement breakaway, such that to the north of the breakaway surface flows are primarily to the north east, draining into Lake Minigwall, whilst to the south of this divide, flows are generally in a south to south-east direction, draining into the Eucla Coastal Barrier (Figure 2.11). Regional surface flow lines (with 1 km² to 100 km² catchment size), derived by Topographic Parameterisation (TOPAZ) of a DEM constructed using the 1 second STRM contour data, are presented in Figure 2.27, along with the modelled regional catchment boundaries. Although defined surface flow lines are shown in Figure 2.27, it is important to note that surface flows are very sluggish across this region, particularly south of the catchment divide (i.e. outcropping breakaway), where the landsurface has a very gently slope of around 0.01° or 0.02%, and has a predominately sandy surface, which facilitates vertical infiltration of rainfall as opposed to surface runoff. Consequently, even under intense storm events (i.e. 1:100 year 72 hour), flow along these modelled flow lines is unlikely to occur.

2.6.2 LOCAL

At a local scale, surface hydrological processes are dominated the aeolian dunes, which tend to concentrate and direct flows towards defined topographic depressions. This is clearly shown in Figure 2.28 for the Shogun and Ambassador East Deposits. These topographic depressions occur throughout the MRUP, resulting in this region being internally draining, with negligible potential for surface waters to leave the site. Even under intense storm events (i.e. 1:100 year 72 hour, equivalent to 158.4 mm rainfall; as occurred during February 2011 associated with the tail end of Cyclone Carlos), the potential for these topographic depressions to fill and then overtop to form a continuous interconnected surface hydrological system is considered very low and localised flooding will be restricted to these depressions only (Plate 2.6). There is also negligible risk for flooding of the open voids during operations, or any of the post-mine landforms, due to the sandy nature of the soils, convergence of surface water within the topographic depressions and the nature of the sand dunes effectively reducing the overall catchment size draining a particular area.

Plate 2.6: Localised flooding with a topographic depression within the MRUP in response to Cyclone Carlos



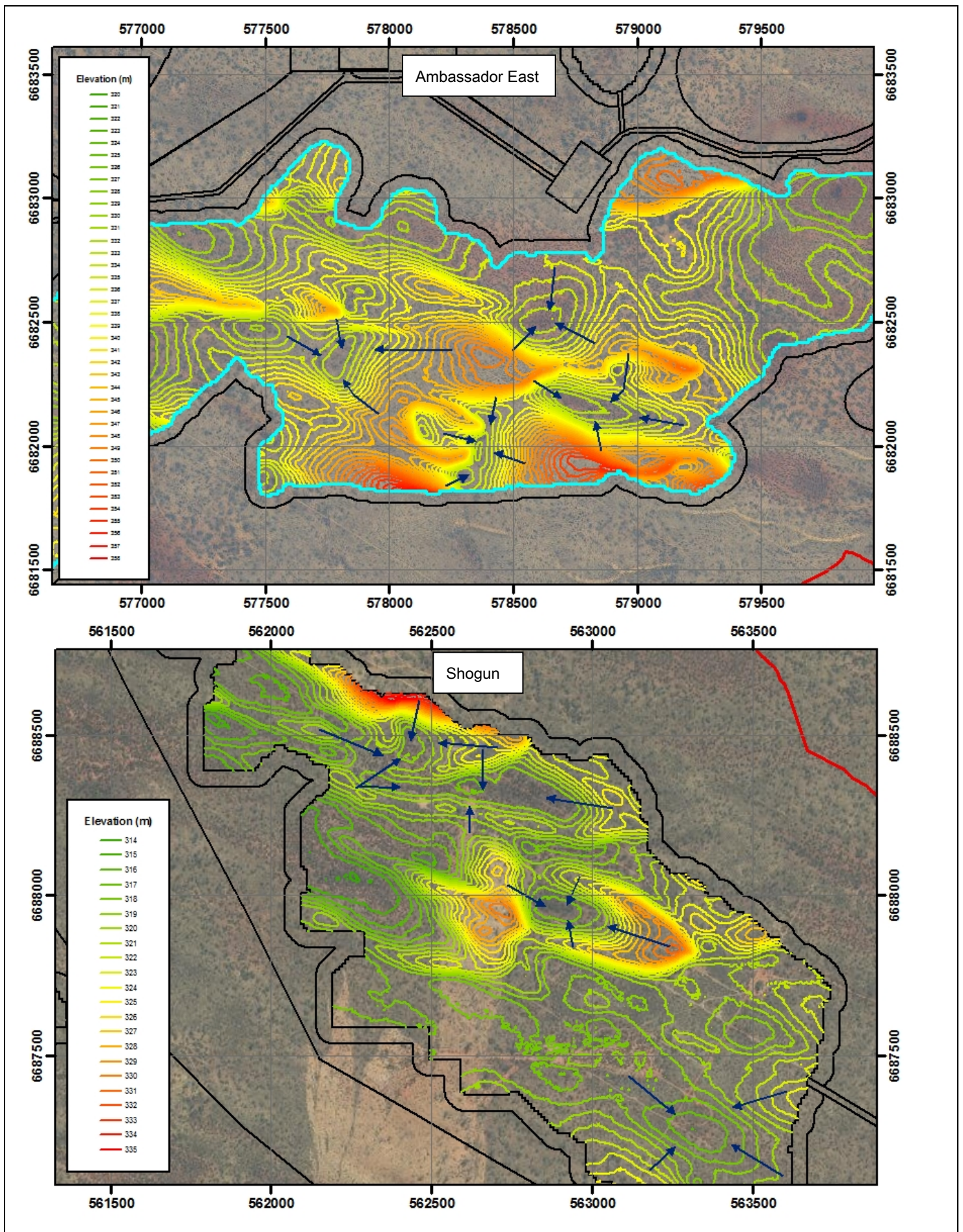


VIMY RESOURCES

TERRAIN ANALYSIS AND MATERIALS
CHARACTERISATION FOR THE MULGA ROCK URANIUM
PROJECT

Figure 2.27: Regional surface hydrology





VIMY RESOURCES

TERRAIN ANALYSIS AND MATERIALS
CHARACTERISATION FOR THE MULGA
ROCK URANIUM PROJECT

Figure 2.28: Local-scale hydrological processes, showing convergence of surface flows into topographic depressions



2.7 REGIONAL SOILS

The soils across the MRUP have been mapped at a regional scale as part of the Australian Soil Resources Information System (ASRIS; CSIRO, 2014). The regional soil-landscape units are shown in Figure 2.29, whilst a description of these units is provided in Table 2.4. The MRUP occurs solely within the Southern Great Victorian Desert Zone (Zone 124), with the majority of the development occurring within soil-landscape unit AB47 which consists of plains and longitudinal and ring dunes, with interdunal corridors and plains and occasional salt pans. The central portion of the production borefield access road traverses the soil-landscape unit My99, which comprises plains of extensive gravel pavements and small tracts of longitudinal dunes.

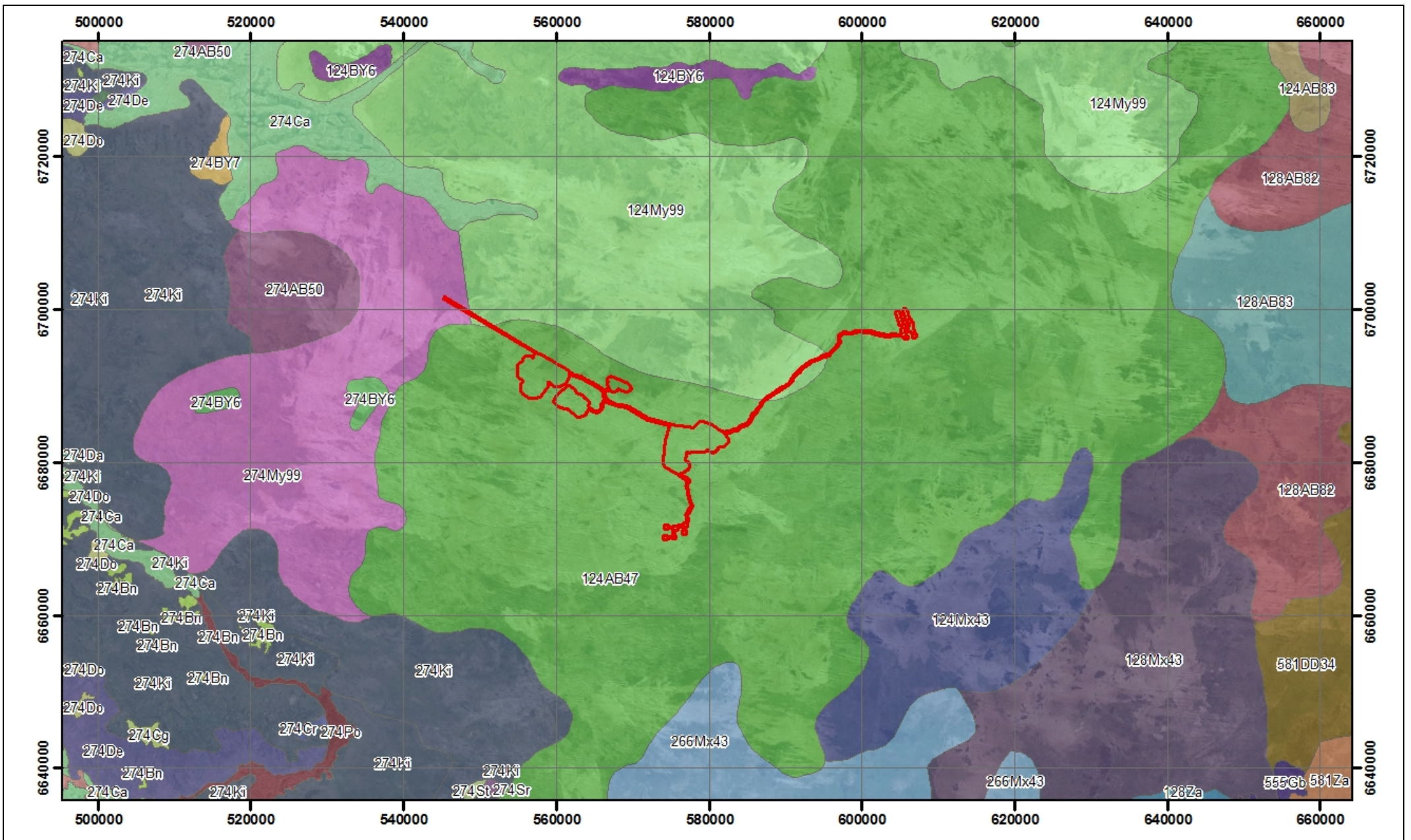
Soil-landscape units belonging to the Sydney Simpson (Zone 128), Norseman (Zone 266), Leemans Sandplain (Zone 274), Nyanga (Zone 555) and Carlisle Plain (Zone 581) Zones border the Southern Great Victorian Desert Zone.

Table 2.4: Soil-landscape units within the MRUP region

Map Unit	Name	
<i>South Great Victorian Desert Zone</i>		
124AB47	AB47	Plains and dunes--longitudinal and ring dunes with interdune corridors and plains; occasional salt pans
124AB83	AB83	Plains with occasional low dunes
124BY6	BY6	Scarpland-breakaways and residuals of various forms, cuestas, mesas, buttes, stony hillocks, and hills commonly with large bare slabs of silcrete; stone and gravel pavements are common;
124Mx43	Mx43	Gently undulating valley plains and pediments; some outcrop of basic rock
124My99	My99	Plains with extensive gravel pavements and small tracts of longitudinal dunes
<i>Sydney Simpson Zone</i>		
128AB82	AB82	Dune fields--very gently undulating plains dominated by longitudinal dunes; small outcrops of calcrete (kunkar) occur in the interdune swales
128AB83	AB83	Plains with occasional low dunes
128Mx43	Mx43	Gently undulating valley plains and pediments; some outcrop of basic rock
<i>Norseman Zone</i>		
266Mx43	Mx43	Gently undulating valley plains and pediments; some outcrop of basic rock
<i>Leemans Sandplain Zone</i>		
274AB50	AB50	Plains with scattered dunes and small breakaways of unit BY7
274Bn	Bandy System	Gritty-surfaced plains and low outcrops of granite with scattered <i>Acacia</i> shrublands.
274BY6	BY6	Scarpland-breakaways and residuals of various forms, cuestas, mesas, buttes, stony hillocks, and hills commonly with large bare slabs of silcrete; stone and gravel pavements are common;

EXISTING ENVIRONMENT

Map Unit	Name	
274BY7	BY7	Scarpland--low lateritic breakaways on granites and gneisses
274Ca	Carnegie System	Salt lakes with fringing saline alluvial plains, kopi dunes and sandy banks, supporting halophytic shrublands and <i>Acacia</i> tall shrublands.
274Cg	Cundlegum System	Breakaways on granite and lower plains supporting eucalypt woodlands.
274Cr	Crete System	Breakaways and lower plains based on weathered granites, supporting halophytic shrublands.
274De	Deadman System	Calcareous plains supporting <i>Acacia</i> , black oak and mallee shrublands/woodlands adjacent to salt lake systems.
274Do	Doney System	Calcareous alluvial plains with eucalypt woodlands adjacent to salt lake systems.
274Ki	Kirgella System	Gently undulating sandplains, with scattered granite outcrop supporting spinifex hummock grasslands, mulga shrublands and mallees.
274My99	My99	Plains with extensive gravel pavements and small tracts of longitudinal dunes
274Po	Ponton System	Channels with narrow flanking alluvial plains supporting chenopod low shrublands.
274Sr	Sturt System	Saline alluvial plains with irregularly arranged drainage foci and sandy banks supporting halophytic shrublands.
274St	Steer System	Gravelly alluvial plains supporting chenopod shrublands.
<i>Nyanga Zone</i>		
555Gb	Gumbelt System	Sandy loam calcrete plains supporting eucalypt woodland with mixed shrub understorey.
<i>Carlisle Plain Zone</i>		
581DD34	DD34	Very gently to gently undulating plains with broad flats and low broad rises, the former being the prominent feature
581Za	Zanthus System	Level sandy loam calcrete plains supporting mallee woodland over spinifex hummock grassland.



VIMY RESOURCES

TERRAIN ANALYSIS AND MATERIALS CHARACTERISATION
FOR THE MULGA ROCK URANIUM PROJECT

Figure 2.29: Regional soil-landscape units



2.8 FLORA AND VEGETATION

The MRUP occurs within the Shield subregion (GVD1) of the Great Victoria Desert bioregion, previously known as the Helms Botanical District. The flora and vegetation across this area has been surveyed and mapped by Matiske Consulting (MCPL, 2015a). A total of 326 vascular plant taxa, representative of 136 genera and 42 families, have been recorded. The majority of taxa recorded were representative of the Fabaceae (52 taxa), Myrtaceae (40 taxa), Goodeniaceae (25 taxa) and Proteaceae (23 taxa) families. A total of nine annual and/or biennial species, equating to 2.8% of the total number of taxa, were recorded.

No threatened flora or Declared Rare Flora (DRF) were recorded in the MRUP and only one State listed Priority 1 (P1) species, *Hibbertia crispula*, (also listed as Vulnerable by the Dote (2015), was present in the area. Targeted survey for *H. crispula* (MCPL, 2015b) has identified an estimated 14,269 plants recorded on dunes in and surrounding the MRUP.

A total of 12 other Priority flora species have been recorded in the MRUP and these are listed in Table 2.5. No introduced weed species or declared plant are present in the MRUP.

Table 2.5: Priority species recorded within the MRUP area

SPECIES	PRIORITY LISTING
<i>Hibbertia crispula</i>	P1 & Vulnerable
<i>Dampiera eriantha</i>	P1
<i>Neurachne lanigera</i>	P1
<i>Malleostemon</i> sp. Officer Basin (D. Pearson 350)	P2
<i>Styphelia</i> sp. Great Victoria Desert (N. Murdoch 44)	P2
<i>Baeckea</i> sp. Sandstone (C.A. Gardner s.n. 26 Oct. 1963)	P3
<i>Labichea eremaea</i>	P3
<i>Ptilotus blackii</i>	P3
<i>Comesperma viscidulum</i>	P4
<i>Dicrastylis cundeeleensis</i>	P4
<i>Grevillea secunda</i>	P4
<i>Olearia arida</i>	P4

The vegetation within the MRUP has been classified into 26 Vegetation Community Types (VCT). The mapped distribution of these VCTs is provided in Figure 2.30 and described in Table 2.6.

Table 2.6: Description of VCTs recorded within the MRUP (MCPL, 2015a)

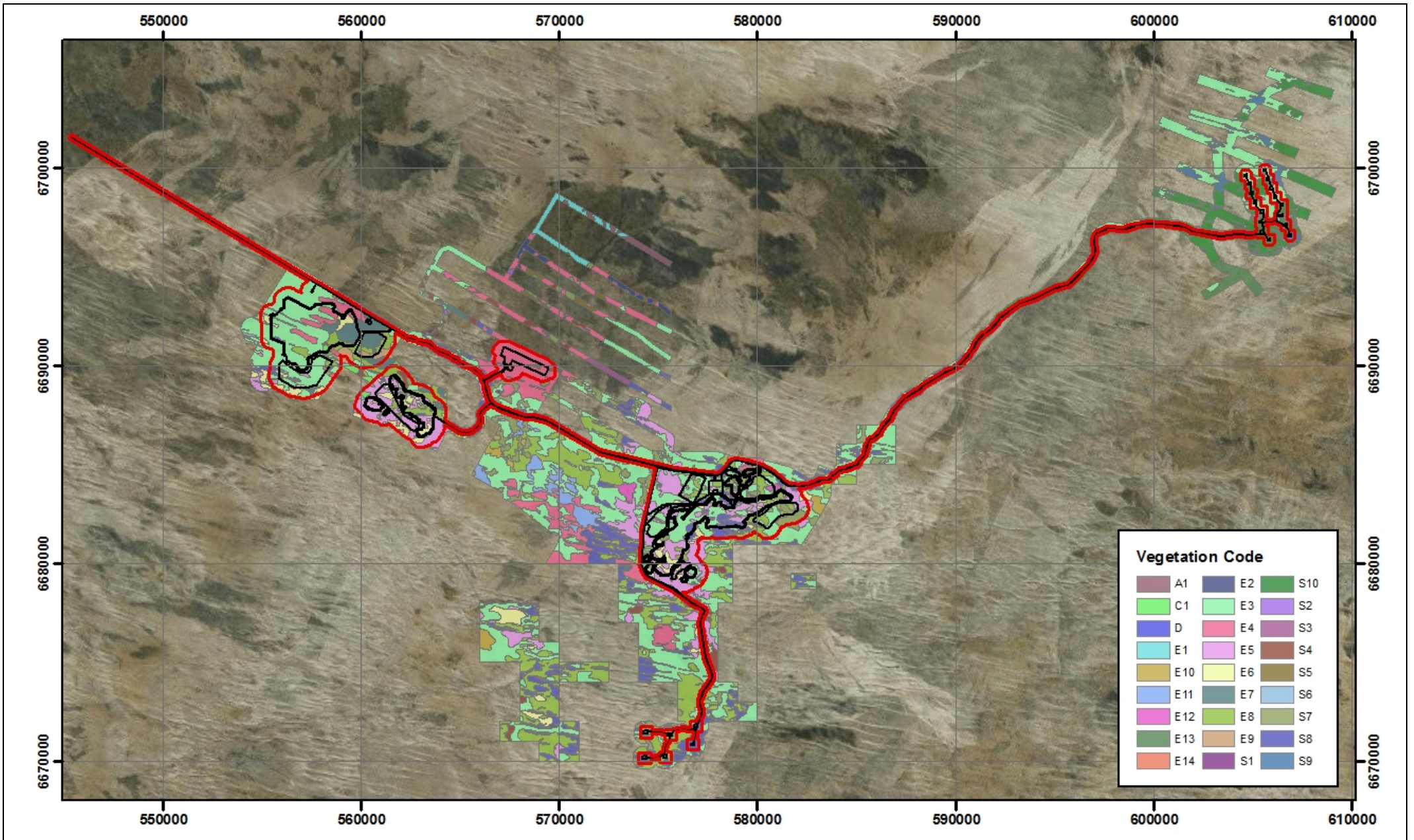
EUCALYPT WOODLANDS	
E1	Low woodland to low open woodland of <i>Eucalyptus concinna</i> with <i>Callitris preissii</i> over <i>Westringia cephalantha</i> , <i>Melaleuca hamata</i> , <i>Acacia colletioides</i> , <i>Acacia hemiteles</i> and <i>Scaevola spinescens</i> over <i>Triodia desertorum</i> . This community occurs on red-orange sandy loams on flats.

E2	Low woodland to open scrub mallee of <i>Eucalyptus trivalva</i> and <i>Eucalyptus platycorys</i> with <i>Callitris preissii</i> and <i>Hakea francisiana</i> over <i>Acacia colletioides</i> , <i>Acacia hemiteles</i> , <i>Melaleuca hamata</i> , <i>Westringia cephalantha</i> , <i>Bertya dimerostigma</i> and mixed shrubs over <i>Triodia desertorum</i> with occasional emergent <i>Eucalyptus gongylocarpa</i> . This community occurs on red orange sandy loams on flats.
E3	Low open woodland of <i>Eucalyptus gongylocarpa</i> over <i>Eucalyptus youngiana</i> , <i>Eucalyptus ceratocorys</i> , <i>Grevillea juncifolia</i> , <i>Hakea francisiana</i> and <i>Callitris preissii</i> over <i>Acacia helmsiana</i> , <i>Cryptandra distigma</i> and mixed low shrubs over <i>Triodia desertorum</i> , <i>Chrysitrix distigmata</i> and <i>Lepidobolus deserti</i> . This community occurs on yellow and yellow-orange sands on flats, slopes and between dunes.
E4	Low open woodland of <i>Eucalyptus gongylocarpa</i> over <i>Callitris preissii</i> with <i>Hakea francisiana</i> and <i>Grevillea juncifolia</i> over <i>Bertya dimerostigma</i> , <i>Westringia cephalantha</i> and mixed shrubs over <i>Triodia rigidissima</i> and <i>Triodia desertorum</i> . This community occurs on orange sands on flats and slopes.
E5	Low open woodland of <i>Eucalyptus gongylocarpa</i> over <i>Eucalyptus rigidula</i> and <i>Eucalyptus</i> sp. Mulga Rock (K.D. Hill & L.A.S. Johnson KH 2668) with <i>Hakea francisiana</i> and <i>Grevillea juncifolia</i> over <i>Westringia cephalantha</i> , <i>Acacia helmsiana</i> , <i>Acacia rigens</i> , <i>Eremophila platythamnos</i> subsp. <i>platythamnos</i> , <i>Cryptandra distigma</i> and mixed low shrubs over <i>Triodia desertorum</i> , <i>Triodia rigidissima</i> and <i>Chrysitrix distigmata</i> . This community occurs on yellow and orange sands on flats and slopes.
E6	Open Scrub Mallee to Very Open Scrub Mallee of <i>Eucalyptus rigidula</i> and/or <i>Eucalyptus</i> sp. Mulga Rock (K.D. Hill & L.A.S. Johnson KH 2668) over <i>Acacia hemiteles</i> , <i>Hakea francisiana</i> , <i>Westringia rigida</i> , <i>Cryptandra distigma</i> , <i>Grevillea acuaria</i> and mixed low shrubs over <i>Triodia rigidissima</i> with <i>Halgania cyanea</i> . This community occurs on red-orange sandy loams on flats and low lying swales.
E7	Open scrub mallee to very open scrub mallee of varying <i>Eucalyptus</i> spp. over <i>Grevillea acuaria</i> , <i>Acacia hemiteles</i> , <i>Cryptandra distigma</i> , <i>Westringia cephalantha</i> and mixed shrubs over <i>Triodia desertorum</i> . This community occurs on red-orange sandy loams in low lying swales.
E8	Open scrub mallee to very open scrub mallee of <i>Eucalyptus ceratocorys</i> and <i>Eucalyptus mannensis</i> subsp. <i>mannensis</i> with <i>Eucalyptus youngiana</i> , <i>Hakea francisiana</i> and <i>Grevillea juncifolia</i> over <i>Acacia fragilis</i> , <i>Acacia helmsiana</i> and mixed low shrubs over <i>Triodia desertorum</i> , <i>Chrysitrix distigmata</i> and <i>Lepidobolus deserti</i> with emergent <i>Eucalyptus gongylocarpa</i> . This community occurs on yellow sands on flats and slopes.
E9	Very open scrub mallee of <i>Eucalyptus mannensis</i> subsp. <i>mannensis</i> with <i>Grevillea juncifolia</i> and <i>Hakea francisiana</i> over <i>Cryptandra distigma</i> , <i>Acacia ligulata</i> and mixed low shrubs over <i>Triodia desertorum</i> with emergent <i>Eucalyptus gongylocarpa</i> . This community occurs on yellow sand on slopes and flats.
E10	Open scrub mallee to very open scrub mallee of <i>Eucalyptus concinna</i> with <i>Eucalyptus platycorys</i> over <i>Hakea francisiana</i> , <i>Cryptandra distigma</i> , <i>Acacia rigens</i> and mixed shrubs over <i>Triodia rigidissima</i> and <i>Chrysitrix distigmata</i> with <i>Leptosema chambersii</i> . This community occurs on orange-red sandy loams on slopes and flats.
E11	Open scrub mallee to very open scrub mallee of <i>Eucalyptus platycorys</i> with <i>Eucalyptus concinna</i> over <i>Acacia helmsiana</i> , <i>Grevillea juncifolia</i> , <i>Hakea francisiana</i> and mixed shrubs over <i>Triodia desertorum</i> and <i>Chrysitrix distigmata</i> . This community occurs on orange-yellow sandy loams on slopes and flats.

E12	Open scrub mallee to very open scrub mallee of <i>Eucalyptus trivalva</i> with <i>Eucalyptus rigidula</i> over <i>Hakea francisiana</i> , <i>Bertya dimerostigma</i> , <i>Acacia helmsiana</i> , <i>Cryptandra distigma</i> and <i>Grevillea juncifolia</i> over <i>Triodia rigidissima</i> , <i>Triodia desertorum</i> , <i>Chrysitrix distigmata</i> and <i>Halgania cyanea</i> . This community occurs on orange and red-orange sandy loams on flats and swales.
E13	Low open mallee woodland of <i>Eucalyptus youngiana</i> over low shrubland of <i>Grevillea didymobotrya</i> subsp. <i>didymobotrya</i> , <i>Cryptandra distigma</i> , <i>Banksia elderiana</i> , <i>Calothamnus gilesii</i> , <i>Acacia desertorum</i> var. <i>desertorum</i> and other <i>Acacia</i> spp. over open <i>Triodia</i> spp. hummock grassland with <i>Chrysitrix distigmata</i> and some low myrtaceous shrubs (and occasional emergent <i>Eucalyptus gongylocarpa</i>). This community occurs on orange-yellow sandy loams on lower slopes and flats.
E14	Low open mallee woodland of <i>Eucalyptus leptophylla</i> or <i>Eucalyptus horistes</i> over open low shrubland of <i>Daviesia ulicifolia</i> subsp. <i>aridicola</i> , <i>Callitris verrucosa</i> and mixed <i>Acacia</i> spp., over <i>Triodia</i> spp., <i>Androcalva melanopetala</i> , <i>Dysphania kalpari</i> and other short-lived perennial or annual herbs. This community occurs on highly leached red-brown-white sandy-clayey soils in swales and drainage areas.
ACACIA WOODLAND	
A1	Low woodland to tall shrubland of <i>Acacia aneura</i> over <i>Aluta maisonneuvei</i> subsp. <i>auriculata</i> , <i>Eremophila latrobei</i> , <i>Phebalium canaliculatum</i> , <i>Prostanthera</i> spp. and mixed shrubs. This community occurs on orange sandy loams or clay loams with some laterite pebbles on flats.
SHRUBLANDS	
S1	Shrubland of <i>Melaleuca hamata</i> with <i>Hakea francisiana</i> and mixed shrubs over <i>Triodia desertorum</i> with emergent <i>Eucalyptus</i> spp.. This community occurs on yellow and orange sand on slopes and flats.
S2	Shrubland of <i>Acacia sibina</i> with <i>Grevillea juncifolia</i> and <i>Eucalyptus youngiana</i> over <i>Phebalium canaliculatum</i> , <i>Grevillea acuaria</i> and mixed shrubs over <i>Triodia desertorum</i> . This community occurs on red clay loams in seasonally wet areas.
S3	Shrubland of <i>Allocasuarina spinosissima</i> and <i>Allocasuarina acutivalvis</i> subsp. <i>acutivalvis</i> with <i>Grevillea juncifolia</i> and <i>Hakea francisiana</i> over <i>Triodia desertorum</i> with emergent <i>Eucalyptus youngiana</i> and <i>Eucalyptus gongylocarpa</i> . This community occurs on yellow sand on slopes.
S4	Shrubland to open shrubland of <i>Acacia desertorum</i> var. <i>desertorum</i> and mixed low shrubs over <i>Triodia desertorum</i> with occasional emergent mallee <i>Eucalyptus</i> spp. This community occurs on yellow or orange sands on mid-slopes.
S5	Shrubland to open shrubland of <i>Acacia sibina</i> with <i>Phebalium tuberculosum</i> over <i>Enekbatus eremaeus</i> , <i>Bertya dimerostigma</i> , <i>Homalocalyx thryptomenoides</i> , <i>Baekkea</i> sp. Great Victoria Desert (A.S. Weston 14813), <i>Melaleuca hamata</i> and mixed low shrubs over <i>Triodia desertorum</i> and <i>Chrysitrix distigmata</i> with occasional emergent <i>Eucalyptus gongylocarpa</i> and <i>Eucalyptus youngiana</i> . This community occurs on yellow-orange sands on flats and lower slopes.
S6	Low shrubland of <i>Thryptomene biseriata</i> , <i>Allocasuarina spinosissima</i> , <i>Allocasuarina acutivalvis</i> subsp. <i>acutivalvis</i> , <i>Jacksonia arida</i> , <i>Calothamnus gilesii</i> , <i>Acacia fragilis</i> , <i>Conospermum toddii</i> (P4), <i>Pityrodia lepidota</i> , <i>Lomandra leucocephala</i> , <i>Anthotroche pannosa</i> and mixed low shrubs over <i>Triodia desertorum</i> with <i>Lepidobolus deserti</i> with emergent <i>Eucalyptus gongylocarpa</i> , <i>Eucalyptus youngiana</i> , <i>Eucalyptus ceratocorys</i> and <i>Eucalyptus mannensis</i> subsp. <i>mannensis</i> . This community occurs on yellow sand dunes.

EXISTING ENVIRONMENT

S7	Low shrubland to low open shrubland of <i>Enekbatus eremaeus</i> , <i>Acacia desertorum</i> var. <i>desertorum</i> , <i>Verticordia helmsii</i> , <i>Homalocalyx thryptomenoides</i> , <i>Leptospermum fastigiatum</i> , <i>Allocasuarina spinosissima</i> , <i>Baeckea</i> sp. Great Victoria Desert (A.S. Weston 14813), <i>Leptosema chambersii</i> and mixed low shrubs over <i>Triodia desertorum</i> and <i>Chrysitrix distigmata</i> with occasional emergent mallee <i>Eucalyptus</i> species, <i>Grevillea juncifolia</i> and <i>Hakea francisiana</i> . This community occurs on yellow and orange sands on lower slopes, undulating plains and swales.
S8	Low open shrubland of <i>Calothamnus gilesii</i> , <i>Persoonia pertinax</i> , <i>Thryptomene biseriata</i> and <i>Leptospermum fastigiatum</i> with <i>Anthotroche pannosa</i> , <i>Acacia helmsiana</i> , <i>Microcorys macredieana</i> , <i>Micromyrtus stenocalyx</i> and mixed low shrubs over <i>Triodia desertorum</i> with <i>Lepidobolus deserti</i> , <i>Chrysitrix distigmata</i> and <i>Caustis dioica</i> with emergent <i>Eucalyptus youngiana</i> , <i>Eucalyptus gongylocarpa</i> and <i>Eucalyptus ceratocorys</i> . This community occurs on yellow sands flats adjacent to yellow sand dunes and undulating sandplains.
S9	Low open shrubland of <i>Melaleuca hamata</i> and mixed <i>Acacia</i> spp. (including <i>Acacia fragilis</i> , <i>Acacia ligulata</i> and <i>Acacia sibina</i>) with <i>Hannafordia bissillii</i> subsp. <i>bissillii</i> , <i>Grevillea didymobotrya</i> subsp. <i>didymobotrya</i> , <i>Mirbelia seorsifolia</i> over <i>Triodia</i> spp. hummock grassland with <i>Leptosema chambersii</i> , <i>Chrysitrix distigmata</i> , <i>Aristida contorta</i> and <i>Goodenia xanthosperma</i> , with emergent eucalypt mallees. This community occurs on orange-red sandyclay loam, in swales and on flats.
S10	Low open shrubland of <i>Banksia elderiana</i> , <i>Calothamnus gilesii</i> , <i>Grevillea didymobotrya</i> subsp. <i>didymobotrya</i> , <i>Acacia desertorum</i> var. <i>desertorum</i> and <i>Grevillea secunda</i> (P4) with <i>Leptospermum fastigiatum</i> and emergent <i>Eucalyptus youngiana</i> (and <i>Eucalyptus rosacea</i>) over <i>Triodia</i> spp. hummock grassland with <i>Chrysitrix distigmata</i> . This community occurs on orange-yellow undulating sandplains and flats.
CHENOPOD SHRUBLAND	
C1	Low shrubland of <i>Atriplex ?vesicaria</i> with <i>Eremophila decipiens</i> subsp. <i>decipiens</i> and <i>Acacia colletioides</i> . This community occurs on red-brown clay loams on clay pans. <i>Callitris preissii</i> with <i>Eucalyptus</i> spp. over mixed shrubs are found in adjacent pockets.
OTHER	
D	Disturbed area
B	Burnt communities (usually assumed to be burnt less than five years prior to the field survey)



VIMY RESOURCES

TERRAIN ANALYSIS AND MATERIALS CHARACTERISATION
FOR THE MULGA ROCK URANIUM PROJECT

Figure 2.30: Vegetation distribution throughout the MRUP (MCPL, 2015a) – See Table 2.6)



2.9 FIRE

Bushfires play an important role in the development and function of the Yellow Sand Plain (YSP), which encompasses the MRUP. Bushfires typically start from lightning strikes during summer storms, and rapidly spread through the spinifex country, with the propagation of the fires strongly influenced by the distribution of previous burns and resulting fuel loads. Given this influence, fire patterns and scars form a complex mosaic across the landscape as shown in Figure 2.31.

The distribution, type and age of the native vegetation within the YSP is a function of the fire regime. In most areas, the vegetation rarely exceeds 50 years of age, as the older vegetation is preferentially burnt given the developed fuel loads and continuity of vegetation. The effect of fire on the landscape within the MRUP is clearly shown in Plate 2.7 and Plate 2.8.

Bushfires also influence pedogenic (soil) development and wind and water erosion processes. During intense fires, which effectively remove all of the vegetation (Plate 2.8), the sandy soil surface is exposed to the prevailing winds and any organic matter accumulation is blown away depleting the surface of organic carbon and nutrients, and limiting the extent to which topsoil development can occur. The exposed sandy surface, with negligible organic matter to bind the sand particle together (i.e. form structure) or vegetation to form a protective boundary layer, is then susceptible to wind erosion, and large dust storms typically occur following high intensity fires. The risk of water erosion also increases following intense fire as the loss of vegetation makes the surface more susceptible to rain-drop impact, and subsequent displacement and erosion of surface particles, and moisture loss (from evaporation) which decreases the permeability or infiltration of the soils, such that infiltration-excess overland flow occurs, even in the sandy soils.

Plate 2.7: Extent of the November 2014 bushfire within the MRUP



Plate 2.8: Intensity of the November 2014 bushfire within the MRUP



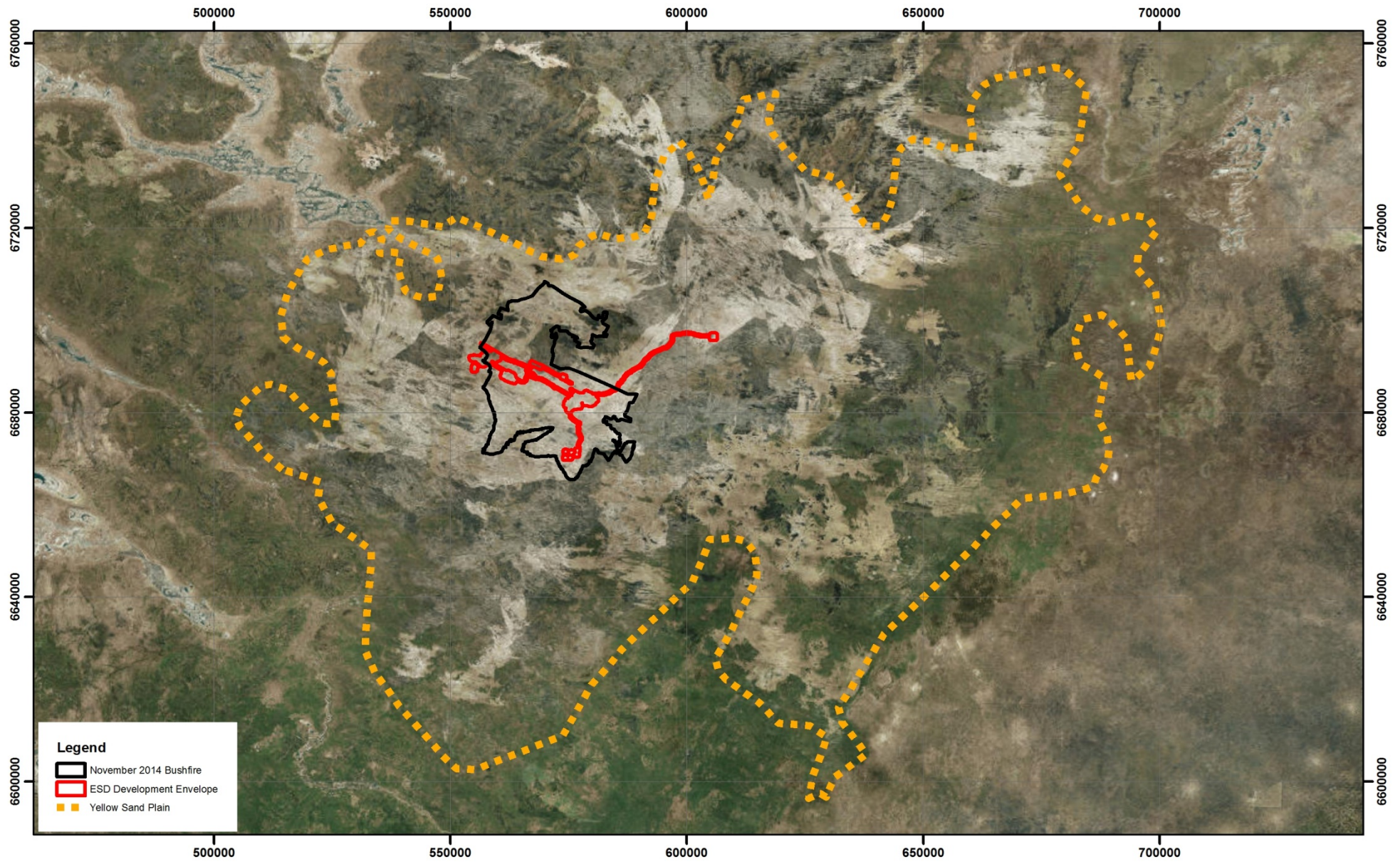
A compilation of bushfires within the MRUP region, since 1995, is shown in Figure 2.32. The most recent large fire occurred in November 2014 when a low to medium fire burnt close to 80,000 ha within a five day period, after having started from a single lightning strike. The extent of the November 2014 fire is shown in Figure 2.32 and the impact of the fire on the native vegetation is shown in Plate 2.7 and Plate 2.8. The complexity and spatial pattern shown in Figure 2.32 is important from a fauna perspective. With any fire there are usually areas that remain unburnt (Plate 2.9) and these represent important refuge areas for the animals to retreat into (Plate 2.10). With the 80,000 ha November bushfire, the area of residual refugia was < 2,000 (< 2.5% of the burnt landscape). The utilisation of these refuge areas results in a significant increase in animal activity and predatory behaviour, and thus fire plays an important part in the overall dynamics and functioning of the terrestrial fauna in the MRUP region.

Plate 2.9: Complexity of the fire front leaving some area unburnt



Plate 2.10: Fire refuge areas



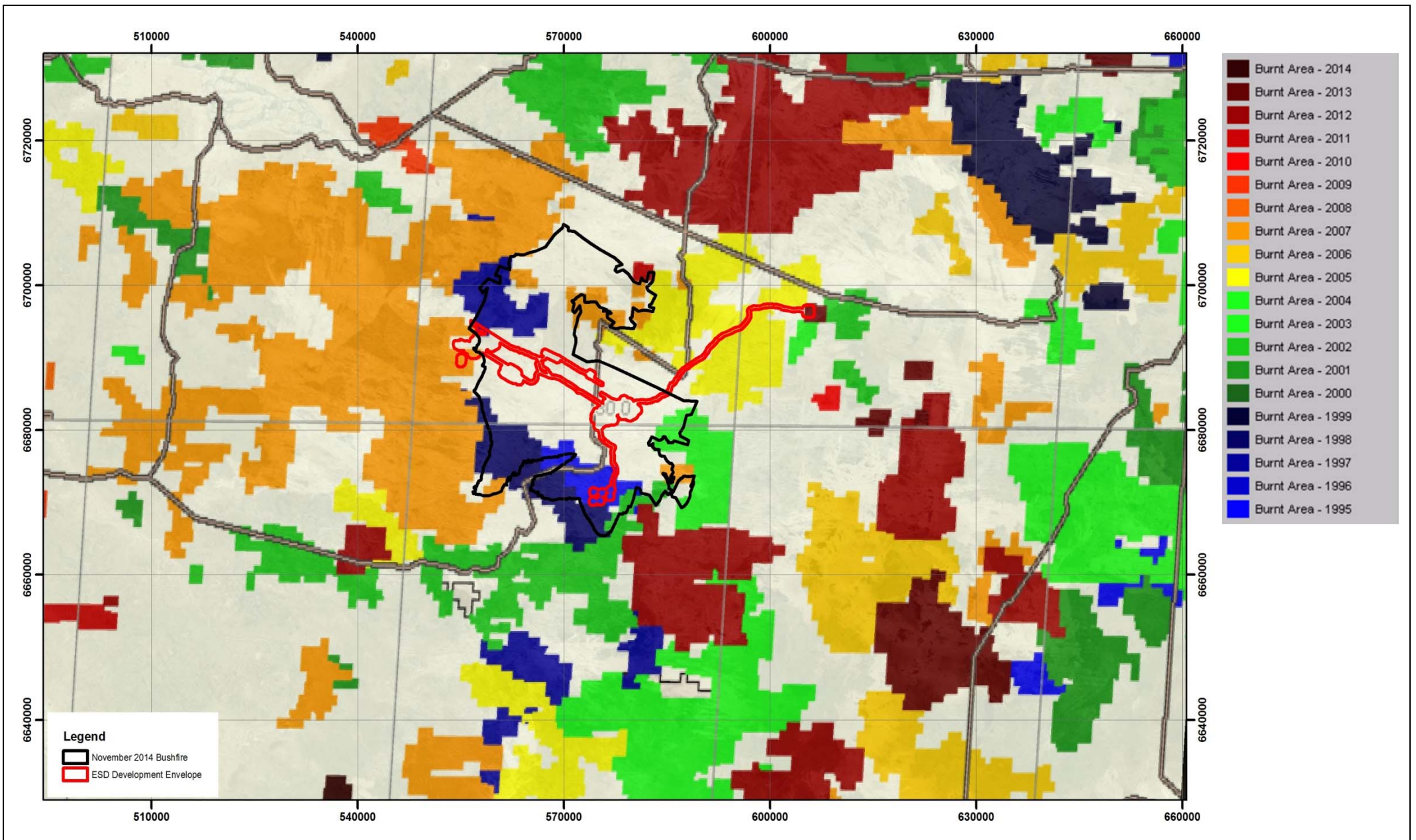


VIMY RESOURCES

TERRAIN ANALYSIS AND MATERIALS CHARACTERISATION
FOR THE MULGA ROCK URANIUM PROJECT

Figure 2.31: Complexity of fire scars within the MRUP region





VIMY RESOURCES

TERRAIN ANALYSIS AND MATERIALS CHARACTERISATION FOR
THE MULGA ROCK URANIUM PROJECT

Figure 2.32: Bushfires from 1995 to 2014 (Data collated from the Landgate's Firewatch)



3 STUDY METHODOLOGY

3.1 SOIL SAMPLING

3.1.1 TRENCH EXCAVATION

To characterise the surficial soils throughout the MRUP, deep trench excavation was undertaken to expose the soil profile. Trenches were excavated using an 8 tonne backhoe, with an extendable arm, to reach a maximum depth of 4 m. Where possible, soil trenches were excavated directly adjacent to existing vegetation (Plate 3.1) to allow for an assessment of the rooting characteristics of the vegetation. By using this approach an appreciable section of the soil profile is exposed for morphological characterisation, as well as soil sampling (Plate 3.2).

Plate 3.1: Deep trench excavation directly adjacent to existing vegetation for this study



For this investigation a total of 24 deep soil trenches were excavated across the Shogun, and Ambassador West and East Deposits. Unfortunately, due to mechanical issues with the backhoe sampling at the Emperor and Princess Deposits was not undertaken. However, the same assemblage of soils occurs throughout these deposits, and these were adequately sampled from the Shogun, and Ambassador West and East Deposits.

Details of the soil sampling location, and the depths sampled, are provided in Table 3.1, whilst a map showing their location within the Shogun and Ambassador Pits is presented in Figure 3.1 and Figure 3.2.

3.1.2 COLLECTION OF SOIL SAMPLES

Soil samples were collected directly from the exposed soil profile (Plate 3.3). The objective of the sampling was to collect samples from each morphologically distinct soil material, so that laboratory analysis could be undertaken (Section 3.2) to characterise the physical, chemical and hydraulic properties of the materials. Disturbed soil samples were placed

immediately into plastic sealable bags, whilst undisturbed cores were wrapped in plastic film (Glad Wrap) and then secured with tape to ensure that the sample remained intact during transport.

Table 3.1: Details of the deep trenches examined in this investigation

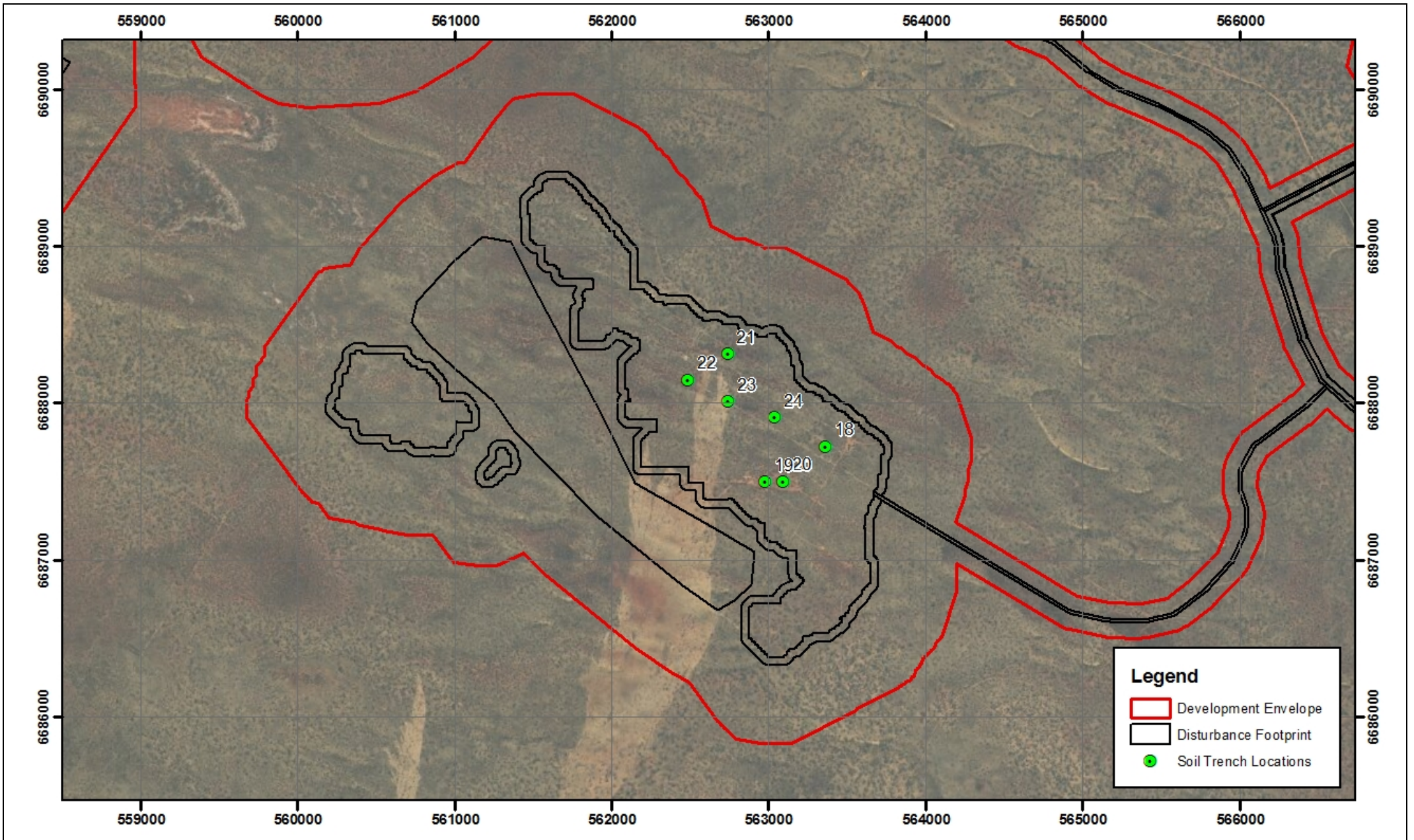
Trench ID	Deposit/Area	GDA94 Zone 51		Depth (m)	
		Easting	Northing		
1	Reinjection Bore	575,532	6,671,194	4.0	
2	Ambassador West	577,016	6,681,557	2.4	
3		576,910	6,681,729	2.7	
4		576,893	6,681,746	3.0	
5		576,900	6,681,737	2.0	
6		576,834	6,681,774	3.2	
7		576,700	6,681,849	3.0	
8		576,452	6,682,003	4.0	
9		575,810	6,682,383	3.0	
10		578,555	6,682,500	2.2	
11		578,567	6,682,569	1.9	
12		578,556	6,682,392	2.8	
13		Ambassador East	578,556	6,682,318	1.6
14			578,575	6,682,284	1.4
15			579,703	6,682,214	2.8
16			579,774	6,682,574	2.7
17			579,866	6,682,497	2.6
18	563,371	6,687,721	2.6		
19	562,986	6,687,494	2.6		
20	563,103	6,687,496	3.2		
21	Shogun	562,746	6,688,309	0.9	
22		562,493	6,688,145	2.9	
23		562,747	6,688,006	3.0	
24		563,043	6,687,905	2.8	

3.1.3 SOIL PROFILE DESCRIPTION

All soil profiles assessed in the field were described in accordance with McDonald and Isbell (2009), whilst the landsurface was assessed using the classification scheme outlined in McDonald *et al.* (2009). Soil profiles were assessed for degree of horizonation, nature of contacts between horizons, presence and abundance of coarse fragments (i.e. gravels) and mottling, and structure, fabric and field texture of soil materials.

3.1.4 SEMI-QUANTITATIVE ASSESSMENT OF ROOT ABUNDANCE

A semi-quantitative assessment of root abundance was made down the soil profile to establish the rooting distribution of the characteristic vegetation within the MRUP. The semi-quantitative assessment followed the rating classes and approach recommended by McDonald *et al.*, 2009) and provided in Table 3.2.

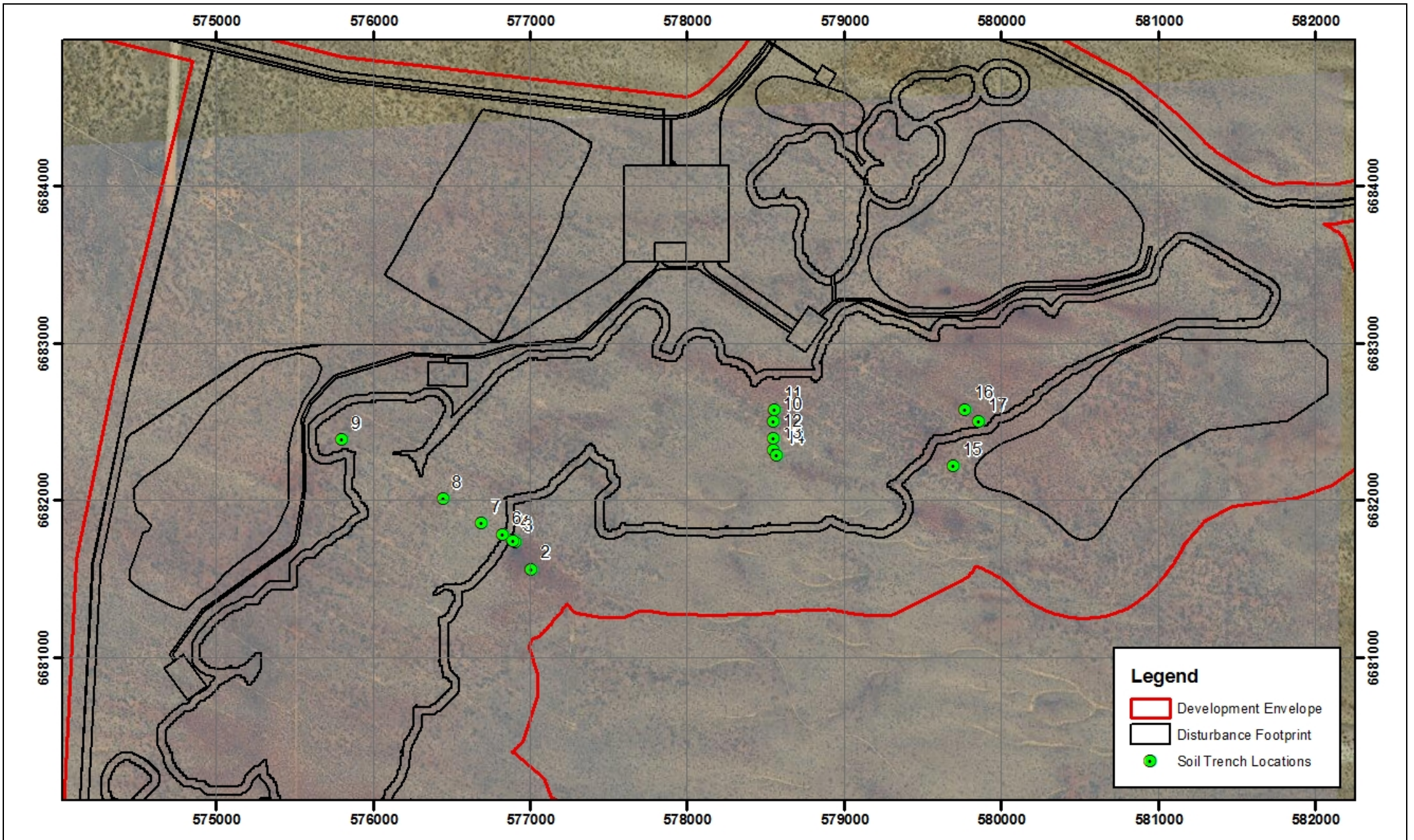


VIMY RESOURCES

TERRAIN ANALYSIS AND MATERIALS CHARACTERISATION
FOR THE MULGA ROCK URANIUM PROJECT

Figure 3.1: Map showing the soil and geochemical sampling locations within the Shogun Deposit





VIMY RESOURCES

TERRAIN ANALYSIS AND MATERIALS CHARACTERISATION
FOR THE MULGA ROCK URANIUM PROJECT

Figure 3.2: Map showing the soil and geochemical sampling locations within the Ambassador West and East Deposits



Plate 3.2: Exposed soil profile achieved through deep trench excavation in this investigation



Plate 3.3: Collection of soil samples from the exposed soil profile surface



Table 3.2: Semi-quantitative assessment of root abundance (McDonald *et al.*, 2009)

Classification	Number of roots/0.01 m ² (10 cm × 10 cm)	
	Very fine (<1mm) and Fine (1-2mm) roots	Medium (2 – 5mm) and Coarse (>5mm) roots
0 = No roots	0	0
1 = Few	1 – 10	1 or 2
2 = Common	10 – 25	2 – 5
3 = Many	25 – 200	> 5
4 = Abundant	> 200	> 5

3.2 LABORATORY ANALYSIS

3.2.1 PHYSICAL, CHEMICAL AND HYDRAULIC PROPERTIES

The physical and chemical properties of the soil materials were assessed at Soilwater Analysis and CSBP Laboratories in Perth. All samples collected in the field were analysed for pH, EC and gravimetric moisture to accurately establish the surface soil horization (i.e. distinction between topsoil, subsoil and overburden), whilst the remaining properties were assessed on a representative number of samples from all soil materials.

Table 3.3: Physical and chemical properties examined in the laboratory

Parameter	Method	Standard Reference
<i>Soil Physical Properties</i>		
Particle size distribution	Pipette sedimentation	McKenzie <i>et al.</i> (2002)
Gravel content	Sieve analysis (> 2 mm soil fraction)	
Bulk density	Constant volume	
Structural stability	Emerson dispersion	
<i>Soil Hydraulic Properties</i>		
Gravimetric moisture content	Oven drying at 105°C	McKenzie <i>et al.</i> (2002)
Saturated hydraulic conductivity	Constant head permeameter	
Water retention characteristics	Pressure plate equipment	
<i>Soil Chemical Properties</i>		
pH	1:5 soil/water extraction	Rayment and Lyons (2011)
Electrical conductivity (EC; salinity)	1:5 soil/water extraction	
Macro-nutrients		
- Mineralised Nitrogen (N) (NH ₄ -N + NO ₃ -N)	KCl extractable	
- Colwell Phosphorus (P)	NaHCO ₃ extraction	Rayment and Lyons (2011)
- Colwell Potassium (K)	NaHCO ₃ extraction	
- Sulfur (S)	KCl extractable S/ICP	
Organic Carbon	Walkley Black Method	Rayment and Lyons (2011)
Exchangeable cations – Calcium (Ca), Magnesium (Mg), Sodium (Na), Potassium (K)	NH ₄ Cl extraction	Rayment and Lyons (2011)
Cation Exchange Capacity (CEC)	Sum of exchangeable cations	-

Parameter	Method	Standard Reference
Exchangeable Sodium Percentage (ESP; sodicity)	$ESP = (Ex. Na/CEC) \times 100$	-

3.2.2 GEOCHEMICAL TESTING

In addition to the surficial soil testing described above (Section 3.1 and 3.2), the baseline geochemical condition or status of the deeper overburden materials was also assessed. This testing involved screening the laboratory pulp samples, from a recent drilling program, for the following parameters:

- pH: this represents the inherent or existing pH of the material and was assessed using a standard 1:5 soil/water extract. The pH results can be used to determine if previous oxidation of sulfides has occurred, and if there is residual released acidity, and the presence/absence of potential acid neutralising materials. For example, if the overburden material has a pH < 7 then it effectively contains no readily available Acid Neutralising Capacity (ANC), whilst if the pH is between 7 and 8.5 then there is minor ANC afforded by gypsum, and if the pH > 8.5 then there is appreciable ANC due to carbonates. If the pH is < 4, then it is likely that previous oxidation of sulfides has occurred.
- Peroxide pH (pH_{ox}): this represents the pH of the material after complete oxidation, namely from sulfides, following hydrogen peroxide (H₂O₂) addition. If the pH_{ox} drops below 3, then there is a fair likelihood that residual sulfides are present in the material. If the pH_{ox} remains above 4 then there are either negligible sulfides or sufficient ANC to neutralise any released acidity.
- Electrical Conductivity (EC): this represents the salinity of the material and is assessed using a standard 1:5 soil/water extract. In essence, EC values < 40 mS/m are considered non-saline, between 40 – 80 mS/m are moderately saline, whilst values > 100 mS/m are considered highly saline and have the potential to impact on plant growth.

For the geochemical testing of the overburden materials, laboratory pulps were screen tested at 2 m vertical intervals, over the entire drillhole length. A total of 12 drillholes from across the Shogun, Ambassador and Princess Deposits were assessed with their details provided in Table 3.4, whilst a map showing their location is provided in Figure 3.1 and Figure 3.2. Given the depth of the drillholes, a total of 235 samples were screen tested.

Table 3.4: Drillholes screen tested in this investigation

Deposit	Drillhole ID	GDA94 Zone 51		Collar Elevation (m AHD)	Depth (m)
		Easting	Northing		
Shogun	5719	562,475	6,688,171		26.5
	5723	563,015	6,687,645		29.0
	5728	563,587	6,686,912		27.5
Ambassador West	5772	576,014	6,681,770	329.2	41.0
	5773	576,265	6,682,110	331.4	35.0
	5774	576,584	6,681,912	334.7	41.0
Ambassador East	5878	578,607	6,682,298	347.2	50.0
	5940	579,687	6,682,610	331.9	39.0
Princess	5549	578,793	6,684,148	339.7	36.0
	5569	579,349	6,684,098	340.1	34.5

Deposit	Drillhole ID	GDA94 Zone 51		Collar Elevation	Depth (m)
	5605	578,913	6,683,653	339.8	39.0
	5614	578,964	6,683,963	339.6	40.0

3.2.3 EROSION TESTING

Laboratory-scale rainfall erosion tests were undertaken on the following samples, which represent the major surficial soil materials throughout the MRUP:

- 'C1': Calcrete (T2, Topographic Depression on the eastern margin of the Ambassador West Deposit; Sample collected from 1 – 2 m depth)
- 'E3': Sand (T8, E3 Vegetation Type within the central portion of the Ambassador West Deposit; Sample collected from 1 – 2 m depth))
- 'E5': Sand (T9, E5 Vegetation Type within the western portion of the Ambassador West Deposit; Sample collected from 1 – 2 m depth)
- 'S6': Sand (T6, S6 Vegetation Type within the large dune along the eastern margin of the Ambassador West Deposit; Sample collected from 1 – 2 m depth))

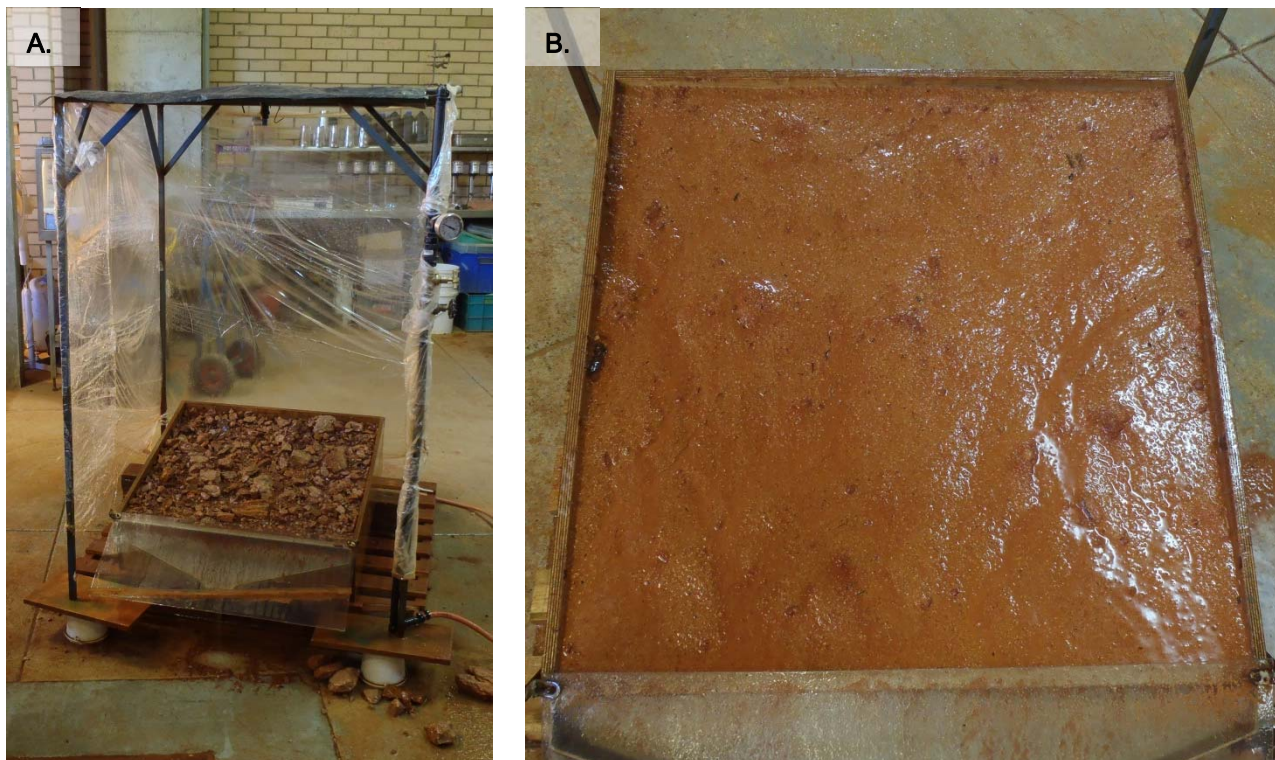
3.2.3.1 Rainfall Simulator

A laboratory-scale rainfall simulator (Plate 3.4) was used to measure the interrill (raindrop impact) erodibility of each material. The rainfall simulator was designed to apply water at an intensity of approximately 100 mm/hr, with a raindrop size and spatial distribution closely resembling natural rainfall. An intensity of 100 mm/hr corresponds to a 1:20, 1:50 and 1:100 year ARI storm event of approximately 6, 10, and 15 min duration, respectively (BOM, 2015a).

Prior to testing, each material was placed into a 0.75 x 0.75 x 0.20 m container and lightly compacted to approximate the expected field conditions. The base of the container was free draining to avoid saturated conditions and air entrapment within the samples. Each material was pre-treated by sequentially wetting and drying the surface to allow natural organisation and settling of the soil particles.

The container was set at a slope angle of 10° to simulate the proposed landform batter angle. The materials were then subjected to a simulated rainfall of approximately 100 mm/hr, and 10 samples of the resulting surface runoff were collected over a 4 hour period. Runoff volume and sediment loss in each sample were determined gravimetrically. Measurements from the rainfall simulator were used to calculate soil erodibility parameters required for the WEPP erosion model. The methods used for calculating these parameters are discussed further in Section 3.2.3.6.

Plate 3.4: Laboratory rainfall simulator. (A) sample C1, (B) sample E3



3.2.3.2 Rill Erosion Measurements

Laboratory scale testing was completed to measure the rill erodibility (K_r) and critical shear stress (τ_c) of the materials under overland flow conditions. The rill erosion test was conducted using SWA's 1.8 metre-long erosion flume (Plate 3.5). The laboratory testing was designed to expose the materials to a range of overland flow depths to simulate storm events of different sizes, and to measure the resulting sediment content in the surface runoff generated by rill erosion.

Each material was subjected to a series of different overland flow rates, and the following measurements were made for each:

- A timed sample of the resulting surface runoff was collected. Surface flow rate and sediment loss were then determined gravimetrically.
- A measurement of surface flow velocity was made using a dye tracer method. The initial breakthrough time of the dye was measured, and the "average" flow velocity was calculated by applying a correction factor ($\alpha = 0.5$) according to (Zhang *et al.*, 2010).
- Measurements of rill width were made at three standardised locations along the rill.

Rill erosion measurements were used to calculate rill erodibility parameters required for the WEPP erosion model. The methods used for calculating these parameters are discussed further in Section 3.2.3.6.

Plate 3.5: Laboratory-scale, rill erosion flume (sample E5).



3.2.3.3 Rainfall Erosion Modelling

The Watershed Erosion Prediction Project (WEPP) model (Flanagan and Livingston, 1995) was used to predict erosion rates from the surface of the proposed post-mine landform given a range of different surface materials placed at a range of slope angles. WEPP accepts input files describing the local soils, climate, slope geometry, and land management regime, and uses them to derive daily sediment loss predictions over a 100-year period.

The SIBERIA model (Willgoose, 2005) was used to predict how the design landform would erode and evolve in the long-term (i.e. 10,000 years), given the most likely development scenarios. The SIBERIA model was calibrated to the average annual erosion rate predicted by WEPP, and used to develop a 3-D picture of landform evolution on an annual time step.

Model input values and assumptions are discussed in the following sections.

3.2.3.4 Climate Data

One of the key inputs to the WEPP model is a 100-year synthetic climate file, typically developed using the CLIGEN stochastic weather generator (Yu, 2003). Given the remote nature of the site, sufficient rainfall data was not available to generate a completely new CLIGEN file. Instead, a CLIGEN file derived for Kalgoorlie (227 km to the south-west of the MRUP) was re-calibrated using the available climate data from the closest long-term climate station at Laverton (BOM station #012305, located approximately 183 km to the north-west of the MRUP) (BOM, 2015b), and the available on-site monitoring data.

Figure 3.3a and Figure 3.3b demonstrate that the 100-year synthetic CLIGEN file used in this investigation is generally consistent with available climate data in the region. Figure 3.3a depicts the frequency of 24-hour storm depths, and demonstrates that the storm intensities predicted by CLIGEN are generally consistent with the available monitoring data,

including the Intensity-Frequency-Duration (IFD) curves supplied by the Bureau of Meteorology (BOM, 2015a). For the more extreme storms (AEP < 0.03), the CLIGEN predicted greater rainfall intensities than are indicated by the actual climate record, and this is likely to result in modelled erosion rates that greater than the erosion rates that will actually be experienced (i.e. this will result in a “conservative” erosion estimate).

Figure 3.3b depicts the average monthly rainfall depth within the CLIGEN file, and shows that it generally falls within the range of monthly averages derived from on-site climate data and data from Laverton. Where the CLIGEN monthly average fell outside of the range of local data, it fell above the upper limit of the measured average. This results in a slightly greater total annual rainfall depth of 299 mm/year in the CLIGEN file, as compared to the measured average annual rainfall depth of 276 mm/yr at Laverton (1985-2014 data).

Figure 3.4 illustrates the annual total rainfall for both the CLIGEN file and measured data sets. It demonstrates that the annual total rainfall depths of the CLIGEN file is slightly higher than the average of the measured data, and that year-to-year variability is similar.

3.2.3.5 Elevation Data

The WEPP model uses slope profile information to model the expected erosion and deposition rates along a unit-width of slope. Three linear slope profiles – 5°, 10°, and 15° linear slopes, each 10 m in height – were input to simulate the range of design options being considered for the post-mine landforms.

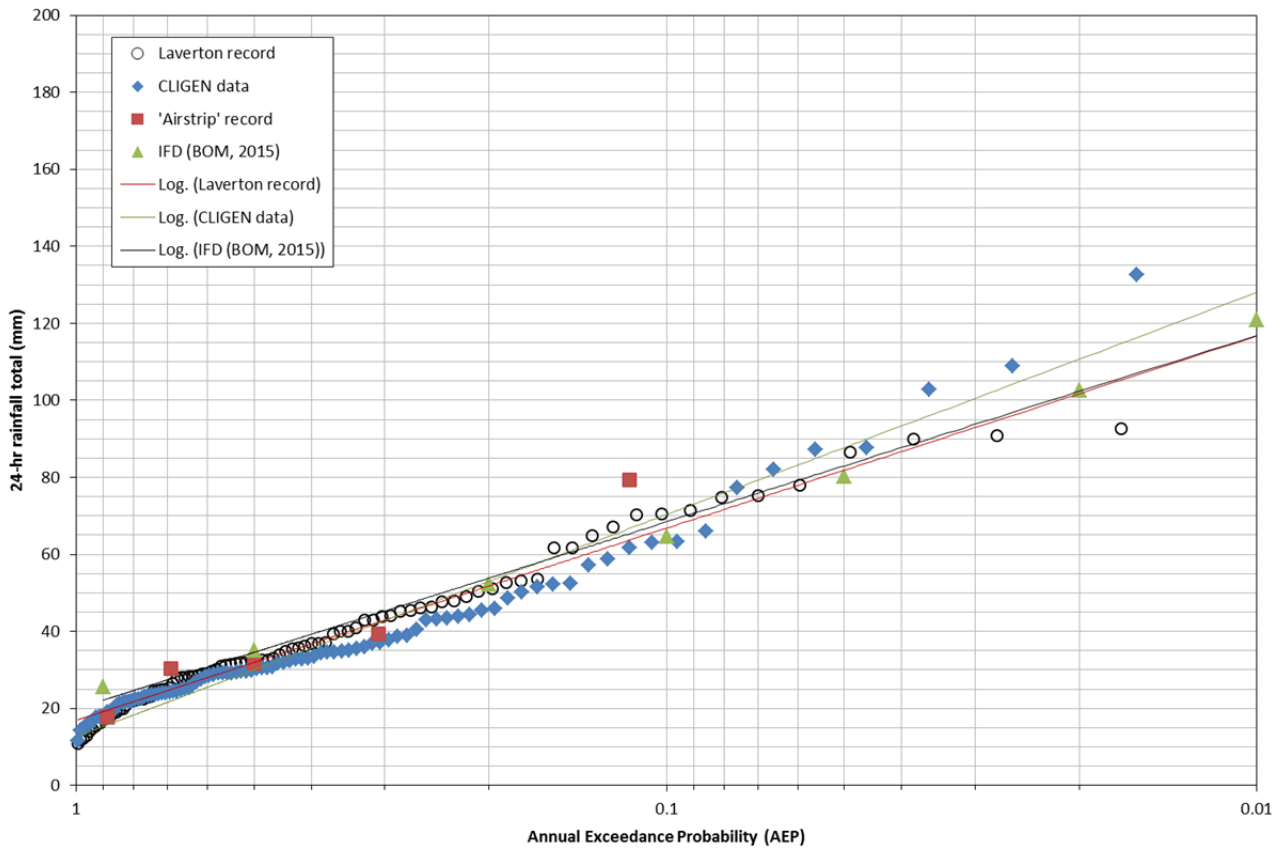
The SIBERIA model uses a digital elevation model (DEM) to predict erosion and deposition, and modifies the DEM accordingly at each time step to predict the final shape of the landform. An input DEM was developed in SURPAC by combining the proposed landform design with the supplied 2 m topographic contours into a single surface. The surface was sampled at 10 m intervals to create a 10x10 m DEM grid over an approximately 25 km² area. This DEM was then used to assess erosion of the landform, in context with the surrounding landscape.

A second DEM was created for more detailed analysis of the landform in SIBERIA, including the layering properties of multiple rehabilitation materials. This DEM was created by sampling the elevation of only the landform surface (i.e. no surrounding landscape) at 4 m intervals to create a 4x4 m DEM grid of the entire landform. This model considered the elevation of sub-soil layers (i.e. not just the surface cover), and consisted of (1) the base clay/tailings core, (2) a 1 metre-thick calcrete layer ('C1' soil), and (3) a 2 metre-thick surface layer consisting of either 'E3' or 'S6' soil.

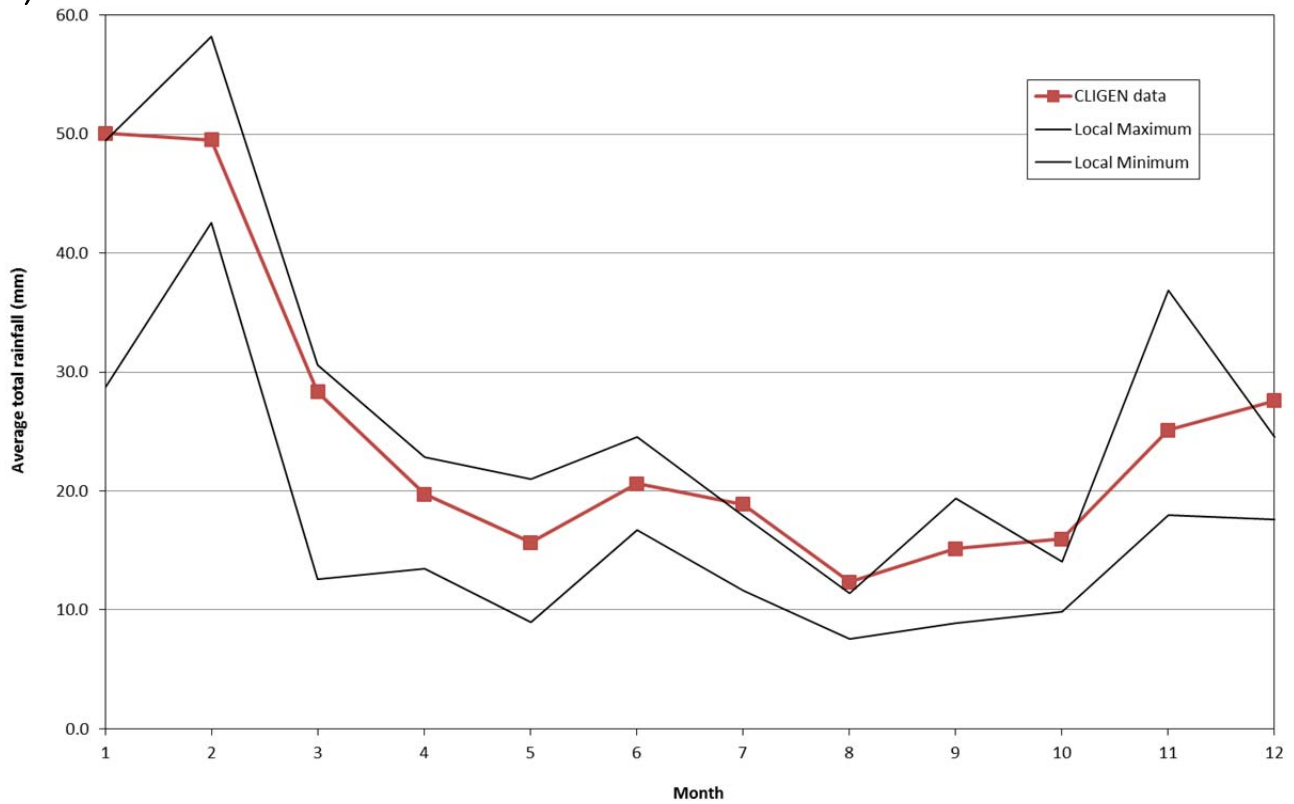
3.2.3.6 Input Soil Parameters

The soil parameters required by WEPP were derived from the laboratory testing undertaken at SWA Laboratories. These parameters include particle size information (% sand, % clay), effective hydraulic conductivity (K_{eff}), interrill erodibility (K_i), rill erodibility (K_r), and soil critical shear stress (τ_c). K_{eff} was estimated by fitting the Green-Ampt equation (Green and Ampt, 1911) to the measured infiltration rates derived from rainfall simulator test. K_i was calculated from the inter-rill erosion rate measured in the rainfall simulator, according to Elliott *et al.* (1989). K_r and τ_c were determined from the shear stress (τ) and rill erosion rate (D_c) measurements collected in the laboratory erosion flume by a linear regression analysis according to the method described by Foster (1982) and Elliott *et al.* (1989). The derived parameters used in the WEPP model are summarised in Table 3.5.

A)



B)

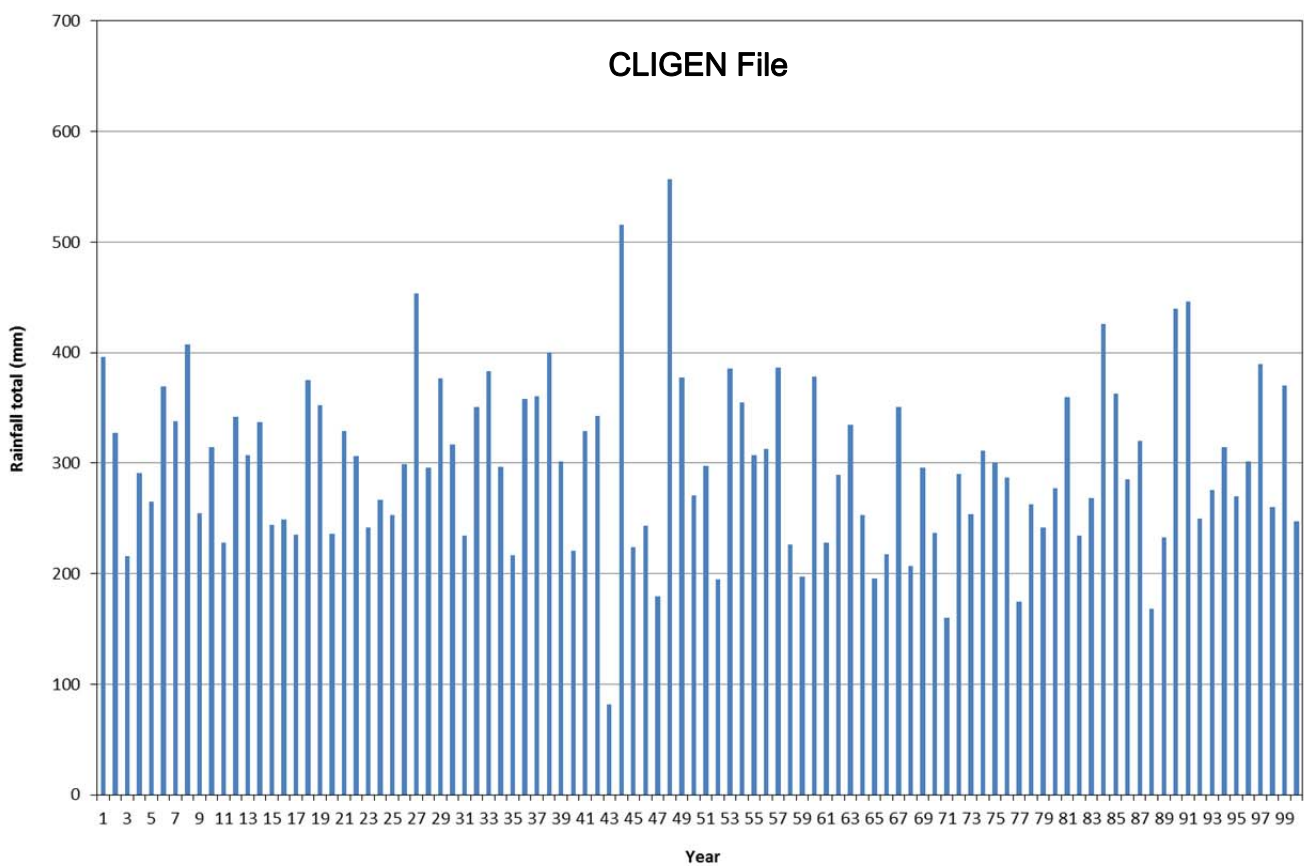
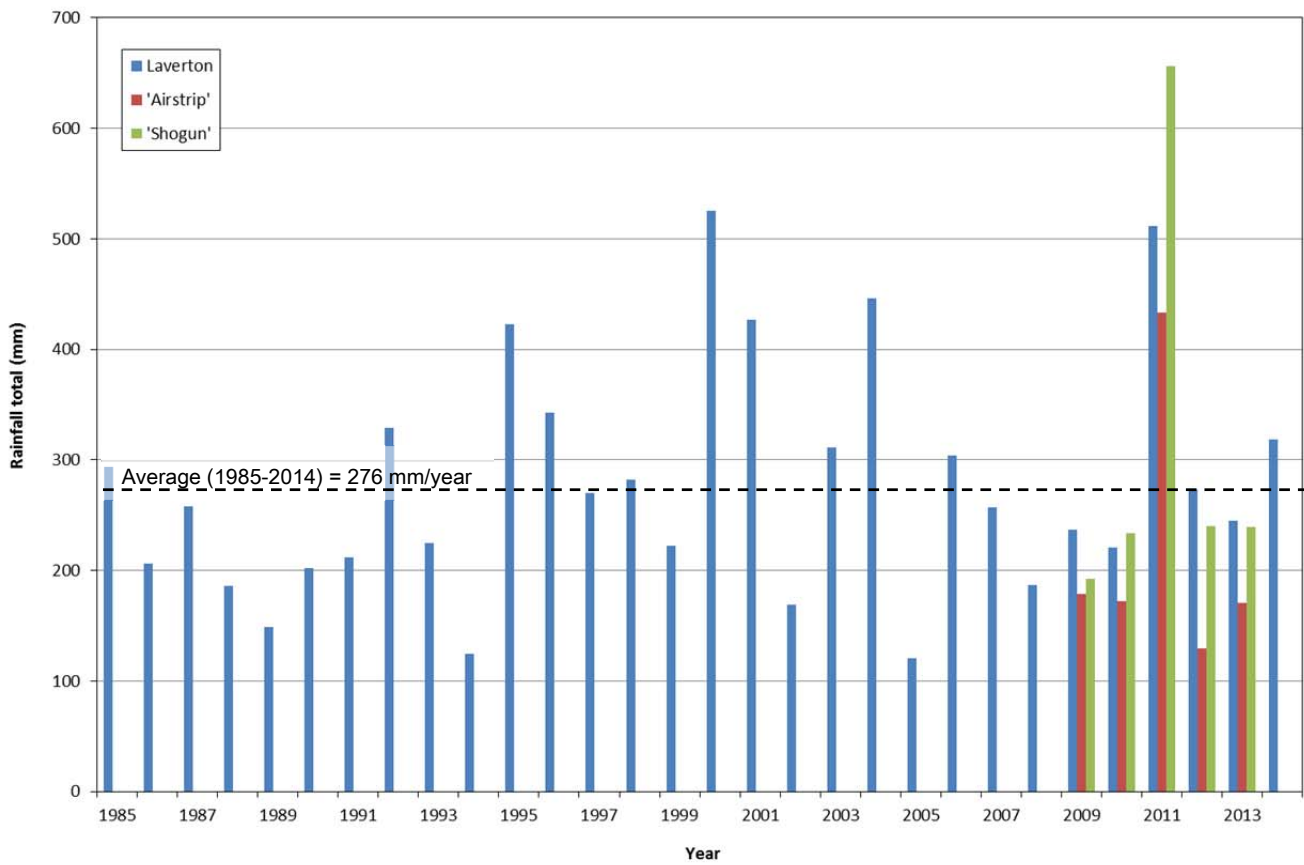


VIMY RESOURCES

TERRAIN ANALYSIS AND MATERIALS
CHARACTERISATION FOR THE MULGA
ROCK URANIUM PROJECT

Figure 3.3: A) 24-hour and B) mean monthly rainfall data





VIMY RESOURCES

TERRAIN ANALYSIS AND MATERIALS
CHARACTERISATION FOR THE MULGA
ROCK URANIUM PROJECT

Figure 3.4: Annual rainfall data



The SIBERIA model was calibrated to the 100-yr average sediment loss rate derived from WEPP, according to the general model calibration methods described in Willgoose (2005). The primary input parameter is the coefficient B_1 in the fluvial transport formula, which defines the magnitude of annual erosion by fluvial processes (rill erosion). The model is also calibrated for diffusive sediment transport (D_z) and the exponent's m_1 and n_1 (exponents on discharge and slope, respectively). The calibrated parameters used in the WEPP model are summarised in Table 3.6.

Table 3.5: Key soil parameters used in the WEPP model.

Material ID	Sand (%)	Clay (%)	OM (%)	CEC (meq/100g)	K_{eff} (mm/hr)	$K_i \times 10^5$ (Kg s / m ⁴)	K_r (s / m)	τ_c (Pa)
C1	88.7	5.9	0.19	17.7	20.2	1.7	0.0006	8.3
E3	91.3	7.5	0.11	1.8	21.7	12	0.0341	1.1
E5	96.1	3.5	0.06	0.8	68.1	17	0.0394	1.0
S6	99.2	0.6	0.09	0.9	100	20	0.0400	0.1

Table 3.6: Key input parameters used in the SIBERIA model.

Material ID	B_1	D_z	m_1	n_1
C1	2.5×10^{-3}	3.5×10^{-4}	1.4	2.10
E3	2.0×10^{-2}	2.0×10^{-3}	1.4	1.18
E5	3.5×10^{-3}	4.5×10^{-4}	1.4	1.35
S6	0.5×10^{-3}	4.5×10^{-4}	1.4	1.80

3.2.3.7 Management Assumptions

The land management input file used in the WEPP model was designed to describe the expected conditions on the remediated waste rock landform. The key features of the input management file include:

- A pre-consolidated soil surface. This means that no further settling is simulated within the model, and that the measured infiltration rates and runoff characteristics apply for the duration of the model (i.e., no further changes in these properties with time). This is reasonable because the laboratory measurements (from which the input parameters were derived) were conducted on pre-consolidated soil samples.
- No vegetation. This assumption will result in conservative (i.e. "worst-case") erosion results, and will apply to the landform during the period prior to vegetation establishment. Subsequent establishment of vegetation will act to enhance the stability of the landform by dissipating rainfall impact energy, producing leaf litter as a ground cover, stabilising the sub-surface and improving infiltration with root growth. The degree of stabilisation will depend on the types of vegetation used and the rates of establishment.
- Zero initial surface cover (i.e. no woody debris or plant litter). This means that no additional surface cover was expected to be added to the soil surface to reduce erosion rates. This assumption does not have any impact on the armouring effect of the rock and gravel fraction in the soil, which was already accounted for within the measured soil parameters discussed in Section 3.2.3.6.

Rill geometry is adjusted internally in the model based on the input soil parameters and on the size of the erosion events encountered.

3.2.3.8 WEPP Modelling Scenarios

A total of three different slope configurations were modelled for each material using the WEPP modelling software. Batter slopes were modelled assuming slope angles of 5°, 10°, and 15° to simulate the range of design options being considered for the post-mine landforms.

3.2.3.9 SIBERIA Modelling Scenarios

The following two model scenarios were tested, with the E3 and S6 soils used as surface cover:

- **Regional model:** An input DEM was developed which incorporated a landform design with 10° external batter slopes within the regional landscape. The primary purpose of this scenario was to determine where sediment eroded from the landform would be deposited, in the long-term (10,000-year), regional context.
- **Layered landform model:** A DEM with a smaller grid size (4x4 m) was developed to investigate how the landform itself would evolve, given the complex layering of different materials likely to be utilised in its construction. The model consisted of (1) the base clay/tailings core, (2) a 1 metre-thick calcrete layer ('C1' soil), and (3) a 2 metre thick surface layer consisting of either 'E3' or 'S6' soil. The primary purpose of this model scenario was to determine if the tailings material was likely to be exposed in the long-term (10,000-years), given different surface soil coverings.

4 STUDY RESULTS

Based on the inferred depositional history over the study area and the morphological characteristics of the various soil profiles exposed by trench excavation three Soil Mapping Units (SMU) were classified across the study area. These are:

- SMU 1: Deep Dunal Sand – occurs predominately as linear (longitudinal) or parabolic dunes;
- SMU 2: Sandy Duplex –occurs on the lower slopes and footslopes of the dunes; and
- SMU 3: Calcareous Loamy Soils –occurs within the inter-dunal depressions.

The relationship between these SMU and the major soil groups of Western Australia (Schoknecht, 2002) and the Australia Soil Classification (Isbell, 1996) are presented in Table 4.1.

Table 4.1: Relationship of identified SMU to Australian soil classification schemes

Identified SMU	Soil Series (Schoknecht, 2002)	Australian Soil Classification (Isbell, 1996)
SMU 1 – Deep Dunal Sand	Yellow Deep Sand	Orthic Tenosol
SMU 2 – Sandy Duplex Soils	Yellow/Brown Deep Sandy Duplex	Yellow or Brown Chromosol
SMU 3 – Calcareous Loamy Soils	Calcareous Shallow Loam	Lithic Calcic Calcarosol

4.1 SOIL DISTRIBUTION

All soils are uniformly and predictably distributed across the MRUP. SMU 1 and 2 represent the Quaternary dunal sands that were deposited by aeolian processes directly onto the pre-existing Miocene surface, for which SMU 3 likely represents the upper portion of this basement surface. In areas not covered by the aeolian dunes, SMU 3 occurs at the surface forming defined and localised topographic depressions. A review of the geological drilling data, and from observations from strategically located soil trenches, it is clear that SMU 3 underlies both SMU 1 and 2, forming a base to the surficial soil profile. Below SMU 3, the Miocene sediments occur, which have been deposited directly onto the underlying Eocene sediments.

As discussed in Section 2.4, and shown in Figure 2.14, the MRUP consists of two defined geomorphic units, representing aeolian dunes and broad relatively flat plains. The association of these geomorphic units with the SMU identified above (Table 4.1) is provided below:

- Aeolian Dunes: comprise predominately SMU 1, and to some extent deeper portions of SMU 2.
- Broad Plain: comprise the shallower portions of SMU 2 and all of SMU 3.

A map showing the broad soil-geomorphic units across the MRUP, derived from the Total Dose Radiometric data, is presented in Figure 4.1. Note: the Aeolian Dunes represented by the blue colours in Total Dose Radiometric data, whilst the Broad Plain is identified by the brown colours.

A good soil-vegetation association occurs across the MRUP, such that defined vegetation types occur within each SMU. For the MRUP the following soil-vegetation association exist:

- SMU 1: composed of > 5 m of yellow dunal sand, supporting the S6 and S8 vegetation types identified by MCPL (2015a).

- SMU 2: composed of 3 – 5 m of yellow sand, grading into a red sand, over SMU 3. This SMU supports the E3 and E5 vegetation types of MCPL (2015a), with the E3 vegetation tending to occur in areas where the surficial yellow sand is around 3 m, whilst the E5 community tends to dominate the deeper (i.e. up to 5 m) yellow sand profiles.
- SMU 3: composed predominately of E6 and E8 vegetation types

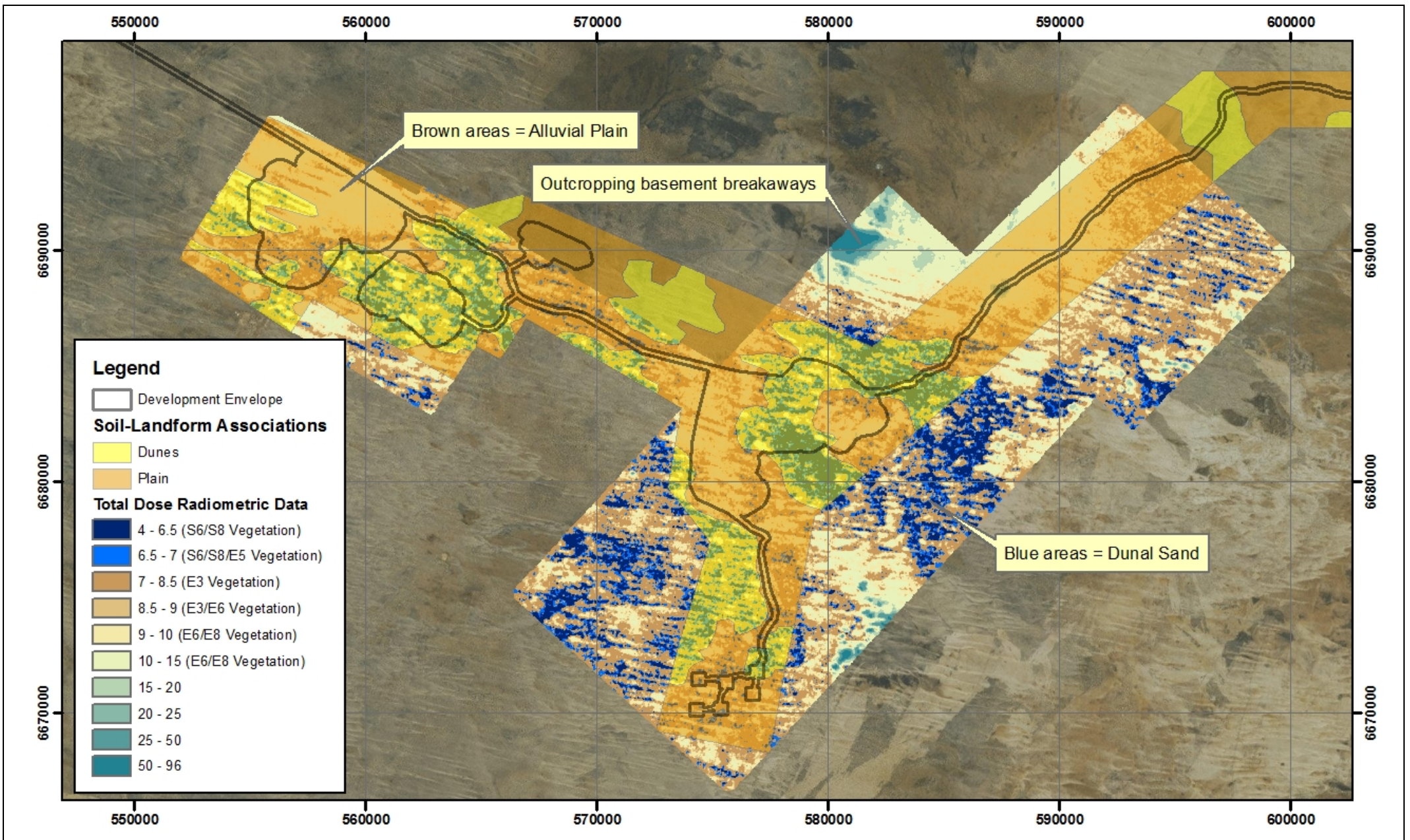
The above soil-vegetation relationship holds across all deposits within the MRUP, and clearly establishes that soil moisture availability (i.e. access to sufficient water to meet their transpiration requirements) controls the distribution of the vegetation.

Maps showing the distribution of the SMUs across entire MRUP are shown in Figure 4.2, whilst Figure 4.3 and Figure 4.4 show the three SMU distributions within the mining areas.

Based on the mapped distribution of the SMU, the percentage of each soil type occurring within the Development Area and the proposed Disturbance Footprint, is provided in Table 4.2.

Table 4.2: SMU coverage within the Development Area and Disturbance Area

SMU	Disturbance Footprint (i.e. Site Layout)	ESD Development Area
Total Area (ha)	3,787	9,997
% SMU 1: Sand Dunes	9.7	10.8
% SMU 2: Sandy Duplex	62.2	69.3
% SMU 3: Calcareous Loam	28.1	19.9

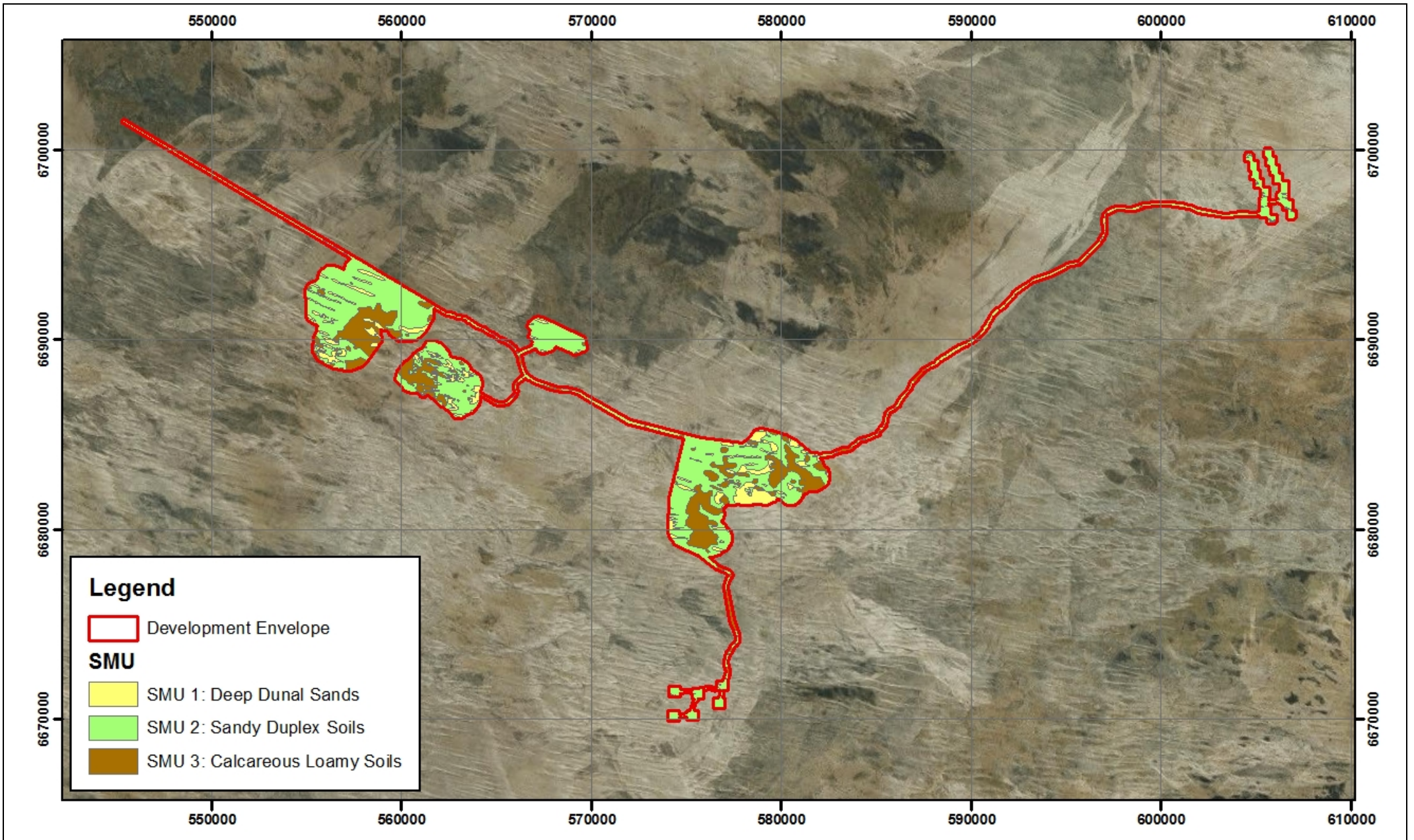


VIMY RESOURCES

TERRAIN ANALYSIS AND MATERIALS CHARACTERISATION
FOR THE MULGA ROCK URANIUM PROJECT

Figure 4.1: Mapping of broad soil landform associations across the MRUP



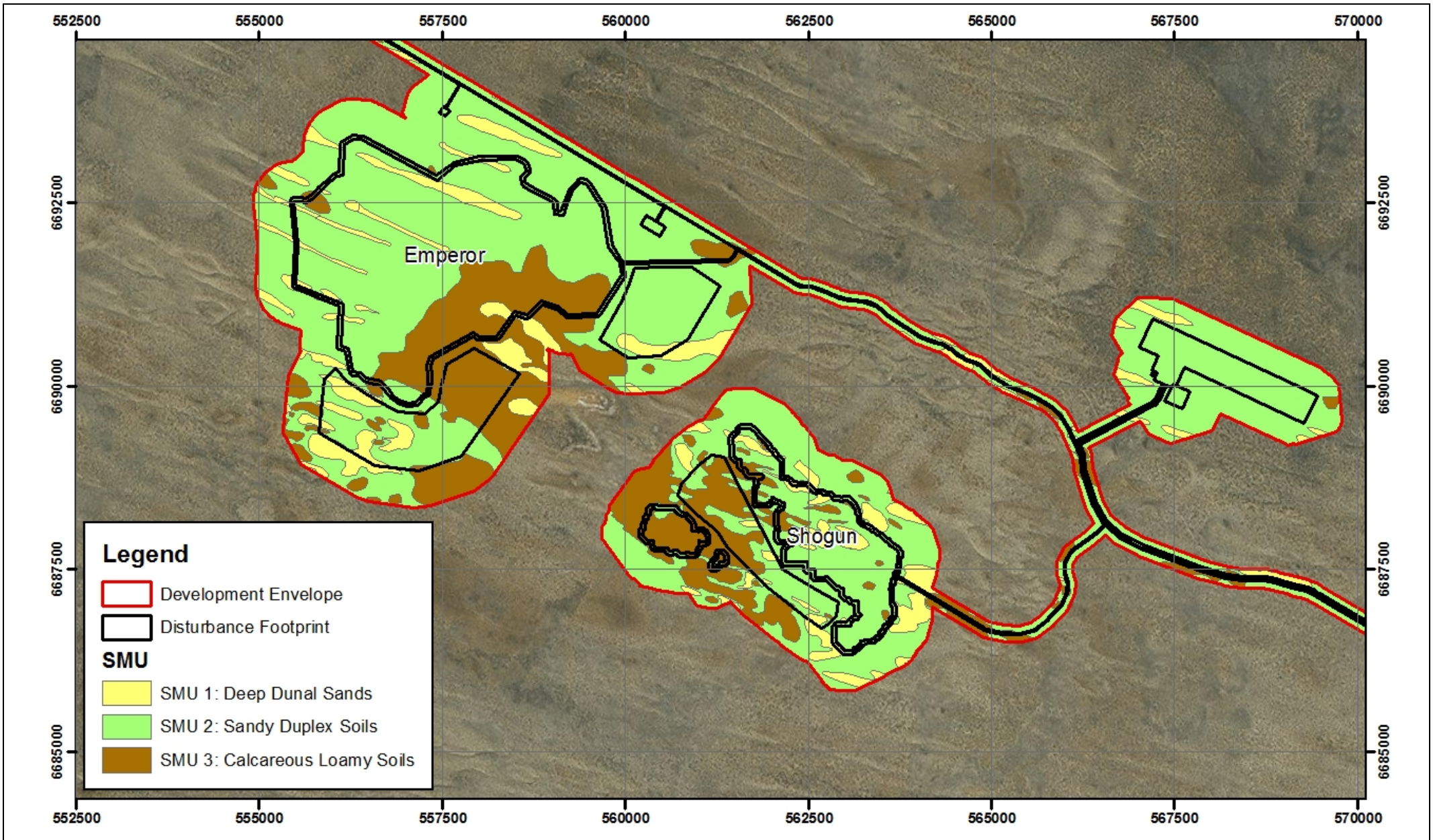


VIMY RESOURCES

TERRAIN ANALYSIS AND MATERIALS CHARACTERISATION FOR
THE MULGA ROCK URANIUM PROJECT

Figure 4.2: SMU Map across the MRUP



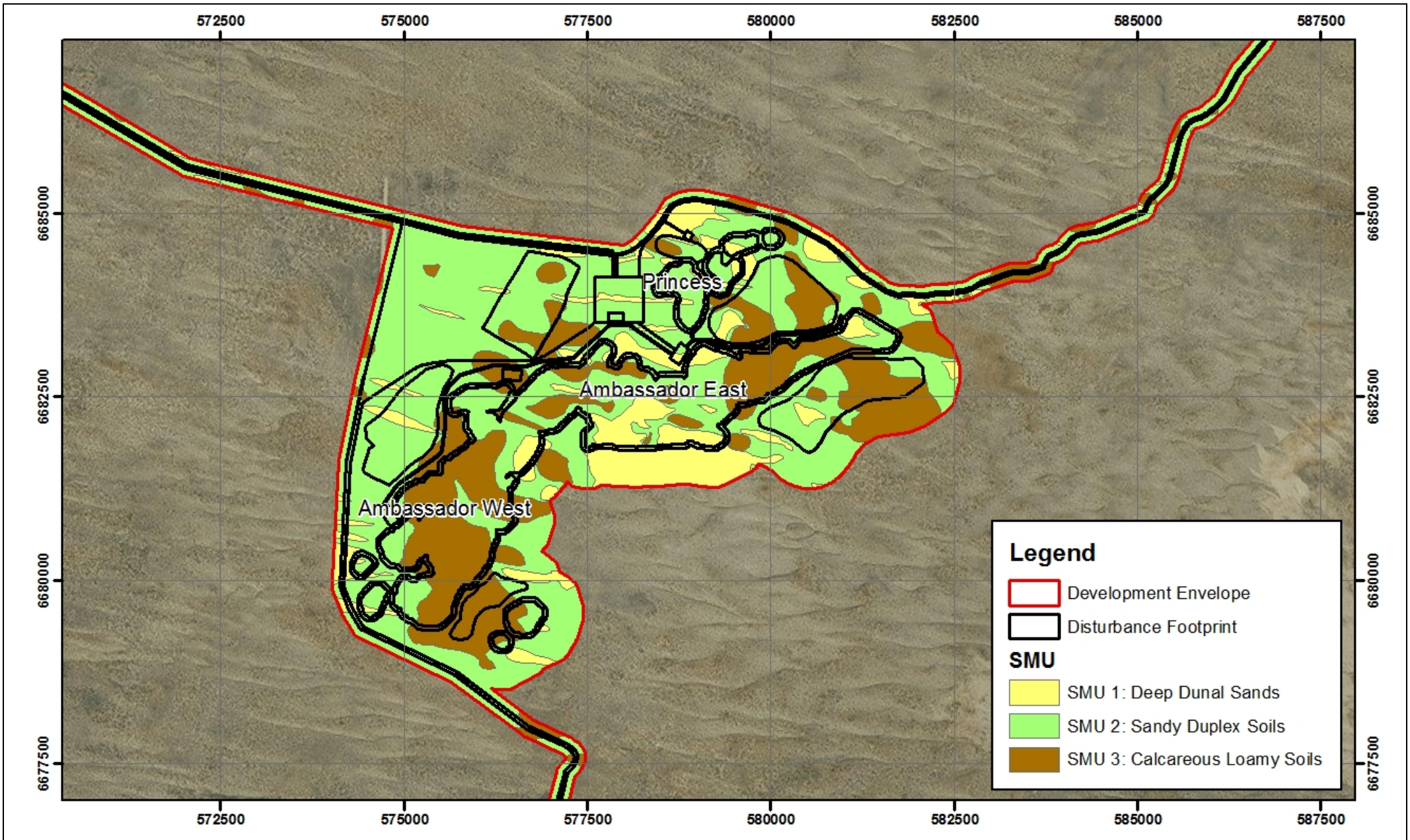


VIMY RESOURCES

TERRAIN ANALYSIS AND MATERIALS CHARACTERISATION
FOR THE MULGA ROCK URANIUM PROJECT

Figure 4.3: SMU map across the Mulga Rock West Deposits





VIMY RESOURCES

TERRAIN ANALYSIS AND MATERIALS CHARACTERISATION
FOR THE MULGA ROCK URANIUM PROJECT

Figure 4.4: SMU map across the Mulga Rock East Deposits



4.2 SMU 1: DEEP DUNAL SANDS

This soil type occurs throughout the study area, and will be regularly encountered during mining (Table 4.2 and Figure 4.2). The distribution of deep sands within SMU 1 conforms to the inactive dunal systems deposited over the topographically subdued loams and developing calcrete layer (i.e. SMU 3) which occur broadly across the region. The sands form low rises and dunes which rise in elevation up to 15 m above the surrounding general landscape.

The deep sandy soils support low shrublands corresponding to the mapped vegetation communities of S6 (steeper slopes of the dunes) and S8 (flatter upper portions of dunes and areas of undulating swales). These vegetation communities consist of low shrubland to low open shrubland of *Acacia desertorum*, *Allocasuarina spinosissima*, *Leptosema chambersii* and other mixed low shrubs over *Triodia desertorum* and *Chrysitrix distigmatosa* with occasional emergent mallee *Eucalyptus* spp (MCPL, 2015a). SMU 1 supports the conservation significant S6 vegetation type, which comprises the majority of the Priority Species occurring within the MRUP (i.e. *Hibbertia crispula* – P1, Vulnerable; *Caesia rigidifolia* – P1; *Dampiera eriantha* – P1; and others listed in Section 2.8).

A typical profile of SMU 1 is shown in Figure 4.5 and was encountered within trenches 6, 7, 12, 13, 14, 18, and 23 (Figure 3.1 and Figure 3.2). The profile generally consists of an upper 10 to 30 cm layer of brownish yellow sand, overlying a deep yellow sand which extends > 5 m in depth. There is a slight accumulation of organic matter in the upper portion of the profile, which would typically be classified as a topsoil material. Although this is the case, 'topsoil' is generally either very poorly developed or completely absent from this SMU.

Over the entire dunal surface comprising SMU 1, a thin, and easily broken, cryptogam layer is present (Plate 4.1). This layer helps to stabilise the surface sands from both water and wind erosion (i.e. provide surface stability), and this is clearly seen in the field whereby a mobile 2 – 5 cm sand fraction occurs above the cryptogam layer, with the underlying sands remaining intact. The stability or anchoring of the actual dune is afforded by the large taproots that the majority of dunal species exhibit (Plate 4.2). When the density of plants over these landforms is considered (Plate 4.3) the anchoring effect of these taproots becomes apparent (Plate 4.4).

The dominant yellow sands in this SMU exist in a dry, friable, single-grain structure, which provides minimal resistance to root growth. Consequently, roots of all sizes easily grow through the soil matrix as shown in Plate 4.5. Roots explore all of the soil profile, and extend and penetrate below 4 m as observed in this investigation. This is expected given the low Plant Available Water (PAW) content of these sands (Table 4.3), and thus the vegetation is required to access a large volume of the soil profile (i.e. extend well below 4 m) to access sufficient soil moisture to meet their transpiration requirements.

Plate 4.1: Layer of cryptogam below thin surface layer of active sand

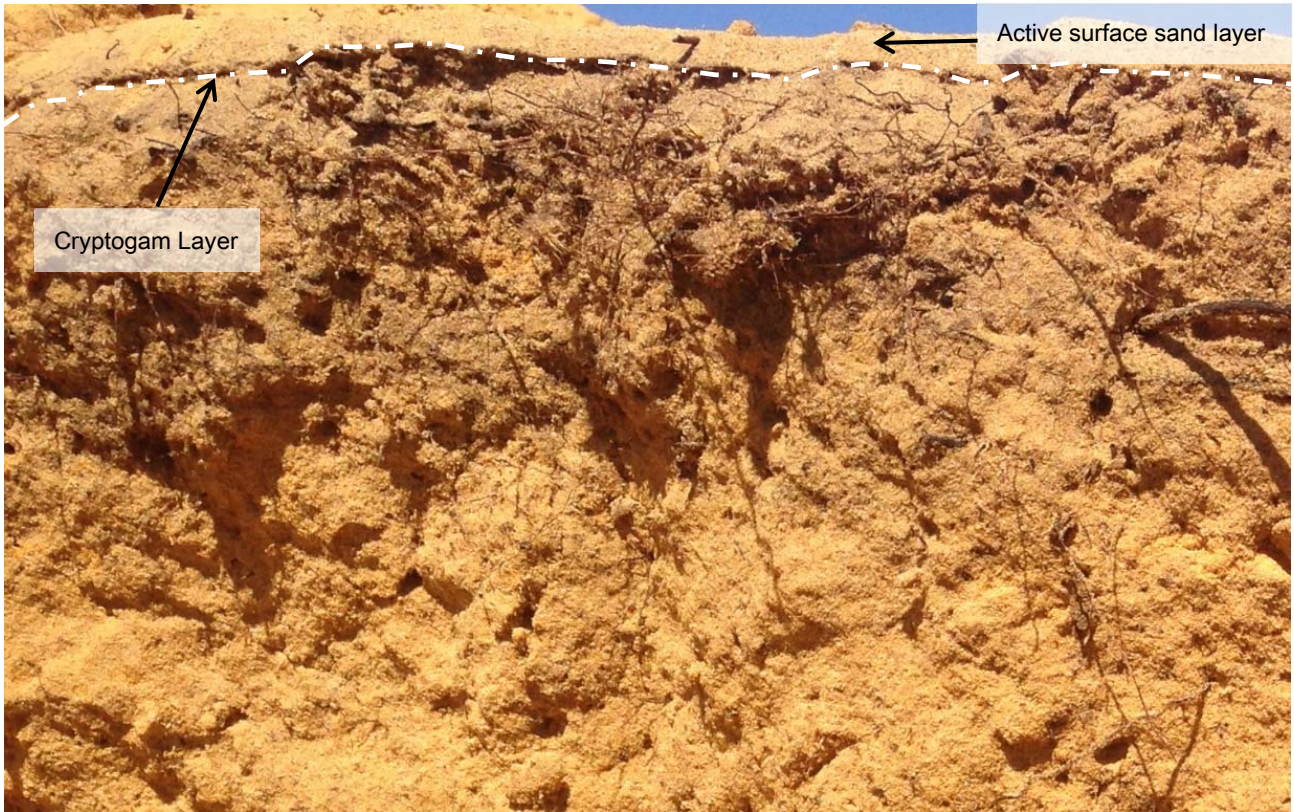


Plate 4.2: Tap roots extending below bottom of trench within dunal sands (SMU 1)



Plate 4.3: Typical density of plant species

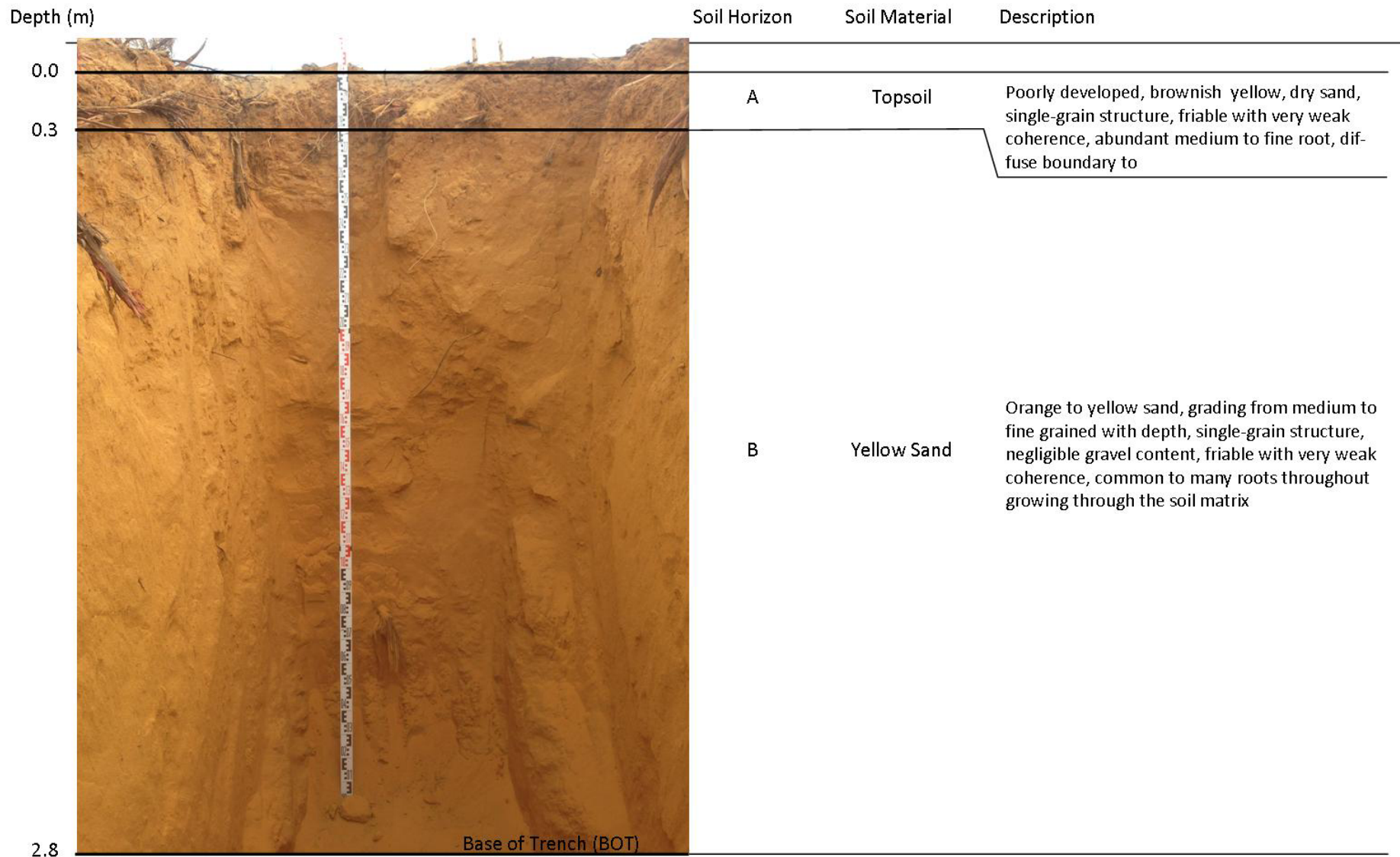


Plate 4.4: Abundance of tap roots effectively anchoring the large sand dunes



Plate 4.5: Root growth through the soil matrix of the yellow sand material





VIMY RESOURCES

TERRAIN ANALYSIS AND MATERIALS
CHARACTERISATION FOR THE MULGA ROCK URANIUM
PROJECT

Figure 4.5: Typical profile of SMU 1 – Deep dunal sands



STUDY RESULTS

4.2.1 PHYSICAL AND HYDRAULIC PROPERTIES

The physical and hydraulic properties existing within SMU 1 (Deep Dunal Sands) are provided in Table 4.3 and shown in Figure 4.6. These results highlight the sandy nature of these soils, ranging from 98.4 – 99.1% sand (i.e. > 20 µm soil fraction). The corresponding bulk density is within the typical range for sands (i.e. 1.6 – 1.8 g/cm³), although the density recorded at 40 – 60 cm of 2.03 g/cm³ suggests some degree of compaction or hardsetting has occurred, This may be another important property that protects the dunes from mobilising.

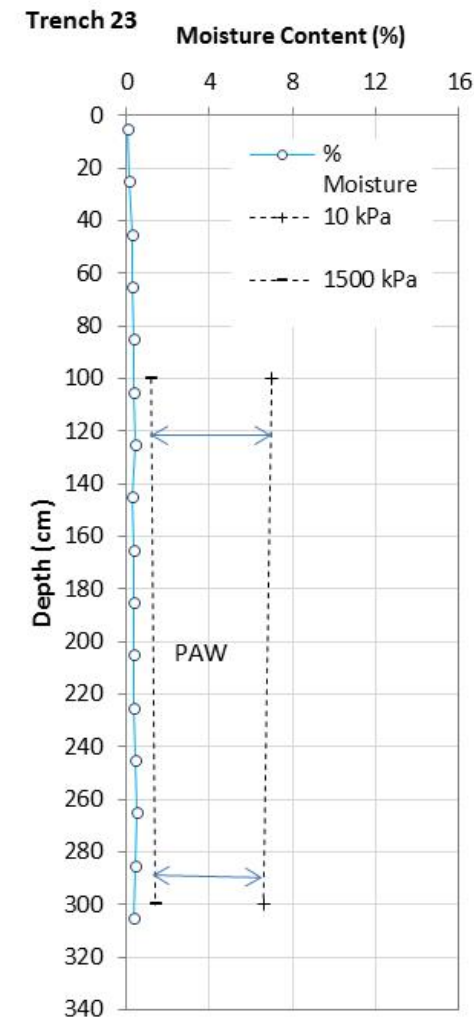
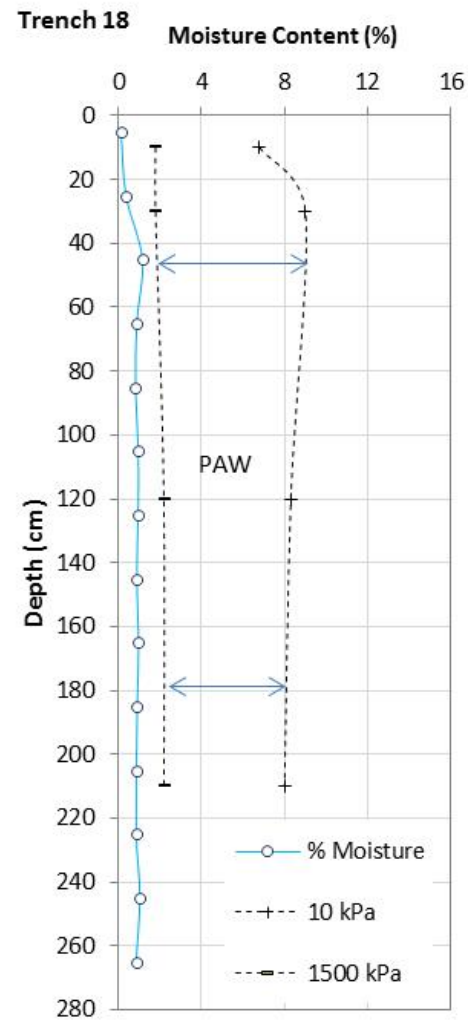
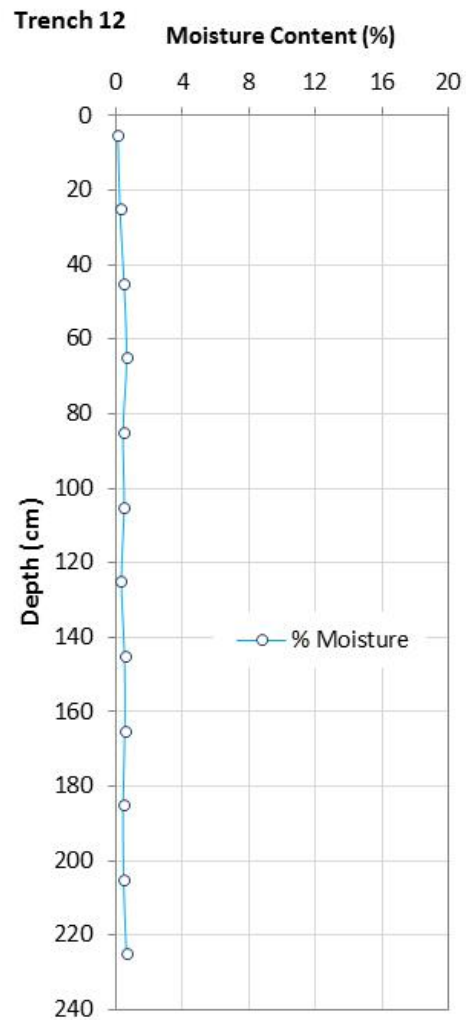
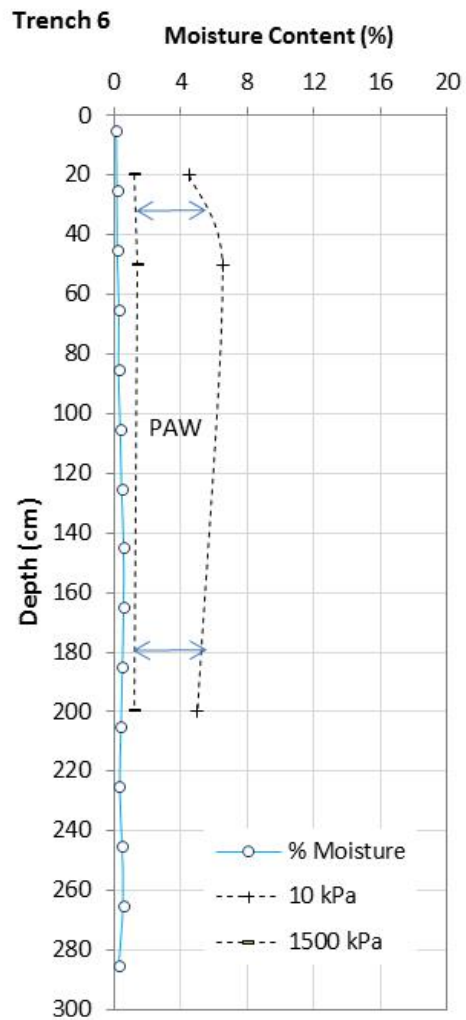
The yellow sands have saturated hydraulic conductivity values of > 5 m/day, and any aggregates that exist rapidly slake (i.e. poor macro-structural stability), with no dispersion being present (i.e. very good microstructural stability). As expected these materials have negligible water holding capacity, with moisture contents (v/v) around 7 %, and corresponding PAW contents of between 4.9 – 6% (49 – 60 mm/m).

At the time of the sampling (i.e. early February 2015) all soils within SMU 1 were at or slightly below Permanent Wilting Point (PWP) to at least 3 m depth, indicating that they are effectively dry to this depth, with no water available for the vegetation to access. Therefore the nature vegetation within SMU either have morphological adaptations to reduce water loss and/or are extracting soil moisture at depths > 3 m. It is likely to be a case of both aspects are being exploited by the vegetation.

Table 4.3: Average physical and hydraulic properties for SMU 1

Depth (cm)	Gravel (%) (> 2 mm)	Particle size distribution (%) (< 2 mm fraction)			Texture	Bulk density (g/cm ³)	Saturated hydraulic conductivity (m/day)
		Sand	Silt	Clay			
0-20	< 1	99.1	0.2	0.7	Sand	1.60	6.5
40-60	< 1	98.8	0.1	1.1	Sand	2.03	6.2
100-150	< 1	98.4	0.3	1.3	Sand	-	5.3
200-290	< 1	98.4	0.2	1.4	Sand	1.76	5.8

Depth (cm)	Water retention characteristics (%; v/v)						Macro structural stability (slaking)	Micro structural stability (dispersion)
	0 kPa	10 kPa	33 kPa	100 kPa	1500 kPa	PAW		
0-20	37.7	6.4	3.1	2.0	1.4	5.1	Poor	Very good
40-60	38.2	6.5	3.0	1.9	1.4	5.1	Poor	Very good
100-150	36.4	7.6	3.9	2	1.7	6	Poor	Very good
200-290	38.5	6.5	2.6	2.0	1.6	4.9	Poor	Very good



VIMY RESOURCES

TERRAIN ANALYSIS AND MATERIALS
CHARACTERISATION FOR THE MULGA ROCK URANIUM
PROJECT

Figure 4.6: Moisture profiles with water retention information for SMU 1



STUDY RESULTS

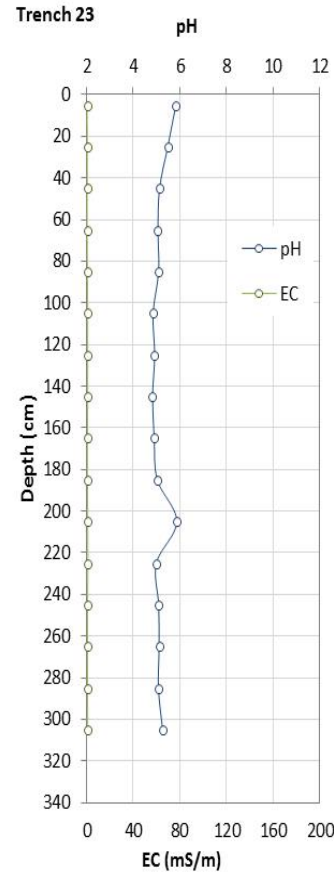
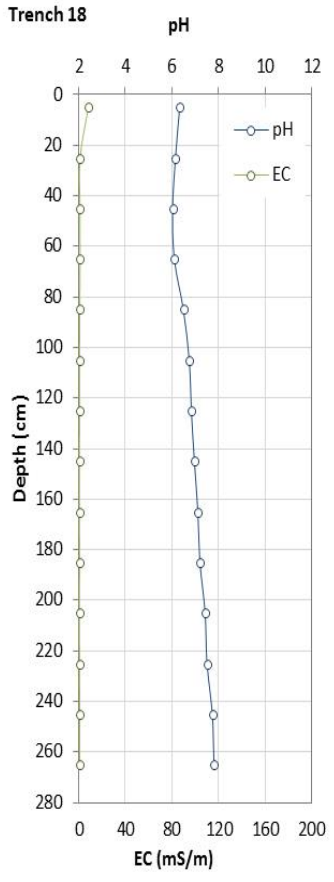
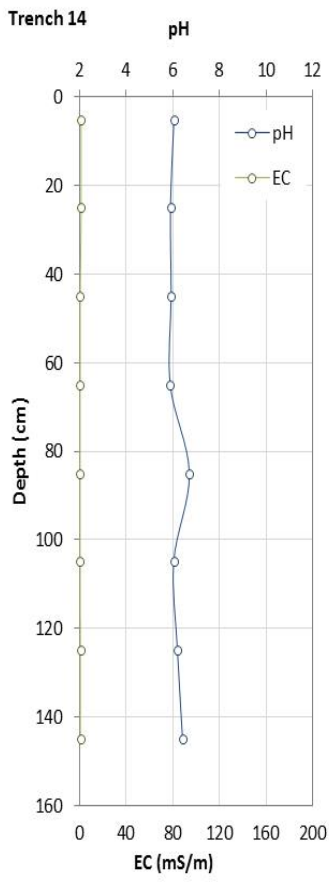
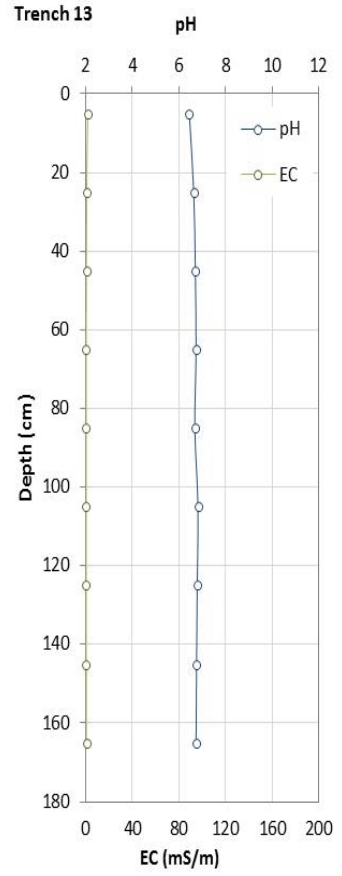
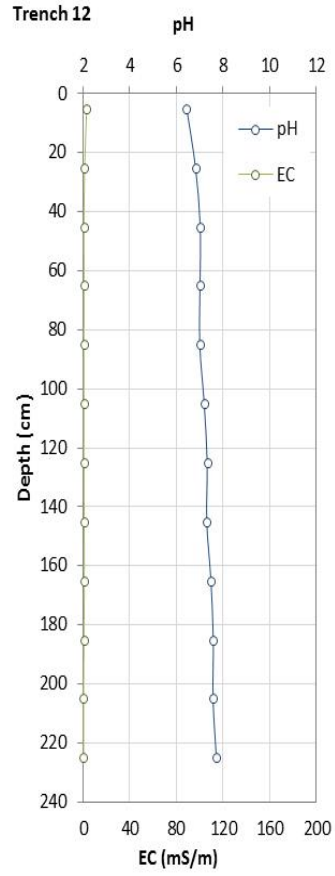
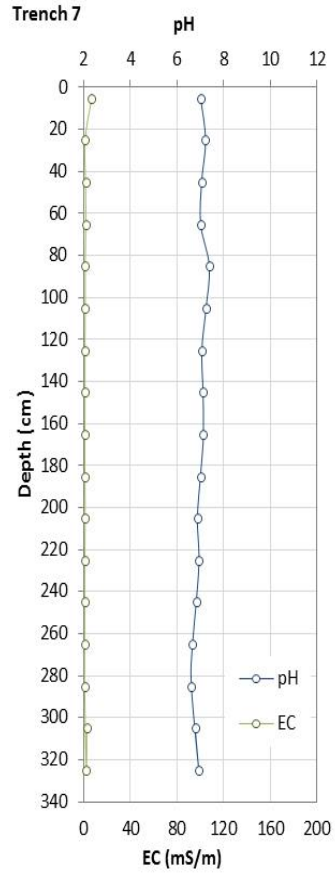
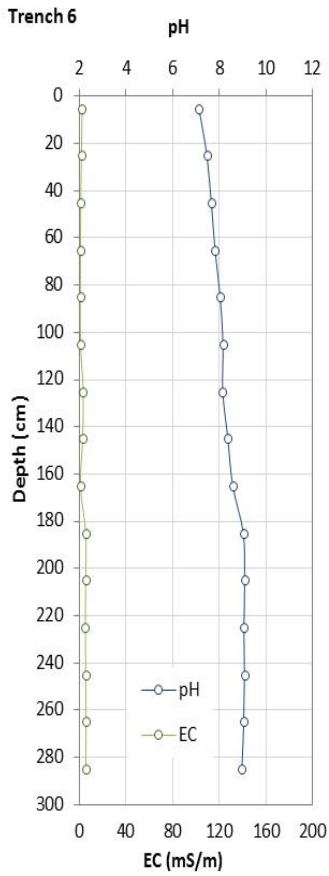
4.2.2 CHEMICAL PROPERTIES

The chemical properties of the yellow sands throughout SMU 1 are presented in Table 4.4 and presented in Figure 4.7. All soils within SMU 1 are chemically benign to a depth of at least 3 m, containing negligible nutrients (even in the “topsoil”), have slightly acidic pH values (i.e. pH 6 – 7), non-saline (EC < 5 mS/m), non-sodic (ESP < 6%) and have very low exchangeable cations and overall CEC (i.e. CEC < 2 meq/100g). The presence of the abundance of roots in the 50 cm of the profile can clearly be seen in the organic C results, dropping from 0.35% to below 0.1% at depth. These chemical properties are expected given the sandy and extensively leached nature of the materials in SMU 1.

Table 4.4: Average chemical properties for SMU 1

Depth (cm)	Nutrients (mg/kg)					Organic C (%)	pH (1:5)	EC 1:5 (mS/m)
	NH ₄ -N	NO ₃ -N	Colwell P	Colwell K	Ext. S			
0-20	1	1.5	4	44	1.8	0.35	6.4	1.6
40-60	<1	1	3.5	42	1.3	0.21	6.5	<1
100-150	<1	<1	3.6	25	2.8	0.09	6.2	<1
200-290	<1	<1	3.5	23	2.7	0.09	6.6	<1

Depth (cm)	Exchangeable cations (meq/100g)					CEC (meq/100g)	ESP (%)
	Ca	Mg	Na	K	Al		
0-20	1.10	0.27	0.02	0.11	0.08	1.49	1.26
40-60	0.81	0.28	0.02	0.10	0.10	1.21	1.40
100-150	0.46	0.26	0.02	0.06	0.13	0.80	2.18
200-290	0.52	0.35	0.03	0.06	0.11	0.95	2.75



VIMY RESOURCES
 TERRAIN ANALYSIS AND MATERIALS
 CHARACTERISATION FOR THE MULGA
 ROCK URANIUM PROJECT

Figure 4.7: pH and EC depth profiles for SMU 1



4.3 SMU 2: SANDY DUPLEX SOILS

SMU 2 occupies the transitional zone between SMU 1 (Dunes) and SMU 3 (Topographic Depressions). This soil type effectively represents the lower portion of SMU 1, where the thickness of the surficial yellow sand is significantly reduced having a total depth above the underlying red sand of between 1 – 3 m. A characteristic profile of SMU 2 is shown in Figure 4.8 and was encountered within trenches 4, 5, 8, 9, 15, 22, and 24.

Given the reduced thickness of the overlying surficial sand, SMU 2 supports the E5 and E3 vegetation types identified by MCPL (2015a). These vegetation communities consist of Low Open Woodlands of *Eucalyptus gongylocarpa*, *E. ceratocorys*, *E. rigidula* and *E. sp.* Mulga Rock, over *Hakea francisiana*, *Cryptandra distigma*, *Acacia rigens* and *Grevillea juncifolia* and other mixed low shrubs over *Triodia* spp and *Chrysitrix distigmata* (MCPL, 2015a). The transition between the E5 and E3 vegetation types corresponds to a reduced thickness of the overlying yellow sand. The E5 vegetation typically occurs in areas where the yellow sand, over the red sand, is > 3 m, whilst the E3 vegetation generally only occurs in areas where the yellow sand is < 3 m over the red sand.

The red sand which occurs at depth in this profile is likely to represent a clay illuviated material, whereby the original clays present in the yellow sand have been leached or eluviated, and subsequently deposited at depth in the profile. This is clearly seen in the increase in clay content with depth (Table 4.5). It is possible that the downward leaching of the clay was restricted by the lower permeability of the underlying reddish brown loam, which represents the upper portion of SMU 3 (Section 4.4).

4.3.1 PHYSICAL PROPERTIES

The physical properties exhibited by the various materials within SMU 2 are provided in Table 4.5, and presented in Figure 4.9. The similarity in physical properties of the sands in SMU 2, with those in SMU 1, is clearly seen in Table 4.5, with the only principal difference being the increasing clay content with depth, corresponding to the red sand soil horizon. The increasing clay content results in a decrease in saturated hydraulic conductivity (i.e. from around 4 m/day to 1.7 m/day), and an increase in the water holding capacity of these soils (this is likely to be the reason why there is a transition from the shrub communities in SMU 1 – e.g. S6 and S8 vegetation types, to an open Eucalypt woodland – e.g. E3 and E5). The increasing clay content with depth also results in a change in the structural properties of the red sand, which exhibits some degree of aggregation, with these aggregates showing minor macro-structural stability and some dispersive potential.

As occurs for the SMU 1 yellow sands, all soils in SMU 2 to at least 3 m depth are effectively dry (< 6%, v/v) and contain no PAW (i.e. the moisture content of the soils is at or slightly below the corresponding PWP). This again implies that the native vegetation is either shutting-down their transpiration or are accessing stored moisture deeper in the soil profile.

Table 4.5: Average physical and hydraulic properties of SMU 2

Depth (cm)	Gravel (%) (> 2 mm)	Particle size distribution (%) (< 2 mm fraction)			Texture	Bulk density (g/cm ³)	Saturated hydraulic conductivity (m/day)
		Sand	Silt	Clay			
0-20	<1	97.6	0.5	1.9	Sand	1.56	3.87
40-80	<1	96.4	0.2	3.4	Sand	1.64	2.56
100-180	<1	95.4	0.6	4.0	Sand	1.77	2.22
200-260	<1	96.3	0.9	2.8	Sand	1.57	1.98

STUDY RESULTS

Depth (cm)	0 kPa	10 kPa	33 kPa	100 kPa	1500 kPa	PAW	Macro structural stability (slaking)	Micro structural stability (dispersion)
300-400	<1	89.7	2.4	7.9	Loamy sand	-	1.69	
Water retention characteristics (% H ₂ O v/v)								
0-20	43.8	13.3	8.5	7.2	5.2	8.1	Poor	Very good
40-80	38.0	8.2	6.3	2.8	2.3	5.9	Poor	Very good
100-180	41.4	15.5	10.2	7.7	5.9	9.6	Poor	Very good
200-260	37.3	10.0	6.2	4.5	3.6	6.4	Fair	Very good
300-400	34.7	8.6	4.1	3.7	2.6	6.0	Fair	Fair

4.3.2 CHEMICAL PROPERTIES

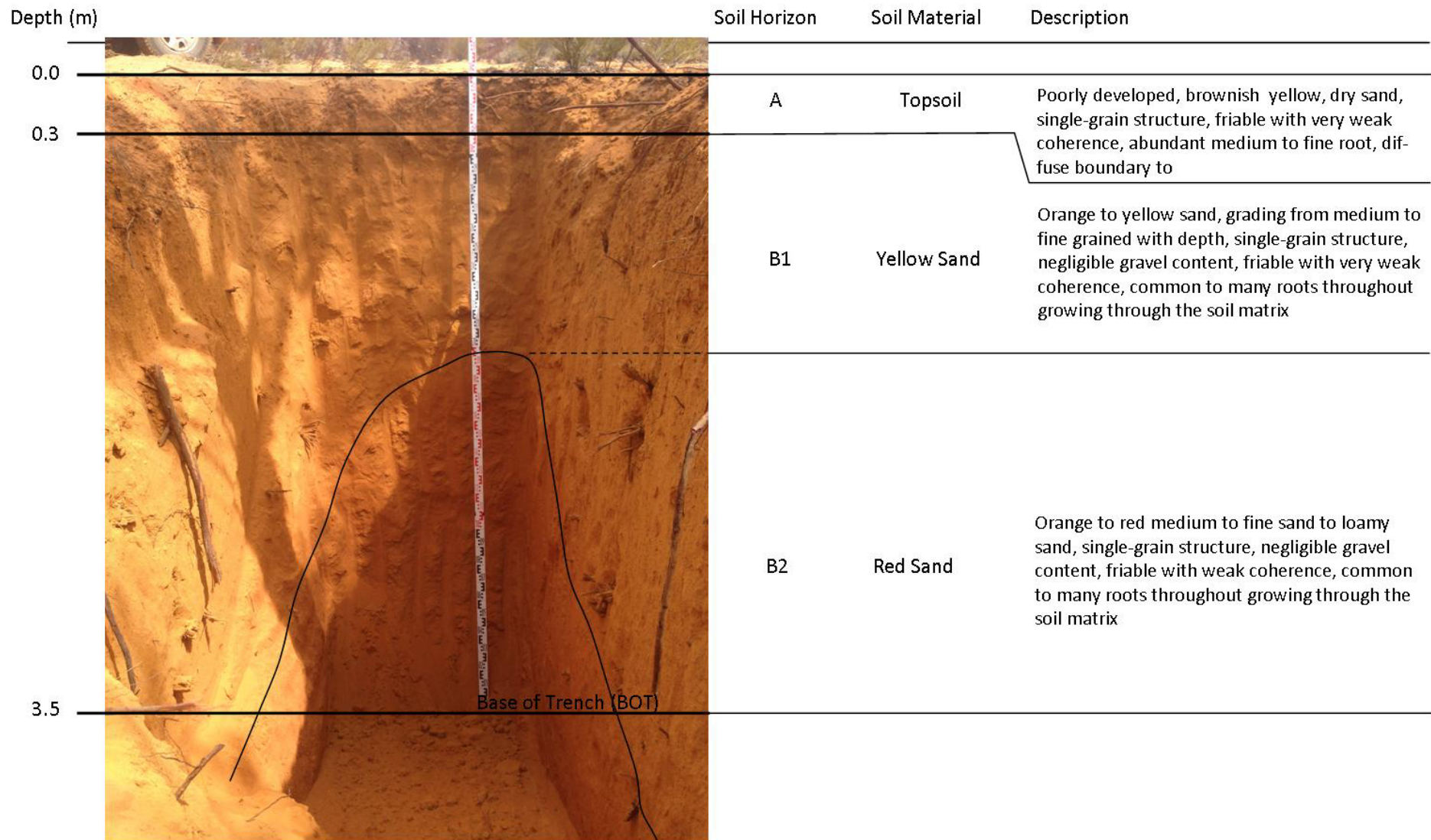
The chemical properties of the various soils occurring within SMU 2 are provided in Table 4.6 and presented in Figure 4.10. Similar to the sandy soils in SMU 1, the soil materials within SMU 2 are considered chemically infertile with very low levels of mineralised N (NH₄-N + NO₃-N) and plant available (Colwell) P. There is a greater abundance of roots in SMU 2, compared to SMU 1, as indicated by the elevated organic C contents to 1.8 m depth. The pH of the various materials in this soil type generally reflect the presence of the underlying calcrete, and thus their pH varies from 7 – 8. The presence of the red sands, which have a higher clay content, resulting in less leaching of salts from this profile, and this is clearly shown with the rapid increase in EC at depth (i.e. salinity values up to 46 mS/m); albeit these materials are still classified as non-saline.

The higher clay content, and lower permeability and leachability of the deeper red sands, also results in them having a relatively high CEC (indicating potentially the presence of illite in the clay mineral fraction) and a dominance of Na in the exchange complex, resulting in them being classified as sodic, with ESP values > 6%.

Table 4.6: Average chemical properties of SMU 2

Depth (cm)	Nutrients (mg/kg)					Organic C (%)	pH (1:5)	EC 1:5 (mS/m)
	NH ₄ -N	NO ₃ -N	Colwell P	Colwell K	Ext. S			
0-20	2.7	1.6	5.0	104	3.4	0.45	7.4	4.9
40-80	2	1	4.0	94	1.1	0.19	7.2	4.9
100-180	<1	<1	3.7	404	55	0.32	8.1	45.4
200-260	<1	<1	3.5	243	38	0.1	7.8	46.1
300-400	<1	<1	4.0	57	9.2	0.1	6.7	2.4

Depth (cm)	Exchangeable cations (meq/100g)					CEC (meq/100g)	ESP (%)
	Ca	Mg	Na	K	Al		
0-20	4.30	0.72	0.04	0.24	0.08	5.30	1.2
40-80	3.91	0.58	0.03	0.22	0.09	4.75	1.1
100-180	4.83	2.90	3.62	0.95	0.09	12.31	16.2
200-260	2.75	2.49	3.28	0.61	0.13	9.13	15.1
300-400	1.33	0.97	0.19	0.15	0.10	2.64	7.2

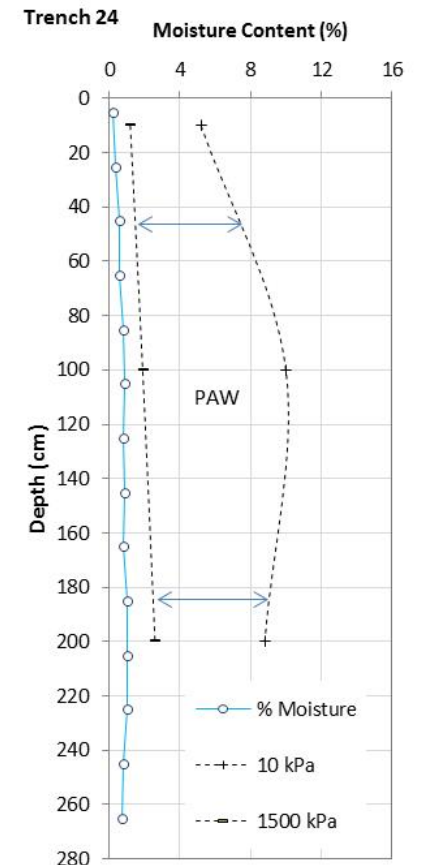
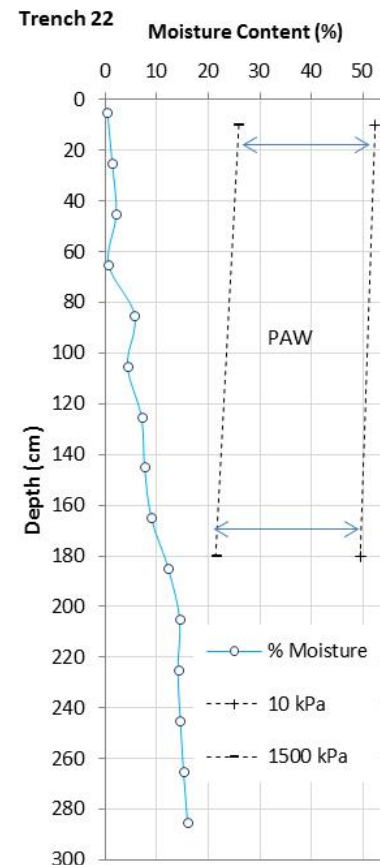
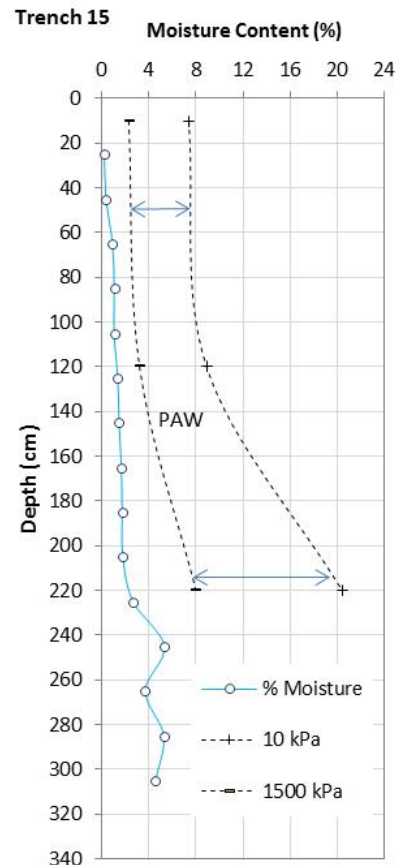
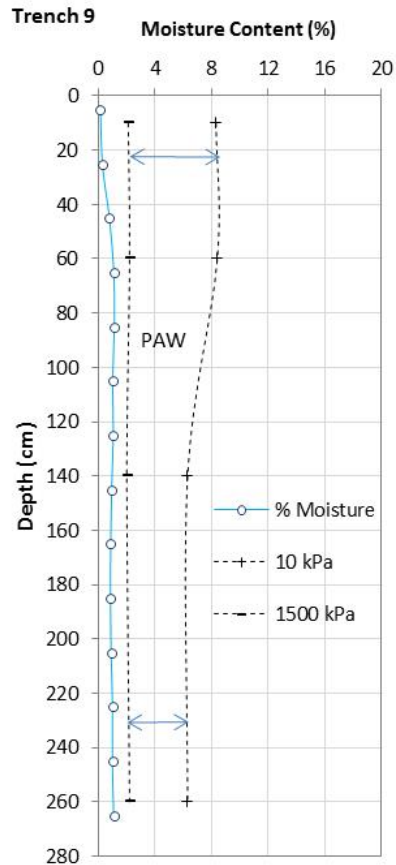
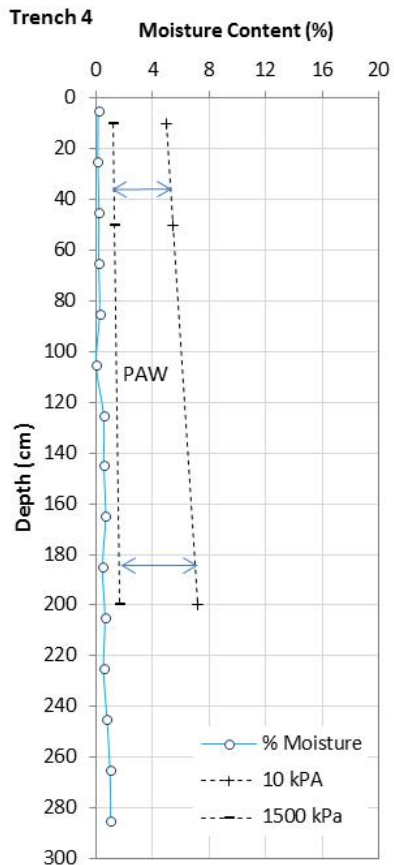


VIMY RESOURCES

TERRAIN ANALYSIS AND MATERIALS
CHARACTERISATION FOR THE MULGA ROCK URANIUM
PROJECT

Figure 4.8: Characteristic soil profile of SMU 2



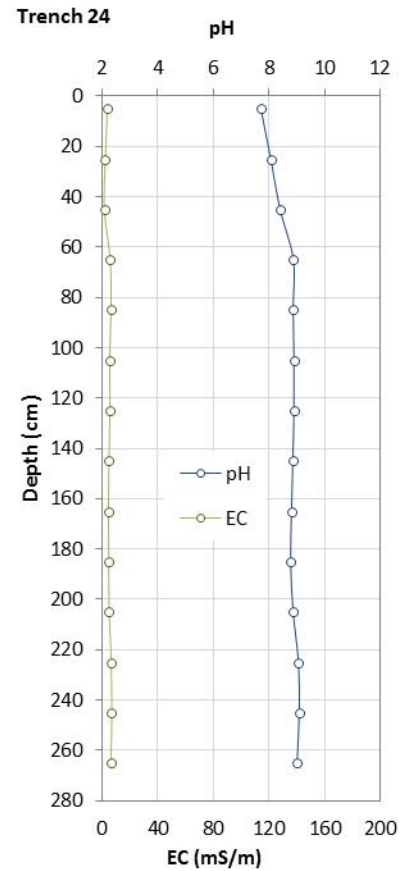
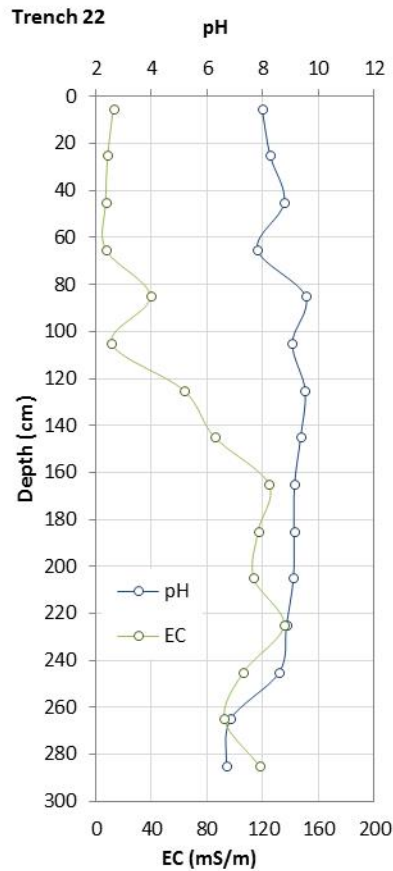
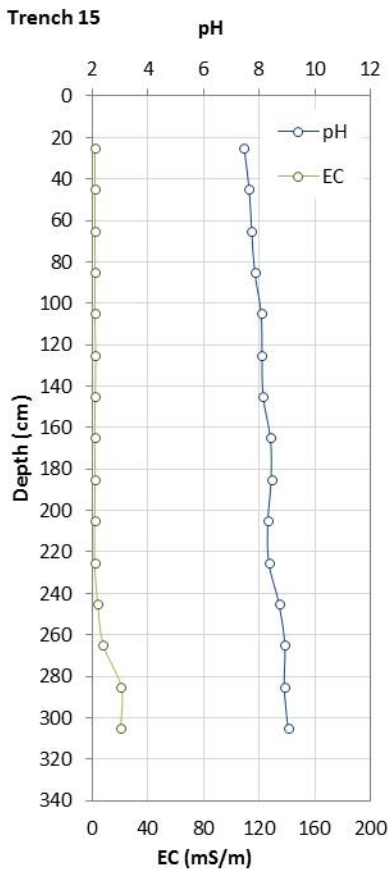
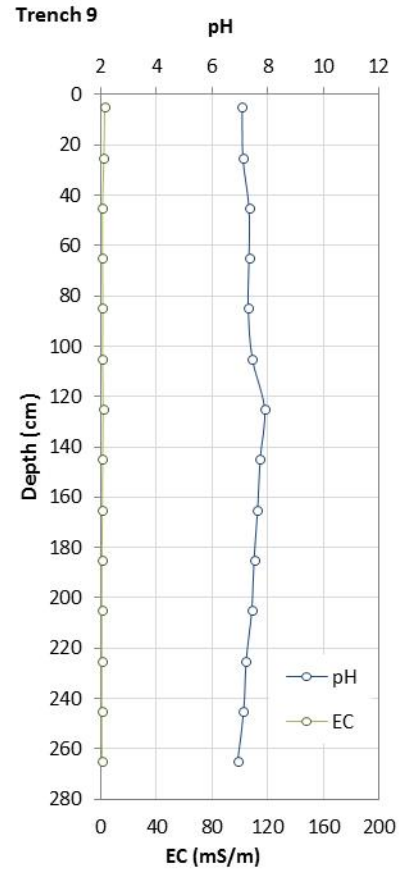
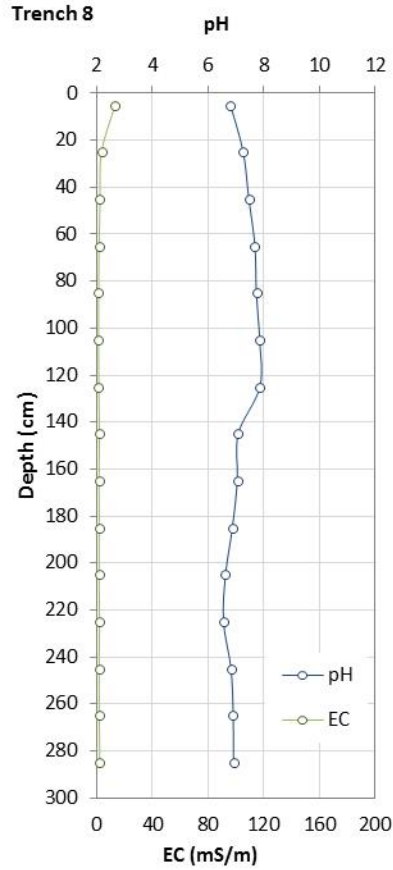
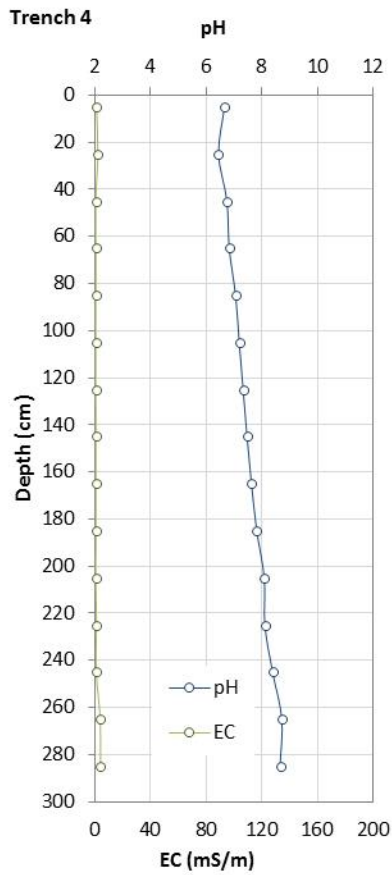


VIMY RESOURCES

TERRAIN ANALYSIS AND MATERIALS
CHARACTERISATION FOR THE MULGA ROCK URANIUM
PROJECT

Figure 4.9: Moisture profiles with water retention information for SMU 2





VIMY RESOURCES

TERRAIN ANALYSIS AND MATERIALS
CHARACTERISATION FOR THE MULGA
ROCK URANIUM PROJECT

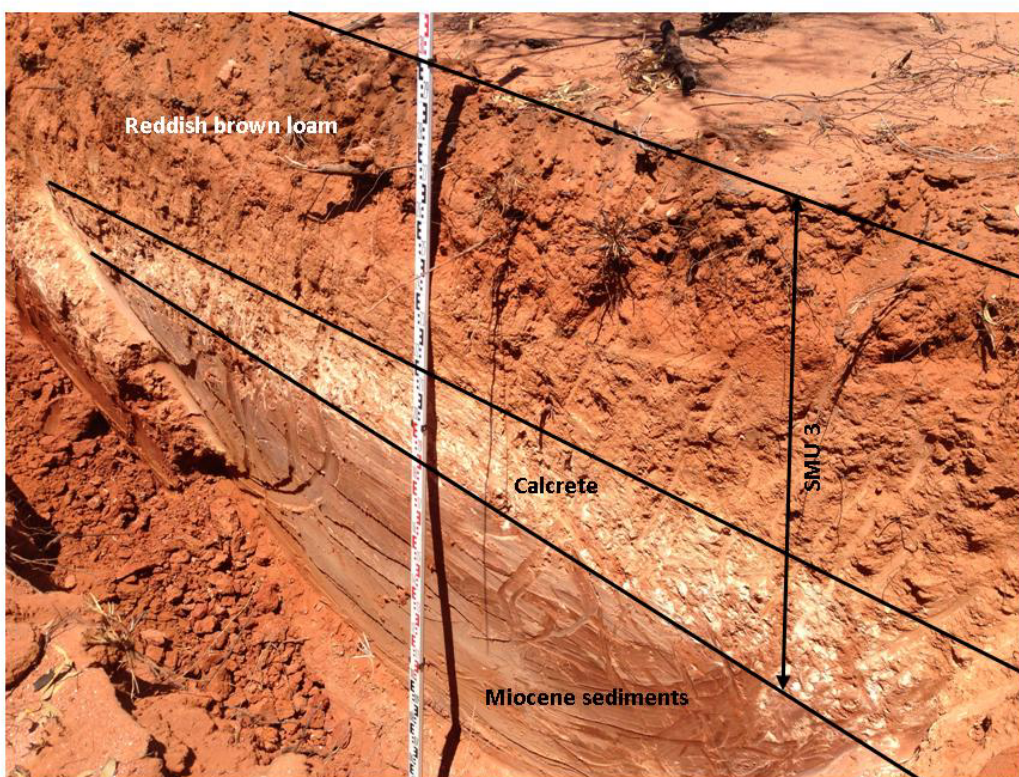
Figure 4.10: pH and EC depth profiles for SMU 2



4.4 SMU 3: CALCAREOUS LOAMY SOILS

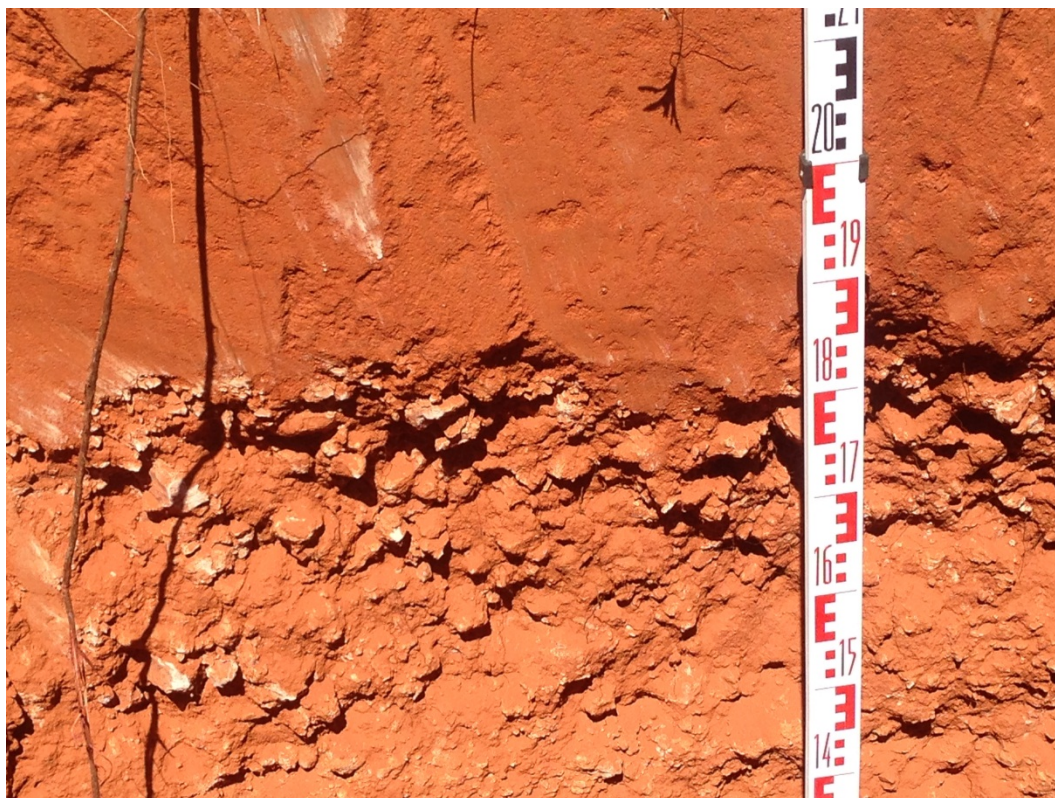
SMU 3 occurs or outcrops within the localised topographic depressions throughout the MRUP. As mentioned in Section 4.1, this soil type underlies both SMU 1 and 2, representing the basal portion of the Quaternary sediments and the upper portion of the Miocene sediments (Plate 4.6). A characteristic soil profile of SMU 3 is provided in Figure 4.11. This soil type consists of an alluvial reddish brown loam that was deposited directly onto the pre-existing calcrete or precursor material (i.e. sandy clay/loam in which the calcrete pedogenically formed). It is clear from the abrupt nature of the loam over the calcrete (Plate 4.7) that they represent two materials of contrasting origin and are not simply due to pedogenesis.

Plate 4.6: Occurrence of SMU 3 directly overlying the Miocene sediments within the Shogun Deposit



SMU 3 supports the E6 and E8 mallee Eucalypt woodland identified by MCPL (2015a), consisting of low open woodland of *Eucalyptus gongylocarpa* over *Eucalyptus youngiana*, *Eucalyptus ceratocorys*, *Grevillea juncifolia*, *Hakea francisiana* and *Callitris preissii* over *Acacia helmsiana*, *Cryptandra distigma* and mixed low shrubs over *Triodia desertorum*, *Chrysitrix distigmata* and *Lepidobolus deserti*. These species, and the associated vegetation community, are likely to be the highest water use vegetation types within the MRUP. These species have ready access to soils that have a high water holding capacity, which is regularly replenished during the winter months due to surface water runoff and accumulation in these areas. A typical soil profile of SMU 3 is provided in **Error! Reference source not found.** and was encountered during the excavation of trenches 2, 3, 10, 11, 16, 17, 19, 20 and 21.

Plate 4.7: Abrupt boundary between the surficial loam overlying the calcrete in SMU 3



4.4.1 PHYSICAL AND HYDRAULIC PROPERTIES

The physical and hydraulic properties of the various soils within SMU 3 are provided in Table 4.7, presented in Figure 4.12. The influence of the higher silt + clay content (up to 22.4%) can clearly be seen on the saturated hydraulic conductivity of the material (i.e. decreasing to around 0.2 m/day) and the water holding capacity of the material (i.e. field capacities of up to 13.8%, and PAW of up to 9.1% or 91 mm/m).

Table 4.7: Average physical and hydraulic properties of SMU 3

Depth (cm)	Gravel (%) (> 2 mm)	Particle size distribution (%) (< 2 mm fraction)			Texture	Bulk density (g/cm ³)	Saturated hydraulic conductivity (m/day)
		Sand	Silt	Clay			
0-20	<1	92.8	2.2	5.0	Sand	1.51	0.8
40-60	<1	91.5	1.4	7.1	Sandy loam	1.68	0.2
100-160	35.7	77.6	9.6	12.8	Loam	-	0.3
180-240	81.8	94.9	2.9	2.2	Sand	-	-

Depth (cm)	Water retention characteristics (% H ₂ O v/v)						Macro structural stability (slaking)	Micro structural stability (dispersion)
	0 kPa	10 kPa	33 kPa	100 kPa	1500 kPa	PAW		
0-20	38.0	10.5	7.2	5.0	3.3	7.1	Good	Fair
40-60	41.4	13.8	8.6	7.0	4.7	9.1	Fair	Fair

Depth (m)

Soil Horizon

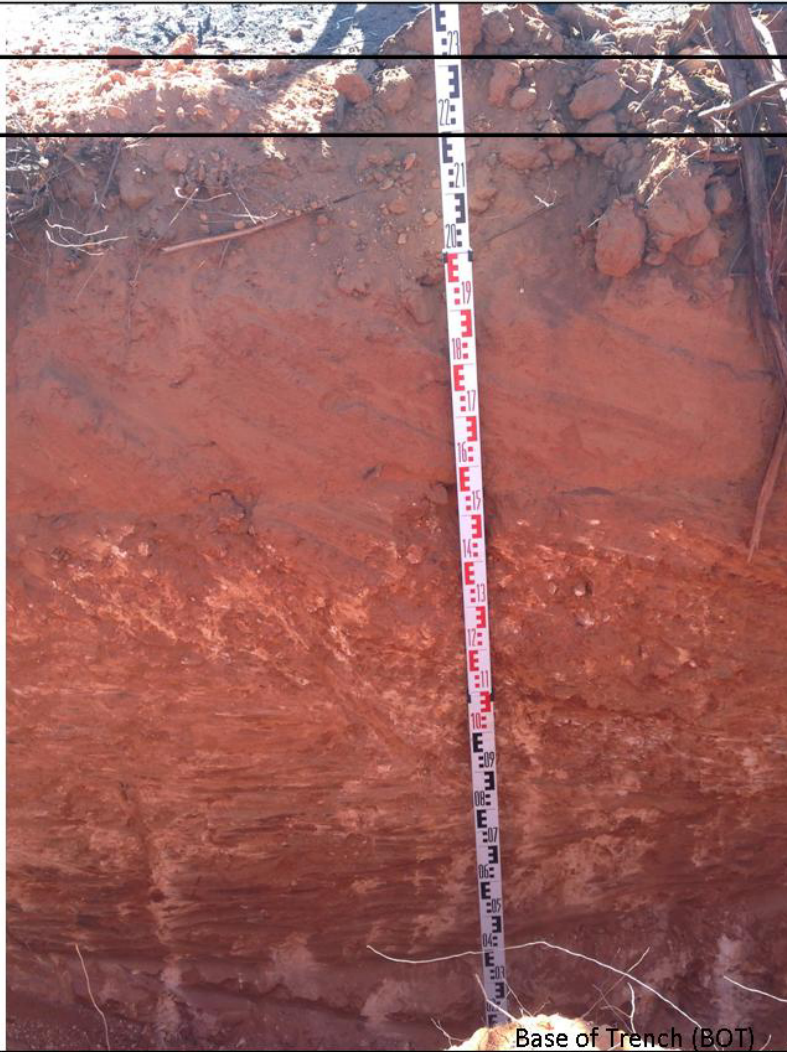
Soil Material

Description

0.0

0.3

2.5



A

Topsoil

Brownish red aggregated loam, well structured with polyhedral peds, strong to very strong coherence, abundant roots of all sizes, gradual boundary to

B1

Reddish Brown Loam

Brownish red loam, well structured with crumb to polyhedral peds, moderate coherence, common to many roots growing along structural surfaces, abrupt boundary to

B2

Calcrete

Light reddish brown to white calcareous loam to consolidated calcrete, represents a developing calcrete layer, moderate to very high coherence, common to many roots growing along structural surfaces

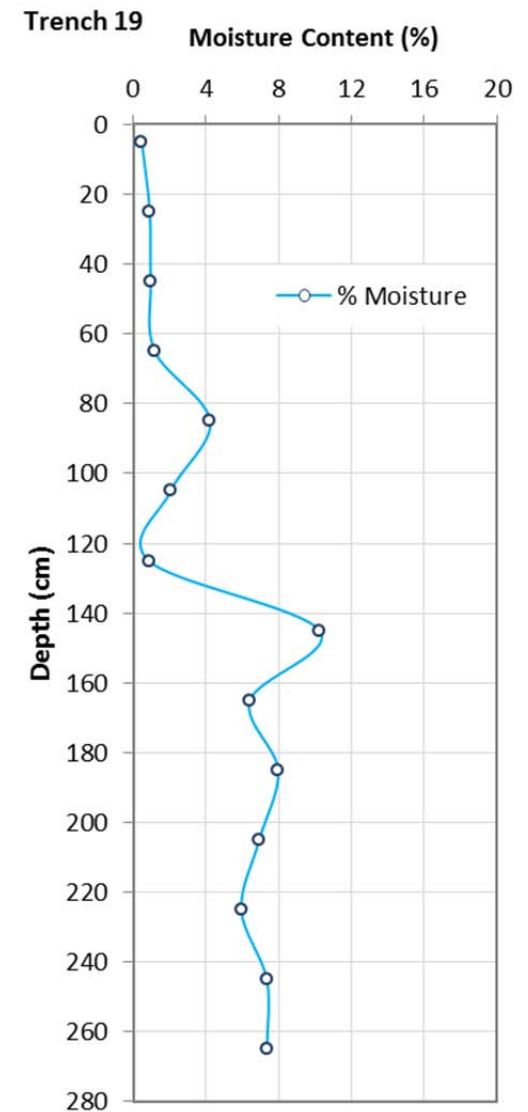
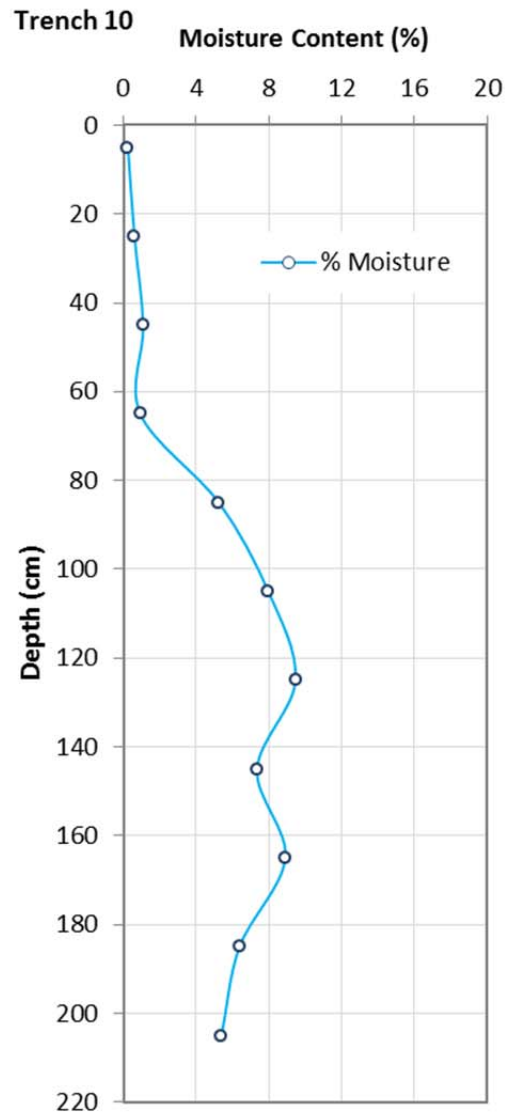
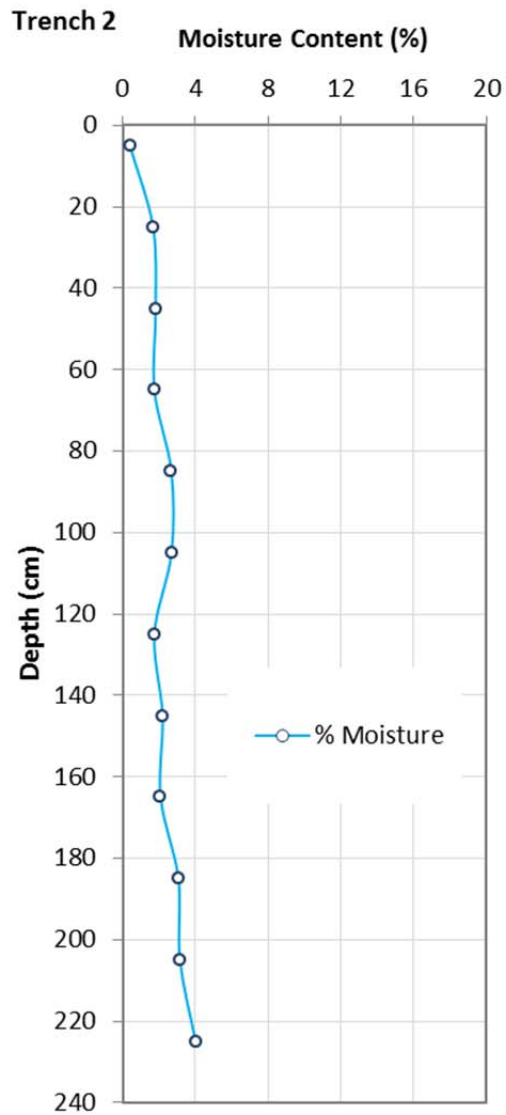
Base of Trench (BOT)

VIMY RESOURCES

TERRAIN ANALYSIS AND MATERIALS
CHARACTERISATION FOR THE MULGA ROCK URANIUM
PROJECT

Figure 4.11: Characteristic soil profile for SMU 3





VIMY RESOURCES

TERRAIN ANALYSIS AND MATERIALS
CHARACTERISATION FOR THE MULGA ROCK URANIUM
PROJECT

Figure 4.12: Moisture profiles for SMU 3



STUDY RESULTS

4.4.2 CHEMICAL PROPERTIES

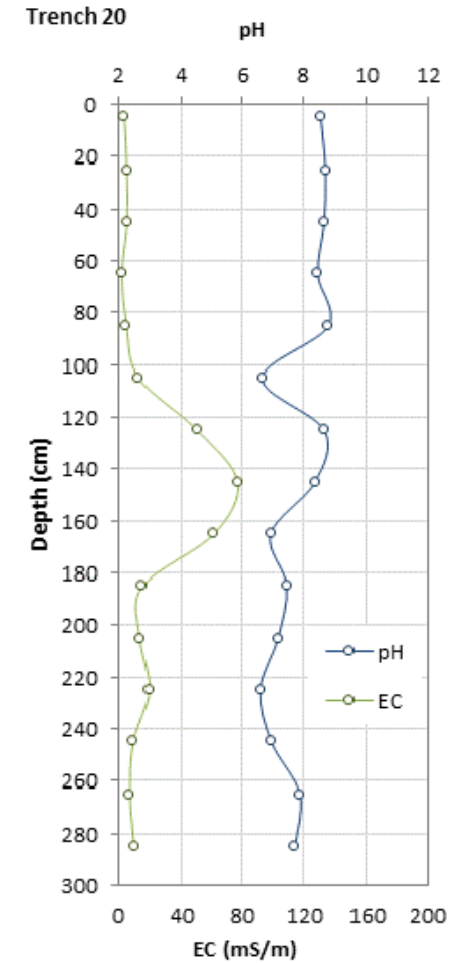
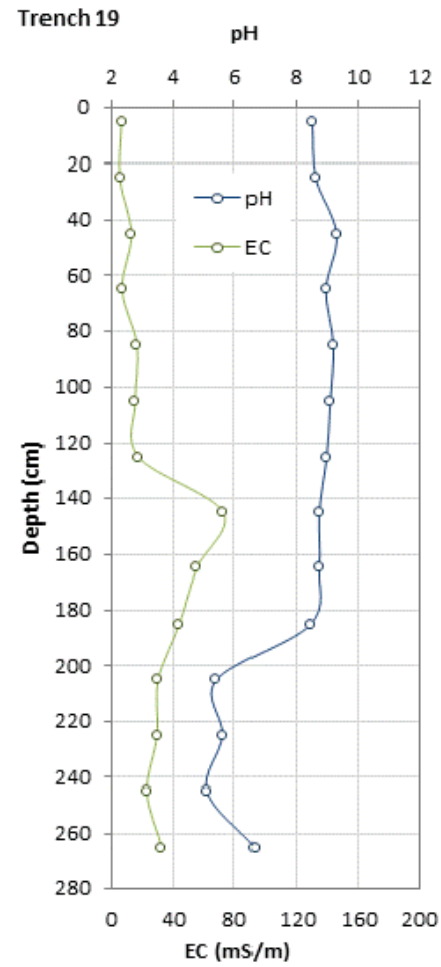
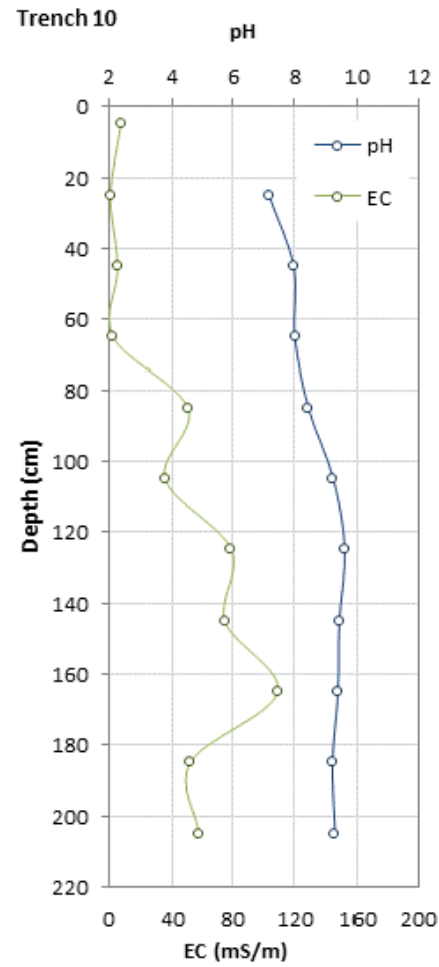
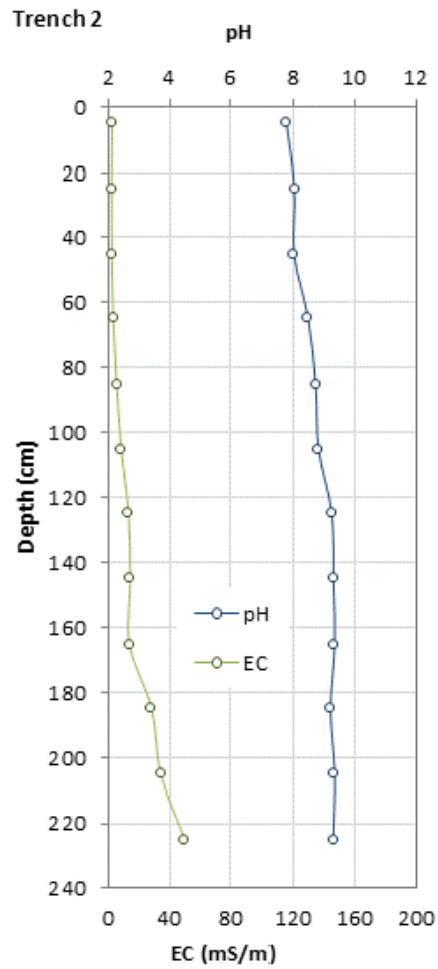
The chemical properties of the soils within SMU 3 are provided in Table 4.8 and shown in Figure 4.13. As with all soils throughout the MRUP, the soil materials within SMU 3 are considered chemical infertile, with low to very low levels of all plant available macro-nutrients (i.e. $\text{NH}_4\text{-N}$ + $\text{NO}_3\text{-N}$, Colwell P & K and Extractable S). The high organic C content in the surface reflects the abundant of plant roots in this surface layer, whilst the moderate to high levels to at least 2.4 m indicates that the vegetation is accessing all of the profile.

Interestingly, there is a significant increase in ESP when the calcrete layer is encountered, and these values are similar to those reported in the upper Miocene sediments (Section 4.7.1), possibly suggesting that the calcrete represents the old Miocene landsurface and was formed by pedogenic precipitation of $\text{Ca}/\text{CO}_3/\text{SO}_4$ in the upper profile.

Table 4.8 Average chemical properties of SMU 3

Depth (cm)	Nutrients (mg/kg)					Organic C (%)	pH (1:5)	EC 1:5 (mS/m)
	$\text{NH}_4\text{-N}$	$\text{NO}_3\text{-N}$	Colwell P	Colwell K	Ext. S			
0-20	3.2	1	5	122	2.8	0.55	7.3	5.5
40-60	2	<1	4	132	1.1	0.21	7.3	2.1
100-160	1	<1	4	188	49	0.12	8.5	23.8
180-240	1	12	3	268	51	0.15	8.4	41.4

Depth (cm)	Exchangeable cations (meq/100g)					CEC (meq/100g)	ESP (%)
	Ca	Mg	Na	K	Al		
0-20	3.94	0.83	0.06	0.29	0.09	5.12	1.2
40-60	2.86	1.07	0.04	0.33	0.10	4.31	1.0
100-160	5.54	1.77	1.82	0.47	0.12	9.61	18.8
180-240	5.34	3.50	2.31	0.68	0.09	11.84	23.7



VIMY RESOURCES

TERRAIN ANALYSIS AND MATERIALS
CHARACTERISATION FOR THE MULGA ROCK URANIUM
PROJECT

Figure 4.13: pH and EC depth profiles for SMU 3



4.5 SOIL MATERIAL MANAGEMENT UNITS (SMMU)

This section summarises the properties of the various soil materials identified throughout the MRUP and groups the materials into Soil Material Management Units (SMMU) to aid their management during mining operations and rehabilitation works (Section 5.1). The following five SMMU were identified within the MRUP:

- Topsoil
- Yellow Dunal Sand (YDS)
- Red Dunal Sand (RDS)
- Red Brown Loam (RBL)
- Calcrete (CT)

A description of the pertinent soil properties that may influence the behaviour of these SMMU during mining and rehabilitation, and subsequently how they should be managed, is provided below, whilst characteristic soil property data is presented in Table 4.9 and Table 4.10.

4.5.1 TOPSOIL

Throughout the MRUP topsoil is poorly developed and exhibits negligible plant available nutrients; hence it is considered chemically infertile. This poor development is likely due to the lack of accumulation of organic matter across the landsurface (Plate 4.8), which is strongly influenced by the current fire regime (and possibly ants and wind following fire), and the arid climate within the MRUP, which limits the breakdown and incorporation of organics into the surface soils.

Plate 4.8: Absence of organic matter accumulation following a fire within the MRUP



Topsoil typically has the following beneficial properties:

STUDY RESULTS

- Nutrient source, which aid germination of the native vegetation
- Microbes, which aids seed germination and nutrient availability
- Seed store

Topsoil within the MRUP is unlikely to contain microbes due to the hot dry climate of the region, and the sandy nature of the surface soils, which rapidly drain and exist well below PWP (i.e. 1,500 kPa) for the majority of the year. SWC have undertaken numerous studies throughout the Goldfields Region to quantify the microbiological properties of native soils to determine their potential benefits to rehabilitation. In all of these studies, across the arid Goldfields Region, minimal microbes, as assessed by Microbial Biomass Carbon (MBC) and Soluble Organic Carbon (SOC), were identified. From this work the role and importance of microbes in ecosystem function, and in particular to facilitate revegetation of post-mine landforms was considered negligible and thus the requirement to strip topsoils or surface soils to preserve this 'biological zone' was not warranted.

Given the surface soils or 'topsoil' within the MRUP are chemically infertile and are unlikely to contain beneficial microbiological properties, its primary benefit is as a seed store. Rehabilitation of the MRUP will involve spreading seed across the rehabilitated post-mine landsurface, and thus the requirement to preserve the seed store within the surface soils is reduced as it will be supplemented by seed. Obviously the utilisation of seed within the surface soil represents a cost-saving (i.e. reduces the quantity of seed to collect or purchase), however this saving needs to be offset by the stripping costs to capture this seed store, which only occurs in the top 5 cm of the soil profile.

4.5.2 YELLOW DUNAL SAND

The Yellow Dunal Sand (YDS) is the most extensive SMMU occurring within the MRUP, and will therefore represent the greatest volume of soil that requires management. Fortunately, this material exhibits optimal soil physical and chemical properties for handling during mining and rehabilitation (i.e. it is non-saline, non-sodic and will not hardset), and is unlikely to result in environmental impact during stripping, stockpiling or utilisation in rehabilitation. Given it has negligible silt + clay content (i.e. 2.5%; Table 4.9), with a dominance of medium sand (i.e. 200 – 400 μm), it has a high saturated permeability (4.87 m/day; Table 4.9) and very low water holding and PAW content (Table 4.9). This material therefore has limited capacity to supply sufficient soil moisture to support the transpiration requirements of the native vegetation and therefore it should only be used as an evaporative buffer to prevent underlying clay soils from drying and hardsetting and to provide revegetation species sufficient depth to develop an extensive lateral root system and maximise the volume of the soil profile accessed.

As occurs in the native environment within the MRUP, the depth of the YDS effectively controls the distribution of the various vegetation communities, such that the more drought-tolerant shrub vegetation units (i.e. S6 and S8) occur in areas where the thickness of YDS exceeds 5 m, whilst the various Eucalypt vegetation communities (i.e. E5, E3, E6 and E8) only occur when this depth is < 5 m. The depth of the YDS effectively controls the volume of PAW accessible to the native species, and therefore its utilisation in rehabilitation can be manipulated to sustainably achieve the desired revegetation community.

4.5.3 RED DUNAL SAND

The Red Dunal Sand (RDS) represents a different pedogenic facies of the YDS, whereby clay eluviated from the overlying YDS is illuviated at depth to form the RDS. This increase in clay content does result in this material potentially hardsetting, when the clay content exceeds 7.5%, with the mobile clay fraction likely to exhibit dispersive properties due to its very low salinity (i.e. the low electrolyte concentration in the soil solution is not sufficient to flocculate the clay

STUDY RESULTS

particles). This potential hardsetting property will restrict the utilisation of this material on the surface of the post-mine landforms; hence it should always underlie an evaporative cover (i.e. YDS) when used in isolation (i.e. not mixed with YDS) in rehabilitation.

In comparison to the YDS, the RDS represents a relatively small portion of the total volume of sand to be handled and utilised during the mining operation. Given this, it is recommended that the RDS is mixed and diluted with the YDS, removing the restrictions on use of the RDS; hence all dunal sand overlying the underlying basal loams and clays can be stripped, stockpiled and utilised as a single homogeneous unit.

4.5.4 RED BROWN LOAM

The Red Brown Loam (RBL) occurs as a relatively thin (i.e. < 1 m in thickness) soil layer across the entire MRUP, forming the base to the overlying Quaternary Dunal Sands (i.e. YDS + RDS). The loamy nature of this material (i.e. 7% silt + clay) result in it having a good water holding and PAW capacity; however, it will hardset if allowed to dry and the mobile clay fraction is dispersive. Based on these properties, it is required that the RBL is stripped separately from the overlying sands, and should only be used at depth (i.e. > 1 m deep) in the rehabilitated soil profile.

4.5.5 CALCRETE

The Calcrete (CT) occurs as a highly variable layer across the entire MRUP and exists in various states of formation (i.e. thin partially formed and unconsolidated, to a thick consolidated calcrete layer). As previously discussed it is likely that this material represents the old Miocene surface, with the calcrete forming from the Miocene sediments. Additional work was undertaken by SWC on the neutralising capacity of the calcrete, to determine its potential for use in either the processing plant or as a basal seepage layer for the TSF to neutralise released or added acidity. The Acid Neutralising Capacity (ANC) of the material varied from 53.4 to 156.9 kg H₂SO₄/t, indicating that this material has an appreciable capacity to buffer acidic seepage or process solutions.

The high fines content typically occurring in this material (i.e. around 17 % silt + clay) will likely limit its use as a capillary break material for the proposed above and in-pit TSF, unless it is screened to remove the < 2 mm soil fraction. In contrast, this fines fraction makes the calcrete material an optimal source for road base.

Table 4.9: Summary physical and hydraulic properties of the identified SMMU

(a) Material	Gravel (%)	Sand size fractions (%)							
		>1.2mm	>600µm	>425µm	>300µm	>200µm	>150µm	>75µm	<75µm
TS	0	1.1	12.2	21.1	23.9	18.5	10.1	6.5	6.5
YDS	0.1	0.7	7.3	16.4	24.1	22.1	12.6	8.8	7.9
RDS	0	0.3	5.5	17.5	29.5	21.5	12.0	8.2	5.5
RBL	0.5	4.3	13.7	13.6	15.7	16.5	11.6	10.3	14.1
CT	51.1	6.9	9.8	14.4	11.4	7.7	6.2	10.4	30.3

(b) Material	Depth (cm)	Fines fractions, < 2 mm [%, g/g]			Texture	BD (g/cm ³)	Ksat (m/day)
		Sand	Silt	Clay			
TS	0-30	97.0	0.8	2.2	Sand	1.56	3.29
YDS	50-380	97.5	0.3	2.2	Sand	1.77	4.87
RDS	180-290	98.6	0.2	1.2	Sand	1.77	-

STUDY RESULTS

(b)	Depth (cm)	Fines fractions, < 2 mm [%, g/g]			Texture	BD	Ksat
RBL	40-400	93.0	1.1	5.9	Sandy loam	1.68	1.17
CT	120-220	83.4	7.4	9.2	Sandy loam	-	-

(c) Material	Depth (cm)	Water retention characteristics (% H ₂ O v/v)				
		0 kPa	10 kPa	100 kPa	1500 kPa	PAW
TS	0-30	40.3	10.5	5.0	3.6	6.9
YDS	50-380	38.1	7.4	2.5	1.9	5.4
RDS	180-290	37.3	7.2	2.0	1.7	5.5
RBL	40-400	36.9	10.9	5.0	3.8	7.1

Table 4.10: Summary chemical properties of the identified SMMU

Material (a)	Nutrients (mg/kg)					Organic C (%)	pH (1:5)	EC 1:5 (mS/m)
	NH ₄ -N	NO ₃ -N	Colwell P	Colwell K	Ext. S			
TS	1.6	1.4	4.5	90	2.4	0.41	7.1	4.0
YDS	<1	<1	3.5	28	2.3	0.09	6.4	<1
RDS	<1	<1	3.5	60	3.8	0.47	7.2	1.3
RBL	1	<1	3.8	102	2.7	0.15	7.3	2.9
CT	1	14	3.8	361	33	0.18	7.9	38

Material (b)	Exchangeable cations (meq/100g)					CEC (meq/100g)	ESP (%)
	Ca	Mg	Na	K	Al		
TS	2.99	0.60	0.04	0.21	0.09	3.85	1.2
YDS	0.56	0.31	0.02	0.06	0.12	0.97	2.2
RDS	1.36	0.77	0.06	0.15	0.12	2.35	3.5
RBL	2.78	1.06	0.13	0.25	0.11	4.23	3.6
CT	7.40	3.81	2.49	0.89	0.10	14.6	15.7

4.6 EROSIONAL STABILITY

4.6.1 WEPP EROSION MODELLING

Table 4.11 and Figure 4.14a show the average sediment yield predicted by the WEPP erosion model, given the input parameters previously summarised in Section 3.2.3.6. In general, erosion rates resulting from the tested soils are considered to be low (i.e. less than 10 t/ha/yr). The sandiest samples, E5 and S6, performed best – these materials exhibited very high infiltration rates, and thus very little runoff and erosion was predicted – with erosion rates of <2 t/ha/yr, even at slope angles up to 15°. Whilst having a slower infiltration rate than the sands, the calcrete sample (C1) also exhibited relatively low erosion rate of <3 t/ha/yr, owing to the high gravel content and resultant self-armouring. Sample E3 exhibited the highest rate of erosion owing to the greater silt/clay content, and low gravel content, as compared to the other samples. Despite this, the E3 soil would be considered “acceptable” (i.e. <10 t/ha/yr) as a mine site rehabilitation material according to Australian mining industry standard practice, so long as slope angles of approximately ≤10° are used. An erosion rate of <10 t/ha/yr is expected to provide sufficient surface stability for rehabilitation species to become established, thus further stabilising the landform.

STUDY RESULTS

As the majority of extreme rainfall events occur during the tropical cyclone season, November-February, the majority of predicted erosion is expected to occur during these months (Figure 4.14b). It is also important to note that while the expected average erosion rates are reported in Table 4.11, considerable year-to-year variability should be expected – with modelled erosion rates ranging from zero erosion in some years, up to 10-times the average rate in other years.

Table 4.11: Summary of WEPP erosion modelling results.

Material ID	Lift height (m)	Slope angle	Average runoff (mm/yr)	Average sediment yield (t/ha/yr)	Average erosion rate (mm/yr)
C1	10	5	8	1.3	0.07
		10	10	2.4	0.13
		15	10	2.9	0.16
E3	10	5	8	2.9	0.16
		10	10	7.1	0.39
		15	11	11.1	0.62
E5	10	5	2	0.5	0.03
		10	2	1.1	0.06
		15	2	1.6	0.09
S6	10	5	1	0.3	0.02
		10	1	0.4	0.02
		15	1	0.7	0.04

4.6.2 SIBERIA EROSION MODELLING

4.6.2.1 Regional Model

The first SIBERIA model scenario was developed in order to investigate the likely sediment transport pathways within the context of the regional landscape. Only one material was considered in the regional model because the erosion pathways are expected to be the same for any soil type, and because the S6 soil was thought to most closely represent the surface conditions across the regional landscape.

The primary model output was a DEM depicting the predicted landform after 10,000 years' worth of erosion. Figure 4.15a depicts the final expected form of the landscape, and Figure 4.15b highlights regions of erosion (greens and blues) and deposition (red). The model results indicate that:

- The erosion rate on the constructed landform is expected to be greater than the erosion rate in surrounding landscape. This is primarily a result of the shape of the constructed landform.
- Deposition of the sediment eroded from the constructed landform is expected to deposit locally, the majority within 100-200 m of the toe of the landform. Sediment is not modelled to travel much farther than this, as the landform is to be built within a natural depression, and any eroded sediment will be captured by the surrounding higher topography.

4.6.2.2 Layered Landform Model

A second SIBERIA model scenario was developed in order to investigate the evolution of the landform in more detail, given the complex layering of different materials likely to be utilised in its construction. The model consisted of (1) the

STUDY RESULTS

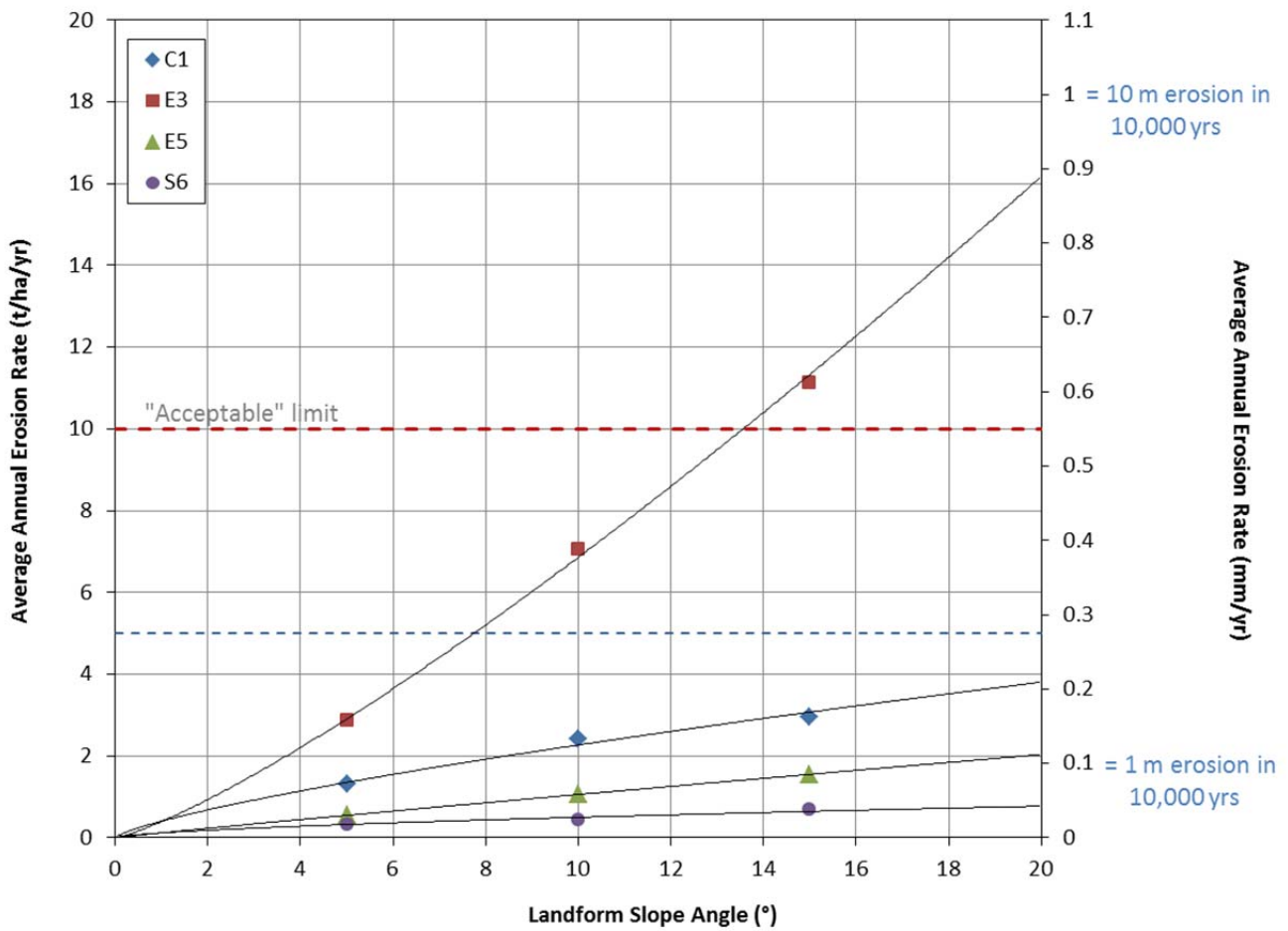
base clay/tailings core, (2) a 1 metre-thick calcrete layer ('C1' soil), and (3) a 2 metre-thick surface layer consisting of either 'E3' or 'S6' soil.

The main model output for an S6 surface covering is depicted in Figure 4.16a, and model output for an E3 surface covering is depicted in Figure 4.16b. The model results indicate:

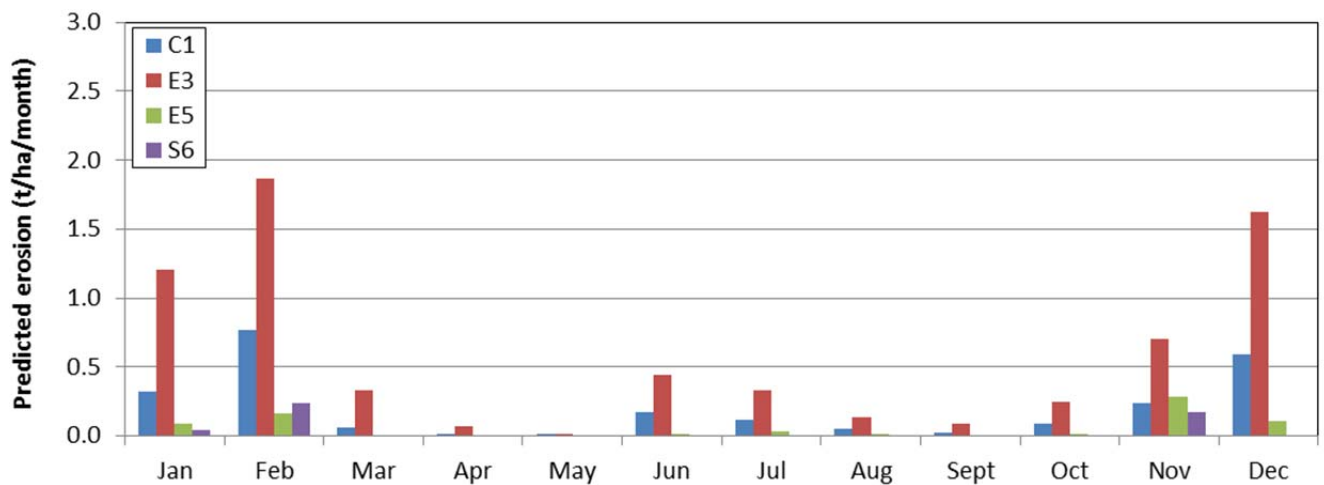
- Given the current landform design and available cover materials, the TSF core would likely be exposed after 10,000 years of rainfall erosion.
- The S6 surface cover resulted in greater rill formation than the E3 surface cover. This is likely to be a result of the extremely sandy nature of the S6 soil, which is expected to result in almost no cohesion between the individual soil particles. Also, given the presence of underlying materials with much lower-permeability, significant base-flow may be expected below the S6 sand, thus increasing tunnelling effects and rill formation.

The S6 surface cover resulted in less overall soil loss than the E3 surface cover. A greater volume of surface runoff (and thus erosion) is expected on the E3 material, given its lower permeability as compared to the S6 material. It is anticipated that most of the upper surface of the TSF core will be exposed after 10,000 years if E3 material is used as the primary cover/growth medium. In contrast, much of the upper surface the TSF may remain covered after 10,000 years if the S6 material is used, with portions of the upper rim and batter slopes being exposed.

A. Modelled annual erosion rates (100-year averages)



B. Modelled monthly erosion rates (100-year averages)



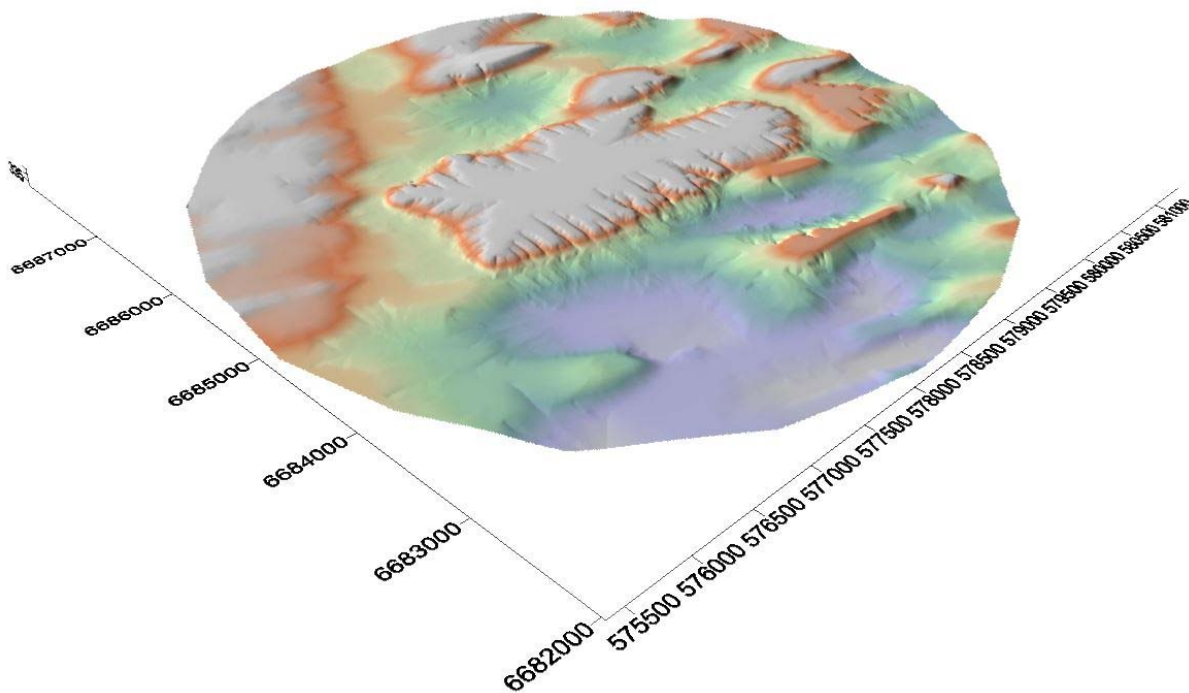
VIMY RESOURCES

TERRAIN ANALYSIS AND MATERIALS CHARACTERISATION FOR THE MULGA ROCK URANIUM PROJECT

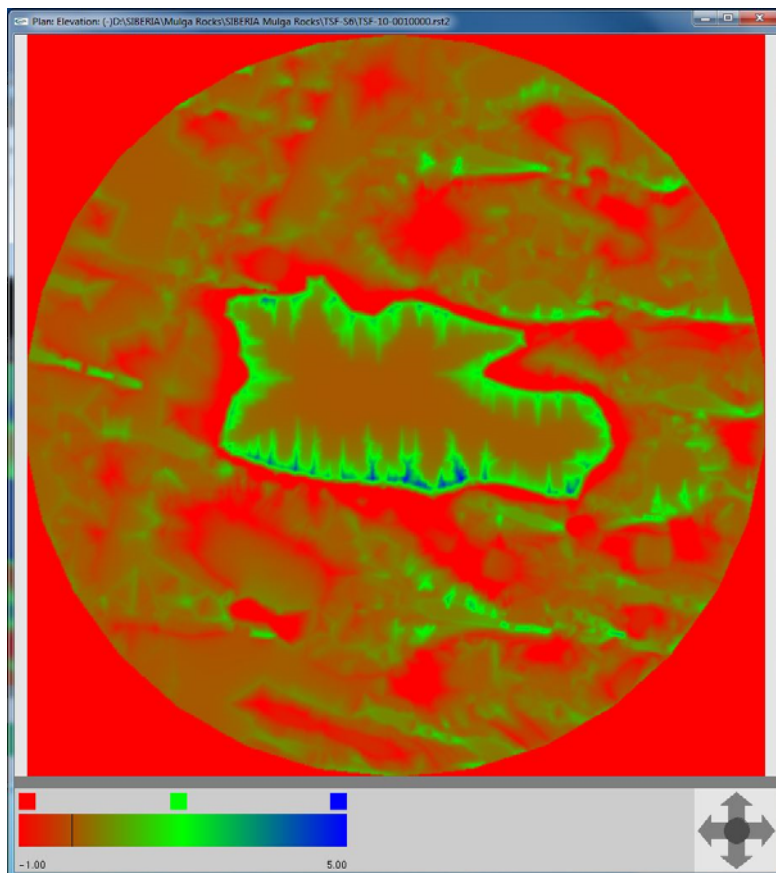
Figure 4.14: Modelled slope erosion rates



A. Regional model DEM output – 10,000 years post-mine



B. Regional model, areas of erosion (green and blue) and deposition (red)



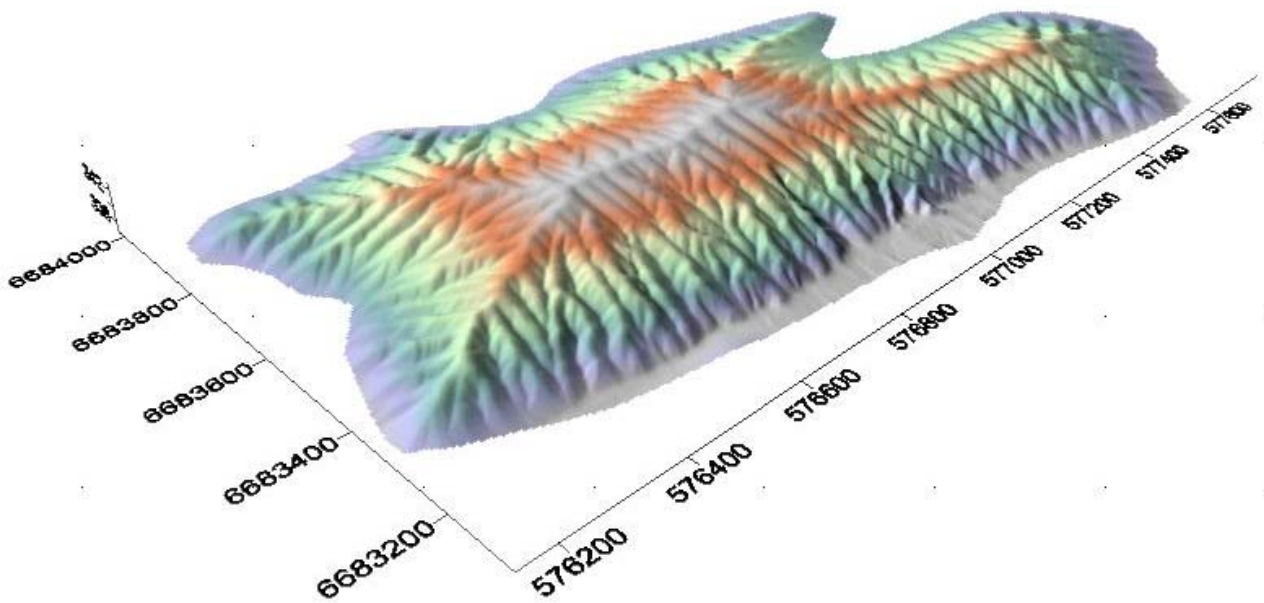
VIMY RESOURCES

TERRAIN ANALYSIS AND MATERIALS CHARACTERISATION FOR THE MULGA ROCK URANIUM PROJECT

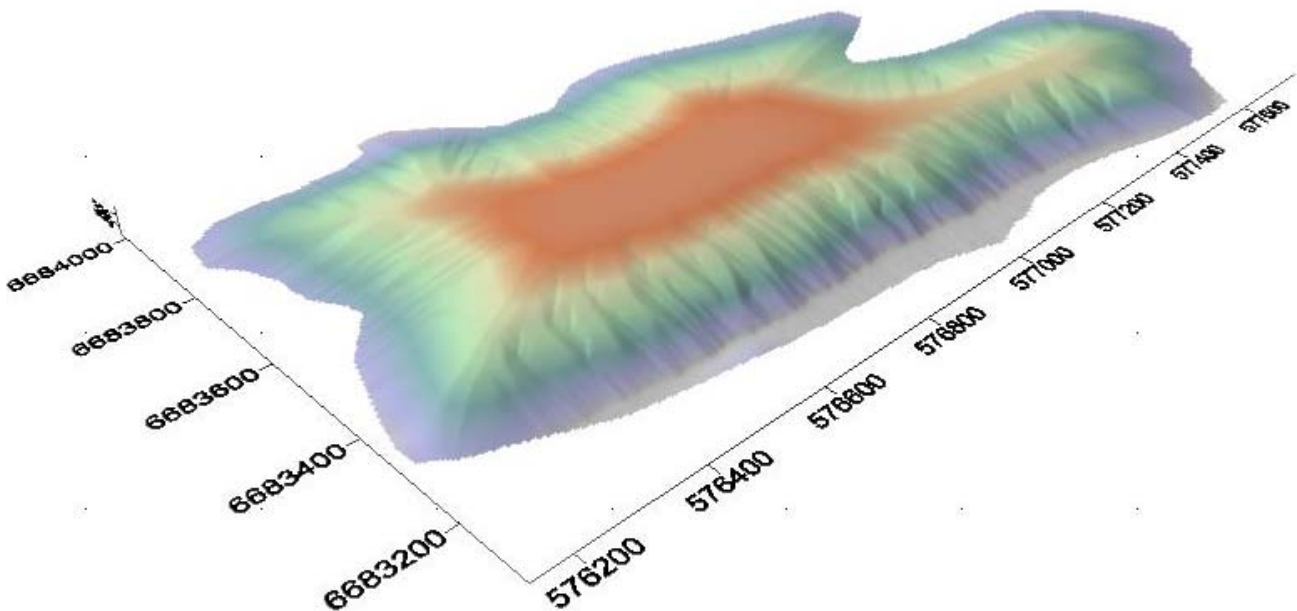
Figure 4.15: Regional SIBERIA model results



A. Layered landform model S6 output DEM – 10,000 years post-mine



B. Layered landform model E3 output DEM – 10,000 years post-mine



VIMY RESOURCES

TERRAIN ANALYSIS AND MATERIALS
CHARACTERISATION FOR THE MULGA
ROCK URANIUM PROJECT

Figure 4.16: Layered SIBERIA landform model results



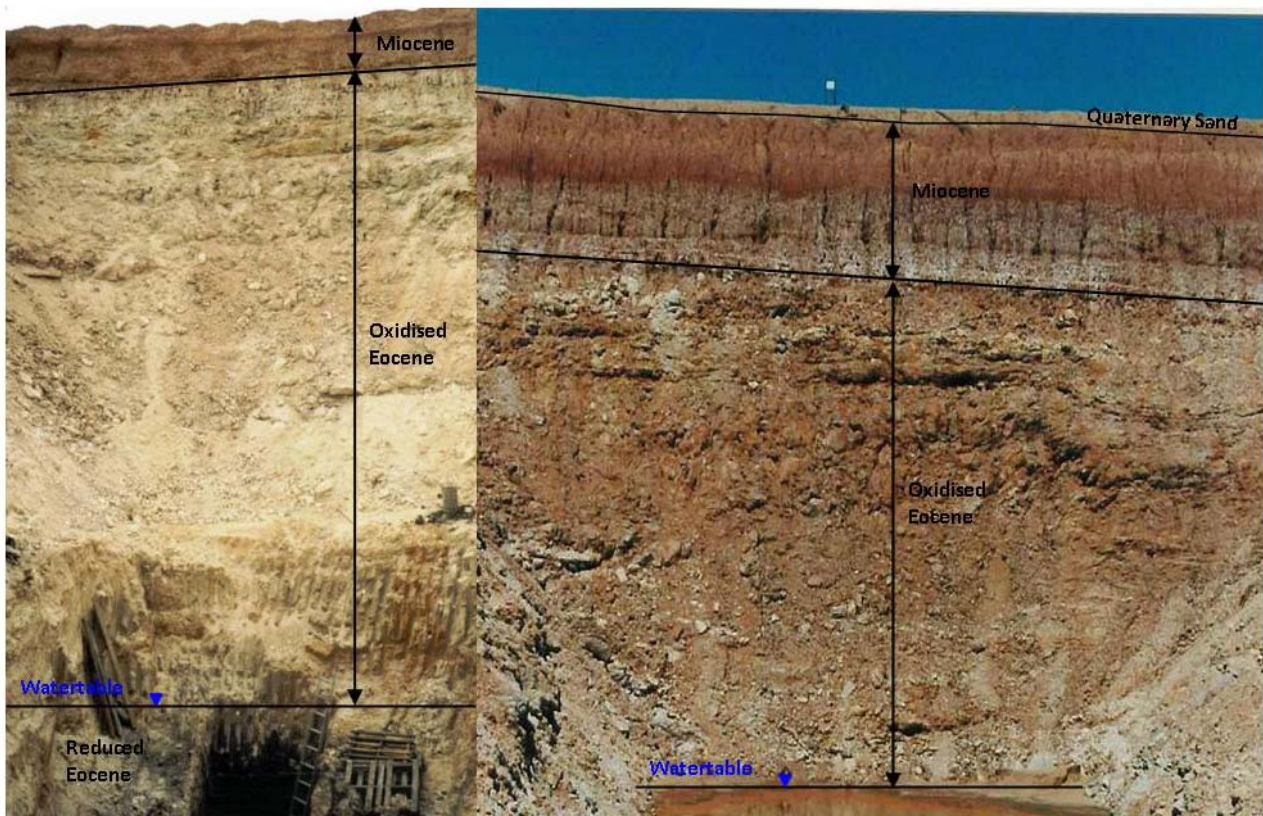
4.7 OVERBURDEN MATERIALS

For the MRUP, all sediment below the surficial calcrete (i.e. underlying SMU 3), comprising the Miocene and Oxidised Eocene profiles are considered overburden materials (Plate 4.9). These materials represent the greatest volume of material to be mined and managed at the MRUP, and thus they represent a substantial environment risk to the operation through the potential to release sediment into the surrounding environment and metalliferous drainage. To assess these risks, the baseline geochemical conditions existing within the deep Miocene and Oxidised Eocene sediments were characterised using the following approaches:

- Screen testing for pH, peroxide pH (pH_{ox}) and EC (salinity) – Section 3.2.2
- Clay dispersion
- Review of multi-element assay results

The results from this analysis for the Miocene and Oxidised Eocene overburden materials are presented in Section 4.7.1 and 4.7.2.

Plate 4.9: Overburden profile comprising the Miocene and Oxidised Eocene Sediments



4.7.1 MIOCENE SEDIMENTS

The Miocene (i.e. 23 – 5 Mya) sediments were deposited unconformably onto the pre-existing lateritic (Tertiary) surface of the Eocene sediments. This deposition resulted in an abrupt boundary occurring between the two sedimentary units, forming a porosity discontinuity and in places a texture contrast boundary. Observations by Vimy geologists, and geophysical assessment, have shown that perching of infiltrating rainfall occurs at this boundary, effectively acting as a deep water supply reservoir for the native vegetation, and that there is a coincident proliferation of plant roots at this

STUDY RESULTS

boundary. No deep roots have been observed in the underlying Oxidised Eocene sediments, and subsequently, the Quaternary Sands and Miocene sediment are been termed the 'Biologically Active Zone'.

The screen test results for the 12 representative drillholes throughout the MRUP are shown in Figure 4.17 to Figure 4.20. This data identifies that the Miocene sediments typically have pH values varying from around 9, in its upper surface where the calcrete layer has formed, to pH 7 at depth. The pH_{ox} values are similar to the corresponding pH data, indicating that no sulfides are present in this material. These alkaline pH values contrast to the slightly – moderately acidic pH values of the overlying Quaternary Sands and the underlying Oxidised Eocene sediments.

The EC (or salinity) of these sediments is generally moderate to high, varying from 50 – 100 mS/m. A defined 'spike' in EC often occurs at the boundary of the Quaternary Sands and the more clayey Miocene sediments, and this is likely due to the deposition and precipitation of salts at the texture contrast boundary. It is important to note that this process of leaching of soluble salts and precipitation of supersaturated mineral species formed by the removal of the water (typically by upward hydraulic connection with the surface) results in the formation of calcrete; hence this elevated salinity layer corresponds with the uniform calcrete layer that is widespread throughout the MRUP.

The dispersive qualities of the Miocene sediments are clearly shown in Plate 4.10. These samples represent a depth profile through the Miocene sediments, ranging from the upper calcrete layer to the base of the Miocene surface. These materials are all classified as sodic (i.e. ESP > 6; Table 4.12), and the influence of salinity in flocculating dispersed clay particles can clearly be seen in Plate 4.10.

Plate 4.10: Dispersive properties of the Miocene sediments, as influenced by salinity

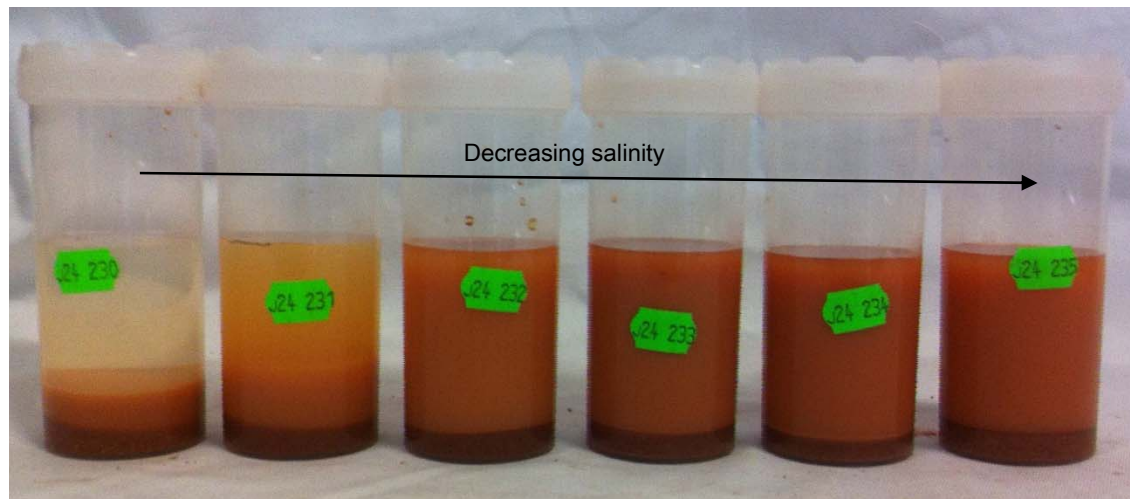


Table 4.12: Characteristic chemical properties of the Miocene sediments

Material	Nutrients (mg/kg)					Organic C (%)	pH (1:5)	EC 1:5 (mS/m)
	NH ₄ -N	NO ₃ -N	Colwell P	Colwell K	Ext. S			
<i>In situ</i> Miocene (Shogun Deposit)	<1	<1	4	372	100	0.09	8.2	63
<i>Rehabilitated Shogun Trial Slot</i>								
1 m depth	< 1	< 1	4	162	34	0.14	9.2	20.4
2 m depth	< 1	< 1	4	84	81	0.09	7.8	56.7

STUDY RESULTS

Material	Exchangeable cations (meq/100g)					CEC (meq/100g)	ESP (%)
	Ca	Mg	Na	K	Al		
<i>In situ</i> Miocene (Shogun)	4.83	3.18	5.20	0.91	0.10	14.1	33.2
<i>Rehabilitated Shogun Trial Slot</i>							
1 m depth	8.64	3.29	4.71	0.92	0.11	17.56	26.82
2 m depth	1	0.5	1.24	0.2	0.06	2.94	42.18

The multi-element composition of the Miocene sediments is provided in Table 4.13. The assay results show that whilst maximum values for several metals and metalloids exceed the corresponding DEC¹ (2010) Ecological Investigation Levels (EIL), average values for the Miocene sediments are all below the EIL, with the exception of Vanadium (Table 4.13). The elevated nature of Vanadium is expected given it is typically isomorphically substituted in the clay crystal mineral structure.

Based on this multi-element composition the risk of metalliferous drainage occurring, in response to rainfall leaching, is considered low.

Table 4.13: Multi-element composition of Miocene sediments (Values in bold exceed the corresponding EIL)

Analyte	Units	DEC (2010) EIL	No. Samples Analysed	Minimum	Maximum	Average	Standard Deviation
Ag	mg/kg		74	0	0.3	0.06	0.07
As	mg/kg	20	31	0	53	10.35	12.77
Au	mg/kg	-	47	0	0.2	0.00	0.03
Ba	mg/kg	300	212	0	1450	117.43	167.40
Cd	mg/kg	3	4	0	3	0.00	1.50
Co	mg/kg	50	79	0	21.3	3.59	3.66
Cr	mg/kg	50	5	20	260	50.00	92.84
Cu	mg/kg	100	79	1	85	15.31	16.19
Fe	%	-	11	0.09	1.5	0.63	0.42
Hg	mg/kg	1	9	0	2.25	0.64	0.80
Mn	mg/kg	500	4	0	50	25	23.81
Ni	mg/kg	60	79	0	83	13.72	14.37
P	%	-	3	0.004	0.005	0.00	0.00
Pb	mg/kg	100	113	0	95	18.18	18.84
Th	mg/kg	-	339	0.47	230	36.49	32.01
S	%	0.3	12	<0.1	<0.1	<0.1	<0.1
Sb	mg/kg	-	5	0	19	9.50	9.94
Se	mg/kg	-	173	0	740	18.38	69.92
Sr	mg/kg	-	65	3.76	506.73	96.75	124.10
U	mg/kg	-	339	0.06	110	15.88	20.29
V	mg/kg	50	65	8	730	123.13	132.25

¹ Now the Department of Environment Regulation (DER)

STUDY RESULTS

Analyte	Units	DEC (2010) EIL	No. Samples Analysed	Minimum	Maximum	Average	Standard Deviation
Zn	mg/kg	200	79	0	178	18.57	27.68

4.7.2 OXIDISED EOCENE SEDIMENTS

The palaeodrainage channel within the Narnoo Basin, hosting the Uranium Orebody, was principally filled with Eocene sediments, varying up to 100 m in thickness (Section 2.2.2). Drier climatic conditions since the Tertiary Period, and uplift along the southeast margin of the Yilgarn Craton, has resulted in a lowering of the watertable, which now stands at approximately 40 m below the surface (2.3.2). In response to this lowering, the surface 40 m of Eocene sediments have been oxidised and significantly weathered resulting in an effectively 'bleached' surface horizon (Plate 4.9); this represents the Oxidised Eocene sediments.

The screen test results show that the Oxidised Eocene sediments are typically slightly – moderately acidic to circum-neutral, with the level of inherent acidity increasing with depth as the watertable (redox boundary) and associated capillary fringe is encountered. The pH_{ox} results show that in the surface portions of the Oxidised Eocene sediments there has been a complete oxidation of sulfides, such that the pH_{ox} resembles the corresponding *in situ* pH; hence there is no residual sulfides present in this material. With depth, and approaching the capillary fringe (i.e. approximately 5 m above the phreatic surface), there are zones of residual sulfides which have the potential to oxidise to pH values around 2 (see Drillholes 5772 and 5940 from the Ambassador West and East Deposits, respectively; Figure 4.18 and Figure 4.19).

The salinity of the Oxidised Eocene sediments (Figure 4.17 to Figure 4.20) is generally low (i.e. < 50 mS/m), with only isolated zones of moderate to high salinities, likely representing clay-rich lenses that have not been completely leached in response to their low permeability. With depth, and approaching the capillary fringe, the salinity of the Oxidised Eocene sediments rises sharply, due to the influence of the hypersaline groundwater. This sharp increase in salinity is clearly seen in Figure 4.17.

The dispersive properties of the Oxidised Eocene sediments are shown in Plate 4.11. The dispersivity of these materials is due to both the low salinity (i.e. low electrolyte concentration in the soil solution) of the majority of the Oxidised Eocene sediments and their sodicity (ESP > 6). The characteristic chemical properties of the Oxidised Eocene sediments are provided in Table 4.14. This data highlights that these sediments are considered chemical infertile, with negligible plant available nutrients, minor organic C (as expected given its bleached properties) and highly sodic (ESP > 20).

The multi-element composition of the Oxidised Eocene sediments is provided in Table 4.15. In contrast to the geochemically inert Miocene sediments, the Oxidised Eocene sediments contain elevated levels of several metals and metalloids, often exceeding the corresponding EIL by several orders of magnitude. Metals and metalloids whose average composition exceeds the DEC (2010) EIL include: Cd, Co, Cr, Cu, Hg, Ni, Pb, V and Zn. These predominately siderophile and chalcophile elements are likely to either be isomorphically substituted within the clay mineral structure (i.e. as in the case for Cr and V), and thus are not available to leaching solutions, or form cationic-hydrolysis (i.e. positively charged) metals in aqueous, with reduced mobility due to the often circum-neutral pH of the Oxidised Eocene sediment (i.e. likely to contain a balance of positive and negatively charge surface complexes). This limited availability and mobility is likely to be the reason why these residual metals and metalloids remain elevated in the highly weathered and oxidised Eocene sediments (i.e. if there were available and mobile they would have been leached out during weathering).

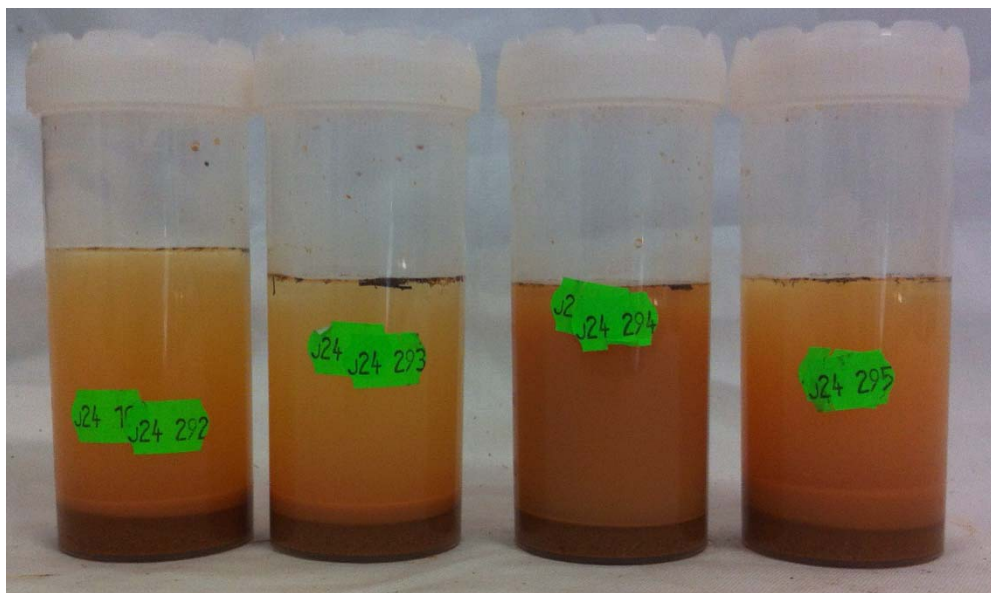
STUDY RESULTS

Table 4.14: Characteristic chemical properties of the Oxidised Eocene sediments

Material	Nutrients (mg/kg)					Organic C (%)	pH (1:5)	EC 1:5 (mS/m)
	NH ₄ -N	NO ₃ -N	Colwell P	Colwell K	Ext. S			
<i>Rehabilitated Shogun Trial Slot</i>								
1 m depth	< 1	< 1	4	72	9.5	0.1	6.9	36.6
2 m depth	1	< 1	4	357	153.1	0.08	6.2	20.4

Material	Exchangeable cations (meq/100g)					CEC (meq/100g)	ESP (%)
	Ca	Mg	Na	K	Al		
<i>Rehabilitated Shogun Trial Slot</i>							
1 m depth	4.44	1.47	1.76	0.41	0.10	8.08	21.78
2 m depth	1.05	0.34	0.49	0.18	0.14	2.06	23.76

Plate 4.11: Dispersive properties of the Oxidised Eocene sediments, as influenced by salinity



Based on the above discussion the risk of metalliferous drainage occurring from the Oxidised Eocene sediment, in response to rainfall leaching, is considered low.

Table 4.15: Multi-element composition of Oxidised Eocene sediments (Values in bold exceed the corresponding EIL)

Analyte	Units	DEC (2010) EIL	No. Samples Analysed	Minimum	Maximum	Average	Standard Deviation
Ag	mg/kg		543	0	24.8	0.49	2.05
As	mg/kg	20	51	0	125	9.20	20.49
Au	mg/kg	-	454	0	2.65	0.03	0.15
Ba	mg/kg	300	569	0	998	60.80	136.18
Cd	mg/kg	3	51	0	260	18.80	42.45
Co	mg/kg	50	556	0	3750	170.14	349.45
Cr	mg/kg	50	48	0	3100	249.92	551.32

STUDY RESULTS

Analyte	Units	DEC (2010) EIL	No. Samples Analysed	Minimum	Maximum	Average	Standard Deviation
Cu	mg/kg	100	556	0	14000	226.45	1032.74
Fe	%	-	543	0.02	12.5	1.21	0.89
Hg	mg/kg	1	35	0.09	166	12.28	36.15
Mn	mg/kg	500	35	0	120	22.29	30.59
Ni	mg/kg	60	556	1	13100	343.44	803.94
P	%	-	35	0	0.05	0.01	0.01
Pb	mg/kg	100	569	0	3630	106.60	362.81
Th	mg/kg	-	588	0	140	7.62	12.17
S	%	0.3	454	0	<0.1	<0.1	<0.1
Sb	mg/kg	-	51	0	1.8	0.15	0.32
Se	mg/kg	-	48	0	665	32.67	107.09
Sr	mg/kg	-	61	0	438	64.10	68.14
U	mg/kg	-	588	0.11	6540	142.71	523.11
V	mg/kg	50	64	4	1400	111.38	208.79
Zn	mg/kg	200	556	0	19600	690.60	1725.36

4.7.3 REHABILITATION POTENTIAL OF OVERBURDEN MATERIALS

The rehabilitation potential of the Miocene and Oxidised Eocene sediments is demonstrated in the rehabilitated mine slot in the Shogun Deposit that was mined by PNC Exploration Australia in the 1990's (Figure 4.21). In this area, two deep trenches were excavated to determine the nature of the reconstructed soil profile, as no records are available as to the nature of the backfilled soil profile. The location of these trenches (corresponding to Trench 19 and 20) is shown in Figure 4.21. Photographs of the reconstructed soil profiles at these locations are presented in Plate 4.12 and Plate 4.13

The most striking feature about the rehabilitation of the mined slot is the dominance of *Eucalyptus* sp. and the general absence of an understory and groundcover (Plate 4.14). Although this rehabilitation likely achieves a similar foliage cover to the native vegetation, it contains appreciably lower species richness and plant density properties than the corresponding and adjacent native vegetation.

It is considered that the relatively saline Miocene and Oxidised Eocene sediments that represent the bulk of the reconstructed soil profile (Plate 4.12 and Plate 4.13) present a chemical limitation to most species other than selected Eucalypt species. As shown in this report (Section 4-1), the surficial Quaternary Sands, comprising SMU 1 and 2, are non-saline, with salinity levels < 10 mS/m. This is likely to represent the growth medium for the majority of understory and groundcover species, and thus the presence of the more saline Miocene and Oxidised Eocene sediment (i.e. up to 100 mS/m) in the root zone restrict the growth and establishment of these species. As observed, and previously mentioned in Section 4.7.1, deep roots, likely to be of Eucalypt species, penetrate through the Miocene sediments and proliferate at the contact between the underlying Oxidised Eocene sediment where higher soil moisture levels prevail. It is therefore likely that the various Eucalypts have a greater tolerance to salinity than do the understory and groundcover species, and this explains their dominance in the rehabilitated trial slot at the Shogun Deposit.

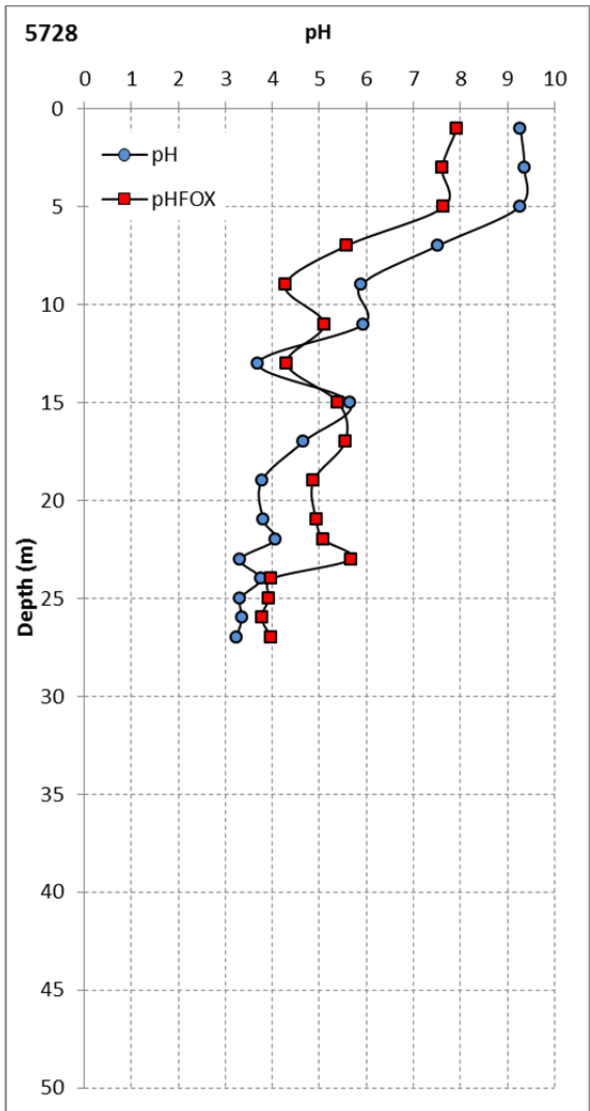
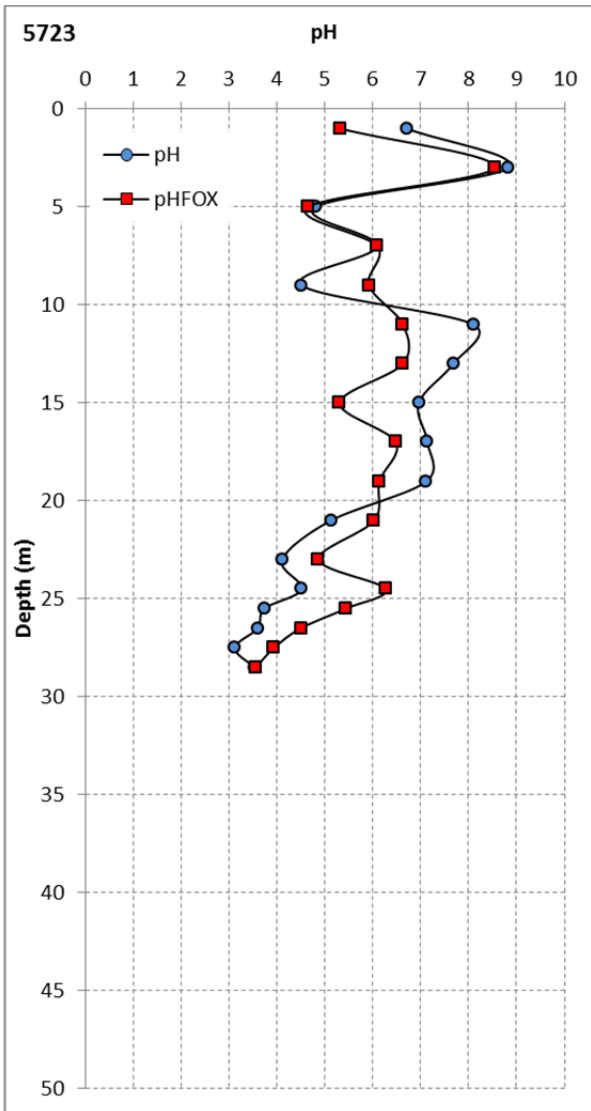
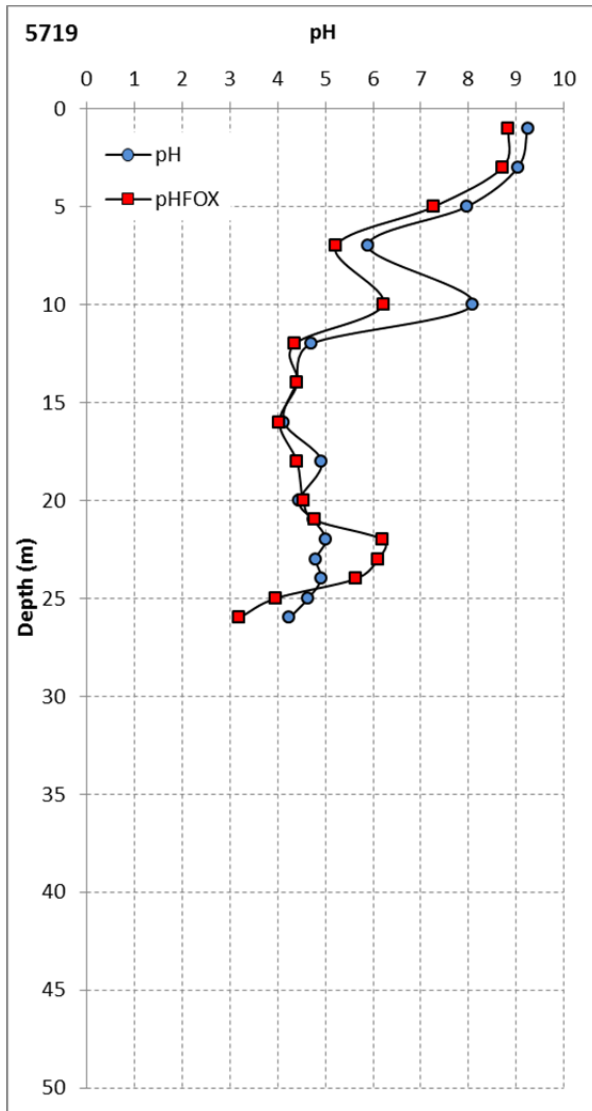
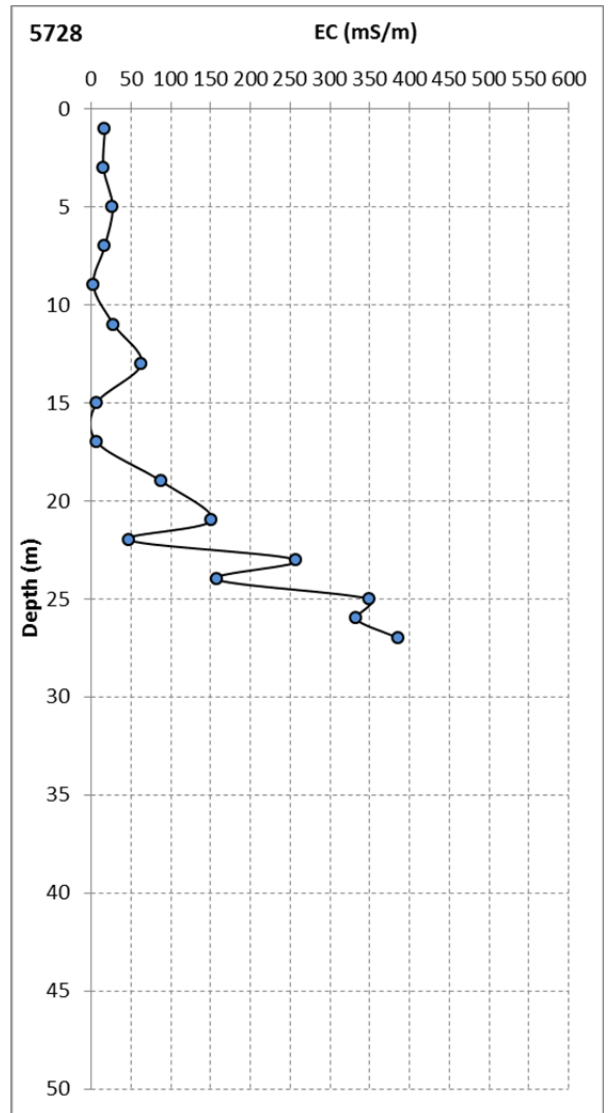
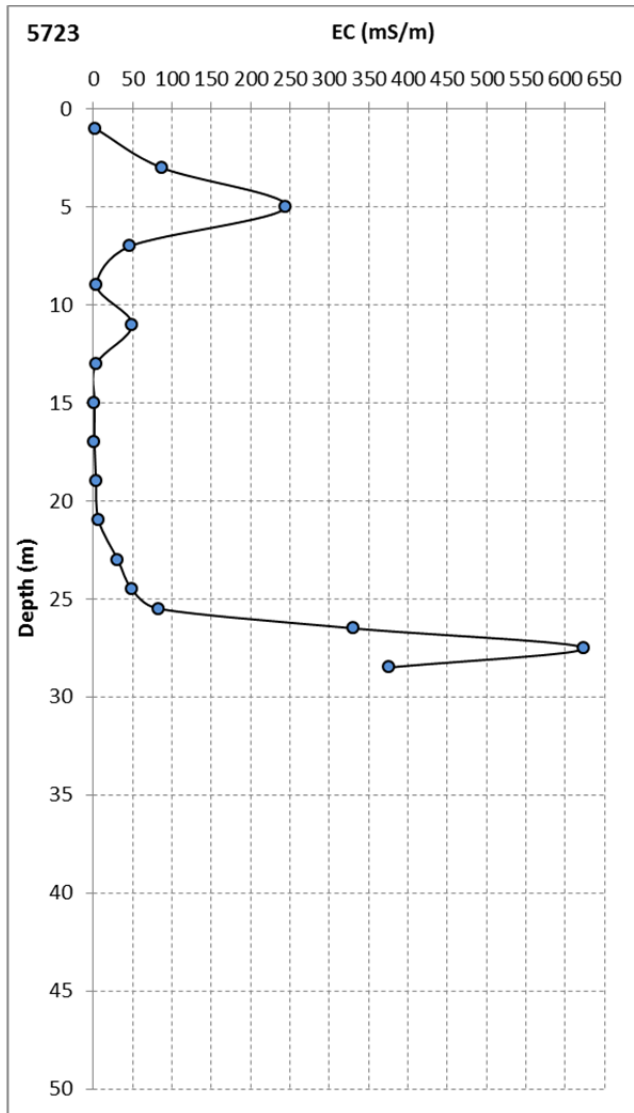
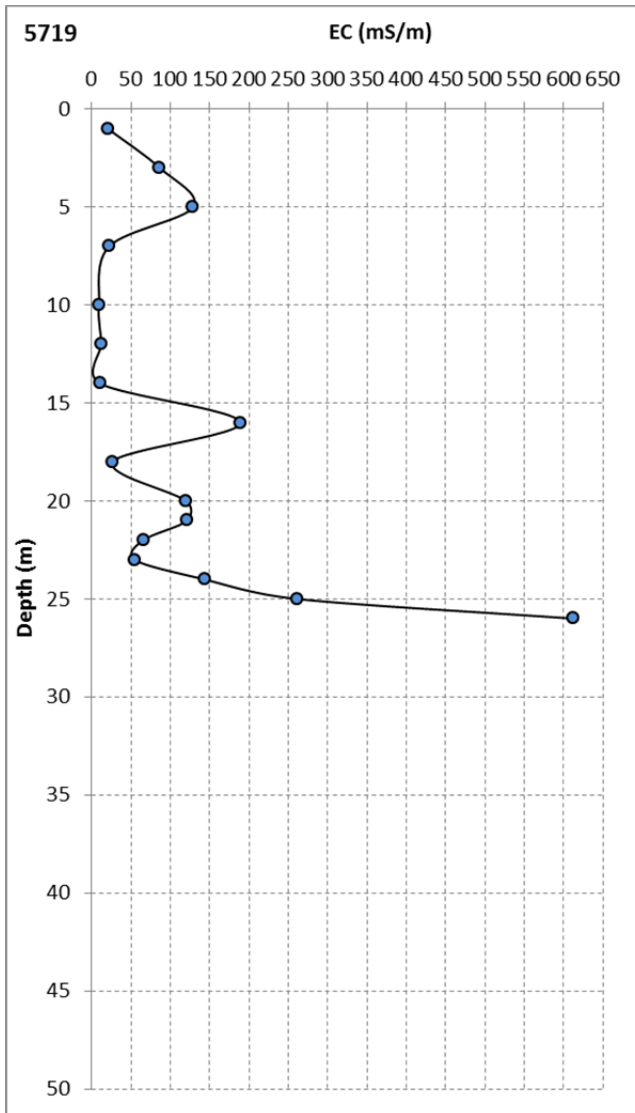


Figure 4.17: Screen test results for the overburden materials within the Shogun Deposit



VIMY RESOURCES

TERRAIN ANALYSIS AND MATERIALS
CHARACTERISATION FOR THE MULGA ROCK URANIUM
PROJECT

Figure 4.16 continued...



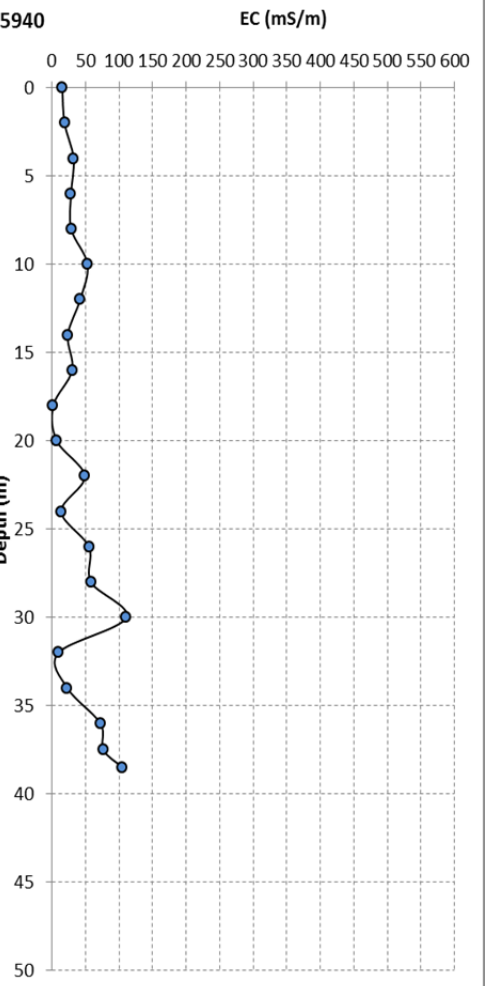
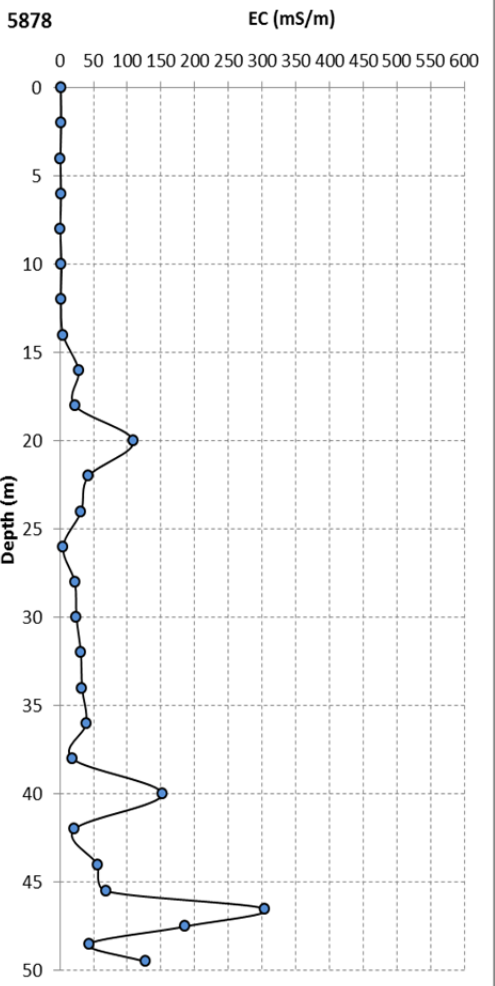
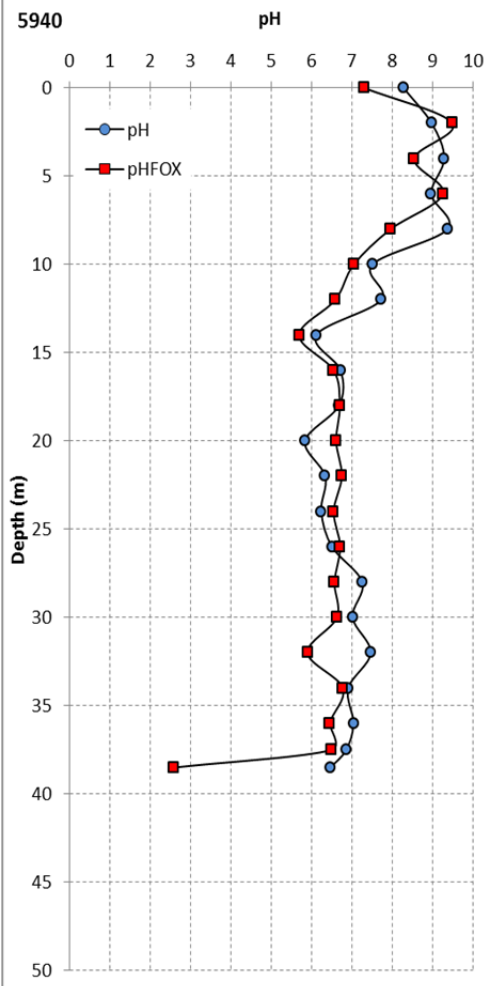
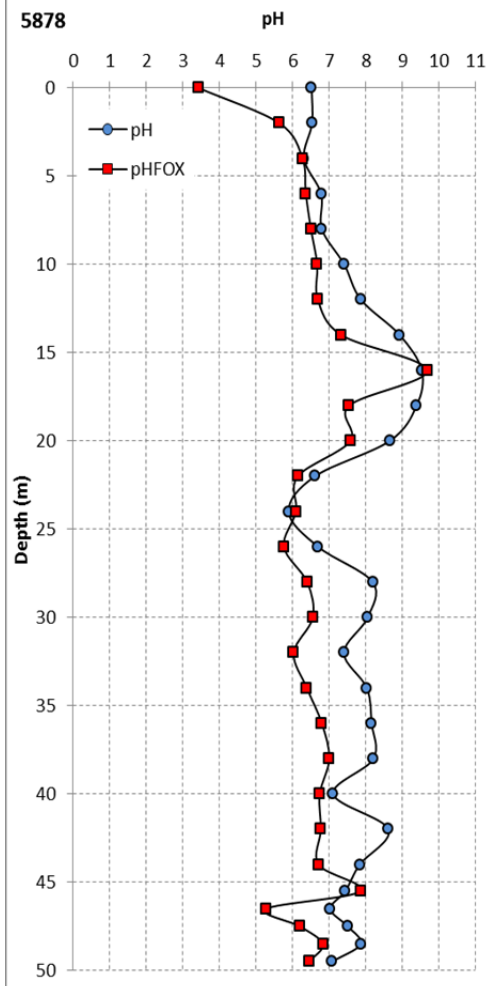
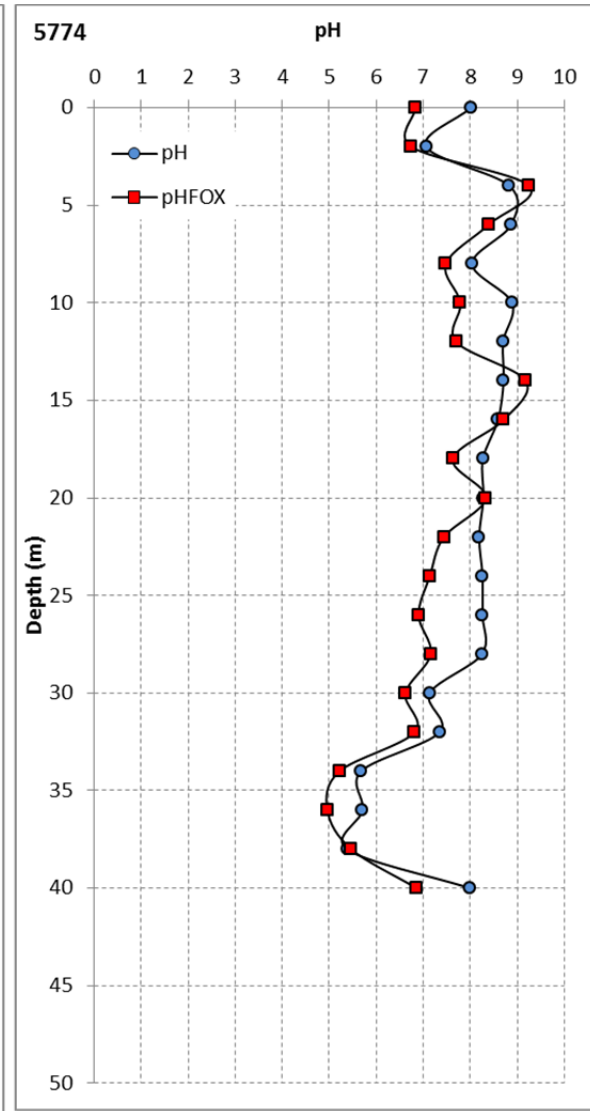
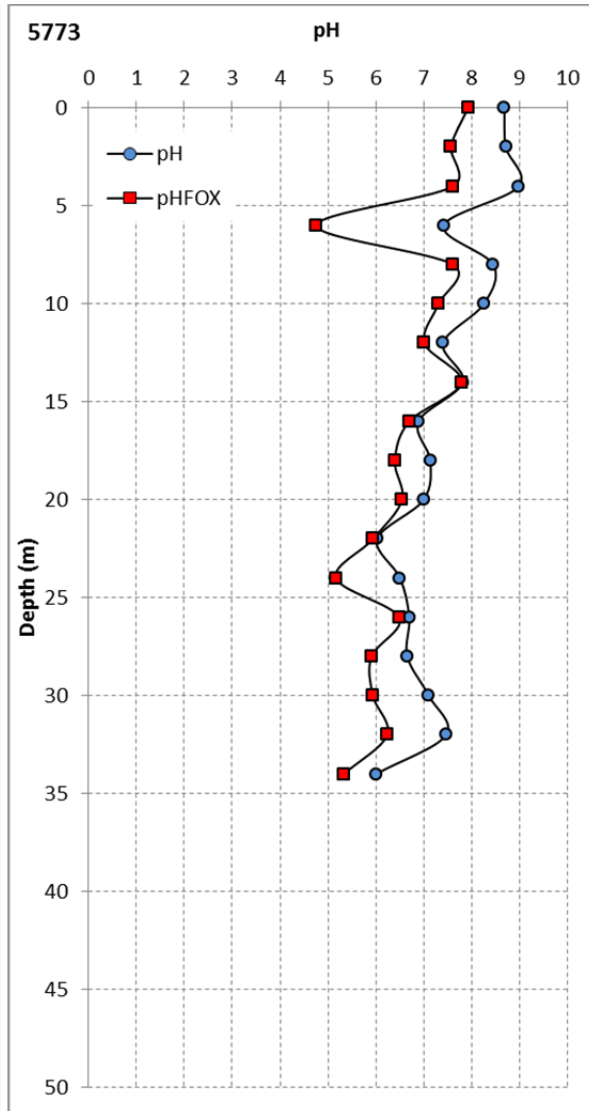
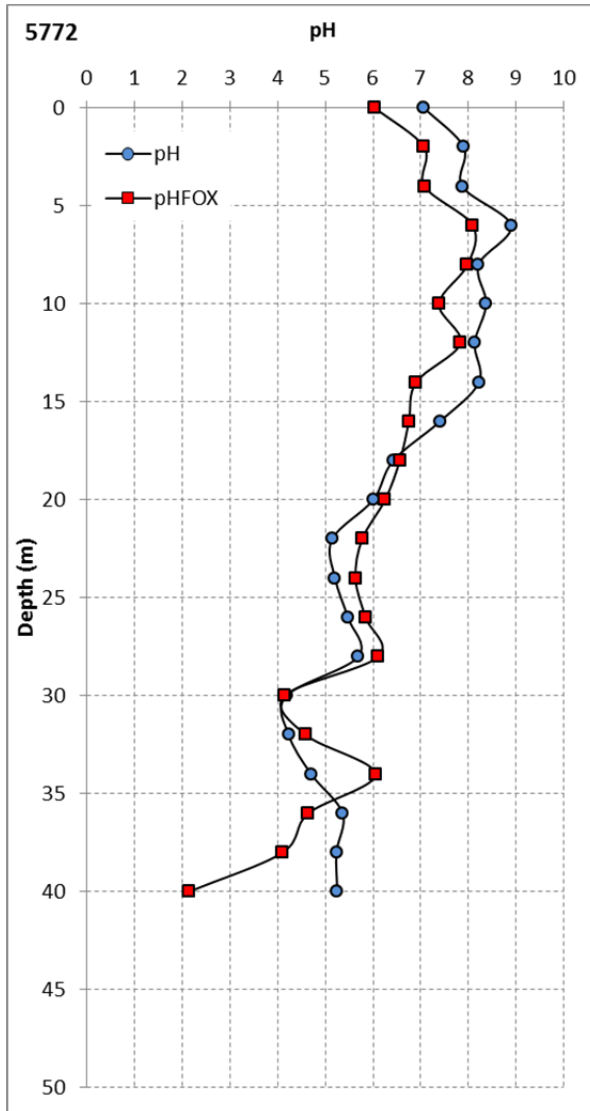


Figure 4.18: Screen test results for the overburden materials within the Ambassador East Deposit

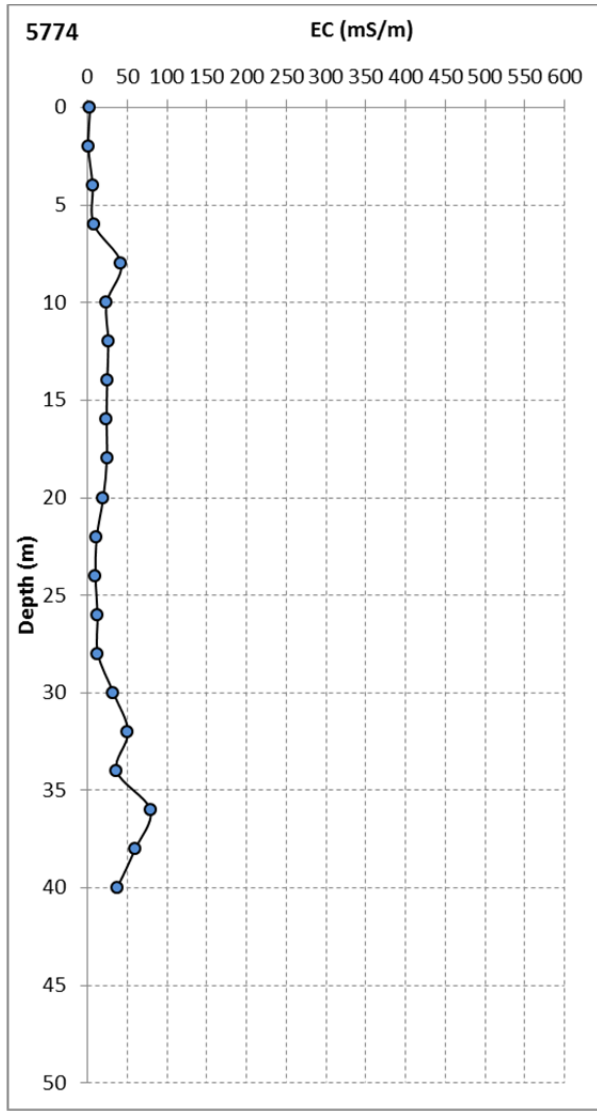
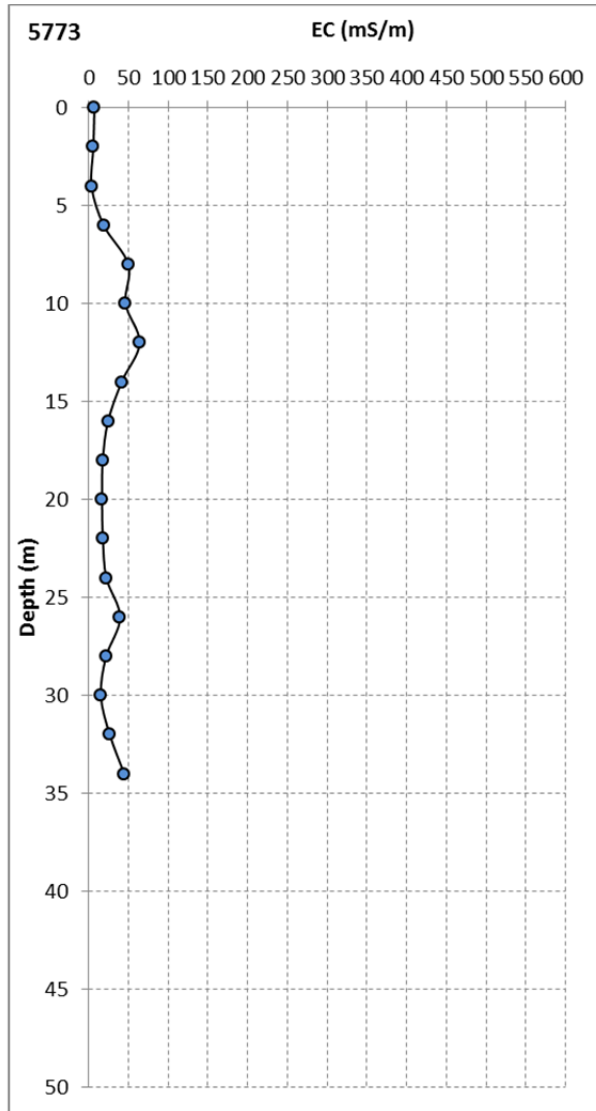
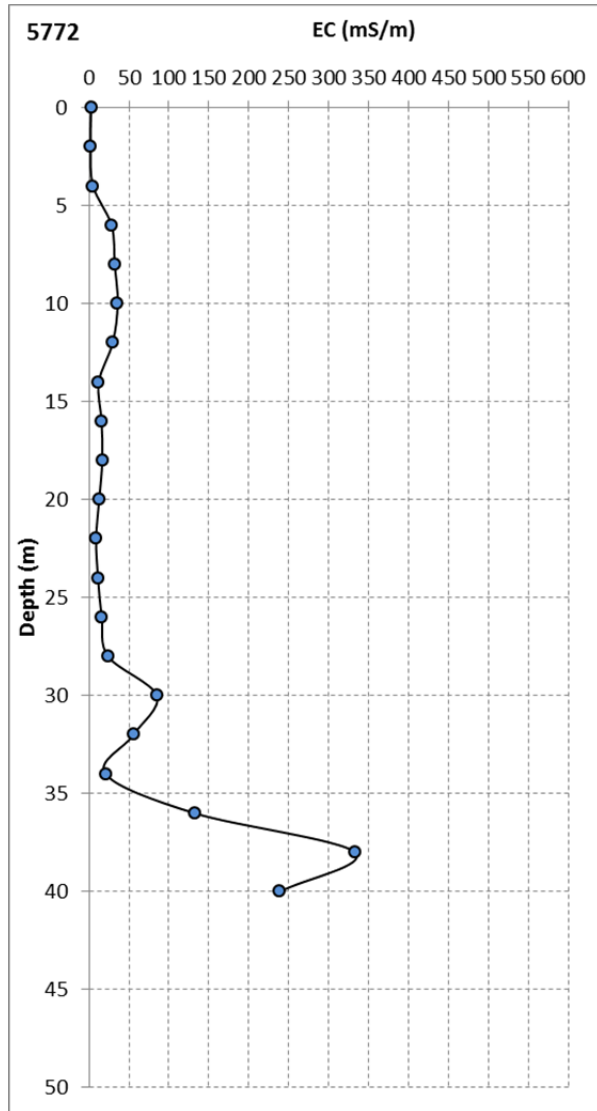


VIMY RESOURCES

TERRAIN ANALYSIS AND MATERIALS
CHARACTERISATION FOR THE MULGA ROCK URANIUM
PROJECT

Figure 4.19: Screen test results for the overburden materials within the Ambassador West Deposit



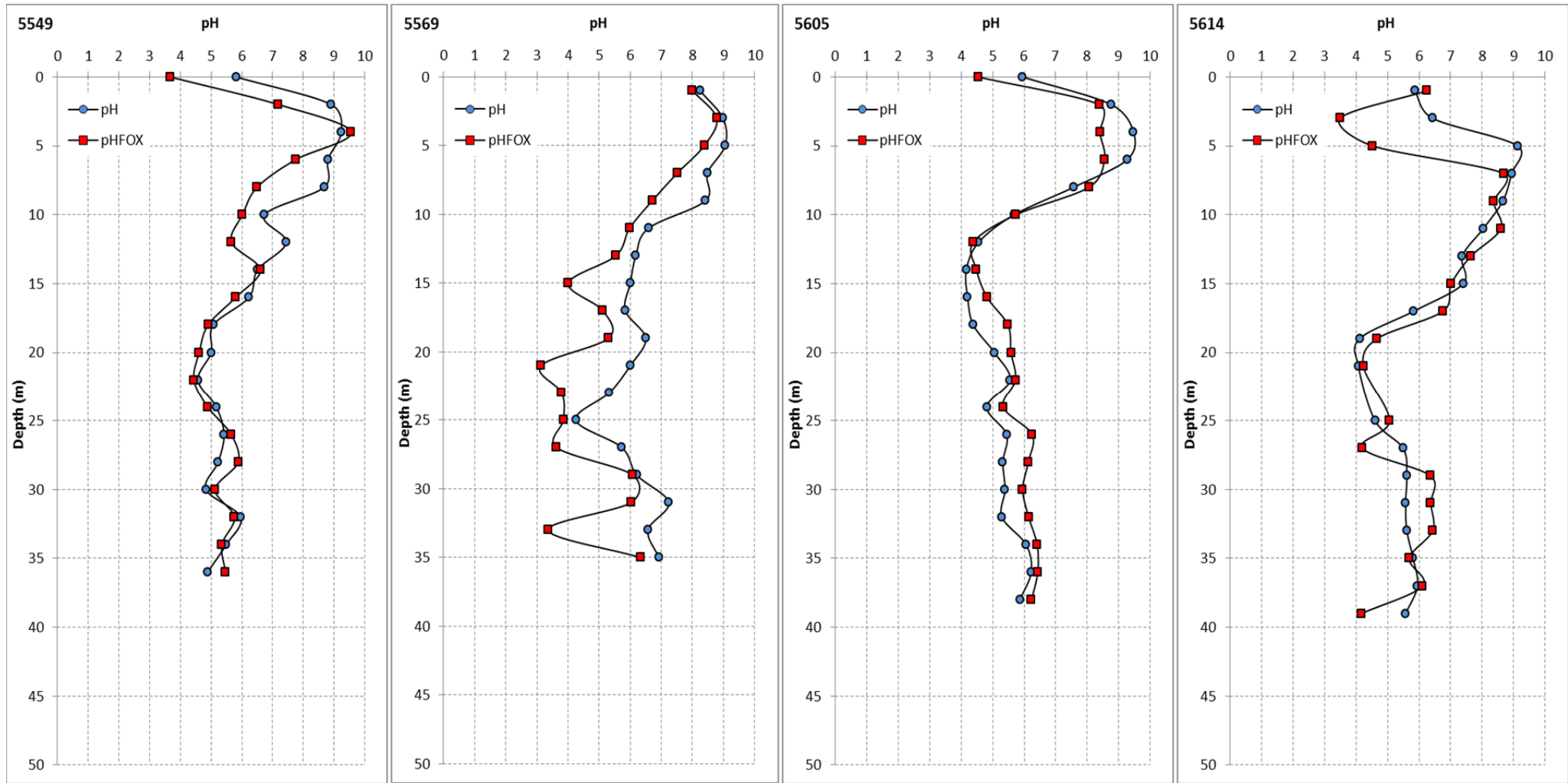


VIMY RESOURCES

TERRAIN ANALYSIS AND MATERIALS
CHARACTERISATION FOR THE MULGA ROCK URANIUM
PROJECT

Figure 4.18 continued...



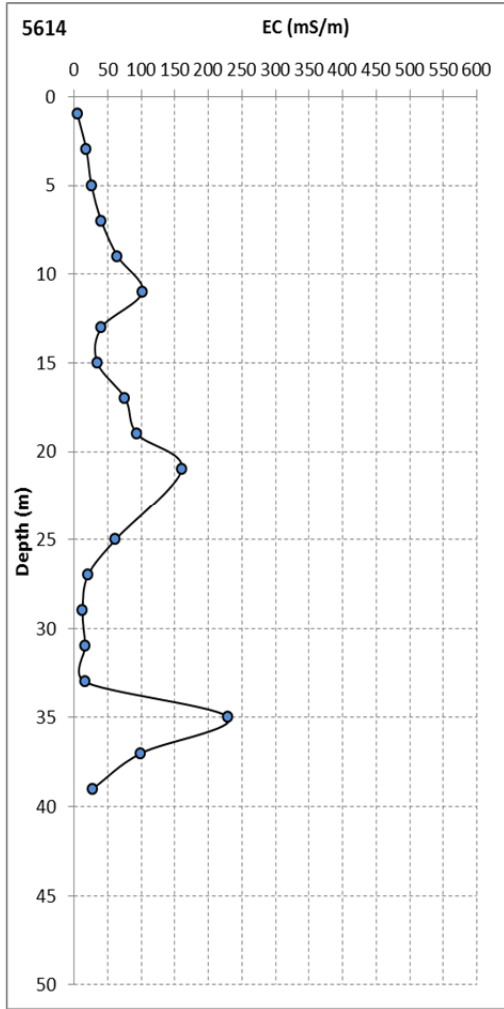
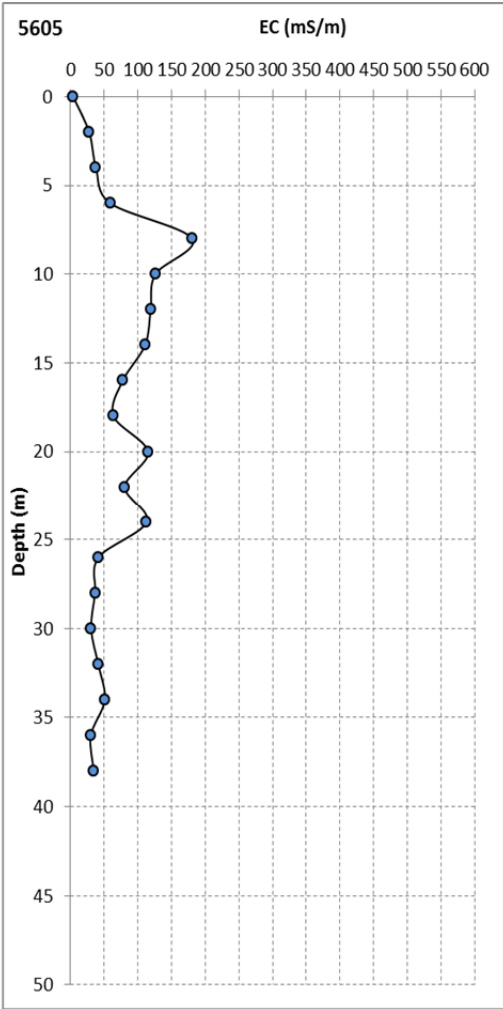
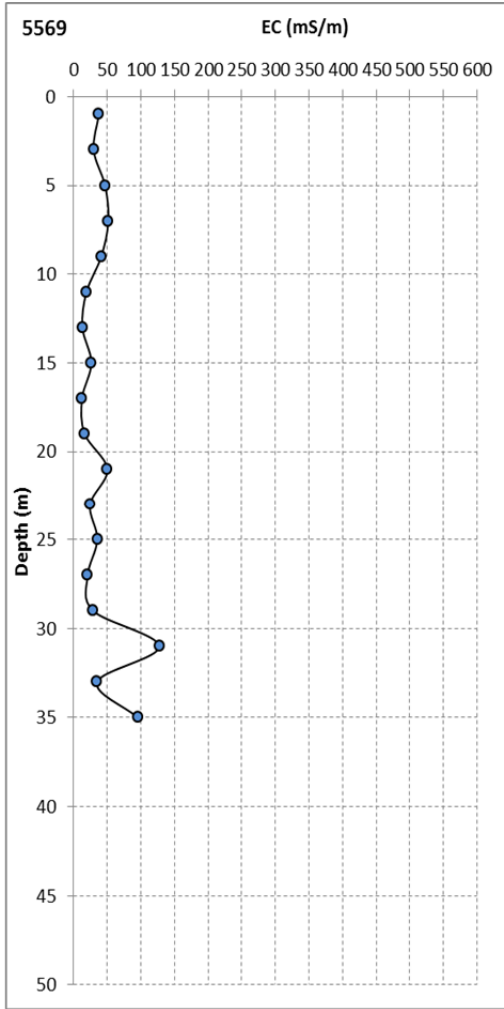
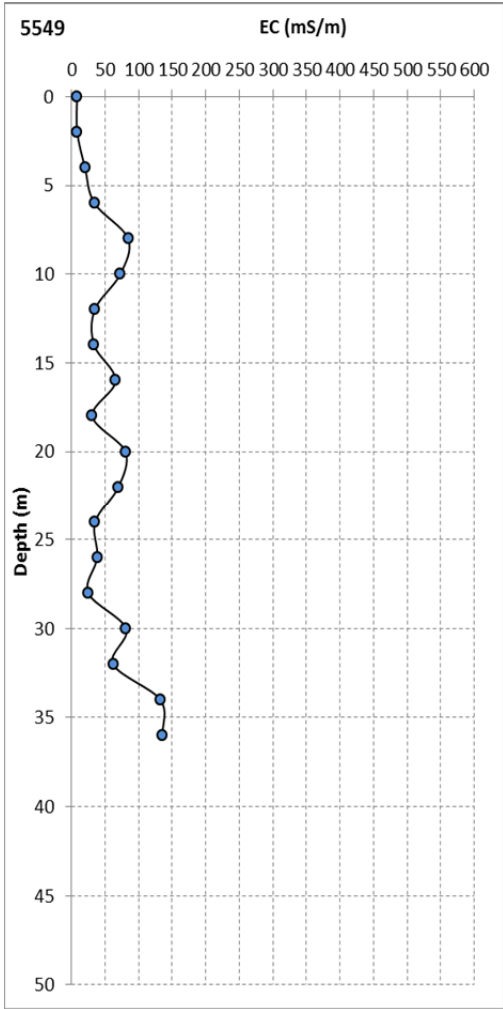


VIMY RESOURCES

TERRAIN ANALYSIS AND MATERIALS
CHARACTERISATION FOR THE MULGA ROCK URANIUM
PROJECT

Figure 4.20: Screen test results for the overburden materials within the Princess Deposit



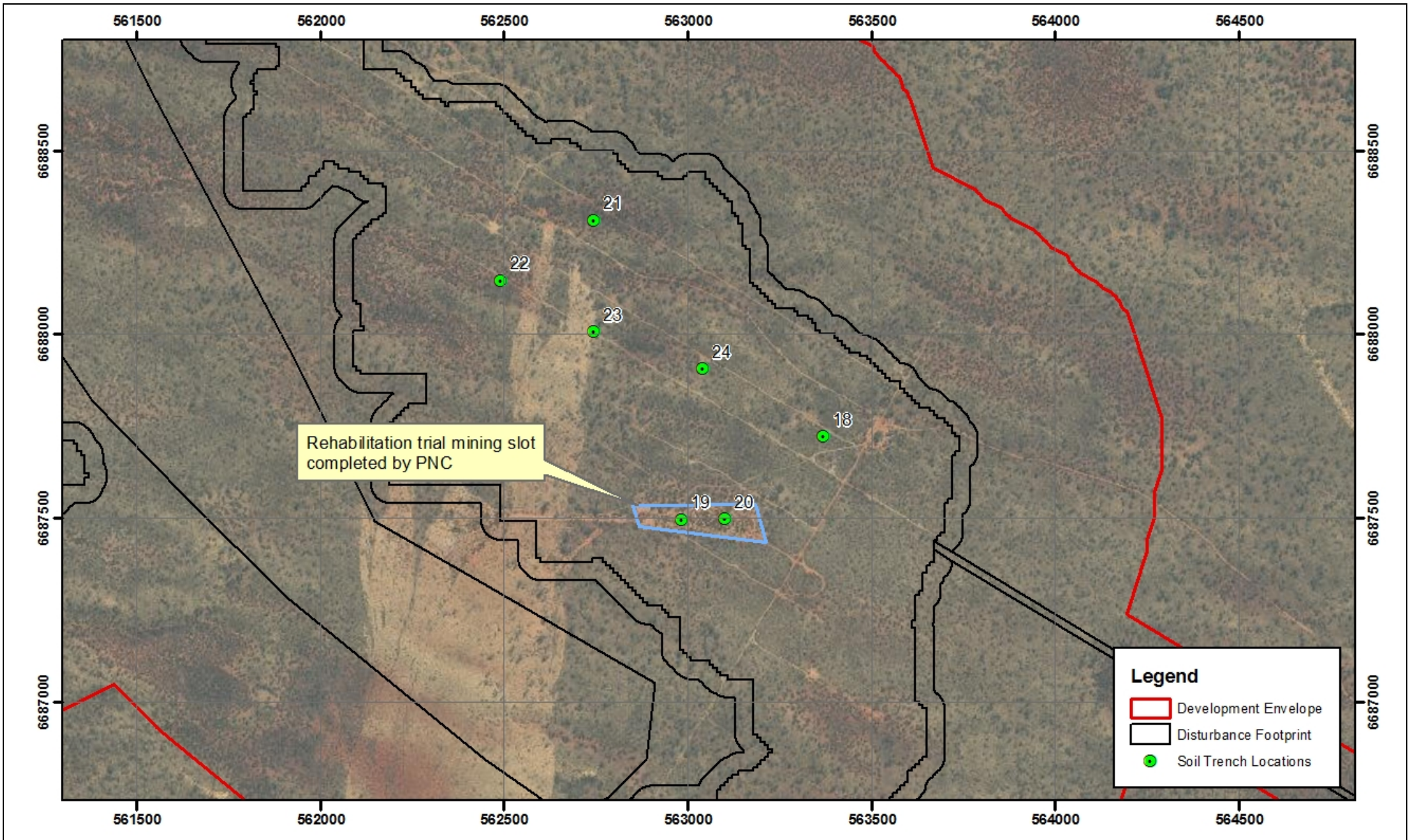


VIMY RESOURCES

TERRAIN ANALYSIS AND MATERIALS
CHARACTERISATION FOR THE MULGA ROCK URANIUM
PROJECT

Figure 4.19 continued...





VIMY RESOURCES

TERRAIN ANALYSIS AND MATERIALS CHARACTERISATION
FOR THE MULGA ROCK URANIUM PROJECT

Figure 4.21: Trial mining slot within the Shogun Deposit



Plate 4.12: Reconstructed soil profile exposed at Trench 19

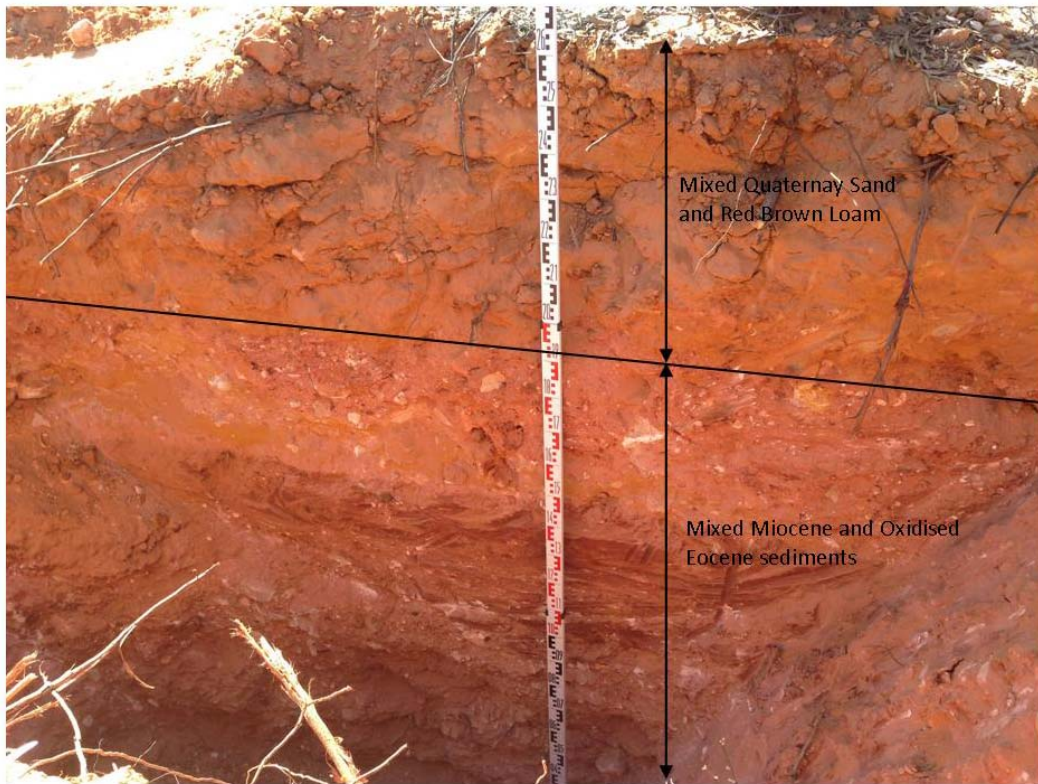


Plate 4.13: Reconstructed soil profile exposed at Trench 20

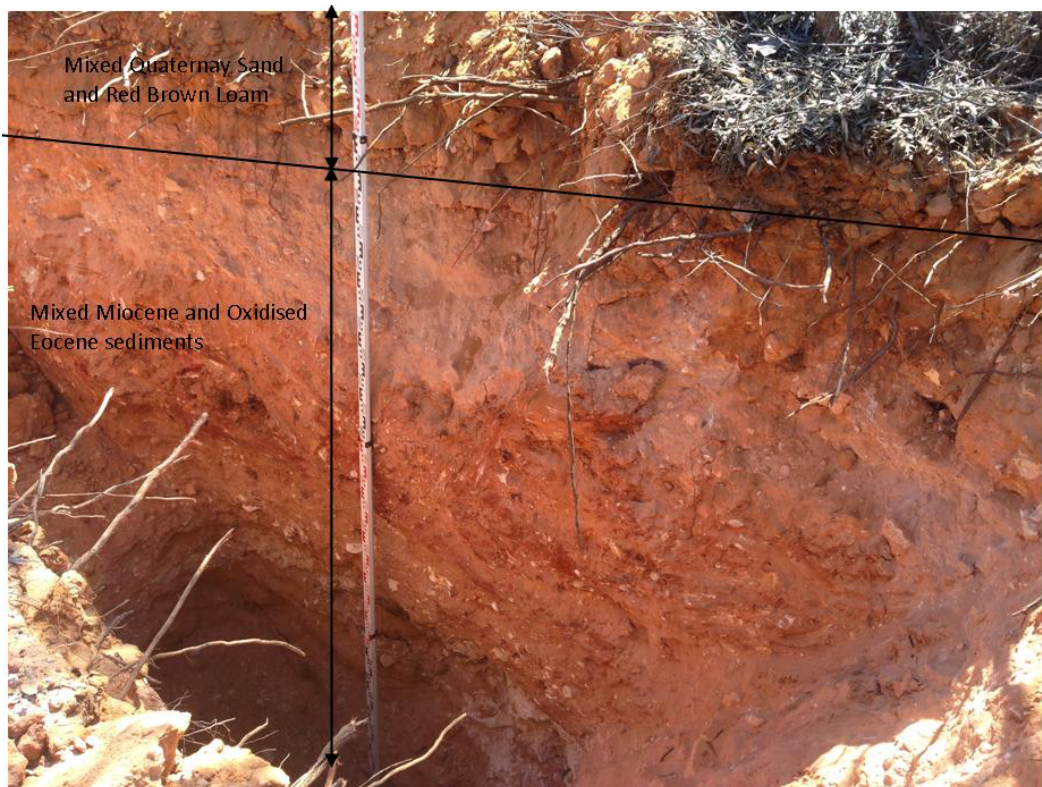


Plate 4.14: Characteristic rehabilitation of the mined slot within the Shogun Deposit



5 STUDY CONCLUSIONS AND RECOMMENDATIONS

5.1 MANAGEMENT OF SOIL AND WASTE MATERIALS

Based on the information and data presented in this report, the soils and deeper overburden materials throughout the MRUP exhibit both beneficial and limiting properties that will require careful management during mining and rehabilitation to ensure that closure can be achieved in a timely manner. A summary of these key properties is provided in Table 5.1.

It is recommended that the management strategies suggested in Table 5.1 are actioned to ensure that inappropriate handling and utilisation of the various soil and overburden materials does not impact on rehabilitation performance and ultimately closure and relinquishment.

5.2 VEGETATION MANAGEMENT

Given the appreciable wind erosion that occurs throughout the MRUP, and the propensity of the surficial sands to displace and be transported by the prevailing winds, management of vegetation (debris) during mining and rehabilitation will be an important aspect in creating stable and sustainable post-mine landforms for this project. As mentioned in Table 5.1, the properties of the surficial Quaternary sand, which will form the upper soil profile for any post-mine land surface, are not conducive to traditional ripping and any mechanised method to create surface complexity or undulation will likely be difficult (i.e. the sands simply fall into the space behind the ripper or tyne without being dislodged vertically); hence the use of vegetation debris to cover and effectively stabilise the rehabilitation surface will be important. The appropriate use of this debris will create a slight boundary layer effect, similar to the role of the sand dunes themselves that will protect the surface from wind erosion. Additional benefits of utilising vegetation debris in rehabilitation include:

- Minimise raindrop impact effects on the surface soils;
- Habitat creation and to provide protection for small terrestrial animals from predatory birds; and
- Seed store for brady孢子ous species (i.e. native species that retain their seed within the canopy of the vegetation).

5.2.1 VEGETATION STRIPPING

All vegetation to be cleared in a designated area should be pushed down and tracked-over by a bulldozer to reduce the vegetation into manageable sizes, which will aid future handling as well as facilitating the decomposition process (i.e. smaller pieces will decompose faster than larger pieces). All vegetation debris should be pushed into windrows to enable an excavator to load the material into truck for stockpiling. It is important during the stripping process that minimal surface soil is captured within the vegetation removed. This can be achieved by ensure that the dozer blade remains slightly above the ground surface and that a batter-bucket is used on the excavator loading the material.

5.2.2 VEGETATION DEBRIS STOCKPILING

All vegetation debris should be stockpiled in a single pile to minimise potential dilution and dispersion effects, and located close to the intend rehabilitation site. There is no height limitation to this stockpile/s as it will remain sufficiently porous to allow oxygen cycling and heat transfer if composting occurs. It is often advantageous to locate the vegetation debris stockpile upwind of any topsoil stockpile to protect against aeolian losses (i.e. wind erosion). This stockpile must not be sprayed with saline water and thus its location must be carefully considered to avoid proximity to traffic and the need for dust suppression.

STUDY CONCLUSIONS AND RECOMMENDATIONS

5.2.3 VEGETATION DEBRIS UTILISATION

Re-application of collected vegetation debris onto post-mine landform surfaces needs to be carefully considered with the pros and cons of each technique identified. The primary reason for this is that the re-application of vegetation debris may actually increase erosion and surface instability if undertaken inappropriately instead of facilitating rehabilitation. Application of vegetation debris to batter surfaces should only occur if there is sufficient volume of material to form a continuous cover across the surface (Plate 5.1 and Plate 5.2). The vegetation debris effectively acts as an adsorptive barrier to raindrop impact and prevents the surface soil particles becoming mobilised and available to erode. If there is insufficient vegetation debris to form a continuous cover then its application to batter surfaces should be avoided as its application and presence on the surface may actually exacerbate erosion and surface water runoff (i.e. by removing water convergence in ripples and directing water down slope in places).

5.3 MULCHING

Mulching of vegetation debris prior to re-application onto post-mine landform surfaces is beneficial as it further reduces the size of the vegetation material facilitating the decomposition process. There is obviously a cost to mulching and a cost-benefit analysis should be undertaken to determine its value.

Plate 5.1: Satisfactory utilisation of vegetation debris providing a continuous cover across a slope surface



STUDY CONCLUSIONS AND RECOMMENDATIONS

Plate 5.2: Unsatisfactory utilisation of vegetation debris providing insufficient surface cover



5.3.1 EFFECTS OF FIRE ON VEGETATION SOURCES

Given the likely importance of utilising vegetation debris in rehabilitation, to both stabilise the post-mine landsurface and facilitate revegetation establishment, it is necessary to consider that following the large fire event that occurred recently within the MRUP, very little vegetation will be available for collection. The lack of vegetation is clearly seen in Plate 5.3. It is therefore critical that during operations, and where vegetation is present, that as much of this resource as practicable is appropriately collected, stockpiled and stored to ensure that is available and viable for use in rehabilitation.

Plate 5.3: Pre- and post-fire vegetation sources

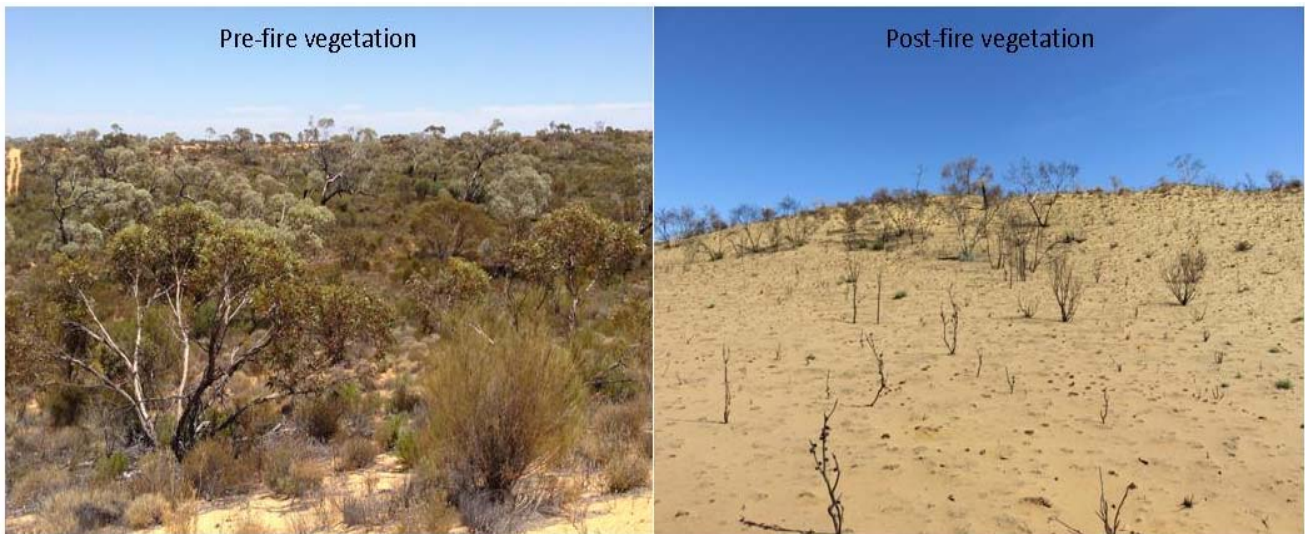


Table 5.1: Key properties of the soil and overburden materials, and their management requirements

Material	Material Class	Beneficial properties	Limiting properties	Management requirements
Quaternary Sand (including Yellow and Red Sands)	Soil	<ul style="list-style-type: none"> • Non-dispersive and non-erodible. • Negligible surface water flow with vertical infiltration dominating. • Friable, low soil strength and not hardsetting. • Optimal soil chemical properties (i.e. slightly acidic to neutral pH, and non-saline). 	<ul style="list-style-type: none"> • Negligible water holding or PAW content. • High permeability that may exacerbate ponding and subsurface lateral flow at a texture contrast boundary. 	<ul style="list-style-type: none"> • Manipulation of the depth of this material will control the revegetation species that establish and are sustainable in rehabilitation. • If placed on slopes overlying a texture contrast boundary then thickness of sand cover must increase with distance down slope to prevent subsurface lateral flows. • Should be used as primarily in rehabilitation as an evaporative cover to prevent the deeper, high PAW materials, from drying-out and hardsetting. • Given its sandy nature, ripping of this material will not be successful. Alternative methods of 'roughing-up' the rehabilitated surface to provide micro-topographic complexity (i.e. similar to a rip line crest and trough) are required.
Red loam or sandy clay	Soil	<ul style="list-style-type: none"> • Good water holding and PAW capacity. • Optimal soil chemical properties (i.e. non-saline and neutral – alkaline pH). 	<ul style="list-style-type: none"> • Although non-sodic, the low salinity results in this material being dispersive and highly erodible. • Hardsetting 	<ul style="list-style-type: none"> • This represents a minor soil material within the MRUP. • Although it contains optimal PAW properties, the small volume will restrict preferential stripping and utilisation in rehabilitation. • Given its association with the underlying calcrete it will likely be stripped with the calcrete and used to construct roads and other infrastructure. • If preferential stripping and utilisation in

rehabilitation is to occur then it will need to be placed below an evaporative cover (i.e. at least 1 m of Quaternary sand) to prevent it from drying and hardsetting.

Calcrete	Soil	<ul style="list-style-type: none"> • Physically stable and non-dispersive, non-erodible and non-hardsetting. • High to very neutralising capacity. 	<ul style="list-style-type: none"> • Strongly alkaline pH and often high salinity that may impact some susceptible species. 	<ul style="list-style-type: none"> • The primary role that the calcrete and overlying Red Brown Loam play is to increase the depth of soil profile that overlies the underlying Miocene and Oxidised Eocene sediments.
Miocene/Oxidised Eocene sediments	Overburden	<ul style="list-style-type: none"> • Optimal water holding and PAW content to support native plant species, although considerable heterogeneity in material properties does occur, ranging from sandy to heavy clay. 	<ul style="list-style-type: none"> • Dispersive, erodible, and hardsetting. • Low permeability facilitating surface runoff and sediment loss. • Salinity often too high for some susceptible species, especially in the basal 5 m which is in contact with the capillary fringe. • Basal 5 m of the Oxidised Eocene sediments often contain residual sulfides. 	<ul style="list-style-type: none"> • These generally clayey soil materials have optimal PAW content, but their elevated salinity limits the growth and sustainable development of salt tolerant species, with only Eucalypt species likely to tolerate these salinities. • Given their dispersive, erosive and hardsetting properties, any use of these materials in rehabilitation should be below an evaporative (i.e. they should not be placed on or near the surface). • Basal 5 m of the Oxidised Eocene sediments should be managed separately from the overlying materials. This material should be placed at depth in the reconstructed mine voids.

6 REFERENCES

- BOM (2015a). *Rainfall IFD Data System*. Available at: <http://www.bom.gov.au/hydro/has/cdirswebx/cdirswebx.shtml> (accessed February 2015).
- BOM (2015b). *Climate Data Online*. Available at: <http://www.bom.gov.au/climate/data/> (accessed February 2015).
- Clark, A. N. (1998) *The Dictionary of Geography*, Second edn. Penguin Books. London.
- CSIRO (2014). *Australian Soil Resource Information System (ASRIS)*, CSIRO Land and Water, Canberra, Australia.
- DEC (2010). *Assessment Levels for Soil, Sediment and Water. Contaminated Sites Management Series, Version 4.* Department of Environment and Conservation (DEC), Perth, Western Australia
- Douglas, G.B., Gray, D.J. and Butt, C.R.M. (1996). *Geochemistry, Mineralogy and Hydrochemistry of the Ambassador Multi-Element Lignite Deposit, Western Australia*. CSIRO Exploration and Mining, Perth, Western Australia.
- Elliott, W. J., Liebenow, A. M., Laflen, J. M. and Kohl, K. D. (1989) *A compendium of soil erodibility data from wepp cropland soil field erodibility experiments 1987 & 1988. Ohio State University and USDA Agricultural Research Service National Soil Erosion Research Laboratory Report*. Lafayette, Indiana, USA.
- Fitzsimmons, K. E. (2007) Morphological variability in the linear dunefields of the Strzelecki and Tirari Deserts, Australia. *Geomorphology*, **91**, 146-160.
- Flanagan, D. and Livingston, S. (1995) *Water erosion prediction project (WEPP) version 95.7 user summary*. In: *WEPP User Summary (Eds: Flanagan and Livingston) NSERL Report*
- Foster, G. R. (1982) Modeling the erosion process. . In *Hydrologic Modeling of Small Watersheds* (ed. by Hahn, CT), pp. 295-380.
- Green, H. W. and Ampt, G. A. (1911) Studies on Soil Physics. *The Journal of Agricultural Science*, **4**, 1-24.
- Isbell, R.F. (1996). *The Australian Soil Classification*. Australian Soil and Land Survey Handbook, Volume 4. CSIRO Publishing, Collingwood, Victoria, Australia.
- Jackson, M.J. and van de Graff, W.J.E. (1981). *Geology of the Officer Basin*, Australia BMR, Bulletin 206.
- Martinson, D.G., Pisias, N.G., Hays, J.D., Imbrie, J., Moore, T.C. and Shackleton, N.J. (1987). 'Age dating and the orbital theory of the ice ages: Development of a high resolution 0 to 300000 year chronostratigraphy'. *Quaternary Research*, **27**, 1-29.
- McKenzie, N., Coughlan, K. and Cresswell, N. (2002). *Soil Physical Measurement and Interpretation for Land Evaluation*, CSIRO Land and Water, Canberra, Australia.
- MCPL (2015a). *Assessment of Flora and Vegetation Surveys Conducted for the Mulga Rock Uranium Project*, Great Victoria Desert, WA. Unpublished report to Vimy Resources prepared by Matiske Consulting Pty Ltd.
- MCPL (2015b). *Regional Hibbertia crispula (P1 & Vulnerable) Survey*, Great Victoria Desert, WA. Unpublished report to Vimy Resources prepared by Matiske Consulting Pty Ltd.
- McDonald, R. C. and Isbell, R.F. 'Landsurface'. In: McDonald, R.C., Isbell, R.F., Speight, J.G., Walker, J. and Hopkins, M.S. (2009). *Australian Soil and Land Survey Field Handbook*, CSIRO Land and Water, Inkata Press, Melbourne, Australia.
- McDonald, R.C., Isbell, R.F., Speight, J.G., Walker, J. and Hopkins, M.S. (2009). *Australian Soil and Land Survey Field Handbook*, CSIRO Land and Water, Inkata Press, Melbourne, Australia.
- Rayment, G., E. and D. Lyons, J. (2011). *Soil Chemical Methods - Australasia*. Collingwood, VIC, CSIRO Publishing.
- Rockwater (2015). *Results of Hydrogeological Investigations and Numerical Modelling, Mulga Rock Mining Areas*, Unpublished report to Vimy Resources prepared by Rockwater Perth, Western Australia.
- Schoknecht, N. (2002). *Soil Groups of Western Australia*, Resource Management Technical Report 246, Department of Agriculture, Perth, Western Australia.

REFERENCES

- Short, N. M. (2010) *The Remote Sensing Tutorial*. Unpublished report prepared by Federation of American Scientists for <http://fas.org/irp/imint/docs/rst/>.
- Walter, M.R., Veevers, J.J., Calver, C.R. and Grey, K. (1995). 'Neoproterozoic stratigraphy of the Centralian Superbasin, Australia', *Precambrian Research*, **73**: 173-195.
- Willgoose, G. (2005) *User Manual for SIBERIA, Version 8.3*. Telluric Research. Scone, NSW.
- Yu, B. (2003) An assessment of uncalibrated CLIGEN in Australia. *Agricultural and Forest Meteorology*, **119**, 131-148.
- Zhang, G.-h., Luo, R.-t., Cao, Y., Shen, R.-c. and Zhang, X. C. (2010) Correction factor to dye-measured flow velocity under varying water and sediment discharges. *Journal of Hydrology*, **389**, 205-213.